NOTICE

AVIS

Canada

The University of Alberta

Matrix Padé Forms and Inverses of Block Hankel Matrices

by

George Labahn

A thesis

submitted to the Faculty of Graduate Studies and Research

in partial fulfillment of the requirements for the degree of

Doctor of Philosophy

Department of Computing Science

Edmonton, Alberta

Fall, 1988

The University of Alberta

Release Form

Name of Author: George Labahn

Title of Thesis: *Matrix Padé Forms and Inverses of Block Hankel Matrices*

Degree for Which Thesis was Presented: Doctor of Philosophy

Year This Degree Granted: 1988

George Labahn

Permanent Address: 11704 - 44 Avenue

Edmonton, Alberta

Canada

Dated 30 June 1988

The University of Alberta

Faculty of Graduate Studies and Research

The undersigned certify that they have read, and recommend to the Faculty of Graduate Studies and Research, for acceptance, a thesis entitled *Matrix Padé Forms and Inverses of Block Hankel Matrices* submitted by George Labahn in partial fulfillment of the requirements for the degree of Doctor of Philosophy

....
Supervisor

....

....

....

Date ....

Dedication

For the children

Philip Labahn, Eve Coppinger, and Allison Leslie

Abstract

For matrix power series with coefficients over a field, the notion of a matrix power series remainder sequence and its corresponding cofactor sequence are introduced and developed. An algorithm for constructing these sequences is presented.

It is shown that the cofactor-sequence yields directly a sequence of Padé fractions for a matrix power series represented as a quotient $B(z)^{-1}A(z)$. When $B(z)^{-1}A(z)$ is normal, the complexity of the algorithm for computing a Padé fraction of type (m,n) is $O(p^3(m+n)^2)$, where p is the order of the matrices A(z) and B(z).

For power series which are abnormal, for a given (m,n), Padé fractions may not exist. However, it is shown that a generalized notion of Padé fraction, the Padé form, introduced in this paper does always exist and can be computed by the algorithm. In the abnormal case, the algorithm can reach a complexity of $O(p^3(m+n)^3)$, depending on the nature of the abnormalities. In the special case of a scalar power series, however, the algorithm complexity is $O((m+n)^2)$, even in the abnormal case.

Matrix Padé forms are also used to give a set of new formulae for the inverse of a block Hankel matrix. The formulae are practical because our algorithm allows for easy computation of these forms. In addition, a by-product of our formulae and the algorithm allows the computation of all inverses of non-singular principal minors.

By using Frobenius-type identities between certain matrix Padé forms, the inversion formulae are shown to generalize the formulae of Gohberg-Heinig, and, in the scalar case, the formulae of Gohberg-Semencul and Gohberg-Krupnik.

The new formulae have the significant advantage of requiring only that the block Hankel matrix itself be nonsingular. The others require, in addition, that certain submatrices be nonsingular.

Acknowledgements

The author would like to take this opportunity to thank the people who helped make this work possible. As with any research project, numerous people were consulted at all stages of its development. Their time and often insightful criticism of this work sparked new ideas and made old ones clear. In particular, I would like to thank the following people.

My first acknowledgements must go to my supervisor Stan Cabay. During the three years I spent under his supervision I grew both academically and professionally. May everyone have such a helpful supervisor.

Second, I would like to thank the members of my examining committee for their time spent in reviewing this thesis.

Without the resources and technical support provided by The Department of Computing Science at the University of Alberta this thesis would not have been possible. In addition a special thanks goes to the Department of Mathematics at the University of Alberta for their support and kindness over the years.

Also, none of this would have been possible without the unlimited patience and kindness of my wife, Laura Leslie, and the ever present encouragement of my parents.

Table of Contents

Chapter 1

Introduction

Let

$$A(z) = \sum_{i=0}^{\infty} a_i z^i, \tag{1.1}$$

where a_i, $i = 0, \ldots$, is a p x p matrix with coefficients from a field K, be a formal power series. Loosely speaking, a matrix Padé approximant of A(z) is an expression of the form $U(z) \cdot V(z)^{-1}$, or $V(z)^{-1} \cdot U(z)$, where U(z) and V(z) are matrix polynomials of degree at most m and n, respectively, whose expansion agrees with A(z) up to and including the term z^{m+n}. Mathematically this is equivalent to the expressions

$$A(z)V(z) - U(z) \quad or \quad V(z)A(z) - U(z) \tag{1.2}$$

being zero for the first m+n+1 terms.

Padé approximants have many applications in mathematics and in engineering-related disciplines. Applications include numerical computations for special power series such as the Gamma function (c.f., Nemeth and Zimanyi [37]), algorithms in the field of numerical analysis (c.f., Gragg [26]), triangulation of block Hankel and Toeplitz matrices (c.f., Rissanen [41]), solution of linear systems of equations with Hankel or Toeplitz coefficient matrices (c.f., Rissanen [39]), digital filtering theory (c.f., Bu. eel [12] and Brophy and Salazar [9]) and linear control theory (c.f., Elgerd [22]).

As an illustration we can single out three areas where formal power series and related rational expressions come into play.

Example 1.1:

Consider the initial valued nonlinear differential equation given by

$$y \cdot \ddot{y} + \dot{y}^2 = \frac{3}{(1 + 2z)^3}, \quad y(0) = 1, \quad \dot{y}(0) = -3/4. \tag{1.3}$$

If we make the assumption that y is analytic in z in a neighborhood of 0, then the coefficients of the

1

MacLaurin expansion can be determined as follows. The first two coefficients are obtained from the initial conditions while the third is determined by substituting 0 into the differential equation and solving for $\ddot{y}(0)$. This gives

$$y = 1 - 3/4z + 39/32z^2 + \cdots .$$

(1.4)

Higher order coefficients can be obtained by differentiating the equation, substituting 0, and solving for $y^{(n)}(0)$. This process is only useful as an approximation since one must stop after a finite number of steps. The result is an approximation of y by a polynomial. However, polynomials are often poor approximations, especially for large z. Instead, one can use a Padé approximation, which, when truncated at the same position, produces the same polynomial. For example, the rational expression

$$\frac{1 + 7/8z}{1 + 13/8z}$$

(1.5)

also has the same first three terms as the power series expansion for y (this is the Padé fraction of type (1,1) for y). This rational expression results in a much closer approximation to the real answer

$$\sqrt{\frac{2 + z}{2 + 4z}}$$

(1.6)

especially for large z. There is, for example, only an 8% difference at infinity (c.f., Baker and Graves-Morris [3]). In this case Padé approximation is used as a method of improving an existing approximation.

Example 1.2:

Consider a linear system having discretized input x_n and discretized output y_n. The outputs are determined by convolution of the inputs with a unit impulse response a_k. (c.f., Bultheel [12])
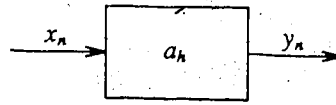
If we think of these discrete sequences in terms of their z-transforms, i.e., as power series

$$X(z) = \sum x_n z^n, \quad Y(z) = \sum y_n z^n, \quad A(z) = \sum a_n z^n, \quad (1.7)$$

then convolution of the impulse response function goes over to polynomial multiplication which results in.

$$Y(z) = A(z)X(z). \quad (1.8)$$

$A(z)$ is called the transfer function of the system. The coefficents of the transfer function are usually determined theoretically or experimentally by measuring the output of a signal from an input that isolates on the particular response. An approximation of $A(z)$ by a rational expression

$$\frac{U(z)}{V(z)} = \frac{\sum_{i=0}^{m} u_i z^i}{\sum_{i=0}^{n} v_i z^i}, \quad with \quad v_0 = 1, \quad (1.9)$$

combined with (1.8) gives

$$V(z) \cdot Y(z) = U(z) \cdot X(z). \quad (1.10)$$

Thus

$$y_t = \left[u_0 x_t + \cdots + u_m x_{t-m} \right] - \left[v_1 y_{t-1} + \cdots + v_n y_{t-n} \right] \quad (1.11)$$

which is a system where the output at time t depends on a particular combination of the last $m+1$ inputs and the previous n outputs. In this case rational approximation is used to obtain a feedforward/feedback model for a linear system (c.f., Gragg and Lindquist [27]).

A variation of this example is to find a closest model to the system having a particular type of rational expression, for example one of the form

$$\frac{u_0}{v_0 + v_1 z + \cdots v_n z^n} \cdot \tag{1.12}$$

By closest, we mean in the least squares sense. Solving the normal equations of this over-determined system results in a Yule-Walker system of equations (c.f, chapter 4) where the coefficients of the system are the autocorrelation coefficients of the sequence a_k (c.f., Wakita [46] or Makhoul [34]). This in turn can be interpreted as a Padé approximation of a particular type for the autocorrelation power series.

Example 1.3

For the power series

$$\frac{1 - 4z^2}{1 + 3z - 3z^2} = 1 - 1/3z + O(z^3), \tag{1.11}$$

the Padé fraction of type (0,2) is given by

$$\frac{1}{1 + 3z + z^2} \tag{1.12}$$

since

$$\frac{1}{1 + 3z + z^2} = \frac{1 - 4z^2}{1 + 3z - 3z^2} + O(z^3). \tag{1.13}$$

Multiplying denominators gives

$$1 + 3z - 3z^2 = (1 + 3z + z^2)(1 - 4z^2) + O(z^3), \tag{1.14}$$

or, more precisely,

$$1 + 3z - 3z^2 = (1 + 3z + z^2)(1 - 4z^2) + z^3(12 + 4z). \tag{1.15}$$

Multiplying both sides by z^{-4} and substituting z for z^{-1} (this is the same as reversing the order of the coefficients of the polynomials) results in

$$z^4 + 3z^3 - 3z^2 = (z^2 + 3z + 1)(z^2 - 4) + (12z + 4) \tag{1.16}$$

which is just polynomial division with remainder. This process shows that polynomial division is equivalent to Padé approximation (of a specific type). More generally, algorithms that are based on polynomial division can also be interpreted in terms of Padé approximation. For example, for any two polynomials $A(z)$ and $B(z)$, the extended Euclidean GCD algorithm calculates a sequence of expressions of the form

$$A(z)S_i(z) + B(z)T_i(z) = R_i(z), \tag{1.17}$$

satisfying various algebraic properties (c.f., [35]), with the last remainder $R_{last}(z)$ being the GCD of $A(z)$ and $B(z)$. If m_i and n_i are the degrees of $S_i(z)$ and $T_i(z)$, respectively, then reversing coefficients in equation (1.16) results in

$$A^{(r)}(z)S_i^{(r)}(z) + B^{(r)}(z)T_i^{(r)}(z) = z^{m_i + n_i + 1} R_i^{(r)}(z). \tag{1.18}$$

where the superscript (r) denotes a polynomial having coefficients in reversed order. Thus the extended Euclidean GCD algorithm can be viewed as a sequence of Padé approximations for the quotient power series $B^{(r)}(z)^{-1} A^{(r)}(z)$.

Note that, although the examples are presented in the scalar case, these are equally valid in the multidimensional case. Matrix Padé approximants can be used when we have a system of nonlinear differential equations with initial conditions. Multidimensional rational approximants are used with linear systems having more than one input and one output.

These examples also illustrate problems that must be considered when generalizing from the scalar case to the matrix case. In example 1.2, commutativity becomes an issue, since equation (1.9) requires that the denominator divide on the left. A denominater dividing on the right will not give a desired model because of the lack of commutativity. Example 1.3 points out the problem of singularity in the matrix case. Matrix polynomial division is equivalent to specific types of matrix Padé approximation, just as in the

scalar case. However, there is no Euclidean-algorithm in the case of matrix polynomials, because nonzero coefficents may be singular, and hence one cannot always divide one nonzero coefficient into another nonzero coefficient. For more on the problem of generalizing scalar polynomials to their matrix counterparts see for example Dennis et al [19] .

An added consideration when generalizing rational approximants is that, unlike the scalar case, the definition of a matrix Padé approximant can be made formal in a variety of ways. For example, the approximation (1.2) can be written as

$$A(z) \approx U'(z) \cdot V'(z)^{-1} = \left\{ U'(z) \cdot adj(V'(z)) \right\} \cdot (det(V'(z))^{-1} = \left\{ U(z) \right\} \cdot V(z)^{-1} \qquad (1.19)$$

so that $V(z)$ is a scalar polynomial while $U(z)$ can be a $p \times q$ matrix. This is the approach taken by Rissanen [40] . Typically, however, $U(z)$ and $V(z)$ are $p \times p$ polynomial matrices, and $V(z)$ is further restricted by the condition that the constant term, $V(0)$, is invertible. In this thesis, we call such approximants matrix Padé fractions, which is consistent with the scalar ($p=1$) case.

For a particular m and n, however, matrix Padé fractions need not exist. Therefore, in this thesis we introduce the notion of a matrix Padé form, in which the condition of invertibility of $V(0)$ is relaxed. The definition is a generalization of a similar one given in the scalar case. It is shown that matrix Padé forms always exist, but that they may not be unique. In general, matrix Padé forms need not have an invertible denominator, $V(z)$. However, for m and n given, by obtaining a basis for all the Padé forms, we are always able to construct a matrix Padé form with an invertible $V(z)$, in the case that one does indeed exist. This, along with additional properties of matrix Padé forms, provides the contents of chapter 2.

Chapter 3 is concerned with the problem of calculating matrix Padé approximants. In the scalar case, existing algorithms can be classified into two categories, those that require that $A(z)$ be a normal power series (c.f., Gragg [26]) and those that do not require this restriction. Algorithms that calculate Padé approximants for normal power series include the ε-algorithm of Wynn [48] , the η-algorithm of Bauer [5] , the Q-D algorithm of Rutishauser [42] along with the well known algorithms of Trench [45] and Levinson

[33] Algorithms that are successful in the degenerate non-normal case can further be divided into two sub-categories according to their complexity costs. The algorithms of Bultheel [11] , Rissanen [39] , McEliece and Shearer [35] , and the slow algorithm of Cabay and Choi [16] calculate the Padé approximant of type (m,n) with a complexity of $O((m+n)^2)$ operations. The algorithms of Brent et al [8] , Sugiyama [44] and the fast algorithm of Cabay and Choi [16] have a complexity of only $O((m+n) \log^2(m+n))$. See the article by Sugiyama for a table listing well known algorithms including their restrictions along with complexities.

Most scalar algorithms can be generalized if the matrix power series is assumed to be normal. While there are examples where the lack of commutativity is a concern (c.f., Draux [20]) this is not a problem with most algorithms. Examples of such generalizations to the matrix case include those given by Bose and Basu [7] , Bultheel [10] , Rissanen [41] , and Starkand [43] . The fast methods of Brent et al [8] , Cabay and Choi [16] , and Sugiyama [44] also work over matrix coefficients, under these strict normality conditions. Fast polynomial multiplication using fast Fourier transforms is required to obtain the improved complexity for these fast algorithms. Since matrix polynomials can be considered as matrices having polynomial coefficients, multiplying two matrix polynomials is the same as a series of scalar polynomial multiplications. Thus fast techniques carry over to the matrix case.

All these algorithms fail, however, if the normality condition is dropped. Without normality there arise problems with matrix singularity. That is, in each algorithm specific nonzero coefficients need to be invertible, a requirement that cannot be guaranteed in the case of matrix coefficients. These specific nonzero coefficients are nonsingular when normality is assumed. An algorithm that calculates Padé approximants in a non-normal case is given by Labahn [32] . However, in this algorithm there are still strict conditions (near-normality) that need to be satisfied by the power series before Padé approximants can be calculated. Some other matrix algorithms that require normality will also work in this slightly less restrictive case (e.g., Rissanen's algorithm).

In chapter 3 we present an algorithm, MPADE, for computing matrix Padé forms for a given matrix power series. The algorithm overcomes the problem of singularity and so, unlike other algorithms, there

are no restrictions placed on the power series in order that MPADE succeed. Central to the development of MPADE are the notions of a matrix power series remainder sequence and the corresponding cofactor sequence, which are introduced in this chapter. These are generalizations of notions developed by Cabay and Kossowski [17] for power series over an integral domain. The cofactor sequence computed by MPADE yields a sequence of matrix Padé fractions along a specific off-diagonal path of the Padé table for $A(z)$.

A complexity analysis of the algorithm is given. For normal power series, we show that the complexity of MPADE is $O(p^3 (m+n)^2)$ operations in K. This is the same complexity as some of the algorithms proposed by Bultheel [10], Bose and Basu [7], Starkand [43], and Rissanen [41]. Overcoming the problem of singularity introduces a degree of uncertainty in the cost complexity, however. In the abnormal case, the algorithm is usually of complexity $O(p^3 \cdot (m+n)^2)$, but can reach $O(p^3 \cdot (m+n)^3)$ operations in K in some pathological cases. In the scalar case, however, MPADE always has a complexity of $O((m+n)^2)$, regardless of the degree of abnormality.

The concept of a matrix Padé approximant is closely related to matrices having a block Hankel structure. These are matrices of the form

$$H_{m,n} = \begin{bmatrix} a_{m-n+1} & \cdots & a_m \\ \cdot & & \cdot \\ \cdot & & \cdot \\ \cdot & & \cdot \\ a_m & \cdots & a_{m+n-1} \end{bmatrix}$$

(1.19)

where the a_i are p x p matrices. The connection between the two follows from equation (1.2) which allows the denominator to be calculated as solutions of a system of equations having as their coefficient matrix a block Hankel matrix. Systems of equations having as their coefficient matrix a Hankel matrix are encountered in such applications as digital filtering, linear control theory and image processing.

Chapter 4 deals with the problem of inverting block Hankel matrices. The approach uses the relationship between these matrices and a related set of matrix Padé forms to determine both when a Hankel

matrix is nonsingular and also how to calculate its inverse. We show that necessary and sufficient conditions for a block Hankel matrix to be nonsingular is the existence of four matrix Padé forms satisfying specific conditions. In addition, a set of closed formulae for the inverse is given in terms of these four matrix Padé forms.

The existence of closed formulae for Hankel matrices is not new. In the scalar case well known formulae of Gohberg and Semencul [23] gives $H_{m,n}^{-1}$ in terms of only the first and last columns of the inverse. Gohberg and Krupnik [24] give a formula for the inverse in terms of only the last two columns of $H_{m,n}^{-1}$.

In the nonscalar case, when $p > 1$, additional problems are encountered in obtaining a closed formula for the inverse. A set of closed formulae of Gohberg and Heinig [25], give the inverse in terms of the first and last columns together with the first and last rows of the inverse.

All of the above formulae depend on the ability to perform certain bordering operations that lend themselves well to matrices with a Hankel structure. However, these bordering operations require the imposition of certain additional restrictions on $H_{m,n}$. For both the Gohberg-Semencul and Gohberg-Heinig formulae, for example, the submatrix $H_{m,n-1}$ must also be nonsingular; whereas, for the Gohberg-Krupnik formula the submatrix $H_{m-1,n-1}$ must also be nonsingular. Inverse formulae are then also given for the relevant submatrices.

By using matrix Padé forms, we are able to avoid bordering techniques and so require only that $H_{m,n}$ be nonsingular. In addition we show, in chapter 5, that formulae that are based on bordering techniques can easily be determined from our formulae by taking advantage of relationships (e.g., Frobenius identities) that exist for neighbors in a Padé table. Thus, by using Padé forms we unify the work done previously in this field.

A major advantage of a closed inverse formula is that it allows for efficient algorithms to calculate the inverses of Hankel matrices. This efficiency comes both in the cost complexity of calculating the inverse and also in the amount of storage required for the final result.

As an application of both our inverse formulae and the MPADE algorithm, we obtain an algorithm for calculating $H_{m,n}^{-1}$. The resulting algorithm has many advantages for our situation. It is successful without any preconditions placed on the original power series. As a by-product, we obtain inverses for all the principal minors of $H_{m,n}$ that are nonsingular. Also, it is iterative on n, allowing cost savings in implementation. The complexity of the resulting algorithm for an n x n matrix is generically $O(p^3 n^2)$, although there are pathological cases where it can be as high as $O(p^3 n^3)$ (for example, when all the principal minors of $H_{m,n}$ are singular). This compares with other nonscalar methods (c.f., Akaike [1], Rissanen [41], Bose and Basu [7]) which are also of complexity $O(p^3 n^2)$, but which succeed only when all principal minors are nonsingular. In the scalar case, however, the cost complexity of MPADE is $O(n^2)$, regardless of the types of singularities found in $H_{m,n}$. This compares favorably with the method described by Rissanen [39], which is of complexity $O(n^2)$ and succeeds in the degenerate case. The $O(n^2)$ methods of Trench [45], Zohar [49], and Kailath et al [30], on the other hand, fail whenever a principal minor of $H_{m,n}$ is singular.

When fast polynomial multiplication methods are available, in the scalar case, the required Padé forms can be calculated by the EMGCD algorithm of Brent et al [8] or the off-diagonal algorithm of Cabay and Choi [16] with a complexity of $O(n \log^2 n)$. The algorithm is also iterative on n and produces the inverses of some of the nonsingular principal minors as a by-product. The $O(n \log^2 n)$ methods of Bitmead and Anderson [6] and de Hoog [28], on the other hand, succeed only in the nondegenerate case. We note that the last two algorithms all use fast $O(n \log^2 n)$ algorithms to determine both the first and last columns of the inverse, and then use one of the inverse formula of Gohberg and Semencul to obtain the inverse. Many of the inefficiencies or restrictions are due to the limitations of this inverse formula.

In the nonscalar case, fast algorithms can also be used to calculate the required Padé forms, but under some restrictions. If the block matrix is positive definite (or, more generally, if the associated power series is nearly-normal (c.f., chapter 3)), for example, and fast polynomial multiplication is allowed, then the inverse formulae can be calculated using the fast algorithm of Labahn [32] with complexity $O(p^3 n \log^2 n)$. This algorithm is also iterative and calculates the inverses of some of the nonsingular principal minors as a

by-product. The algorithm of Bitmead and Anderson, generalized to the nonscalar case by the use of the inverse formulae of Gohberg and Heinig, is also of complexity $O(p^3 \cdot n \, \log^2 n)$, but works only in the normal case.

Chapter 2

Matrix Padé Forms

2.1. Introduction

Let

$$A(z) = \sum_{i=0}^{\infty} a_i z^i, \tag{2.1}$$

where a_i, $i = 0, \ldots$, is a p x p matrix with coefficients from a field K, be a formal power series. In this chapter we present the basic definitions and properties of a matrix Padé approximant for A(z). Roughly speaking this is an expression of the form $U(z) \cdot V(z)^{-1}$, or $V(z)^{-1} \cdot U(z)$, where U(z) and V(z) are p x p matrix polynomials of degree at most m and n, respectively, whose expansion agrees with A(z) up to and including the term z^{m+n}.

Typically V(z) is further restricted by the condition that the constant term, V(0), is invertible (c.f., Bose and Basu [7] , Bultheel [10] , and Starkand [43]). In this thesis, we call such approximants matrix Padé fractions, which is consistent with the scalar (p=1) case (c.f., Gragg [26]).

For a particular m and n, however, matrix Padé fractions need not exist. Therefore we introduce the notion of a matrix Padé form, in which the condition of invertibility of V(0) is relaxed. The definition is a generalization of a similar one given for the scalar case (c.f., Gragg [26]). We show that matrix Padé forms always exist, but that they may not be unique. In general, matrix Padé forms need not have an invertible denominator, V(z). However, for m and n given, by obtaining a basis for all the Padé forms, we are also able to construct a matrix Padé form with an invertible V(z), in the case that one does exist. In addition, properties that will be used (in chapter 3) to establish an algorithm to construct such forms are also included in this chapter.

For purposes of presentation, we adopt the following notation. We let D denote the non-commutative ring of p x p matrices over a field. The domain of formal power series with coefficients over D and indeter-

minant z is denoted by D[[z]]. For any $A(z) \, \varepsilon \, D[[z]]$, A(z) is formally represented by

$$A(z) = \sum_{i=0}^{\infty} a_i z^i,$$ (2.2)

where the coefficients $a_i \, \varepsilon \, D$ are always written in lower case. The domain of polynomials (finite power series) over D with indeterminant z is denoted by D[z]. Any polynomial $P_n(z) \, \varepsilon \, D[z]$ is represented formally by

$$P_n(z) = \sum_{i=0}^{n} p_i z^i,$$ (2.3)

where again the coefficients $p_i \, \varepsilon \, D$ are written in lower case. The degree of $P_n(z)$ (i.e., the largest i such that $p_i \neq 0$) is denoted by $\partial(P_n(z))$.

2.2. Basic Definitions

Let

$$A(z) = \sum_{i=0}^{\infty} a_i z^i \quad , \quad B(z) = \sum_{i=0}^{\infty} b_i z^i \quad \varepsilon \, D[[z]]$$ (2.4)

be formal power series with coefficients from the ring D of p x p matrices over some field K. Throughout this paper it is assumed that the leading coefficient, b_0, of B(z) is an invertible matrix. For non-negative integers m and n, let

$$U(z) = \sum_{i=0}^{m} u_i z^i \quad , \quad V(z) = \sum_{i=0}^{n} v_i z^i \quad \varepsilon \, D[z]$$ (2.5)

denote p x p matrix polynomials.

Definition 2.1: The triple (U (z),V (z),W(z)) is defined to be a **Right Matrix Padé Form** (RMPFo) of type (m,n) for the pair (A(z),B(z)) if

I. $\partial(U(z)) \leq m$, $\partial(V(z)) \leq n$,

II. $A(z) \cdot V(z) + B(z) \cdot U(z) = z^{m+n+1} W(z)$ *with* $W(z) \in D[[z]]$ and . $\qquad$ (2.6)

III. The columns of $V(z)$ are linearly independent over the field K.

The matrix polynomials U(z), V(z), and W(z) are usually called the right **numerator, denominator,** and **residual** (all of type (m,n)), respectively. Note that when B(z) = -I, Definition 2.1 corresponds to the definition of Padé form for a single matrix power series A(z) given in Labahn [32].

There is an equivalent definition for a left matrix Padé form (LMPFo). Condition II is replaced with an equivalent version with matrix multiplication by U(z) and V(z) being on the left. Condition III is replaced with the condition that the rows, rather than the columns, of the denominator are linearly independent over the base field K.

However, there is a one-to-one correspondence between RMPFo's and LMPFo's. By taking the transposes of the matrices on both sides of equation (2.6), it follows that

$$V^t(z) \cdot A^t(z) + U^t(z) \cdot B^t(z) = z^{m+n+1} W^t(z). \qquad (2.7)$$

The degree and order conditions are identical. It is clear that if (U(z),V(z),W(z)) is a RMPFo for (A(z), B(z)), then $(U^t(z), V^t(z), W^t(z))$ is a LMPFo for $(A^t(z), B^t(z))$. Thus, any algorithm that calculates a right matrix Padé form of a certain type can also be used to calculate the left matrix Padé form of the same type.

For ease of discussion, we use the following notation. For any matrix polynomial

$$U(z) = u_0 + u_1 z + \cdots + u_k z^k \in D[z], \qquad (2.8)$$

we write U (i.e., the same symbol but without the z variable) to mean the p(k+1) by p vector of matrix coefficients

$$U = \begin{bmatrix} u_0, u_1, \cdots, u_k \end{bmatrix}^t. \qquad (2.9)$$

Let

$$S_{m,n} = \begin{bmatrix} a_0 & & & & b_0 & & & \\ \cdot & \cdot & & & & & & \\ \cdot & & \ddots & & & & & b_0 \\ \cdot & & & a_0 & & & & \\ \cdot & & & & & & & \\ a_{m+n} & \cdots & a_m & & b_{m+n} & \cdots & & b_n \end{bmatrix} \tag{2.10}$$

denote a Sylvestor matrix for A(z) and B(z) of type (m,n). Then equation (2.6) can be written as

$$S_{m,n} \cdot \begin{bmatrix} V \\ U \end{bmatrix} = 0. \tag{2.11}$$

Theorem 2.2: (Existence of Matrix Padé Forms) For any pair of power series (A(z), B(z)) and any pair of nonzero integers (m,n), there exists a RMPFo of type (m,n).

Proof: Let X denote a vector of length p(m+n+2), and consider the homogeneous system of linear equations

$$S_{m,n} \cdot X = 0. \tag{2.12}$$

Because $S_{m,n}$ has p(m+n+1) rows, it follows that (2.12) has at least p linearly independent solutions. Let $\begin{bmatrix} V,U \end{bmatrix}^t$ denote p such solutions arranged by columns. Then $\begin{bmatrix} V,U \end{bmatrix}^t$ satisfies (2.11), and consequently U(z) and V(z) determined according to the convention (2.8) and (2.9) satisfy (2.6). Clearly, the pair (U(z),V(z)) also satisfies condition I in Definition 2.1. The linear independence of the columns of V(z) is equivalent to the linear independence of the columns of $\begin{bmatrix} V,U \end{bmatrix}^t$ because of the nonsingularity of b_0. Hence condition III of Definition 2.1 also holds.

From the proof of Theorem 2.2, it follows that if $S_{m,n}$ has maximal rank, then Padé forms are unique up to multiplication of U(z) and V(z) on the right by a nonsingular matrix. On the other hand, if the rank of

$S_{m,n}$ is less than maximal, then more than one independent Padé form exists.

Example 2.3: Let $B(z) = -I$ and

$$A(z) = \begin{bmatrix} 1 & 0 \\ 0 & 1 \end{bmatrix} + \begin{bmatrix} 1 & 0 \\ 0 & 1 \end{bmatrix} z^2 + \begin{bmatrix} 2 & 0 \\ 0 & 1 \end{bmatrix} z^4 + \begin{bmatrix} -1 & 0 \\ -1 & 0 \end{bmatrix} z^5 + \cdots .$$ (2.13)

With $m = 2$ and $n = 3$, a basis for the solution space of (2.9) is given by the two vectors

$$X_1 = \begin{bmatrix} 0, 1, 0, 0, 0, -1, 0, 0, 0, 1, 0, 0, 0, 0 \end{bmatrix}^t$$ (2.14)

and

$$X_2 = \begin{bmatrix} 0, 0, 0, 1, 0, 0, 0, -1, 0, 0, 0, 1, 0, 0 \end{bmatrix}^t .$$ (2.15)

Thus,

$$V = \begin{bmatrix} 0 & 1 & 0 & 0 & 0 & -1 & 0 & 0 \\ 0 & 0 & 0 & 1 & 0 & 0 & 0 & -1 \end{bmatrix}^t$$ (2.16)

and

$$U = \begin{bmatrix} 0 & 1 & 0 & 0 & 0 & 0 \\ 0 & 0 & 0 & 1 & 0 & 0 \end{bmatrix}^t$$ (2.17)

is a solution of (2.11), and the pair $(U(z), V(z))$, where

$$V(z) = \begin{bmatrix} 0 & 0 \\ 1-z^2 & z-z^3 \end{bmatrix} \quad \text{and} \quad U(z) = \begin{bmatrix} 0 & 0 \\ 1 & z \end{bmatrix}$$ (2.18)

defines a Padé form of type (2,3) for $(A(z), B(z))$.

In Example 2.3, note that that columns of $V(z)$ are linearly independent over the field K, but that they are linearly dependent over the ring of polynomials $K[z]$ (i.e., $V(z)$ is singular). Indeed, for this example, a RMPFo $(U(z), V(z), W(z))$ of type (2,3) for which $V(z)$ is nonsingular cannot be found. The problem occurs because, although the solution space has dimension 2 when considered as a vector space over the

field K, it has only dimension 1 when considered as a module over the ring $K[z]$.

We note that having an invertible denominator is highly desirable, since usually the purpose of Padé forms is to approximate the infinite power series

$$-(B(z))^{-1} \cdot A(z) \qquad (2.19)$$

by the finite rational form

$$U(z) \cdot (V(z))^{-1} , \qquad (2.20)$$

where the approximation is to be exact for the first m+n+1 terms. When the denominator is singular, we cannot form this rational expression and this limits the usefulness of Padé approximation. For example, a singular denominator gives no information about the poles since every point is a pole in this case.

2.3. Matrix Padé Fractions.

One case when the denominator of a RMPFo is invertible is given by

Definition 2.4. The triple (U(z),V(z),W(z)) is said to be a **Right Matrix Padé Fraction** (RMPFr) of type (m,n) for the pair (A(z),B(z)) if

I. (U(z),V(z), W(z)) is a RMPFo of type (m,n) for (A(z),B(z)), and

II. The constant term, V(0), of the denominator is an invertible matrix.

Condition II ensures that the denominator, V(z), is an invertible matrix polynomial.

As in the case of Padé forms, there is an equivalent definition for a left matrix Padé fraction (LMPFr). Also, there is a correspondence between right matrix Padé fractions for (A(z),B(z)) and left matrix Padé fractions for $(A(z)^t, B(z)^t)$. It is interesting to note that a power series may have a matrix

Padé fraction on one side but not on the other. In Example 2.3, the power series A(z) does not have a right matrix Padé fraction of type (2,3), but it does have a left matrix Padé fraction of type (2,3). When a power series does have both a right and a left matrix Padé fraction of the same type, then the two resulting rational forms are equal (c.f., Baker [2]).

The problem with Padé fractions is that, as mentioned in the previous section, they do not always exist. However, let

$$
T_{m,n} = \begin{bmatrix} a_0 & & & | & b_0 & & \\ \cdot & & \cdot & | & \cdot & & \\ \cdot & & & | & & b_0 \\ \cdot & & a_0 & | & \cdot & & \cdot \\ & & \cdot & | & & & \cdot \\ & & \cdot & | & & & \\ a_{m+n-1} & \cdot & \cdot & a_m & | & b_{m+n-1} & \cdot & \cdot & b_n \end{bmatrix}
$$

(2.21)

and define

$$
d_{m,n} = \begin{cases} 1, & m = 0, n = 0, \\ det\,(T_{m,n}), & otherwise. \end{cases}
$$

(2.22)

Then, a sufficient condition for the existence of a RMPFr is given by

Theorem 2.5. If $d_{m,n} \neq 0$, then every RMPFo of type (m,n) is an RMPFr of type (m,n). In addition, a RMPFr of type (m,n) is unique up to multiplication on the right by a nonsingular p x p matrix having coefficients from the field K.

Proof: Equation (2.11) may be written

$$
\begin{bmatrix}
0 & & & b_0 & & \\
a_0 & & & & & \\
\cdot & & a_0 & \cdot & & \\
\cdot & & & & b_0 & \\
\cdot & & & \cdot & & \\
a_{m+n-1} & \cdot & a_m & b_{m+n} & \cdot & b_n
\end{bmatrix}
\cdot
\begin{bmatrix}
v_1 \\
\\
v_n \\
u_0 \\
\\
\\
u_m
\end{bmatrix}
= -
\begin{bmatrix}
a_0 \\
\\
\cdot \\
\cdot \\
\cdot \\
\\
a_{m+n}
\end{bmatrix}
\cdot v_0 \cdot
\tag{2.23}
$$

The matrix on the left of (2.23) is nonsingular, since $d_{m,n} \neq 0$ and b_0 is nonsingular. Thus, all the solutions of (2.23) can be obtained by assigning v_0 arbitrarily and solving (2.23) for the remaining components (v_1, ... v_n, u_0, ... , u_m). If v_0 is chosen to be a singular matrix, then the solution obtained by solving (2.23) violates condition III in the definition of Padé form. Thus, in this case, all RMPFo's are RMPFr's.

To show uniqueness, suppose $(U(z),V(z),W(z))$ and $(U'(z),V'(z),W'(z))$ are two RMPFr's for $(A(z),B(z))$. Then, v_0 and v'_0 are both nonsingular matrices with coefficients from the field K. Thus, there exists a nonsingular matrix, M, with coefficients from K satisfying $v_0 = v'_0 \cdot M$. It follows that

$$
V(z) = V'(z) \cdot M \quad \text{and} \quad U(z) = U'(z) \cdot M , \tag{2.24}
$$

while from (2.6) and (2.24)

$$
z^{m+n+1} W(z) = z^{m+n+1} W'(z) \cdot M \tag{2.25}
$$

and so uniqueness holds.

A basic requirement for results in both chapter 3 and chapter 4 is

Theorem 2.6. Let A(z) and B(z) be given by (2.4). If m and n are positive integers such that $d_{m,n} \neq 0$, then RMPFo's (P(z),Q(z),R(z)) of type (m-1,n-1) for (A(z),B(z)) are unique up to multiplication of P(z), Q(z) and R(z) on the right by a nonsingular matrix from K. In addition, the leading term R(0) of the residual is a

nonsingular matrix:

Proof: $S_{(m-1),(n-1)}$ can be obtained from $T_{m,n}$ by deleting the last block row (i.e., the last p rows). Since $T_{m,n}$ is of maximal rank p(m+n), then $S_{(m-1),(n-1)}$ has rank p(m+n-1). Consequently, the dimension of the solution space to

$$S_{(m-1),(n-1)} \cdot X = 0 \tag{2.26}$$

is exactly p. Then, $[Q, P]^t$ is obtained by collecting by columns a basis for the solution space of (2.26). Clearly, if $[Q', P']^t$ and $[Q, P]^t$ are two such collections, then there exists a nonsingular matrix M from K such that

$$[Q, P]^t = [Q', P']^t \cdot M . \tag{2.27}$$

Thus, $P(z) = P'(z) \cdot M$ and $Q(z) = Q'(z) \cdot M$, and, from (2.6), $R(z) = R'(z) \cdot M$, proving uniqueness.

To prove the invertibility of R(0), let $r_0 = R(0)$ and suppose that r_0 is a singular p x p matrix. Then, there is a nonzero p x 1 vector X that satisfies

$$r_0 \cdot X = 0. \tag{2.28}$$

But, from (2.6) and (2.26), it follows that

$$T_{m,n} \cdot \begin{bmatrix} Q \\ P \end{bmatrix} = \begin{bmatrix} 0 \\ \cdot \\ 0 \\ r_0 \end{bmatrix} . \tag{2.29}$$

Thus,

$$T_{m,n} \cdot \begin{bmatrix} Q \\ P \end{bmatrix} \cdot X = 0 . \tag{2.30}$$

Since the coefficient matrix for the above system is invertible, we deduce that

$$\begin{bmatrix} Q \\ P \end{bmatrix} \cdot X = 0 . \tag{2.31}$$

But this contradicts the fact that the columns of $[Q, P]^t$ are made up of linearly independent vectors. This implies that r_0 is invertible.

The fact that Padé forms of type (m,n) and (m-1,n-1) are uniquely determined after suitable normalizations, when $T_{m,n}$ is nonsingular, allows us to prove such properties as argument invariance (c.f., Baker [2]) for the Padé forms computed by the algorithm MPADE given in chapter 3, and is central to our commutativity results of chapter 4.

Chapter 3

The MPADE Algorithm

3.1. Matrix Power Series Remainder Sequences

We define a **Right Matrix Padé Table** for $(A(z), B(z))$ to be any infinite two-dimensional collection of RMPFo's of type (m,n) for $(A(z),B(z))$ with m = 0, 1, ... and n = 0, 1, ... It is assumed that there is precisely one entry (i.e., one RMPFo) assigned to each position in the table. From Theorem 2.2, it follows that a right matrix Padé table exists for any given $(A(z), B(z))$. However, the table is not unique, because RMPFo's are not unique. This is unlike the definition of a Padé table for scalar power series (c.f. Gragg [26]), since here a Padé table consists of a collection of Padé fractions, which are unique.

A matrix power series pair $(A(z),B(z))$ is said to be **normal** (c.f., Bultheel [10]) if $d_{m,n} \neq 0$ for all m,n. For normal power series, it follows from Theorem 2.5 that every entry in the right matrix Padé table is a RMPFr. Consequently, from condition II in Definition 2.4 of RMPFr's, a right matrix Padé table for normal power series may be made unique by insisting that the constant term, V(0), in the denominator of any Padé fraction be the identity matrix.

Given the power series (2.4) and any non-negative integers m and n, we introduce a sequence of points

$$(m_0,n_0), \ (m_1,n_1), \ (m_2,n_2), \ \cdots \tag{3.1}$$

in the right matrix Padé table satisfying

$$(m_0,n_0) = \begin{cases} (m-n-1,-1) & , \ m \geq n , \\ (-1,n-m-1) & , \ m < n , \end{cases} \tag{3.2}$$

and

$$(m_{i+1},n_{i+1}) = (m_i + s_i \ ,n_i + s_i \ ), \ i = 0, 1, 2, \cdots , \tag{3.3}$$

where $1 \leq s_i \leq \infty$. Observe that

$$m_i \qquad = m - n \ , \ i = 0, 1, 2, \cdots , \tag{3.4}$$

and consequently the sequence (3.1) lies along the m-n off-diagonal path of the right matrix Padé table. In (3.3), the s_i are selected so that

$$d_{m_i,n_i} \neq 0 \tag{3.5}$$

and

$$d_{(m_i+j),(n_i+j)} = 0 \ , \tag{3.6}$$

for $j = 1, 2, \cdots , s_i - 1$.

For i = 1, 2, ..., let $(U_i(z), V_i(z), W_i(z))$ be the unique RMPFr (c.f., Theorem 2.5) of type (m_i, n_i) for $(A(z), B(z))$. Then $\begin{bmatrix} V_i \ , \ U_i \end{bmatrix}'$ satisfies

$$S_{m_i,n_i} \cdot \begin{bmatrix} V_i \\ U_i \end{bmatrix} = 0. \tag{3.7}$$

and

$$A(z) \cdot V_i(z) + B(z) \cdot U_i(z) = z^{m_i+n_i+1} W_i(z). \tag{3.8}$$

Generalizing the notions of Cabay and Kossowski [17] , we introduce

Definition 3.1. The sequence

$$\left\{ W_i(z) \right\}, i = 1, 2, \cdots , \tag{3.9}$$

is called the **Power Series Remainder Sequence** for the pair (A(z),B(z)). The sequence of pairs

$$\left\{ (U_i(z), V_i(z)) \right\}, i = 1, 2, \cdots , \tag{3.10}$$

is called the corresponding cofactor sequence. The integer pairs $\{(m_i, n_i)\}$ are called **nonsingular nodes** along the m - n off-diagonal path of the Padé table for (A(z),B(z)).

We note that each term of a power series remainder sequence is unique up to multiplication on the right by a nonsingular matrix. This is also true for each term of the corresponding cofactor sequence.

Initially, when $m \geq n$, observe that $m_1 = m - n$ and $n_1 = 0$ (i.e., $s_0 = 1$), because in (2.22) the non-singularity of b_0 implies that $d_{(m-n),0} \neq 0$. Thus, $V_1(z)$ is some arbitrary nonsingular matrix from K and, using (3.6), $U_1(z)$ can be obtained by solving

$$
\begin{bmatrix} b_0 \\ \cdot & \cdot \\ \cdot & & \cdot \\ b_{m_1} & \cdots & b_0 \end{bmatrix} U_1 = - \begin{bmatrix} a_0 \\ \cdot \\ \cdot \\ a_{m_1} \end{bmatrix} V_1 .
\tag{3.11}
$$

That is, $U_1(z)$ can be obtained by multiplying the first $m_1 + 1$ terms of the quotient power series $B^{-1}(z) \cdot A(z)$ on the right by $-V_1(z)$.

Initially, when $m < n$, depending on a_0 there are two cases to consider. The simple case, when $det(a_0) \neq 0$, yields

$$
d_{0,(n-m)} = \det \begin{bmatrix} a_0 \\ \cdot & & \cdot \\ \cdot & & & \cdot \\ a_{n-m-1} & \cdots & a_0 \end{bmatrix} \neq 0 .
\tag{3.12}
$$

Thus, $s_0 = 1$, $m_1 = 0$, and $n_1 = n - m$. Then, the RMPFr $(U_1(z), V_1(z), W_1(z))$ of type (m_1, n_1) is determined by setting $U_1(z)$ to be an arbitrary nonsingular matrix from K and then solving

$$
\begin{bmatrix} a_0 \\ \cdot & \cdot \\ \cdot & & \cdot \\ a_{n_1} & \cdots & a_0 \end{bmatrix} V_1 = - \begin{bmatrix} b_0 \\ \cdot \\ \cdot \\ b_{n_1} \end{bmatrix} U_1 .
\tag{3.13}
$$

That is, when $m < n$ and $det(a_0) \neq 0$, $V_1(z)$ can be obtained by multiplying the first n_1+1 terms of the quotient power series $A^{-1}(z) \cdot B(z)$ on the right by $-U_1(z)$.

When $m < n$ and $det(a_0) = 0$, we must first determine the smallest positive integer s_0 (i.e., the smallest $m_1 = m_0 + s_0$ and $n_1 = n_0 + s_0$) so that $d_{m_1,n_1} \neq 0$. Then, $(U_1(z), V_1(z))$ is obtained by solving

$$S_{m_1,n_1} \cdot \begin{bmatrix} V_1 \\ U_1 \end{bmatrix} = 0 . \tag{3.14}$$

In the next section, we give an algorithm which computes a RMPFo of type (m,n) for $(A(z),B(z))$ by performing a sequence of the above types of initializations (albeit, each for different power series).

When the power series pair $(A(z),B(z))$ is normal, only the initializations corresponding to (3.11) and (3.13) are required. Thus, for normal power series $s_i = 1$ for all i, and the algorithm reduces to a sequence of truncated power series divisions.

There are also some non-normal power series that share this property. For each pair of integers m and n, let $r_{m,n}$ be the rank of the matrix $T_{m,n}$. Then normality is equivalent to

$$r_{m,n} = (m+n) \cdot p \tag{3.15}$$

for all m and n. A matrix power series pair $(A(z), B(z))$ is said to be **nearly-normal** (c.f., Labahn [32]) if, for all integers m and n,

$$r_{m,n} = k_{m,n} \cdot p \tag{3.16}$$

for some integer $k_{m,n}$. Clearly, every normal power series is also a nearly-normal power series. In addition, all scalar power series are nearly-normal.

For a nearly-normal power series pair $(A(z),B(z))$ it is easy to see that when a_0 is singular, then $a_0 = 0$. This follows from the observation that the rank of a_0 is just $r_{0,1}$, which, if it is not p, must be zero. Also, if $a_0 = \cdots = a_{k-1} = 0$ and $a_k \neq 0$, then a_k must be a nonsingular matrix for similar reasons. When $k > m$ this implies that there are no nonsingular nodes along the m - n off-diagonal path before and includ-

ing the node (m,n). Otherwise, when $k \le m$, the initialization (3.14) becomes

$$\begin{bmatrix} 0 & & & | & b_0 & & \\ & & & | & & & \\ a_{m_1} & & & | & & & \\ \cdot & & & | & \cdot & & b_0 \\ \cdot & & & | & \cdot & & \\ a_{m_1+n_1} & \cdots & a_{m_1} & | & b_{m_1+n_1} & \cdots & b_{n_1} \end{bmatrix} \cdot \begin{bmatrix} V_1 \\ \\ U_1 \end{bmatrix} = 0, \tag{3.17}$$

where $s_0 = k+1$, $m_1 = k$ and $n_1 = n-m+k$. Consequently the RMPFr $(U_1(z), V_1(z), W_1(z))$ of type (m_1, n_1) is obtained from (3.17) first by setting $U_1(z) = z^{m_1} \cdot U$, where U is any nonsingular matrix from K. Then, $V_1(z)$ is obtained by multiplying the first n_1+1 terms of the quotient power series $(z^{-m_1} \cdot A(z))^{-1} \cdot B(z)$ on the right by $-U$. Thus, also for nearly-normal power series (and therefore also for all scalar power series), all initializations reduce to truncated power series divisions.

Corresponding to the Power Series Remainder Sequence, we introduce

Definition 3.2. The sequence

$$\left\{ (P_i(z), Q_i(z)) \right\}, \; i = 1, 2, \cdots , \tag{3.18}$$

where $(P_i(z), Q_i(z), R_i(z))$ is a Padé form of type (m_i-1, n_i-1) for $(A(z), B(z))$, is called a **predecessor sequence** of the power series remainder sequence.

The triple $(P_i(z), Q_i(z), R_i(z))$ satisfies the equation

$$A(z) \cdot Q_i(z) + B(z) \cdot P_i(z) = z^{m_i + n_i - 1} \cdot R_i(z) \tag{3.19}$$

by (2.6). Initially, when $s_0 = 1$, the predecessor pair $(P_1(z), Q_1(z))$ is defined to be

$$P_1(z) = z^{m-n-1} I_p \; , \; \text{and} \; Q_1(z) = 0 \tag{3.20}$$

if $m \ge n$, and

$$P_1(z) = 0 \ , \ Q_1(z) = z^{n-m-1} I_p \qquad (3.21)$$

if $m < n$. Both (3.20) and (3.21) satisfy (3.19), and therefore condition II for RMPFo's, but not necessarily conditions I and III.

Theorem 3.3: For $i = 1, 2, \ldots$, the predecessors $(P_i(z), Q_i(z))$ are unique up to right multiplication by a nonsingular matrix from K. In addition, the leading term of the residual, $R_i(0)$, is nonsingular.

Proof: The results are an immediate consequence of (3.20), (3.21) and Theorem 2.6.

The main result of this section is

Theorem 3.4. For any positive integer k, (k - 1, k) is a nonsingular node in the Padé table for $(W_i(z), R_i(z))$ if and only if $(m_i + k, n_i + k)$ is a nonsingular node in the Padé table for $(A(z), B(z))$.

Proof: Let M_{11}, M_{21}, M_{12}, and M_{22} be matrices of dimension $p(n_i + k) \times pk$, $p(m_i + k) \times pk$, $p(n_i + k) \times p(k-1)$, and $p(m_i + k) \times p(k-1)$, respectively, defined by

$$M_{11} = \begin{bmatrix} v_0 & & & \\ & \cdot & & \\ v_{n_i} & & \cdot & \\ & \cdot & & v_0 \\ & & \cdot & \\ & & & v_{n_i} \end{bmatrix} \ , \ M_{12} = \begin{bmatrix} 0 & & \\ 0 & & \\ q_0 & & \\ & \cdot & \\ q_{n_i-1} & \cdot & q_0 \\ & \cdot & \\ & & q_{n_i-1} \end{bmatrix} \ , \qquad (3.22)$$

$$M_{21} = \begin{bmatrix} u_0 & & & \\ & \cdot & & \\ u_{m_i} & & \cdot & \\ & \cdot & & u_0 \\ & \cdot & & \\ & & & u_{m_i} \end{bmatrix} \ , \ M_{22} = \begin{bmatrix} 0 & & \\ 0 & & \\ p_0 & \cdot & \\ & \cdot & \\ p_{m_i-1} & \cdot & p_0 \\ & \cdot & \\ & & p_{m_i-1} \end{bmatrix} \qquad (3.23)$$

Also, let M be

$$M = \begin{bmatrix} M_{11} & M_{12} \\ M_{21} & M_{22} \end{bmatrix}. \tag{3.24}$$

If we set

$$R_i(z) = \sum_{j=0}^{\infty} r_j z^j , \quad \text{with} \quad \det(r_0) \neq 0, \quad \text{and} \quad W_i(z) = \sum_{j=0}^{\infty} w_j z^j , \tag{3.25}$$

then, from (3.8) and (3.19), it follows that

$$T_{(m_i+k),(n_i+k)} \cdot M = \begin{bmatrix} 0 & \cdots & 0 & | & 0 & \cdots & 0 \\ & & & | & & & \\ & & & | & & & \\ 0 & \cdots & 0 & | & 0 & \cdots & 0 \\ w_0 & & & | & r_0 & & \\ \cdot & & & | & \cdot & & \\ \cdot & & w_0 & | & \cdot & & r_0 \\ \cdot & & & | & \cdot & & \cdot \\ w_{2k-2} & \cdots & w_{k-1} & | & r_{2k-2} & \cdots & r_k \end{bmatrix}$$

$$= \begin{bmatrix} 0 \\ T'_{(k-1),k} \end{bmatrix}, \tag{3.26}$$

where 0 represents a zero matrix of size $p(m_i+n_i+1) \times p(2k-1)$ and

$$T'_{(k-1),k} = \begin{bmatrix} w_0 & & & | & r_0 & & \\ \cdot & & & | & & \cdot & \\ \cdot & & w_0 & | & & & r_0 \\ & & & | & & & \\ w_{2k-2} & \cdots & w_{k-1} & | & r_{2k-2} & \cdots & r_k \end{bmatrix}. \tag{3.27}$$

We are now in a position to prove the theorem. Assume $T_{(m_i+k),(n_i+k)}$ is nonsingular. We show that $T'_{(k-1),k}$ is then also nonsingular. Let

$$X = \left[X_1, \cdots, X_{2k-1} \right]'$$

(3.28)

be a p(2k-1) x 1 vector that satisfies

$$T'_{(k-1),k} \cdot X = 0 ;$$

(3.29)

Since $T_{(m_i+k),(n_i+k)}$ is nonsingular, (3.26) implies

$$M \cdot X = 0,$$

(3.30)

From (3.30), we then obtain that

$$v_0 \cdot X_1 = 0,$$

(3.31)

and consequently $X_1 = 0$, because v_0 is nonsingular. The first block equation from (3.29) then implies

$$r_0 \cdot X_{k+1} = 0.$$

(3.32)

Thus, $X_{k+1} = 0$ because r_0 is nonsingular. In a similar fashion, it follows that $X_2 = 0$ and $X_{k+2} = 0$. Continuing in this way, we obtain that X = 0, that is, $T'_{(k-1),k}$ is nonsingular.

Conversely, suppose that $T'_{(k-1),k}$ is nonsingular. Let $X = (X_1, \cdots, X_{2k-1})$ be a 1 x p(2k-1) vector, $Y = (Y_1, \cdots, Y_{m_i+n_i})$ a 1 x p(m_i+n_i) vector and Z a 1 x p vector. Consider

$$(Z, Y, X) \cdot T_{(m_i+k),(n_i+k)} = 0.$$

(3.33)

Multiplying both sides of (3.33) on the right by M, and using equation (3.26), it follows that

$$X \cdot T'_{(k-1),k} = 0.$$

(3.34)

Since $T'_{(k-1),k}$ is nonsingular, then X = 0. Then, in (3.33), using block columns 2 through n_i+1 and block columns n_i+k+2 through to m_i+n_i+k+1 of $T_{(m_i+k),(n_i+k)}$, we obtain

$$Y \cdot T_{m_i,n_i} = 0.$$

(3.35)

Since T_{m_i,n_i} is nonsingular, Y = 0. Finally, block column n_i+k+1 of $T_{(m_i+k),(n_i+k)}$ now yields

$$Z \cdot b_0 = 0.$$

(3.36)

Since b_0 is nonsingular, $Z = 0$. Hence, $T_{(m+k),(n+k)}$ is nonsingular.

Theorem 3.4 allows us to calculate nonsingular nodes of a pair of power series by calculating non-singular nodes of the residual pair of power series. This gives us an iterative method of calculating non-singular nodes.

Theorem 3.5: The cofactor and predecessor sequences for $(A(z),B(z))$ satisfies

$$\begin{bmatrix} U_{i+1}(z) & P_{i+1}(z) \\ V_{i+1}(z) & Q_{i+1}(z) \end{bmatrix} = \begin{bmatrix} U_i(z) & P_i(z) \\ V_i(z) & Q_i(z) \end{bmatrix} \cdot \begin{bmatrix} I & 0 \\ 0 & z^2 I \end{bmatrix} \cdot \begin{bmatrix} V'(z) & Q'(z) \\ U'(z) & P'(z) \end{bmatrix} \tag{3.37}$$

where $(U'(z),V'(z))$ are the numerator and denominator of the RMPFr of type (s_i-1, s_i) for $(W_i(z),R_i(z))$, and where $(P'(z),Q'(z))$ is its predecessor.

Proof: From Theorem 3.4, (s_i-1, s_i) is the first nonsingular node for $(W_i(z),R_i(z))$. Thus, $(U'(z),V'(z))$ satisfies

$$W_i(z) \cdot V'(z) + R_i(z) \cdot U'(z) = z^{2s_i} W'(z), \tag{3.38}$$

where $V'(0)$ is nonsingular and $W'(z)$ is some matrix power series which we show later is exactly $W_{i+1}(z)$. Then, using (3.8), (3.19), (3.37) and (3.38) we get

$$A(z) \cdot V_{i+1}(z) + B(z) \cdot U_{i+1}(z)$$

$$= A(z) \cdot \left\{ V_i(z) \cdot V'(z) + z^2 Q_i(z) \cdot U'(z) \right\} + B(z) \cdot \left\{ U_i(z) \cdot V'(z) + z^2 P_i(z) \cdot U'(z) \right\}$$

$$= \left\{ A(z) \cdot V_i(z) + B(z) \cdot U_i(z) \right\} \cdot V'(z) + \left\{ A(z) \cdot Q_i(z) + B(z) \cdot P_i(z) \right\} \cdot z^2 \cdot U'(z)$$

$$= z^{m+n+1} \cdot \left\{ W_i(z) \cdot V'(z) + R_i(z) \cdot U'(z) \right\}$$

$$= z^{(m_i+n_i)+(n_i+s_i)+1} \cdot W'(z).$$

(3.39)

Thus, $W'(z) = W_{i+1}(z)$ and condition II for a RMPFo is satisfied.

To verify condition I, expanding (3.37) gives

$$U_{i+1}(z) = U_i(z) \cdot V'(z) + z^2 P_i(z) \cdot U'(z),$$

(3.40)

so that

$$\partial(U_{i+1}(z)) \le max(\, m_i + s_i \,,\, 2 + (\, m_i - 1\,) + s_i - 1\,)$$
$$= m_i + s_i.$$

(3.41)

Similarly,

$$\partial(V_{i+1}(z)) \le n_i + s_i.$$

(3.42)

Finally, to verify condition II for RMPFr, observe that

$$V_{i+1}(0) = V_i(0) \cdot V'(0),$$

(3.43)

and, consequently, $V_{i+1}(0)$ is invertible since both $V_i(0)$ and $V'(0)$ are invertible.

Thus, $(U_{i+1}(z), V_{i+1}(z), W'(z))$ is a RMPFr of type (m_i+s_i, n_i+s_i) for $(A(z), B(z))$.

A similar argument shows that $(P_{i+1}(z), Q_{i+1}(z), R'(z))$ is the RMPFo of type $(m_{i+1}-1, n_{i+1}-1)$ and hence we have our predecessor.

3.2. The Algorithm

Given non-negative integers m and n, the algorithm MPADE below makes use of Theorem 3.5 to compute the cofactor and predecessor sequences (3.10) and (3.18), respectively. Thus, intermediate results available from MPADE include those RMPFr's $(U_i(z), V_i(z), W_i(z))$ for $(A(z), B(z))$ at all the nonsingular nodes (m_i, n_i), i=1,2, ... , k-1, smaller than (m,n), along the off-diagonal path $m_i - n_i = m-n$. The output

gives results associated with the final node (m_k, n_k). If (m,n) is also a nonsingular node, then the output $(U_k(z), V_k(z), W_k(z))$ is a RMPFr of type (m,n) for $(A(z), B(z))$, and $(P_k(z), Q_k(z), R_k(z))$ is a RMPFo of type $(m-1, n-1)$. If (m,n) is a singular node, then the output $(U_k(z), V_k(z), W_k(z))$ is simply a RMPFo of type (m,n) for $(A(z), B(z))$, and now $(P_k(z), Q_k(z), R_k(z))$ is set to be the RMPFr of type (m_{k-1}, n_{k-1}).

Note that, when (m,n) is not a nonsingular node, a simple modification of MPADE allows the computation of all RMPFo's of type (m,n) for $(A(z), B(z))$. It is only necessary to arrange to compute q columns of $[V'_k, U'_k]$, rather than p, in order to form a basis for the solution space of the equation in step 3.1 of MPADE. Here q (with $q \geq p$) is the number of linearly independent solutions of the system (2.11). From this basis, it is then possible to construct a p x p matrix $V(z)$, and a corresponding $U(z)$ and $W(z)$, for which $(U(z), V(z), W(z))$ is a RMPFo of type (m,n) for $(A(z), B(z))$ and has the property that $V(z)$ is an invertible matrix, assuming such a RMPFo exists. This enhancement is not included in MPADE primarily to simplify the presentation of the algorithm.

ALGORITHM (MPADE):

INPUT: A(z), B(z), m, n, and p, where

1) m and n are nonnegative integers, p is a positive integer,

.2) A(z) and B(z) are p x p matrix power series with $det(B(0)) \neq 0$. Note that

A(z) mod z^{m+n+1} and B(z) mod z^{m+n+1}, only, are required.

OUTPUT: Matrix polynomials $P_k(z)$, $Q_k(z)$, $U_k(z)$, $V_k(z)$, matrix power series $R_k(z)$, $W_k(z)$ and a boolean SUCCESS defined as follows:

1) If SUCCESS is true, then $(U_k(z), V_k(z), W_k(z))$ is a RMPFr of type (m,n) for $(A(z), B(z))$ and $(P_k(z), Q_k(z), R_k(z))$ is its predecessor;

2) If SUCCESS is false, then $(U_k(z), V_k(z), W_k(z))$ is a RMPFo of type (m,n) and $(P_k(z), Q_k(z), R_k(z))$ is a RMPFr at the largest nonsingular node along the m-n off-diagonal path.

Step 1: # Initialization #

If $m \geq n$

then set

1.1) $i \leftarrow 1$

1.2) $s_0 \leftarrow m - n$

1.3) $\begin{bmatrix} m_1 \\ n_1 \end{bmatrix} = \begin{bmatrix} s_0 \\ 0 \end{bmatrix}$

1.4) $\begin{bmatrix} U_1(z) & P_1(z) \\ V_1(z) & Q_1(z) \end{bmatrix} = \begin{bmatrix} -B(z)^{-1} \cdot A(z) \bmod z^{s_0+1} & z^{s_0-1} \cdot I \\ I & 0 \end{bmatrix}$

else set

1.5) $i \leftarrow 0$

1.6) $\begin{bmatrix} m_0 \\ n_0 \end{bmatrix} = \begin{bmatrix} m-n \\ 0 \end{bmatrix}$

1.7) $\begin{bmatrix} U_0(z) & P_0(z) \\ V_0(z) & Q_0(z) \end{bmatrix} = \begin{bmatrix} 0 & z^{m-n-1} \cdot I \\ I & 0 \end{bmatrix}$

Step 2: # Search for next nonsingular node #

2.1) $s_i \leftarrow 0$

2.2) $d \leftarrow 0$

2.3)   Do while $n_i + s_i < n$ and $d = 0$

2.4)   Set $s_i \leftarrow s_i + 1$

2.5)   Compute the residual $W_i(z)$ such that

$$(A(z) \cdot V_i(z) + B(z) \cdot U_i(z)) \bmod z^{m_i+n_i+2s_i+1} = z^{m_i+n_i+1} \cdot W_i(z)$$

2.6)   Compute the residual $R_i(z)$ such that

$$(A(z) \cdot Q_i(z) + B(z) \cdot P_i(z)) \bmod z^{m_i + n_i + 2s_i - 1} = z^{m_i + n_i - 1} \cdot R_i(z)$$

2.7)   Compute

$$d = det(T'_{(s_i - 1), s_i}).$$

determined from the power series $W_i(z)$ and $R_i(z)$ (c.f., (3.27)).

2.8)   End do

Step 3: # Compute RMPFr for residuals #

3.1)   Solve

$$S'_{(s_i - 1), s_i} \cdot \begin{bmatrix} V' \\ U' \end{bmatrix} = 0,$$

where S' is the Sylvester matrix determined from $W_i(z)$ and $R_i(z)$

Step 4: # Compute predecessor for residuals #

4.1)   If $s_i > 1$ and $d \neq 0$,

then solve

$$S'_{(s_i - 2), (s_i - 1)} \cdot \begin{bmatrix} Q' \\ P' \end{bmatrix} = 0,$$

where again S' is the Sylvester matrix determined from $W_i(z)$ and $R_i(z)$

else set

4.2) $\begin{bmatrix} Q'(z) \\ P'(z) \end{bmatrix} = \begin{bmatrix} I \\ 0 \end{bmatrix}$

Step 5: # Advance along off-diagonal for Padé fractions #

5.1) $m_{i+1} \leftarrow m_i + s_i$

5.2) $n_{i+1} \leftarrow n_i + s_i$

5.3) $\begin{bmatrix} U_{i+1}(z) & P_{i+1}(z) \\ V_{i+1}(z) & Q_{i+1}(z) \end{bmatrix} \leftarrow \begin{bmatrix} U_i(z) & P_i(z) \\ V_i(z) & Q_i(z) \end{bmatrix} \cdot \begin{bmatrix} I & 0 \\ 0 & z^2 \cdot I \end{bmatrix} \cdot \begin{bmatrix} V'(z) & Q'(z) \\ U'(z) & P'(z) \end{bmatrix}$

5.4) $i \leftarrow i + 1$

Step 6: # termination test #

If $n_i < n$

then go to step 2

Else

    If $d \neq 0$

    then SUCCESS $\leftarrow$ true,

    else SUCCESS $\leftarrow$ false;

    Exit.

    Theorem 3.6: The MPADE algorithm is valid.

Proof: The argument is by induction on i.

When $m \geq n$, the initial step, i=1, to compute $(U_1(z), V_1(z))$ and $(P_1(z), Q_1(z))$ in step 1 is clearly valid. When $m < n$, the initialization in step 1 uses negative powers of z (invoked in order to simpli.
algorithm presentation) and, consequently, $(U_0(z), V_0(z))$ and $(P_0(z), Q_0(z))$ d not satisfy the requirements of a RMPFo in a strict sense. However, it is a simple, but tedious, matter to show that one pass through MPADE yields $(U_1(z), V_1(z))$ and $(P_1(z), Q_1(z))$ which meet all the requirements for the first term in the cofactor and predecessor sequences (3.10) and (3.18), respectively (see the Appendix for details).

The inductive step along the nonsingular nodes of the off-diagon. path $m_i - n_i = m - n$ follows directly from Theorem 3.5 (compare (3.37) with step 5.3 of MPADE). Thus, when $(m, n) = (m_k, n_k)$ is a nonsingular node, the proof is complete. On the other hand, when $(m, n) = (m_k, n_k)$ is not a nonsingular node, arguments similar to those of Theorem 3.5 can be used to show that $(U'(z), V'(z), W'(z))$ is a RMPFo of type $(s_{k-1} - 1, s_{k-1})$ for $(W_{k-1}(z), R_{k-1}(z))$ if and only if $(U_k(z), V_k(z), W_k(z))$ determined according to (3.37) is a

RMPFo of type (m_k, n_k) for $(A(z), B(z))$.

Remark 1. In the scalar case the MPADE algorithm reduces to the $O(n^2)$ off-diagonal algorithm of Cabay and Choi [16] . By reversing coefficients and with $B(z)=-I$, the anti-diagonal algorithm of McEliece and Shearer [35] is obtained.

Remark 2. For normal matrix power series, intermediate results are identical to those of Rissanen [41] . The algorithm of Rissanen does generalize to non-normal power series, but only in the scalar case (c.f., Rissanen [39]). It is not clear how to express this in the matrix case because of the problem of matrix singularity.

3.3. Complexity of the MPADE Algorithm

In assessing the costs of MPADE, it is assumed that classical algorithms are used for the multiplication of polynomials. Only the more costly steps are considered. For these steps, Table 5.1 below provides crude upper bounds on the number of multiplications in K performed during the i-th pass through MPADE.

Step	Bound on Number of Multiplications
2.5	$2p^3(m_i+n_i+2)(s_i+1)$
2.6	$2p^3(m_i+n_i+2)(s_i+1)$
2.7	$4p^3(s_i-1)^3$
3.1	$6p^3s_i^2$
4.1	$6p^3s_i^2$
5.3	$4p^3(m_i+n_i+2)(s_i+1)$

Table 3.6
Bounds on Operations per Step

In step 2.7 of MPADE, it is assumed that the Gaussian elimination method is used to obtain the LU decomposition of $T_{(n-1),n}$. In addition, it is assumed that Gaussian elimination is accompanied with border-

ing techniques. Thus, as s_i increases by 1 in step 2.4, the results of the previous pass through the **while** loop are used to achieve the current LU decomposition. The bound for step 2.7 in Table 3.6 assumes we do not take any advantage of the special nature of $T_{(s_i-1),s_i}$.

For step 3.1, it is assumed that the LU decomposition of $T_{(s_i-1),s_i}$ from step 2.7, is used to simplify the triangularization of $S_{(s_i-1),s_i}$. The solution $[V', U']$ is obtained finally by solving this triangularized $S_{(s_i-1),s_i}$. Similar observations apply to step 4.1.

An upper bound for the number of multiplications in K required by MPADE is obtained by summing the costs in Table 3.6 for i=0,1, ... ,k. We use the fact that

$$\sum_{i=0}^{k} s_i = m \text{ , if } m \ge n \text{ , and } \sum_{i=0}^{k} s_i = n \text{ , if } m < n \text{ .} \tag{3.44}$$

In addition,

$$\sum_{i=0}^{k} m_i{}^{\alpha} s_i{}^{\beta} \le m^{\alpha+\beta} \text{ and } \sum_{i=0}^{k} n_i{}^{\alpha} s_i{}^{\beta} \le n^{\alpha+\beta} \text{ .} \tag{3.45}$$

Then, step 2.7 has a complexity of $O(p^3(m+n)^3)$ and the remaining steps a complexity of $O(p^3(m+n)^2)$, at worst.

Theorem 3.7 When the quotient power series $B(z)^{-1}A(z)$ is nearly-normal, the MPADE algorithm calculates a RMPFr of type (m,n) with a complexity of $O(p^3(m+n)^2)$.

Proof: When $(A(z),B(z))$ is nearly-normal s_i is often larger than one, but the matrix $T_{(s_i-1),s_i}$ is always in triangular form (c.f., Labahn [32]). Thus the cost of step 2.7 of MPADE is zero. Using table 3.6 along with (3.44) and (3.45) gives the result.

Corollary 3.8 When the quotient matrix power series $B(z)^{-1}A(z)$ is normal, the MPADE algorithm calculates a RMPFr of type (m,n) with complexity $O(p^3(m+n)^2)$.

Proof: Corollary 3.8 follows from Theorem 3.7 since all normal matrix power series are nearly-normal.

Corollary 3.9 For scalar quotient power series $B(z)^{-1}A(z)$, the MPADE algorithm calculates a RMPFr of type (m,n) with a complexity of $O((m+n)^2)$.

Proof: Corollary 3.9 follows from Theorem 3.7 since all scalar power series are nearly-normal.

When the matrix power series is not nearly-normal or normal the complexity of MPADE depends on the distribution of the nonsingular nodes along the particular off-diagonal. However, even one nonsingular node can reduce the cost substantially. For example, if the midpoint (n/2,n/2) is the only nonsingular node along the main diagonal then MPADE requires $1/3(n/2)^3 + 1/3(n/2)^3 = 1/12n^3$ operations, versus $1/3n^3$ operations needed for Gaussian elimination, a cost saving of a factor of 4. Algorithms that require normality, on the other hand, break down when even one node is singular.

Chapter 4

Inverse Formulae of Block Hankel Matrices

4.1. Introduction

Let

$$H_{m,n} = \begin{bmatrix} a_{m-n+1} & \cdots & a_m \\ \cdot & & \cdot \\ \cdot & & \cdot \\ \cdot & & \cdot \\ a_m & \cdots & a_{m+n-1} \end{bmatrix} \tag{4.1}$$

be a nonsingular block Hankel matrix with coefficients from the ring of p x p matrices over a field (with $a_i = 0$ for negative i). [1] The primary contribution of this chapter is a set of new closed formulae for $H_{m,n}^{-1}$. We require only that $H_{m,n}$ be nonsingular. When p=1, one of the formulae agrees with that obtained by Choi [18].

The representations for $H_{m,n}^{-1}$ depend on the concept of a matrix Padé form developed in chapter 2 for the matrix polynomial

$$A(z) = \sum_{i=0}^{m+n} a_i z^i. \tag{4.2}$$

Central to our approach are commutativity relationships which are shown to exist between certain matrix Padé forms. These commutativity relationships allow us to overcome the limitations imposed when using bordering techniques (which require additional nonsingularity conditions) that are the traditional methods for obtaining closed inverse formulae. Indeed, the conditions that we impose are both necessary and sufficient for the existence of an inverse.

A major advantage of a closed inverse formula is that it allows for efficient algorithms to calculate the inverses of Hankel matrices. This efficiency comes both in the cost complexity of calculating the

---

[1] All results hold, with minor modifications, for block Toeplitz matrices.

inverse and also in the amount of storage required for the final result.

When discussing Padé forms in the context of Hankel matrices, we use a minor change of notation from the previous chapters. A subscript on the numerator and denominator of a matrix Padé will now signify the type (i.e., maximal allowed degree) of the Padé form. This is done for purposes of simplification and clarification of our presentation.

4.2. Nonsingular Block Hankel Matrices and Matrix Padé Forms

For any block Hankel matrix (4.1), there is an associated matrix polynomial A(z) given by (4.2). The nonsingularity of a block Hankel matrix, is closely related to the existence of certain matrix Padé forms for the pair (A(z),-I). Notice that, for this special case, Condition II of Definition 2.1 becomes

$$
\begin{bmatrix} & & a_0 \\ & \cdot & \cdot \\ & \cdot & \cdot \\ a_{m-n} & \cdots & a_m \end{bmatrix} \begin{bmatrix} v_n \\ \cdot \\ \cdot \\ v_0 \end{bmatrix} = \begin{bmatrix} u_0 \\ \cdot \\ \cdot \\ u_m \end{bmatrix} \tag{4.3}
$$

and

$$
\begin{bmatrix} a_{m-n+1} & \cdots & a_{m+1} \\ \cdot & & \cdot \\ \cdot & & \cdot \\ a_m & \cdots & a_{m+n} \end{bmatrix} \begin{bmatrix} v_n \\ \cdot \\ \cdot \\ v_0 \end{bmatrix} = \begin{bmatrix} 0 \\ \cdot \\ \cdot \\ 0 \end{bmatrix}. \tag{4.4}
$$

The matrix polynomial $V_n(z)$ can be determined by solving (4.4), that is solving a system of equations with the block Hankel matrix (4.1) as the coefficient matrix. Once $V_n(z)$ has been obtained, then $U_m(z)$ can be obtained from (4.3).

For purposes of presentation, we use the following convention. For a given pair of positive integers (m,n), let the triples $(U_m(z),V_n(z),W(z))$ and $(U_m^*(z),V_n^*(z),W^*(z))$ denote a RMPFo and a LMPFo, respectively, of type (m,n) for A(z). For the same (m,n), a RMPFo and a LMPFo of type (m-1,n-1) for A(z) will be represented, respectively, by $(P_{m-1}(z),Q_{n-1}(z),R(z))$ and $(P_{m-1}^*(z),Q_{n-1}^*(z),R^*(z))$. For these

Padé forms, collectively, condition II of Definition 2.1 becomes

$$A(z)V_n(z) - U_m(z) = z^{m+n+1} \cdot W(z), \tag{4.5}$$

$$V_n^*(z)A(z) - U_m^*(z) = z^{m+n+1} \cdot W^*(z), \tag{4.6}$$

$$A(z)Q_{n-1}(z) - P_{m-1}(z) = z^{m+n-1} \cdot R(z), \tag{4.7}$$

and

$$Q_{n-1}^*(z)A(z) - P_{m-1}^*(z) = z^{m+n-1} \cdot R^*(z). \tag{4.8}$$

In section 3, in the case that $H_{m,n}$ is nonsingular, the inverse is given in terms of these four matrix Padé forms.

Theorem 4.1: For a pair of positive integers (m,n), the following statements are equivalent:

$$det(H_{m,n}) \neq 0, \tag{4.9}$$

$$det(r_0) \neq 0 \quad \text{and} \quad det(v_0) \neq 0, \tag{4.10}$$

$$det(r_0^*) \neq 0 \quad \text{and} \quad det(v_0^*) \neq 0. \tag{4.11}$$

Proof: That (4.9) implies (4.10) and (4.9) implies (4.11) was proved in Theorems 2.5 and 2.6 since $det(T_{m,n}) \neq 0$ if and only if $det(H_{m,n})$, and so we show only the converses here. To see that (4.10) implies (4.9), let $X = (x_1, \cdots, x_n)$ be a row vector of length np and suppose that

$$X \cdot H_{m,n} = 0. \tag{4.12}$$

We shall show that $X = 0$. We accomplish this by showing that (4.12) implies that $x_n = 0$ and

$$(0, x_1, \cdots, x_{n-1}) \cdot H_{m,n} = 0. \tag{4.13}$$

By repeated application of this property, it then follows that $x_{n-1} = \cdots = x_1 = 0$, and so $X = 0$.

First observe that equating coefficients of z^i, for $m+1 \leq i \leq m+n$, in (4.5) yields

$$H_{m,n} \cdot \begin{bmatrix} v_n \\ \cdot \\ \cdot \\ v_1 \end{bmatrix} = - \begin{bmatrix} a_{m+1} \\ \cdot \\ \cdot \\ a_{m+n} \end{bmatrix} v_0 , \qquad (4.14)$$

where v_0 is invertible since we are assuming statement (4.10). Similarly, equating coefficients of z^i, for $m \le i \le m+n-1$, in (4.7) yields

$$H_{m,n} \cdot \begin{bmatrix} q_{n-1} \\ \cdot \\ \cdot \\ q_0 \end{bmatrix} = \begin{bmatrix} 0 \\ \cdot \\ 0 \\ r_0 \end{bmatrix}, \qquad (4.15)$$

where, by assumption, r_0 is invertible. From (4.12) and (4.15), it follows that

$$x_n \cdot r_0 = X \cdot \begin{bmatrix} 0 \\ \cdot \\ 0 \\ r_0 \end{bmatrix} = X \cdot H_{m,n} \cdot \begin{bmatrix} q_{n-1} \\ \cdot \\ \cdot \\ q_0 \end{bmatrix} = 0. \qquad (4.16)$$

Since r_0 is invertible, it then follows that $x_n = 0$.

Having shown that $x_n = 0$, equation (4.12) then yields

$$(x_1, \cdots, x_{n-1}) \cdot \begin{bmatrix} a_{m-n+2} & \cdots & a_m \\ \cdot & & \cdot \\ \cdot & & \cdot \\ a_m & \cdots & a_{m+n-2} \end{bmatrix} = 0. \qquad (4.17)$$

But, from (4.12) and (4.14), we have

$$(x_1, \cdots, x_{n-1}, 0) \cdot \begin{bmatrix} a_{m+1} \\ \cdot \\ \cdot \\ a_{m+n} \end{bmatrix} \cdot v_0 = X \cdot H_{m,n} \begin{bmatrix} v_n \\ \cdot \\ \cdot \\ v_1 \end{bmatrix} = 0. \qquad (4.18)$$

Since v_0 is invertible, (4.18) implies that

$$(x_1, \cdots, x_{n-1}) \cdot \begin{bmatrix} a_{m+1} \\ \cdot \\ \cdot \\ a_{m+n-1} \end{bmatrix} = 0. \qquad (4.19)$$

Equations (4.17) and (4.19) imply that

$$(x_1, \cdots, x_{n-1}) \cdot \begin{bmatrix} a_{m-n+2} & \cdots & a_{m+1} \\ \cdot & & \cdot \\ \cdot & & \cdot \\ a_m & \cdots & a_{m+n-1} \end{bmatrix} = 0, \tag{4.20}$$

which is equivalent to (4.13).

Thus, we have shown that (4.10) implies (4.9). A similar argument shows that (4.11) implies (4.9).

Note that both conditions in (4.10) and in (4.11) of Theorem 4.1 are necessary. Consider

$$A(z) = z^3 + 0 \cdot z^4 + \cdots . \tag{4.21}$$

Then a RMPFo, $(P_1(z), Q_2(z), R(z))$, of type (1,2) is given by

$$P_1(z) = 0, \quad Q_2(z) = z, \quad R(z) = 1 + \cdots . \tag{4.22}$$

But $\det(H_{2,3}) = 0$, so that $\det(r_0) \neq 0$ alone does not imply (4.9). Also, consider

$$A(z) = \begin{bmatrix} 1 & 0 \\ 0 & 1 \end{bmatrix} + \begin{bmatrix} 1 & 0 \\ 0 & 1 \end{bmatrix} z^2 + \begin{bmatrix} 2 & 0 \\ 0 & 1 \end{bmatrix} z^4 + \begin{bmatrix} 0 & 0 \\ 0 & 0 \end{bmatrix} z^5 + \cdots . \tag{4.23}$$

Then one RMPFo, $(U_2(z), V_3(z), W(z))$, of type (2,3) is given by

$$U_2(z) = \begin{bmatrix} 1 & 0 \\ 0 & 1 \end{bmatrix} - \begin{bmatrix} 1 & 0 \\ 0 & 0 \end{bmatrix} z^2, \quad V_3(z) = \begin{bmatrix} 1 & 0 \\ 0 & 1 \end{bmatrix} - \begin{bmatrix} 2 & 0 \\ 0 & 1 \end{bmatrix} z^2. \tag{4.24}$$

But, here again, $\det(H_{2,3}) = 0$. Thus, $\det(v_0) \neq 0$ alone does not imply (4.9).

Theorem 4.1 has important computational significance since the singularity of $H_{m,n}$ can be detected simply by recognizing a singular r_0 or a singular v_0. If both r_0 and v_0 are nonsingular, then the results of chapter 2 implies that the matrix Padé forms identified by (4.5), (4.6), (4.7) and (4.8) are unique, except for the specification of the nonsingular matrices $v_0, v_0^*, r_0,$ and r_0^*. As a consequence it can be assumed

without loss-of generality that

$$v_0 = v_0^\bullet = r_0 = r_0^\bullet = I. \tag{4.25}$$

This nonrestrictive assumption simplifies the presentation of subsequent results.

A key relationship between matrix Padé forms which enables, in sections 3 and 4, the presentation of the inverse of $H_{m,n}$, is given by

Lemma 4.2. Let $\det(H_{m,n}) \neq 0$. Then the matrix Padé forms identified by (4.5), (4.6), (4.7) and (4.8) ε normalized according to (4.25) satisfy

$$\begin{bmatrix} Q_{n-1}^\bullet(z) & -P_{m-1}^\bullet(z) \\ -V_n^\bullet(z) & U_m^\bullet(z) \end{bmatrix} \cdot \begin{bmatrix} U_m(z) & P_{m-1}(z) \\ V_n(z) & Q_{n-1}(z) \end{bmatrix} = z^{m+n-1} \begin{bmatrix} I & 0 \\ 0 & I \end{bmatrix}, \tag{4.26}$$

$$\begin{bmatrix} U_m(z) & P_{m-1}(z) \\ V_n(z) & Q_{n-1}(z) \end{bmatrix} \cdot \begin{bmatrix} Q_{n-1}^\bullet(z) & -P_{m-1}^\bullet(z) \\ -V_n^\bullet(z) & U_m^\bullet(z) \end{bmatrix} = z^{m+n-1} \begin{bmatrix} I & 0 \\ 0 & I \end{bmatrix}, \tag{4.27}$$

$$\begin{bmatrix} R^\bullet(z) & -Q_{n-1}^\bullet(z) \\ -z^2 W^\bullet(z) & V_n^\bullet(z) \end{bmatrix} \cdot \begin{bmatrix} V_n(z) & Q_{n-1}(z) \\ z^2 W(z) & R(z) \end{bmatrix} = \begin{bmatrix} I & 0 \\ 0 & I \end{bmatrix} \tag{4.28}$$

and

$$\begin{bmatrix} V_n(z) & Q_{n-1}(z) \\ z^2 W(z) & R(z) \end{bmatrix} \cdot \begin{bmatrix} R^\bullet(z) & -Q_{n-1}^\bullet(z) \\ -z^2 W^\bullet(z) & V_n^\bullet(z) \end{bmatrix} = \begin{bmatrix} I & 0 \\ 0 & I \end{bmatrix}. \tag{4.29}$$

Proof: Multiplying (4.5) on the left by $Q_{n-1}^\bullet(z)$ and (4.8) on the right by $V_n(z)$, and subtracting the first from the second, we obtain

$$Q_{n-1}^\bullet(z) \cdot U_m(z) - P_{m-1}^\bullet(z) \cdot V_n(z) = z^{m+n-1} \cdot (R^\bullet(z) V_n(z) - z^2 Q_{n-1}^\bullet(z) W(z))$$

$$= z^{m+n-1} r_0^\bullet v_0$$

$$= z^{m+n-1} I.$$
(4.30)

In (4.30), we have used the normalizing condition (4.25) and the fact that the left hand side, and consequently the right hand side, is a matrix polynomial of degree at most m+n-1.

Multiplying (4.5) on the left by $V_n^\bullet(z)$ and (4.6) on the right by $V_n(z)$, and subtracting the second from the first, we obtain

$$-V_n^\bullet(z) \cdot U_m(z) + U_m^\bullet(z) \cdot V_n(z) = z^{m+n+1} \cdot (V_n^\bullet(z) W(z) - W^\bullet(z) V_n(z))$$

$$= 0.$$
(4.31)

In (4.31), the last equality is true because the left hand side and consequently the right hand side, is a matrix polynomial of degree at most m+n.

In a similar fashion, (4.7), (4.8) and (4.25) yield

$$Q_{n-1}^\bullet(z) P_{m-1}(z) - P_{m-1}^\bullet(z) Q_{n-1}(z) = z^{m+n-1} \cdot (Q_{n-1}^\bullet(z) R(z) - R^\bullet(z) Q_{n-1}(z))$$

$$= 0;$$
(4.32)

whereas, (4.6), (4.7) and (4.25) give

$$P_{m-1}(z) + U_m^\bullet(z) Q_{n-1}(z) = z^{m+n-1} \cdot (V_n^\bullet(z) R(z) - z^2 W^\bullet(z) Q_{n-1})$$

$$= z^{m+n-1} I.$$
(4.33)

Equations (4.30), (4.31), (4.32) and (4.33) together comprise (4.26). Equation (4.27) follows directly from (4.26), since matrix inverses are two sided.

Equations (4.30) also gives

$$z^{m+n-1} \cdot (R^\bullet(z) V_n(z) - z \, Q_{n-1}^\bullet(z) W(z)) = z^{m+n-1} \cdot I,$$
(4.34)

from which we obtain

$$R^*(z)V_n(z)-z^2 Q_{n-1}^*(z)W(z)=I.$$

(4.35)

Similarly, from equation (4.31), we obtain

$$V_n^*(z)W(z)-W^*(z)V_n(z)=0.$$

(4.36)

From (4.32), we obtain

$$Q_{n-1}^*(z)R(z)-R^*(z)Q_{n-1}(z)=0,$$

(4.37)

and (4.33) gives

$$V_n^*(z)R(z)-z^2 W^*(z)Q_{n-1}=I.$$

(4.38)

Equations (4.35), (4.36), (4.37) and (4.38) comprise (4.28). As before, (4.29) follows from (4.28), since matrix inverses are two sided.

4.3. The Off-diagonal Inverse Formulae

The main result of this chapter is

Theorem 4.3. Let $H_{m,n}$ be the block Hankel matrix (4.1). If there are RMPFo's and LMPFo's of type (m-1,n-1) and (m,n) for A(z) satisfying the normalizing condition (4.25), then $H_{m,n}$ is nonsingular with inverse

$$H_{m,n}^{-1} = \begin{bmatrix} v_{n-1} & & v_0 \\ & \ddots & \\ v_0 & & \end{bmatrix}\begin{bmatrix} q_{n-1}^* & & q_0^* \\ & \ddots & \\ & & q_{n-1}^* \end{bmatrix} - \begin{bmatrix} q_{n-2} & q_0 & 0 \\ & \ddots & \\ q_0 & & \\ 0 & & \end{bmatrix}\begin{bmatrix} v_n^* & & v_1^* \\ & \ddots & \\ & & v_n^* \end{bmatrix},$$

(4.38)

or, equivalently,

$$H_{m,n}^{-1} = \begin{bmatrix} q_{n-1} & & \\ & \ddots & \\ q_0 & & q_{n-1} \end{bmatrix}\left(\begin{bmatrix} v_{n-1}^* & & v_0^* \\ & \ddots & \\ v_0^* & & \end{bmatrix} - \begin{bmatrix} v_n & & \\ & \ddots & \\ v_1' & & v_n \end{bmatrix}\right)\begin{bmatrix} q_{n-2}^* & q_0^* & 0 \\ & \ddots & \\ q_0^* & & \\ 0 & & \end{bmatrix}$$

(4.39)

Proof. Using

$$U_m(z)Q^*_{n-1}(z) - P_{m-1}(z)V^*_n(z) = z^{m+n-1}I,$$

which is from (4.27), we can equate coefficients of z^i, $m \leq i \leq m+n-1$, to obtain

$$\begin{bmatrix} u_m & & u_{m-n+1} \\ & \cdot & \\ & & \cdot \\ & & u_m \end{bmatrix} \cdot \begin{bmatrix} q^*_{n-1} & & q^*_0 \\ & \cdot & \\ & & \cdot \\ & & q^*_{n-1} \end{bmatrix} - \begin{bmatrix} p_{m-1} & & p_{m-n} \\ & \cdot & \\ & & \cdot \\ & & p_{m-1} \end{bmatrix} \cdot \begin{bmatrix} v^*_n & & v^*_1 \\ & \cdot & \\ & & \cdot \\ & & v^*_n \end{bmatrix} = I. \qquad (4.40)$$

Similarly,

$$V_n(z)Q^*_{n-1}(z) - Q_{n-1}(z)V^*_n(z) = 0,$$

also from (4.27), yields

$$\begin{bmatrix} & & v_n \\ & \cdot & \\ & \cdot & \\ v_n & & v_1 \end{bmatrix} \begin{bmatrix} q^*_{n-1} & & q^*_0 \\ & \cdot & \\ & & \cdot \\ & & q^*_{n-1} \end{bmatrix} - \begin{bmatrix} & & q_{n-1} \\ & \cdot & \\ & \cdot & \\ q_{n-1} & & q_0 \end{bmatrix} \begin{bmatrix} v^*_n & & v^*_1 \\ & \cdot & \\ & & \cdot \\ & & v^*_n \end{bmatrix} = 0. \qquad (4.41)$$

Now, from (4.7), we obtain

$$H_{m,n} \cdot \begin{bmatrix} q_{n-2} & & q_0\,0 \\ & \cdot & \\ q_0 & & \\ 0 & & \end{bmatrix} = \begin{bmatrix} p_{m-i} & & p_{m-n} \\ & \cdot & \\ & & \cdot \\ & & p_{m-1} \end{bmatrix} - H_{m-n,n} \cdot \begin{bmatrix} & & q_{n-1} \\ & \cdot & \\ & & \cdot \\ q_{n-1} & & q_0 \end{bmatrix}. \qquad (4.42)$$

Observe that, for $1 \leq i,j \leq n$, the (i,j) component in (4.42) is obtained by equating coefficients of $z^{m+i-j-1}$ in (4.7). Similarly, (4.5) yields

$$H_{m,n} \cdot \begin{bmatrix} v_{n-1} & & v_0 \\ & \cdot & \\ & & \cdot \\ v_0 & & \end{bmatrix} = \begin{bmatrix} u_m & & u_{m-n+1} \\ & \cdot & \\ & & \cdot \\ & & u_m \end{bmatrix} - H_{m-n,n} \cdot \begin{bmatrix} & & v_n \\ & \cdot & \\ & & \cdot \\ v_n & & v_1 \end{bmatrix}. \qquad (4.43)$$

Combining (4.42) and (4.43) and using (4.40) and (4.41), it then follows that

$$
H_{m,n}\left\{\begin{bmatrix} v_{n-1} & & v_0 \\ & \cdot & \\ & \cdot & \\ v_0 & & \end{bmatrix}\begin{bmatrix} q_{n-1}^* & & q_0^* \\ & \cdot & \\ & & q_{n-1}^* \end{bmatrix} - \begin{bmatrix} q_{n-2} & & q_0\ 0 \\ & \cdot & \\ q_0 & & \\ 0 & & \end{bmatrix}\begin{bmatrix} v_n^* & & v_1^* \\ & & \\ & & \\ & & v_n^* \end{bmatrix}\right\}
$$

$$
= \left\{\begin{bmatrix} u_m & & u_{m-n+1} \\ & \cdot & \\ & & \\ & & u_m \end{bmatrix} - H_{m-n,n}\cdot\begin{bmatrix} & & v_n \\ & \cdot & \\ & & \\ v_n & & v_1 \end{bmatrix}\right\}\begin{bmatrix} q_{n-1}^* & & q_0^* \\ & \cdot & \\ & & q_{n-1}^* \end{bmatrix}
$$

$$
- \left\{\begin{bmatrix} p_{m-1} & & p_{m-n} \\ & \cdot & \\ & & \\ & & p_{m-1} \end{bmatrix} - H_{m-n,n}\begin{bmatrix} & & q_{n-1} \\ & \cdot & \\ & & \\ q_{n-1} & & q_0 \end{bmatrix}\right\}\begin{bmatrix} v_n^* & & v_1^* \\ & & \\ & & \\ & & v_n^* \end{bmatrix}
$$

$$
= \left\{\begin{bmatrix} u_m & & u_{m-n+1} \\ & & \\ & \cdot & \\ & & u_m \end{bmatrix}\begin{bmatrix} q_{n-1}^* & & q_0^* \\ & \cdot & \\ & & q_{n-1}^* \end{bmatrix} - \begin{bmatrix} p_{m-1} & & p_{m-n} \\ & & \\ & & \\ & & p_{m-1} \end{bmatrix}\begin{bmatrix} v_n^* & & v_1^* \\ & & \\ & & \\ & & v_n^* \end{bmatrix}\right\}
$$

$$
- H_{m-n,n}\left\{\begin{bmatrix} & & v_n \\ & \cdot & \\ & & \\ v_n & & v_1 \end{bmatrix}\begin{bmatrix} q_{n-1}^* & & q_0^* \\ & \cdot & \\ & & q_{n-1}^* \end{bmatrix} - \begin{bmatrix} & & q_{n-1} \\ & \cdot & \\ & & \\ q_{n-1} & & q_0 \end{bmatrix}\begin{bmatrix} v_n^* & & v_1^* \\ & & \\ & & \\ & & v_n^* \end{bmatrix}\right\}
$$

$$
= I.
$$

(4.44)

Thus, $H_{m,n}$ is nonsingular with inverse given by (4.38).

The second formula (4.39) for the inverse is proved using (4.6), (4.8) and the second column of (4.27).

Remark 1. In the scalar case, formula (4.38) was first obtained by Choi [18].

Remark 2: The assumptions of Theorem 4.3 can be equivalently replaced by the requirement that we obtain solutions to

$$H_{m,n} \cdot \left[q_{n-1}, \cdots, q_0 \right]^t = \left[0, \cdots, 0, I \right]^t, \tag{4.45}$$

$$\left[q_{n-1}, \cdots, q_0 \right] \cdot H_{m,n} = \left[0, \cdots, 0, I \right], \tag{4.46}$$

$$H_{m,n} \cdot \left[v_n, \cdots, v_1 \right]^t = - \left[a_{m+1}, \cdots, a_{m+n+1}, a_{m+n} \right]^t, \tag{4.47}$$

and

$$\left[v_n, \cdots, v_1 \right] \cdot H_{m,n} = - \left[a_{m+1}, \cdots, a_{m+n+1}, a_{m+n} \right], \tag{4.48}$$

where a_{m+n} can be any $p \times p$ matrix. Equations (4.47) and (4.48) are block versions of the Yule-Walker equations.

4.4. The Anti-diagonal Inverse Formulae

Theorem 4.3 provides inverse formulae for the block Hankel matrix $H_{m,n}$ in terms of RMPFo and LMPFo of type (m-1,n-1) and (m,n) for the associated matrix polynomial A(z). There are some algorithms (c.f., [8], [35], [44]) that calculate Padé forms along an anti-diagonal, rather than along an off-diagonal path of the Padé table. For this reason, it is useful to provide inverse formulae in terms of RMPFo's and LMPFo's of type (m-1,n) and (m,n-1) for A(z).

Let $(E_m(z),F_{n-1}(z),G(z))$ and $(E_m^*(z),F_{n-1}^*(z),G^*(z))$ be a RMPFo and a LMPFo, respectively, of type (m,n-1) for A(z). Also, let $(B_{m-1}(z),C_n(z),D(z))$ and $(B_{m-1}^*(z),C_n^*(z),D^*(z))$ be a RMPFo and a LMPFo, respectively, of type (m-1,n) for A(z). Then, the following equations are satisfied:

$$A(z)F_{n-1}(z) - E_m(z) = z^{m+n}G(z),$$

(4.49)

$$F_{n-1}^*(z)A(z) - E_m^*(z) = z^{m+n}G^*(z),$$

(4.50)

$$A(z)C_n(z) - B_{m-1}(z) = z^{m+n}D(z)$$

(4.51)

and

$$C_n^*(z)A(z) - B_{m-1}^*(z) = z^{m+n}D^*(z).$$

(4.52)

Corollary 4.1: Let $H_{m,n}$ be the block Hankel matrix (4.1). Then the following are equivalent:

$$det(H_{m,n}) \neq 0,$$

(4.53)

$$det(e_m) \neq 0 \text{ and } det(c_n) \neq 0,$$

(4.54)

$$det(e_m^*) \neq 0 \text{ and } det(c_n^*) \neq 0.$$

(4.55)

If any (and therefore all) of (4.53), (4.54) or (4.55) hold, then an inverse is given by

$$H_{m,n}^{-1} = \begin{bmatrix} c_n & & \\ & \cdot & \\ & & \cdot \\ c_1 & & c_n \end{bmatrix} \begin{bmatrix} f_{n-1}^* & & f_0^* \\ & \cdot & \\ f_0^* & & \end{bmatrix} - \begin{bmatrix} 0 & & \\ f_{n-1} & & \\ & \cdot & \\ f_1 & & f_{n-1} & 0 \end{bmatrix} \begin{bmatrix} c_{n-1}^* & & c_1^* \\ & \cdot & \\ c_0^* & & \end{bmatrix},$$

(4.56)

or, equivalently,

$$H_{m,n}^{-1} = \begin{bmatrix} f_{n-1} & & f_0 \\ & \cdot & \\ f_0 & & \end{bmatrix} \begin{bmatrix} c_n^* & & c_1^* \\ & \cdot & \\ & & c_n^* \end{bmatrix} - \begin{bmatrix} c_{n-1} & & c_0 \\ & \cdot & \\ c_0 & & \end{bmatrix} \begin{bmatrix} 0 & f_{n-1}^* & f_1^* \\ & \cdot & \\ & \cdot & f_{n-1}^* \\ & & 0 \end{bmatrix},$$

(4.57)

where we have normalized the Padé forms so that

$$e_m = e_m^* = c_n = c_n^* = I. \tag{4.58}$$

Proof: Let $a_i^\# = a_{2m-i}$, for $0 \le i = m+n$, and define a truncated power series $A^\#(z) = \sum_{i=0}^{m+n} a_i^\# z^i$.

Observe that, if

$$H_{m,n}^\# = \begin{bmatrix} a_{m-n+1}^\# & \cdots & a_m^\# \\ \cdot & & \cdot \\ a_m^\# & \cdots & a_{m+n-1}^\# \end{bmatrix}, \tag{4.59}$$

then

$$H_{m,n}^\# = J \cdot H_{m,n} \cdot J, \tag{4.60}$$

where

$$J = \begin{bmatrix} 0 & I \\ I & 0 \end{bmatrix}.$$

Equating coefficients of z^i, for $m \le i \le m+n-1$, in (4.49) gives

$$H_{m,n} \begin{bmatrix} f_{n-1} \\ \cdot \\ \cdot \\ f_0 \end{bmatrix} = \begin{bmatrix} e_m \\ 0 \\ \cdot \\ 0 \end{bmatrix}. \tag{4.61}$$

From (4.60) and (4.61), it then follows that

$$H_{m,n}^\# \begin{bmatrix} f_0 \\ \cdot \\ \cdot \\ f_{n-1} \end{bmatrix} = \begin{bmatrix} 0 \\ \cdot \\ 0 \\ e_m \end{bmatrix}. \tag{4.62}$$

Thus,

$$Q_{n-1}(z) = \sum_{i=0}^{n-1} f_{n-1+i} z^i \tag{4.63}$$

is a right denominator of type (m-1,n-1) for $A^{\#}(z)$. Similarly, (4.50) yields

$$\left[f_0^{*}, \cdots , f_{n-1}^{*} \right] H_{m,n}^{\#} = \left[0, \cdots , 0, e_m^{*} \right] \tag{4.64}$$

and so

$$Q_{n-1}^{*}(z) = \sum_{i=0}^{n-1} f_{n-1+i}^{*} z^{i} \tag{4.65}$$

is a left denominator of type (m-1,n-1) for $A^{\#}(z)$.

Next, from (4.51), we obtain

$$H_{m,n} \begin{bmatrix} c_{n-1} \\ . \\ c_0 \end{bmatrix} = \begin{bmatrix} a_{m-n} \\ . \\ a_{m-1} \end{bmatrix} c_n , \tag{4.66}$$

and so (4.60) then gives

$$H_{m,n}^{\#} \begin{bmatrix} c_0 \\ . \\ c_{n-1} \end{bmatrix} = \begin{bmatrix} a_{m+1}^{\#} \\ . \\ a_{m+n}^{\#} \end{bmatrix} c_n , \tag{4.67}$$

Thus,

$$V_n(z) = \sum_{i=0}^{n} c_{n-i} z^{i} \tag{4.68}$$

is a right denominator of type (m,n) for $A^{\#}(z)$. Similarly, (4.52) can be used to obtain

$$\left[c_0^{*}, \cdots , c_{n-1}^{*} \right] H_{m,n}^{\#} = c_n^{*} \left[a_{m+1}^{\#}, \cdots a_{m+n}^{\#} \right] \tag{4.69}$$

and so

$$V_n^{*}(z) = \sum_{i=0}^{n} c_{n-i}^{*} z^{i} \tag{4.70}$$

is a left denominator of type (m,n) for $A^{\#}(z)$. Since $\det(H_{m,n}^{\#}) \neq 0$ if and only if $\det(H_{m,n}) \neq 0$, the equivalence of (4.53), (4.54) and (4.55) now follows from the equivalence of (4.9), (4.10) and (4.11).

To prove (4.56), normalize according to (4.58) and substitute (4.63), (4.65), (4.68) and (4.70) into (4.38) to obtain

$$
H_{m,n}^{\#^{-1}} =
\begin{bmatrix} c_1 & & c_n \\ & \ddots & \\ c_n & & \end{bmatrix}
\begin{bmatrix} f_0^* & & f_{n-1}^* \\ & \ddots & \\ & & f_0^* \end{bmatrix}
-
\begin{bmatrix} f_1 & & f_{n-1} & 0 \\ & \ddots & \\ f_{n-1} & & \\ 0 & & \end{bmatrix}
\begin{bmatrix} c_0^* & & c_{n-1}^* \\ & & \\ & & c_0^* \end{bmatrix},
\tag{4.71}
$$

By using (4.60), (4.56) follows immediately from (4.70). In a similar fashion, (4.57) can be obtained using (4.39).

Chapter 5

Other Inverse Formulae

5.1. Introduction

The special structure of Hankel matrices has resulted in a number of proposed formulae for the inverse of $H_{m,n}$ other than those given in chapter 4. When p = 1 (the scalar case) well known formulae of Gohberg and Semencul [23] gives $H_{m,n}^{-1}$ in terms of only the first and last columns of the inverse. Gohberg and Krupnik [24] give a formula for the inverse in terms of the last two columns of $H_{m,n}^{-1}$.

When p > 1, there are closed formulae due to Gohberg and Heinig [25] (these are actually given when the coefficients are from a noncommutative algebra). These are given provided the first and last columns together with the first and last rows of the inverse are known.

All of the above formulae depend on the ability to perform certain bordering operations that lend themselves well to matrices with a Hankel structure. However, these bordering operations require the imposition of certain additional restrictions on $H_{m,n}$. For the Gohberg-Krupnik formula, the matrix $H_{m-1,n-1}$ must also be nonsingular; whereas, for the Gohberg-Semencul and Gohberg-Heinig formulae, the matrix $H_{m,n-1}$ must be nonsingular.

In this chapter, we show that these formulae are simply special cases of the formulae from chapter 4. Indeed, when we add the condition that $H_{m,n-1}$ also be nonsingular, certain Frobenius-type identities for matrix Padé forms are used to show that our formulae yields the formulae of Gohberg and Heinig. On the other hand, when we add the condition that $H_{m-1,n-1}$ be nonsingular, a different set of Frobenius-type identities applied to our results yields inverse formulae, which in the scalar case corresponds to the Gohberg-Krupnik formulae. Finally, we show that additional formulae can be obtained using the results of chapter 4 along with various relationships existing in the Padé table of a power series.

5.2. The Inverse Formulae of Gohberg-Heinig

In this and the next section, we compare our off-diagonal inverse formulae (4.38) and (4.39) with other similar well-known formulae. In terms of matrix Padé forms of type (m-1,n-1) and (m,n-1), the inverse of $H_{m,n}$ is given by

Corollary 5.1. Let the matrix Padé forms identified by (4.7), (4.8), (4.49) and (4.50) be given. Then the following statements are equivalent:

$$det\,(H_{m,n-1}) \neq 0 \ \text{ and }\ det\,(H_{m,n}) \neq 0, \tag{5.1}$$

$$det\,(r_0) \neq 0 \ \text{ and }\ det\,(f_0) \neq 0, \tag{5.2}$$

$$det\,(r_0^*) \neq 0 \ \text{ and }\ det\,(f_0^*) \neq 0. \tag{5.3}$$

In addition, if any (and therefore all) of conditions (5.1), (5.2) or (5.3) are satisfied, then

$$H_{m,n}^{-1} = \begin{bmatrix} f_{n-1} & .. & f_0 \\ . & & \\ . & & \\ f_0 & & \end{bmatrix} \begin{bmatrix} q_{n-1}^* & .. & q_0^* \\ & . & \\ & & q_{n-1}^* \end{bmatrix} - \begin{bmatrix} q_{n-2} & q_0 & 0 \\ . & & \\ q_0 & & \\ 0 & & \end{bmatrix} \begin{bmatrix} 0 & f_{n-1}^* & f_1^* \\ . & & \\ & & f_{n-1}^* \\ & & 0 \end{bmatrix}, \tag{5.4}$$

where the Padé forms have been normalized by

$$r_0 = r_0^* = f_0 = f_0^* = I. \tag{5.5}$$

Proof: We first show that (5.1) implies (5.2). Since $\det(H_{m,n}) \neq 0$, Theorem 4.1 implies that $\det(r_0) \neq 0$. Since $\det(H_{m,n-1}) \neq 0$, Theorem 4.1 also implies that $\det(f_0) \neq 0$. Therefore (5.1) implies (5.2). In a similar fashion (5.1) implies (5.3).

To show that (5.2) implies (5.1), let

$$U_m(z) = E_m(z) - z \cdot P_{m-1}(z) r_0^{-1} \cdot g_0 \tag{5.6}$$

$$V_n(z) = F_{n-1}(z) - z \cdot Q_{n-1}(z) r_0^{-1} \cdot g_0. \tag{5.7}$$

Then, $\partial(U_m(z)) \leq m$ and $\partial(V_n(z)) \leq n$. Also,

$$A(z)V_n(z) - U_m(z)$$

$$= \left\{ A(z)F_{n-1}(z) - E_m(z) \right\} - z \left\{ A(z)Q_{n-1}(z) - P_{m-1}(z) \right\} r_0^{-1} g_0$$

$$= z^{m+n} \left\{ G(z) - R(z)r_0^{-1} g_0 \right\}$$

$$= z^{m+n+1} W(z), \tag{5.8}$$

where

$$W(z) = z^{-1} \left\{ G(z) - R(z)r_0^{-1} g_0 \right\} \varepsilon D[[z]]. \tag{5.9}$$

Finally, the columns of $V_n(z)$ are linearly independent, since, from (5.7), $v_0 = f_0$, and by assumption f_0 is nonsingular. Thus, $(U_m(z), V_n(z), W(z))$ is a RMPFo of type (m,n) for $A(z)$, satisfying $\det(v_0) \neq 0$. From Theorem 4.1, it follows that $H_{m,n}$ is nonsingular since both $\det(r_0) \neq 0$ and $\det(v_0) \neq 0$. To see that $H_{m,n-1}$ is also nonsingular, observe that

$$\begin{bmatrix} a_{m-n+1} & \cdots & a_m \\ \cdot & & \cdot \\ \cdot & & \cdot \\ a_m & \cdots & a_{m+n-1} \end{bmatrix} \begin{bmatrix} I & & f_{n-1} \\ & \cdot & \cdot \\ & & I & \cdot \\ 0 & \cdots & 0 & f_0 \end{bmatrix} = \begin{bmatrix} a_{m-n+1} & \cdots & a_{m-1} & e_m \\ a_{m-n+2} & & a_m & 0 \\ \cdot & & \cdot & \cdot \\ a_m & \cdots & a_{m+n-2} & 0 \end{bmatrix}, \tag{5.10}$$

where the last column is determined by equating coefficients of z^i, for $m \leq i \leq m+n-1$ in (4.49). Thus, $\det(H_{m,n}) \neq 0$ and $\det(f_0) \neq 0$ implies that $\det(H_{m,n-1}) \neq 0$. Thus, (5.2) implies (5.1).

In a similar fashion, by defining

$$-U_m^*(z) = E_m^*(z) - z g_0^* r_0^{*-1} P_{m-1}^*(z), \tag{5.11}$$

$$V_n^*(z) = F_{n-1}^*(z) - z g_0^* r_0^{*-1} Q_{n-1}^*(z), \tag{5.12}$$

can be shown that (5.3) implies (5.1).

To obtain the inverse formula, substitution of (5.6), (5.7), (5.11) and (5.12), after normalization by (5.5), into equation (4.38) gives

$$
H_{m,n}^{-1} = \begin{bmatrix} f_{n-1} & . & . & f_0 \\ . & & & \\ . & & & \\ f_0 & & & \end{bmatrix} \begin{bmatrix} q_{n-1}^* & . & . & q_0^* \\ & & . & . \\ & & & \\ & & & q_{n-1}^* \end{bmatrix} - \begin{bmatrix} q_{n-2} & & q_0 & 0 \\ . & & . & . \\ q_0 & & . & \\ 0 & & & \end{bmatrix} \begin{bmatrix} 0 f_{n-1}^* & . & f_1^* \\ . & & \\ & & f_{n-1}^* \\ & & 0 \end{bmatrix}
$$

$$
+ \begin{bmatrix} q_{n-2} & & q_0 & 0 \\ . & & . & . \\ q_0 & & . & \\ 0 & & & \end{bmatrix} (g_0 - g_0^*) \begin{bmatrix} q_{n-1}^* & . & . & q_0^* \\ & & . & \\ & & & . \\ & & & q_{n-1}^* \end{bmatrix} . \tag{5.13}
$$

But, equations (4.49) and (4.50) imply that

$$
E_m^*(z)F_{n-1}(z) - F_{n-1}^*(z)E_m(z) = z^{m+n} \left\{ F_{n-1}^*(z)G(z) - G^*(z)F_{n-1}(z) \right\}. \tag{5.14}
$$

Consequently,

$$
F_{n-1}^*(z)G(z) - G^*(z)F_{n-1}(z) = 0 \tag{5.15}
$$

and, in particular,

$$
g_0 = g_0^*. \tag{5.16}
$$

Thus, (5.13) is exactly (5.4), since the last product cancels.

Remark 1: Corollary 5.1 can be proved directly from (4.7), (4.8), (5.1) and (5.2). Indeed, using the same arguments as in Lemma 4.2, we can obtain

$$
\begin{bmatrix} r_0^{*-1} Q_{n-1}^*(z) & -r_0^{*-1} P_{m-1}^*(z) \\ -f_0^{*-1} F_{n-1}^*(z) & f_0^{*-1} E_m^*(z) \end{bmatrix} \begin{bmatrix} E_m(z)f_0^{-1} & P_{m-1}(z)r_0^{-1} \\ F_{n-1}(z)f_0^{-1} & Q_{n-1}(z)r_0^{-1} \end{bmatrix} = z^{m+n-1} \begin{bmatrix} I & 0 \\ 0 & I \end{bmatrix} \tag{5.17}
$$

and the commutative relationship

$$\begin{bmatrix} E_m(z)f_0^{-1} & P_{m-1}(z)r_0^{-1} \\ F_{n-1}(z)f_0^{-1} & Q_{n-1}(z)r_0^{-1} \end{bmatrix} \begin{bmatrix} r_0^{*-1}Q_{n-1}^*(z) & -r_0^{*-1}P_{m-1}^*(z) \\ -f_0^{*-1}F_{n-1}^*(z) & f_0^{*-1}E_m^*(z) \end{bmatrix} = z^{m+n-1}\begin{bmatrix} I & 0 \\ 0 & I \end{bmatrix}. \tag{5.18}$$

Consequently, we can normalize our Padé forms according to (5.5) and the formulae will follow in a fashion similar to the proof of Theorem 4.3.

The actual proof, in addition to being simpler, serves to illustrate the existence of Frobenius-type relationships (generalized from the scalar case (c.f., Gragg [26]) to the matrix case) between matrix Padé forms of types (m,n), (m,n-1) and (m-1,n-1). These relationships, which exist under the assumptions of Corollary 5.1, are given by (5.6), (5.7), (5.11) and (5.12) (see also [10] , [14] , [13]).

Remark 2: From (5.17), it follows from equating coefficients of degree m+n-1 that

$$e_m^* q_{n-1} = f_0^* r_0 \tag{5.19}$$

and

$$q_{n-1}^* e_m = r_0^* f_0 \tag{5.20}$$

Thus, if the conditions of Corollary 5.1 are satisfied, then $e_m^*, q_{n-1}, q_{n-1}^*$ and e_m are all nonsingular. Normalizing (4.7), (4.8), (4.49) and (4.50) by setting

$$r_0 = r_0^* = e_m = e_m^* = I., \tag{5.21}$$

rather than by (5.5), we obtain

$$H_{m,n}\cdot\begin{bmatrix} q_{n-1} , \cdots , q_0 \end{bmatrix}^t = \begin{bmatrix} 0 , \cdots , 0 , I \end{bmatrix}^t \tag{5.22}$$

$$\begin{bmatrix} q_{n-1}^* , \cdots , q_0^* \end{bmatrix}\cdot H_{m,n} = \begin{bmatrix} 0 , \cdots , 0 , I \end{bmatrix} \tag{5.23}$$

$$H_{m,n}\cdot\begin{bmatrix} f_{n-1} , \cdots , f_0 \end{bmatrix}^t = \begin{bmatrix} I , 0 , \cdots , 0 \end{bmatrix}^t \tag{5.24}$$

$$- \left[f_{n-1}^{\bullet} , \cdots , f_0^{\bullet} \right] \cdot H_{m,n} = \left[I, 0, \cdots , 0 \right].\tag{5.25}$$

These conditions, together with the requirement that $\det(q_{n-1}) \neq 0$ and $\det(q_{n-1}^{\bullet}) \neq 0$, are exactly the conditions given by Gohberg and Heinig [25] in deriving the inverse formula (5.4). Because of the different normalization requirement, their formula includes the term q_{n-1}^{-1} between the first two matrices and $q_{n-1}^{\bullet -1}$ between the last two matrices. This is permissible because of (5.19), (5.20) and (5.21). In the scalar case, this is the well known formula of Gohberg and Semencul [23].

Remark 3: The assumptions of Corollary 5.1, which are equivalent to conditions (5.22), (5.23), (5.24) and (5.25) of Gohberg and Heinig, are far more restrictive than the assumptions of Theorem 4.3, which are equivalent to (4.45), (4.46), and the block Yule-Walker equations (4.47) and (4.48). The formula of Gohberg and Heinig has the additional requirement that q_{n-1} and $q_{n-1}^{\bullet}$ be nonsingular (which is equivalent to $H_{m,n-1}$ being nonsingular). Thus, for example, (4.38) can be used to obtain the inverse of

$$H_{2,3} = \begin{bmatrix} I & 0 & 0 \\ 0 & 0 & I \\ 0 & I & 0 \end{bmatrix},\tag{5.26}$$

whereas, (5.4) cannot be applied.

Remark 4: Since the assumptions of Corollary 5.1 require that not only $H_{m,n}$ but also $H_{m,n-1}$ be nonsingular, it should be possible to express the inverse of $H_{m,n-1}$ in closed form as well. Indeed, by deriving Frobenius-type identities similar to (5.6), (5.7), (5.11) and (5.12) (c.f., Bultheel [10] , [14] , [13]), the matrix Padé form of type (m-1,n-2) can be expressed in terms of matrix Padé forms of type (m,n-1) and (m-1,n-1). Then, substituting the Padé forms of type (m,n-1) and (m-1,n-2) into (4.38) (with n replaced by n-1) and simplifying, we obtain as another corollary to Theorem 4.3 the second inverse formula of Gohberg and Heinig, namely,

$$H_{m,n-1}^{-1} = \begin{bmatrix} f_{n-2} & \cdots & f_0 \\ & \cdot & \\ & \cdot & \\ f_0 & & \end{bmatrix} \begin{bmatrix} q_{n-1}^{\bullet} & \cdots & q_1^{\bullet} \\ & \cdot & \\ & & q_{n-1}^{\bullet} \end{bmatrix} - \begin{bmatrix} q_{n-2} & & q_0 \\ \cdot & \cdot & \\ q_0 & & \end{bmatrix} \begin{bmatrix} f_{n-1}^{\bullet} & \cdots & f_1^{\bullet} \\ & \cdot & \\ & & f_{n-1}^{\bullet} \end{bmatrix}.\tag{5.27}$$

Here, we have again normalized according to (5.5). We also note that the Gohberg-Heinig formulae given here are both determined from formula (4.38). Additional formulae, based on (4.39) rather than (4.38), can also be derived.

Remark 5: Gohberg and Heinig prove their formulae with the coefficients over a non-commutative algebra. Our formulae and results also carry over with minor alterations. In particular, Theorem 4.1 and Corollary 5.1 would both require that (4.9) be equivalent to (4.10) and (4.11), simultaneously.

5.3. The Inverse Formulae of Gohberg-Krupnik

Let $(L_{m-2}(z), M_{n-2}(z), N(z))$ and $(L_{m-2}^*(z), M_{n-2}^*(z), N^*(z))$ be a RMPFo and LMPFo, respectively, of type (m-2,n-2) for $A(z)$. These matrix Padé forms then satisfy

$$A(z)M_{n-2}(z) - L_{m-2}(z) = z^{m+n-3}N(z) \tag{5.28}$$

$$M_{n-2}^*(z)A(z) - L_{m-2}^*(z) = z^{m+n-3}N^*(z). \tag{5.29}$$

The inverse of $H_{m,n}$ in terms of matrix Padé forms of types (m-2,n-2) and (m-1,n-1) is given by

Corollary 5.2. Let the matrix Padé forms identified by (4.7), (4.8), (5.28) and (5.29) be given. Then, the following statements are equivalent:

$$det(H_{m,n}) \neq 0 \quad \text{and} \quad det(H_{m-1,n-1}) \neq 0, \tag{5.30}$$

$$det(n_0) \neq 0, \ det(q_0) \neq 0, \ \text{and} \ det(r_0) \neq 0, \tag{5.31}$$

and

$$det(n_0^*) \neq 0, \ det(q_0^*) \neq 0, \ \text{and} \ det(r_0^*) \neq 0. \tag{5.32}$$

In addition, if any (and therefore all) of the conditions (5.30), (5.31) or (5.32) are satisfied, then

$$H_{m,n}^{-1} = \begin{bmatrix} q_{n-2} & q_0 & 0 \\ & & \\ q_0 & & \\ 0 & & \end{bmatrix} q_0^{-1} \begin{bmatrix} m_{n-2}^* & m_{-1}^* \\ & \\ m_0^* & \\ & \\ m_{n-2}^* & \end{bmatrix} - \begin{bmatrix} m_{n-3} & m_0 & 0 & 0 \\ & \\ m_0 & \\ 0 & \\ 0 & \end{bmatrix} q_0^{*-1} \begin{bmatrix} q_{n-1}^* & q_0^* \\ & \\ & \\ q_{n-1}^* & \end{bmatrix}$$

$$+ \begin{bmatrix} q_{n-1} \\ \cdot \\ \cdot \\ \cdot \\ q_0 \end{bmatrix} q_0^{-1} \begin{bmatrix} q_{n-1}^*, & \cdots & , q_0^* \end{bmatrix}. \tag{5.33}$$

Here, the matrix Padé forms have been normalized so that [2]

$$n_0 = n_0^* = r_0 = r_0^* = I. \tag{5.34}$$

Proof: To prove that (5.30) is equivalent to (5.31), it follows directly from Theorem 2.3 that $\det(H_{m,n}) \neq 0$ implies that $\det(r_0) \neq 0$ while $\det(H_{m-1,n-1}) \neq 0$ implies that $\det(n_0) \neq 0$ and $\det(q_0) \neq 0$. Conversely, suppose that (5.31) holds. Again, from Theorem 4.1, we have that $\det(n_0) \neq 0$ and $\det(q_0) \neq 0$ implies $\det(H_{m-1,n-1}) \neq 0$. But, then

$$\begin{bmatrix} a_{m-n+1} & \cdots & a_m \\ \cdot & & \cdot \\ \cdot & & \cdot \\ a_m & \cdots & a_{m+n-1} \end{bmatrix} \begin{bmatrix} I & & q_{n-1} \\ & \cdot & \cdot \\ & I & \cdot \\ & \cdots & q_0 \end{bmatrix} = \begin{bmatrix} a_{m-n+1} & \cdots & a_{m-1} & 0 \\ \cdot & & & \cdot \\ a_{m-1} & \cdots & a_{m+n-2} & 0 \\ a_m & & a_{m+n-1} & r_0 \end{bmatrix}, \tag{5.35}$$

together with the assumption that $\det(r_0) \neq 0$, implies that also $\det(H_{m,n}) \neq 0$.

A similar argument shows that (5.30) is equivalent to (5.32).

To prove (5.33), we first establish some identities. Observe that, under the normalization condition (5.34), $(L_{m-2}(z), M_{n-2}(z), N(z))$, $(L_{m-2}^*(z), M_{n-2}^*(z), N^*(z))$, $(P_{m-1}(z)q_0^{-1}, Q_{n-1}(z)q_0^{-1}, R(z)q_0^{-1})$, and $(q_0^{*-1}P_{m-1}^*(z), q_0^{*-1}Q_{n-1}^*(z), q_0^{*-1}R^*(z))$, satisfy the conditions of Lemma 4.2, with (m,n) replaced by (m-1,n-1). Here, (4.29) becomes

---

[2] Rather than normalizing with $r_0 = r_0^* = I$, it is equally proper to normalize with $q_0 = q_0^* = I$.

$$\begin{bmatrix} Q_{n-1}(z)q_0^{-1} & M_{n-2}(z) \\ z^2 R(z)q_0^{-1} & N(z) \end{bmatrix} \begin{bmatrix} N^*(z) & -M_{n-2}^*(z) \\ -z^2 q_0^{*-1} R^*(z) & q_0^{*-1} Q_{n-1}^*(z) \end{bmatrix} = \begin{bmatrix} I & 0 \\ 0 & I \end{bmatrix} \tag{5.36}$$

and, in particular,

$$\left\{ R(z)q_0^{-1} \right\} N^*(z) = N(z) \left\{ q_0^{*-1} R^*(z) \right\}. \tag{5.37}$$

Note that the constant and linear terms in (5.37) yield

$$q_0 = q_0^* \tag{5.38}$$

and

$$q_0^{*-1}(n_1^* - r_1^*) = (n_1 - r_1)q_0^{-1}. \tag{5.39}$$

For later purposes, also observe the identity

$$\begin{bmatrix} q_{n-1} & \cdots & q_0 \\ & \ddots & \\ q_0 & & \end{bmatrix} q_0^{-1} \begin{bmatrix} q_{n-1}^* & \cdots & q_0^* \\ & \ddots & \\ & & q_{n-1}^* \end{bmatrix} - \begin{bmatrix} q_{n-2} & \cdots & q_0 & 0 \\ & \ddots & & \\ q_0 & & & \\ 0 & & & \end{bmatrix} q_0^{*-1} \begin{bmatrix} 0 & q_{n-1}^* & & q_0^* \\ & & \ddots & \\ & & & q_{n-1}^* \end{bmatrix}$$

$$= \begin{bmatrix} q_{n-1} \\ \cdot \\ \cdot \\ \cdot \\ q_0 \end{bmatrix} q_0^{-1} \begin{bmatrix} q_{n-1}^* , & \cdots & , q_0^* \end{bmatrix}, \tag{5.40}$$

which follows using (5.38).

Next, we proceed as in Corollary 5.1 by constructing right and left matrix Padé forms of type (m,n) for A(z). Set

$$U_m(z) = \left\{ P_{m-1}(z) \left[I + (n_1 - r_1)z \right] - L_{m-2}(z)z^2 \right\} q_0^{-1} \tag{5.41}$$

and

$$V_n(z) = \left\{ Q_{n-1}(z) \left[I + (n_1 - r_1)z \right] - M_{n-2}(z)z^2 \right\} q_0^{-1} .$$

(5.42)

Then, $U_m(z)$ and $V_n(z)$ provide a RMPFo of type (m,n) for A(z). To see this, note that the degree requirements are clearly satisfied. In addition, the columns of $V_n(z)$ are linearly independent since, in (5.42), $v_0 = I$. Finally,

$$A(z)V_n(z) - U_m(z)$$

$$= \left\{ \left[A(z)Q_{n-1}(z) - P_{m-1}(z) \right] \left[I + (n_1 - r_1)z \right] - z^2 \left[A(z)M_{n-2}(z) - L_{m-2}(z) \right] \right\} q_0^{-1}$$

$$= \left\{ z^{m+n-1}R(z) \left[I + (n_1 - r_1)z \right] - z^{m+n-1}N(z) \right\} q_0^{-1}$$

$$= z^{m+n-1} \left\{ (r_0 - n_0) + (r_1 + r_0(n_1 - r_1) - n_1)z + z^2 \left[\cdots \right] \right\} q_0^{-1}$$

$$= z^{m+n+1} \left\{ \cdots \right\} q_0^{-1} ,$$

(5.43)

since $n_0 = r_0 = I$.

Similarly, it can be shown that

$$U_m^*(z) = q_0^{*-1} \left\{ \left[I + (n_1^* - r_1^*)z \right] P_{m-1}^*(z) - L_{m-2}^*(z)z^2 \right\}$$

(5.44)

$$V_n^*(z) = q_0^{*-1} \left\{ \left[I + (n_1^* - r_1^*)z \right] Q_{n-1}^*(z) - M_{n-2}^*(z)z^2 \right\} .$$

(5.45)

provides a LMPFo of type (m,n) for A(z).

Note that (5.42) and (5.45), respectively, yield

$$-\begin{bmatrix} v_{n-1} & \cdots & v_0 \\ & & \\ & \cdot & \\ v_0 & & \end{bmatrix} = \begin{bmatrix} q_{n-1} & \cdots & q_0 \\ & & \\ & \cdot & \\ q_0 & & \end{bmatrix} q_0^{-1} + \begin{bmatrix} q_{n-2} & \cdots & q_0\, 0 \\ & & \\ q_0 & \cdot & \\ 0 & & \end{bmatrix} (n_1 - r_1) q_0^{-1}$$

$$-\begin{bmatrix} m_{n-3} & \cdots & m_0\, 0\, 0 \\ m_0 & & \\ 0 & \cdot & \\ 0 & & \end{bmatrix} q_0^{-1} \qquad (5.46)$$

and

$$\begin{bmatrix} v_n^* & \cdots & v_1^* \\ & & \\ & \cdot & \\ & & v_n^* \end{bmatrix} = q_0^{*-1} \begin{bmatrix} 0\, q_{n-1}^* & & q_1^* \\ & q_{n-1}^* & \\ & \cdot & \\ & 0 & \end{bmatrix} + q_0^{*-1} (n_1^* - r_1^*) \begin{bmatrix} q_{n-1}^* & & q_0^* \\ & \cdot & \\ & \cdot & \\ & & q_{n-1}^* \end{bmatrix}$$

$$- q_0^{*-1} \begin{bmatrix} m_{n-2}^* & & m_{-1}^* \\ & \cdot & \\ & \cdot & \\ & & m_{n-2}^* \end{bmatrix}. \qquad (5.47)$$

where $m_{-1}^* = 0$. Substituting (5.46) and (5.47) into (4.38), and rearranging terms, we obtain

$$H_{m,n}^{-1} = \begin{bmatrix} q_{n-2} & & q_0\, 0 \\ & & \\ q_0 & & \\ 0 & & \end{bmatrix} q_0^{-1} \begin{bmatrix} m_{n-2}^* & & m^* \\ & \cdot & \\ & & m_{n-2}^* \end{bmatrix} - \begin{bmatrix} m_{n-3} & & m_0\, 0\, 0 \\ & & \\ m_0 & & \\ 0 & & \\ 0 & & \end{bmatrix} q_0^{*-1} \begin{bmatrix} q_{n-1}^* & & q_0^* \\ & \cdot & \\ & & q_{n-1}^* \end{bmatrix}$$

$$+ \begin{bmatrix} q_{n-1} & \cdots & q_0 \\ & & \\ q_0 & & \end{bmatrix} q_0^{-1} \begin{bmatrix} q_{n-1}^* & \cdots & q_0^* \\ & \cdot & \\ & & q_{n-1}^* \end{bmatrix} - \begin{bmatrix} q_{n-2} & \cdots & q_0\, 0 \\ & & \\ q_0 & & \\ 0 & & \end{bmatrix} q_0^{*-1} \begin{bmatrix} 0\, q_{n-1}^* & & q_1^* \\ & \cdot & \\ & q_{n-1}^* & \\ & 0 & \end{bmatrix}$$

$$+ \begin{bmatrix} q_{n-2} & \cdots & q_0 & 0 \\ & & & \\ q_0 & \cdot & & \\ 0 & & & \end{bmatrix} \left\{ (n_1 - r_1)q_0^{-1} - q_0^{*^{-1}}(n_1^* - r_1^*) \right\} \begin{bmatrix} q_{n-1}^* & \cdots & q_0^* \\ & \cdot & \\ & & q_{n-1}^* \end{bmatrix}. \tag{5.48}$$

But, using (5.38) and (5.39), it is easy to see that (5.48) is exactly (5.33)

Remark 1. The inverse formula (5.33) can also be determined by bordering techniques. Indeed, equation (5.35) can be further manipulated to obtain

$$H_{m,n}^{-1} = \begin{bmatrix} H_{m-1,n-1}^{-1} & 0 \\ & \cdot \\ 0 & \cdots & 0 \end{bmatrix} + \begin{bmatrix} q_{n-1} \\ \cdot \\ \cdot \\ q_0 \end{bmatrix} q_0^{-1} \begin{bmatrix} q_{n-1}^* , & \cdots & , q_0^* \end{bmatrix}. \tag{5.49}$$

Equation (4.38) applied to $H_{m-1,n-1}^{-1}$, along with simplification using Lemma 4.2, converts (5.49) into (5.33).

The present proof takes its cue from the approach of sections 4 and 5. In each case, the inverse formula is obtained from (4.38) using Frobenius-type identities for matrix Padé forms. The Frobenius-type identities (5.41), (5.42), (5.44) and (5.45) used here can be found in [13] (see also chapter 2).

Remark 2. Notice that, if the matrix Padé forms (4.7), (4.8), (5.28) and (5.29) satisfy the conditions of Corollary 5.2 and are normalized according to (5.34), then

$$H_{m,n} \cdot \left\{ \begin{bmatrix} m_{n-2} \\ \cdot \\ m_0 \\ 0 \end{bmatrix} - \begin{bmatrix} q_{n-1} \\ \cdot \\ \cdot \\ q_0 \end{bmatrix} \cdot n_1 \right\} = \begin{bmatrix} 0 \\ 0 \\ I \\ n_1 \end{bmatrix} - \begin{bmatrix} 0 \\ 0 \\ 0 \\ I \end{bmatrix} n_1 = \begin{bmatrix} 0 \\ \cdot \\ 0 \\ I \\ 0 \end{bmatrix}. \tag{5.50}$$

Thus, the second last column of $H_{m,n}^{-1}$ is a combination of the coefficients of $M_{n-2}(z)$ and $Q_{n-1}(z)$. Similarly, one can obtain the second last row of $H_{m,n}^{-1}$ as a combination of the coefficients of $M_{n-2}^*(z)$ and

$Q^{\bullet}_{n-1}(z)$.   −

Conversely, suppose $X = [\, x_{n-1}, \; \cdots \; , x_0\,]^t$ and $Q = [\, q_{n-1}, \; \cdots \; , q_0\,]^t$, respectively, represent the second last and last block columns of the inverse of $H_{m,n}$. Then, if $\det(q_0) \neq 0$, we have that

$$H_{m,n}\left\{ \begin{bmatrix} x_{n-1} \\ \\ x_0 \end{bmatrix} - \begin{bmatrix} q_{n-1} \\ \\ q_0 \end{bmatrix} q_0^{-1}x_0 \right\} = \begin{bmatrix} 0 \\ 0 \\ I \\ -q_0^{-1}x_0 \end{bmatrix} \qquad (5.51)$$

so that

$$H_{m-1,n-1}\left\{ \begin{bmatrix} x_{n-1} \\ \\ x_1 \end{bmatrix} - \begin{bmatrix} q_{n-1} \\ \\ q_1 \end{bmatrix} q_0^{-1}x_0 \right\} = \begin{bmatrix} 0 \\ 0 \\ I \end{bmatrix}. \qquad (5.52)$$

This implies that

$$M_{n-2}(z) = z^{-1}\left\{ X(z) - Q_{n-1}(z)q_0^{-1}x_0 \right\} \qquad (5.53)$$

is a RMPFo denominator of type (m-2,n-2) for A(z). Similarly, we can obtain a LMPFo denominator of type (m-2,n-2) when we have the last and second last block rows of the inverse of $H_{m,n}$. Then substitution into (5.33) yields

$$H_{m,n}^{-1} = \begin{bmatrix} q_{n-2} & q_0 & 0 \\ \cdot & & \\ q_0 & & \\ 0 & & \end{bmatrix} q_0^{-1} \begin{bmatrix} x^{\bullet}_{n-1} & x^{\bullet}_0 \\ & \\ & x^{\bullet}_{n-1} \end{bmatrix} - \begin{bmatrix} x_{n-2} & x_0 & 0 \\ \cdot & & \\ x_0 & & \\ 0 & & \end{bmatrix} q_0^{\bullet-1} \begin{bmatrix} q^{\bullet}_{n-1} & q^{\bullet}_0 \\ & \cdot \\ & q^{\bullet}_{n-1} \end{bmatrix}$$

$$+ \begin{bmatrix} q_{n-2} & q_0 & 0 \\ \cdot & & \\ q_0 & & \\ 0 & & \end{bmatrix} q_0^{-1}(x^{\bullet}_0 - x_0)q_0^{\bullet-1} \begin{bmatrix} q^{\bullet}_{n-1} & q^{\bullet}_0 \\ & \cdot \\ & q^{\bullet}_{n-1} \end{bmatrix} + \begin{bmatrix} q_{n-1} \\ \cdot \\ \cdot \\ q_0 \end{bmatrix} q_0^{-1}\left[q^{\bullet}_{n-1}, \; \cdots \; , q^{\bullet}_0 \right]; \qquad (5.54)$$

whereas, substitution into (4.38) gives

$$
H_{m-1,n-1}^{-1} = \begin{bmatrix} q_{n-2} & & q_0 \\ \cdot & & \\ & \ddots & \\ q_0 & & \end{bmatrix} q_0^{-1} \begin{bmatrix} \overset{\bullet}{x}_{n-1} & & \overset{\bullet}{x}_1 \\ \cdot & & \\ & \ddots & \\ & & \overset{\bullet}{x}_{n-1} \end{bmatrix} - \begin{bmatrix} x_{n-2} & & x_0 \\ \cdot & & \\ & \ddots & \\ x_0 & & \end{bmatrix} \overset{\bullet}{q_0}^{-1} \begin{bmatrix} \overset{\bullet}{q}_{n-1} & & \overset{\bullet}{q}_1 \\ \cdot & & \\ & \ddots & \\ & & \overset{\bullet}{q}_{n-1} \end{bmatrix}.
\tag{5.55}
$$

Remark 3. In the scalar case, if $X = [\, x_{n-1}, \cdots, x_0 \,]^t$, and $Q = [\, q_{n-1}, \cdots, q_0 \,]^t$, respectively, represent the second last and last columns of the inverse of $H_{m,n}$, and $q_0 \neq 0$, then (5.54) and (5.55) reduce to

$$
H_{m,n}^{-1} = q_0^{-1} \left\{ \begin{bmatrix} q_{n-2} & & q_0 & 0 \\ \cdot & & \\ & \ddots & \\ q_0 & & \\ 0 & & \end{bmatrix} \begin{bmatrix} x_{n-1} & & x_0 \\ \cdot & & \\ & \ddots & \\ & & x_{n-1} \end{bmatrix} - \begin{bmatrix} x_{n-2} & & x_0 & 0 \\ \cdot & & \\ & \ddots & \\ x_0 & & \\ 0 & & \end{bmatrix} \begin{bmatrix} q_{n-1} & & q_0 \\ \cdot & & \\ & \ddots & \\ & & q_{n-1} \end{bmatrix} \right.
$$

$$
\left. + \begin{bmatrix} q_{n-1}^2 & \cdots & q_{n-1}q_0 \\ & & \\ & & \\ q_{n-1}q_0 & \cdots & q_0^2 \end{bmatrix} \right\}.
\tag{5.56}
$$

and

$$
H_{m-1,n-1}^{-1} = q_0^{-1} \left\{ \begin{bmatrix} q_{n-2} & & q_0 \\ \cdot & & \\ & \ddots & \\ q_0 & & \end{bmatrix} \begin{bmatrix} x_{n-1} & & x_1 \\ \cdot & & \\ & \ddots & \\ & & x_{n-1} \end{bmatrix} - \begin{bmatrix} x_{n-2} & & x_0 \\ \cdot & & \\ & \ddots & \\ x_0 & & \end{bmatrix} \begin{bmatrix} q_{n-1} & & q_1 \\ \cdot & & \\ & \ddots & \\ & & q_{n-1} \end{bmatrix} \right\}.
\tag{5.57}
$$

These are the original formulae of Gohberg and Krupnik [24].

Remark 4. Following the approach of section 4, we can also obtain conditions and inverse formulae for $H_{m-1,n-1}$ and $H_{m,n}$ when the first and second block column, along with the first and second block row, of the inverse of $H_{m,n}$ is given (c.f., Iohvidov [29]). Here, conditions and inverse formulae for $H_{m-1,n-1}$ and $H_{m,n}$ are stated in terms of matrix Padé forms of type (m,n-1) and (m+1,n-2). Additional formulae,

based on (4.39) rather than (4.38) can also be given.

5.4. Additional Inverse Formulae

The Frobenius-type relationships given in this chapter are but a small sample of similar recurrence relationships which exist between matrix Padé forms and which are developed by Bultheel ([10] , [14] , [13]). All the relationships require the existence of inverses of certain coefficients in the Padé forms involved. These requirements are always satisfied for normal matrix power series (where $H_{m,n}$ is nonsingular for all m and n). For this restricted class of power series, many of the recursive relationships provide directly algorithms for the computation of Padé forms. Depending on the path (within the Padé table) determined by the recurrence, Bultheel observes that the algorithms ([1] , [7] , [21] , [33] , [36] , [41] , [47]) which explicitly or implicitly compute the inverse of Hankel or Toeplitz matrices are equivalent to using an appropriate recurrence formula.

For a subset of these relationships, this chapter shows that each recurrence yields a separate closed formula for the inverse of a block Hankel. Algorithms based on recurrences which specify computations along an off-diagonal path (e.g., [1] , [7] , [41] [47]) yield closed formulae expressed by (4.38), (4.39) and (5.33). Those that specify computations along a staircase (e.g., [21] , [33] , [36]) yield formulae (5.4) and (5.27); whereas, those that specify computations along an anti-diagonal path yield (4.56) and (4.57). Additional closed formulae can be derived corresponding to other recurrences given by Bultheel.

5.5. Computation of Block Hankel Inverses

Formulas (5.4), (5.27), and (5.33) are equivalent to ones given by Gohberg-Heinig, and Gohberg-Krupnik, whereas (4.38), (4.39), (4.56) and (4.57) are new. A major advantage of the new formulae is that the underlying assumptions are far less restrictive than they are for (5.4), (5.27) and (5.33). Whereas, the new formulae require only that $H_{m,n}$ be nonsingular, the latter also require that an additional submatrix be

nonsingular. In addition, necessary and sufficient conditions for the existence of $H_{m,n}^{-1}$ are directly available from the coefficients of Padé forms. This provides a significant computational advantage.

Relaxed conditions provide little computational gain, however, if the available algorithms can function only under the more severe restrictions of normality. Unfortunately, this is true for most algorithms that compute nonscalar Padé forms or decompose block Hankel matrices. One exception in this regard is the MPADE algorithm of chapter 3. This algorithm is based on a recurrence relationship between Padé forms at successive nonsingular nodes along an off-diagonal path of the matrix Padé table (or, by reversing coefficients, along an anti-diagonal path). When the power series is normal, or, less restrictively, when all minors of the associated Hankel matrix are nonsingular (e.g., when the block Hankel matrix is positive definite), all the nodes along the path are nonsingular and then the recurrence relationship reduces to (5.42), which is one of many given by Bultheel. The methods based on this relationship are special cases of the MPADE algorithm.

For purposes of expressing the inverse of $H_{m,n}$ in terms of the new formulae (4.38), (4.39), (4.56) and (4.57), the MPADE algorithm is particularly suitable. Singularity is detected with no additional effort. When $H_{m,n}$ is nonsingular, the necessary Padé forms (i.e., the solutions of the associated block Yule-Walker equations) appearing in the formulae are simultaneously available on termination. The algorithm has no restrictions of normality. In addition, intermediate results enable the computation of the inverses of any nonsingular principal minors. When the power series is normal, the cost is the same as that of previously mentioned algorithms.

Using fast polynomial arithmetic in the normal case, Bitmead and Anderson [6] indicate that their scalar algorithm, based on a divide-and-conquer partitioning of the Hankel matrix, can be generalized to the nonscalar case with a cost complexity of $O(p^3 n \log^2 n)$. Under somewhat relaxed normality conditions (i.e., near-normality), Labahn [32] also gives an algorithm, an adaption of MPADE, with the same complexity.

In the scalar case, one call of an algorithm given by Cabay and Choi [16] can be used to construct the inverse formulae (4.38), (4.39), (4.56) or (4.57) with cost complexity $O(n \log^2 n)$ under no restrictions of normality. There are other methods (c.f. Sugiyama [44] for a survey) that also have the same complexity and succeed in the abnormal case. In particular, this is true of the scalar method of Bren -t al [8]. They use two calls of a fast anti-diagonal GCD algorithm, EMGCD, to determine the two Padé s required by the Gohberg-Semencul formula (5.4). The algorithm succeeds immediately if both $H_{m,n}$ and $H_{m,n-1}$ are nonsingular. If $H_{m,n-1}$ is singular (but $H_{m,n}$ is not), then a nonsingular matrix $H_{m,n+1}$ is first constructed. Two additional calls of the anti-diagonal algorithm are then made to yield the two Padé forms required by the second formula (5.27) of Gohberg and Semencul. By computing the inverse of $H_{m,n}$ using formula (4.56) or (4.57) their algorithm can now be altered so as to only require one call of their anti-diagonal algorithm.

Another significant drawback in basing an algorithm on the inverse formulae of Gohberg and Semencul has been observed by Bunch [15]. Because two distinct formulae are used to represent $H_{m,n}^{-1}$, depending on the status of singularities of relevant minors, the results are subject to numerical instability. No such problems are encountered with the use of the new formulae.

Chapter 6

Summary and Suggestions for Future Research

We have considered the problem of determining an adequate definition for a rational approximant of a formal matrix power series and also, given a suitable definition, the problem of computing it. We have restricted our attention to square matrix power series.

In attempting to extend the notion of Padé approximation to matrix power series, we have followed the classical theory of Padé approximants for scalar power series. We introduce the notion of a matrix Padé form, which always exist but may not be unique, and also the notion of matrix Padé fraction, which is unique but need not exist. The definition of matrix Padé form is meant to be as broad as possible. By constructing all the matrix Padé forms of type (m,n), it is always possible to determine ones for which the denominator is invertible, should one exist.

The notion of a matrix power series remainder sequence introduced in chapter 3 is a generalization of one given by Cabay and Kossowski [17] for scalar power series. The cofactor sequence, which is shown to be associated with the remainder sequence, yields directly all the matrix Padé fractions at the nonsingular nodes of a particular off-diagonal path of the matrix Padé table. By determining also the (unique) matrix Padé form at nodes preceeding the nonsingular nodes, we are able to compute matrix Padé fractions iteratively from one nonsingular node to the next. The resulting algorithm, MPADE, is at least as fast as other algorithms for computing matrix Padé fractions, and it is the only one that succeeds in the abnormal case.

The relationship between matrix Padé forms and block Hankel matrices has also between investigated in the study of the invertibility of such matrices. We show that a necessary and sufficient condition for the nonsingularity of a block Hankel matrix is the existence of four matrix Padé forms satisfying special conditions. Furthermore, when a block Hankel matrix is nonsingular we have presented a new set of closed formulae for the inverse in terms of these four matrix Padé forms. Unlike other inverse formulae, no extra conditions are required for these formulae to hold. The resulting formulae are practical since the required matrix Padé forms can be calculated by the MPADE algorithm of chapter 3. Indeed, the iterative

algorithm also calculates inverses of all nonsingular principal minors. It is at least as fast as other algorithms for computing inverses in the block case and is the only one that imposes no additional conditions. In the scalar case the required Padé forms can be calculated by the off-diagonal algorithm of Cabay and Choi [16]. The result is also an iterative algorithm that calculates inverses of some of the nonsingular principal minors and is faster than existing algorithms.

By using various Frobenius-type identities for matrix Padé forms, the formulae of chapter 4 give additional inverse formulae. Specifically, we have shown that the well known, more restrictive formulae of Gohberg-Krupnik [24], Gohberg-Semencul [23] and Gohberg-Heinig [25] follow from our closed formulae. Thus our approach, using matrix Padé forms, results in the unification of existing work on Hankel inverses.

With regards to the study of matrix Padé forms, there are many areas that can be researched. The MPADE algorithm can be improved in a number of ways. We expect that the cost of the decomposition of $T_{(s_i-1),s_i}$ in step 2.7 and consequently of $S_{(s_i-1),s_i}$ in step 3.1, can be achieved in time faster than $O(p^3 s_i^3)$, by taking advantage of the special structure of Sylvester matrices. The algorithm would also experience an improvement if it were possible to identify additional points between nonsingular nodes for which Theorem 3.5 is valid. This would improve the algorithm by decreasing the s_i. This, and in general the nature of matrix Padé forms between nonsingular nodes, is a subject for further research. Finally, by appealing to fast methods for polynomials, it is of interest to attempt to develop a recursive divide-and-conquer version of MPADE, in a fashion similar to one developed by Cabay and Choi [16] for the scalar case. This was done in the matrix case by Labahn [32] but under the restriction of near-normality.

For normal and nearly-normal power series, progressing from one nonsingular node to the next is equivalent to power series division of the residuals associated with the nonsingular nodes (because $S_{(s_i-1),s_i}$ in step 3.1 of MPADE, with the exception of one column, reduces to a triangular matrix). Thus, in this case when, in addition, $A(z)$ and $B(z)$ are matrix polynomials, there is a strong analogy between MPADE and Euclid's algorithm (for the scalar case, see Cabay and Choi [16]). It is thus of interest to use MPADE to

calculate the greatest common divisor of two matrix polynomials.

The calculation of a greatest common divisors of two matrix polynomials plays an important role in the study of minimal partial realizations of matrix sequences (c.f., Gragg and Lindquist [27]). The calcu' - tion problems in the matrix case, however, are significantly more complicated than the scalar case. Polynomial division is not always possible, hence Euclid's algorithm is not always applicable. Furthermore, the notion of relative primeness differs from the scalar case. Two matrix polynomials are relatively prime if their only common divisor is a unimodular polynomial, i.e., a matrix polynomial having a constant determinant (and hence, having a matrix polynomial as an inverse). Unlike the scalar case , trivial divisors (i.e., unimodular polynomials) may have nonzero degrees. Factoring out a common divisor may result in a rational expression having higher degrees though decreasing the degrees of the determinants).

At present we have partial results when matrix Padé forms are used in the study of the matrix GCD problem. For example, the numerator and denominater of a matrix Padé fraction occurring at a nonsingular node are relatively prime. The only common factors of the numerator and denominater of a predecessor Padé form must have a determinant of the form z^k. If the (m,n) node of the Padé table of (A(z),B(z)) is non-singular, where A(z) and B(z) have degrees n and m, respectively, then A(z) and B(z) are relatively prime.

The closed inverse formulae presented opens up many new potential research topics. At present we are also investigating closed inverse formulae for Sylvester matrices of the form (2.21) where it is not assumed that b_0 is nonsingular. More generally, we can follow the approach of chapter 4 to obtain closed inverse formulae for matrices of the form

$$S_{m,n} = \begin{bmatrix} a_0 & \cdots & a_n & | & b_0 & \cdots & b_m \\ & & & | & & & \\ & & & | & & & \\ & & & | & & & \\ a_{m+n+1} & \cdot & a_{m+2n+1} & | & b_{m+n+1} & \cdot & b_{2m+n+1} \end{bmatrix} \tag{6.1}$$

that is, of two Hankel-like matrices adjoined together to form one square matrix. Besides their use in Padé

approximantion, these matrices are also important in applying the Sylvester criterion for the relative prime-ness of two polynomials and for studying propagation through layered media . Necessary and sufficient conditions for determination of the nonsingularity of such generalized Sylvester matrices in the scalar case depends on the existence of three Hermite-Padé approximants (c.f., Baker [4]) for the pair $(A(z), z^{m-n} B(z))$. A closed formula for the inverse is then given in terms of these Hermite-Padé approximants. Unlike existing methods (c.f., Kailath et al [31]), our formula requires only that $S_{m,n}$ is nonsingular. The approach taken essentially follows the methods introduced in chapter 4. At present the formula has many favorable properties, especially in terms of storage requirements and evaluation costs. However, the formula is long and unwieldy so is not yet fully understood. In addition, there remains the problem of obtaining an efficient algorithm for the calculation of the required Hermite-Padé approximants that avoids unnecessary requirements of nonsingularity of certain submatrices. Existing recurrence relationships (c.f., Paszkowski [38]) have strong invertibilty requirements. A recurrence relation that does not require extra-invertibility has been obtained and an algorithm, using a similar approach found with the MPADE algo-rithm , is in progress. It is also expected that corresponding formulae, similar to the scalar formulae, also exists in the block generalized Sylvester case.

There is also the problem of obtaining a closed inverse formula for square matrices of the form

$$H'_{n_1, \cdots, n_k} = \begin{bmatrix} a_0 & \cdots & a_{n_r} & | & & | & b_0 & \cdots & b_{n_k} \\ & & \cdot & | & \cdots & | & & \\ & & \cdot & | & & | & & \\ a_u & \cdots & a_{u+n_1} & | & & | & b_u & \cdots & b_{u+n_k} \end{bmatrix}$$

(6.2)

where $u = n_1 + \cdots + n_k + k - 1$, that is, in the case where the matrix consists of k Hankel-like matrices where k is arbitrary. This is a problem in both the scalar and block cases. Again it is expected that neces-sary and sufficient conditions for the inverse will depend on the existence of certain Hermite-Padé approxi-mants (or block Hermite-Padé approximants), and that a closed formula can be given in terms of these approximants. We note that this problem ranges from the very structured case (k = 1) to the totally unstruc-tured (k = u) case.

An interesting corollary of any inverse formulae in the k Hankel-like case is that it will then provide inverse formulae in the block Hankel matrix case where the blocks are no longer square matrices, but rather matrices of a specific rectangular size. This follows from the ability to transform these block matrices into other block k Hankel-like matrices. For example, if

$$H_n = \begin{bmatrix} a_0 & \cdots & a_n \\ \vdots & & \vdots \\ a_{pn} & \cdots & a_{(p+1)n} \end{bmatrix} \tag{6.3}$$

where the a_i are 1 x p vectors

$$a_i = (b_i, \ldots, c_i), \tag{6.3}$$

then H_n can be transformed into

$$H'_{n,\ldots,n} = \begin{bmatrix} b_0 & \cdots & b_n & | & & | & c_0 & \cdots & c_n \\ & & & | & \cdots & | & & & \\ & & & | & & | & & & \\ b_{pn} & \cdots & b_{(p+1)n} & | & \cdots & | & c_{pn} & \cdots & c_{(p+1)n} \end{bmatrix} \tag{6.4}$$

by a permutation of the columns. H_n is nonsingular if and only if $H'_{n,\ldots,n}$ is nonsingular. In addition, any closed inverse formula for the scalar matrix $H'_{n,\ldots,n}$ will provide a closed inverse formula for H_n. When the a_i are q x p matrices, with $q > 1$, then H_n will be transformed into a block matrix $H'_{n,\ldots,n}$ and so a closed formula for the block matrix will provide an inverse formula for H_n in this case.

Chapter 7

Appendix: Validity of Initialization in MPADE Algorithm

It is required to show, in the case where $m < n$, that the $(U_1(z), V_1(z))$ computed by MPADE is a RMPFr for $(A(z), B(z))$ at the first nonsingular node (m_1, n_1) along the m-n offdiagonal path of the right matrix Padé table for $(A(z), B(z))$. In addition, we need to show that $(P_1(z), Q_1(z))$ is the predecessor of this nonsingular node.

To show the validity of the initialization step when $m < n$, we need

Lemma 7.1. $(U(z), V(z))$ is an RMPFo (RMPFr) of type (m, n) for $(A(z), B(z))$ if and only if $(z^k U(z), V(z))$ is an RMPFo (RMPFr) of type $(m+k, n)$ for $(z^k A(z), B(z))$

Proof: The result follows directly from (2.11).

When $m < n$, one complete pass through MPADE is required before $(U_1(z), V_1(z))$ are computed. Given the initial values (m_0, n_0), $(U_0(z), V_0(z))$ and $(P_0(z), Q_0(z))$ defined by steps 1.6 and 1.7 of MPADE (note that (m_0, n_0) defined here is different from the initialization given in (3.2)), the residuals computed in steps 2.5 and 2.6 then satisfy

$$R_0(z) = B(z) \tag{7.1}$$

and

$$W_0(z) = z^{n-m-1} A(z), \tag{7.2}$$

where, for convenience, the modulo operation has been dropped. Let s_0 be the smallest positive integer in step 2.1 such that $det(T_{(s-1),s}) \neq 0$, where $T_{(s-1),s}$ is determined from $R_0(z)$ and $W_0(z)$. Clearly, because of (7.2), $s_0 \geq n - m$.

Let $(U'(z), V'(z))$ be the RMPFr of type (s_0-1, s_0) for $(W_0(z), R_0(z))$ computed in step 3.1. Then, from (7.1) and (7.2) and Lemma 7.1, it follows that $U'(z)$ can be expressed as

$$U'(z) = z^{n-m-1} \cdot U^*(z),\tag{7.3}$$

where $(U^*(z), V'(z))$ is the RMPFr of type (s_0+m-n, s_0) for $(A(z), B(z))$ at the first nonsingular node along the m-n offdiagonal path of the right matrix Padé table for $(A(z), B(z))$.

Thus, it is required to show that $(U_1(z), V_1(z))$ computed by MPADE is equal to $(U^*(z), V'(z))$. But, step 5.3 yields

$$
\begin{bmatrix} U_1(z) \\ V_1(z) \end{bmatrix} = \begin{bmatrix} U_0(z) & P_0(z) \\ V_0(z) & Q_0(z) \end{bmatrix} \cdot \begin{bmatrix} I & 0 \\ 0 & z^2 \cdot I \end{bmatrix} \cdot \begin{bmatrix} V'(z) \\ U'(z) \end{bmatrix}
$$

$$
= \begin{bmatrix} 0 & z^{m-n-1} \cdot I \\ I & 0 \end{bmatrix} \cdot \begin{bmatrix} I & 0 \\ 0 & z^2 \cdot I \end{bmatrix} \cdot \begin{bmatrix} V'(z) \\ z^{n-m-1} \cdot U^*(z) \end{bmatrix}
$$

$$
= \begin{bmatrix} U^*(z) \\ V'(z) \end{bmatrix}\tag{7.4}
$$

as required. In addition, steps 5.1 and 5.2 yield

$$m_1 = m_0 + s_0 = s_0 + m - n\tag{7.5}$$

and

$$n_1 = n_0 + s_0 = s_0,\tag{7.6}$$

which specifies correctly the first nonsigular node along the m-n offdiagonal.

In a similar fashion, it can be shown that $(P_1(z), Q_1(z))$ computed in step 5.3 is the predecessor of $(U_1(z), V_1(z))$.

References

[1]   H. Akaike , "Block Toeplitz Matrix Inversion ", *SIAM J. Appl. Math* , Vol. 24, 1973, pp. 234-241 .

[2]   G.A. Baker, *Essentials of Padé Approximants*, Academic Press, New York, 1975.

[3]   G.A. Baker and P. Graves-Morris, *Padé Approximants Part I: Basic Theory*, Addison-Wesley , Reading , 1981.

[4]   G.A. Baker, "Invariance Properties in Hermite-Padé Approximation Theory", *J. of Comp. and Appl. Math*, Vol. 11, No. 1, 1984, pp. 49-56.

[5]   F.L. Bauer, The Quotient-Difference and Epsilon Algorithms, in *On Numerical Approximation*, R.E. Langer (ed.), University of Wisconsin Press, Madison, 1959, pp. 361-370.

[6]   R.R. Bitmead and B.D.O. Anderson , "Asmptotically Fast Solutions of Toeplitz and Related Systems of Linear Equations", *Linear Algebra Appl.* , Vol. 34 , 1980, pp. 103-116 .

[7]   N.K. Bose and S. Basu, "Theory and Recursive Computation of 1-D Matrix Padé Approximants", *IEEE Trans. on Circuits and Systems*, Vol. 4, 1980, pp. 323-325 .

[8]   R. Brent, F.G. Gustavson and D.Y.Y. Yun, "Fast Solution of Toeplitz Systems of Equations and Computation of Padé Approximants ", *J. of Algorithms* , Vol. 1, 1980, pp. 259-295.

[9]   F. Brophy and A.C. Salazar, "Considerations of the Padé Approximant Technique in the Synthesis of Recursive Digital Filters", *IEEE Trans. Audio and Electroacoustics*, Vol. AU-21, No. 6, Dec 1973, pp. 500-505.

[10]   A. Bultheel, "Recursive Algorithms for the Matrix Padé Table ", *Math. of Computation*, Vol. 35, 1980, pp. 875-892.

[11]   A. Bultheel , "Recursive Algorithms for Nonnormal Padé Tables", *SIAM J. Appl. Math*, Vol. 39, No. 1, 1980, pp. 106-118.

[12]   A. Bultheel, "Algorithms To Compute The Reflection Coefficients of Digital Filters", *Num. Methods of Approx. Theory*, Vol. 7, 1983, .

[13]   A. Bultheel , "Recursive Relations for Block Hankel and Toeplitz Systems Part I: Direct Recursions ", *J. Comp. and Appl. Math*, Vol. 10 , 1984, pp. 301-328 .

[14]   A. Bultheel , "Recursive Relations for Block Hankel and Toeplitz Systems Part II: Dual Recursions ", *J. Comp. and Appl. Math*, Vol. 10 , 1984, pp. 329-354 .

         J.R. Bunch , "Stability of Methods for Solving Toeplitz Systems of Equations", *SIAM J. Sci. Comput.*, Vol. 6, 1985, pp. 349-364 .

[16]   S. Cabay and D.K. Choi, Algebraic Computations of Scaled Padé Fractions, *SIAM J. of Computation* , Feb, 1986 , pp. 243-270.

[17]   S. Cabay and P. Kossowski , Power Series Remainder Sequences and Padé Fractions over Integral Domains , *J. of Symbolic Computation* , to appear .

[18]   D.K. Choi , *Algebraic Computations of Scaled Padé Fractions* , Ph.D. Thesis, University of Alberta, 1984.

[19]   J.E. Dennis , J.F. Traub and R.P. Weber , "The Algebraic Theory of Matrix Polynomials.", *SIAM J. Numer. Anal.*, Vol. 13 , 1976, pp. 831-845.

[20]   A. Draux , "The Epsilon Algorithm in a Non-commutative Algebra ", *J. Comp. Appl. Math* , Vol. 19 , 1987, pp. 9-21.

[21]   J. Durbin , "The Fitting of Time-Series Models ", *Rev. Inst. Internat. Stat.* , Vol. 28 , 1960 , pp. 233-244 .

[22]   O.I. Elgerd, *Control Systems Theory*, McGraw-Hill, New York, 1967.

[23]   I.C. Gohberg and A.A. Semencul , "On the Inversion of Finite Toeplitz Matrices and their Continuous Analogs ", *Mat. Issled*, Vol. 2 , 1972, pp. 201-233. (in Russian) .

[24]   I.C. Gohberg and N.Ya. Krupnik , "A Formula for the Inversion of Finite Toeplitz Matrices ", *Mat. Issled* , Vol. 2 , 1972, pp. 272-283. (in Russian) .

[25]   I.C. Gohberg and G. Heinig , "Inversion of Finite Toeplitz Matrices made of elements of a Non-commutative Algebra "; *Rev. Roum. Math. Pures Et Appl.*, Vol. XIX, No. 5 , 1974, pp. 623-663. (in Russian) .

[26]   W.B. Gragg , "The Padé Table and its Relation to Certain Algorithms of Numerical Analysis ", *SIAM Rev.*, Vol. 14, 1972 , pp. 1-61.

[27]   W.B. Gragg and A. Lindquist, "On the Partial Realization Problem ", *Lin. Alg. and Appl.* , Vol. 50 , 1983, pp. 277-319 .

[28]   F. de Hoog, "A New Algorithm for Solving Toeplitz Systems of Equations", *Linear Algebra Appl.* , Vol. 88 , 1987, pp. 123-138 .

[29]   I.S. Iohvidov , *Hankel and Toeplitz Matrices and Forms* , Birkhauser , Boston, 1982.

[30]   T. Kailath , A. Vieira and M. Morf , "Inverses of Toeplitz Operators, Innovations and Orthogonal Polynomials ", *SIAM Review* , Vol. 20, 1978 , pp. 106-119.

[31]   T. Kailath , S.Y. Kung and M. Morf , "Displacement Ranks of Matrices and Linear Equations", *J. Math. Anal. Appl.* , Vol. 68 , 1979 , pp. 395-407 .

[32]   G. Labahn , *Matrix Padé Approximants* , M.Sc. Thesis, Dep't of Computing Science, University of Alberta, Edmonton, Canada, 1986.

[33]   N. Levinson , "The Wiener RMS (root mean square) Error in Filter Design ", *J. Math. and Phys.* , Vol. 25 , 1947, pp. 261-278 .

[34]   J. Makhoul, "Linear Prediction: A Tutorial Review", *Proc. IEEE*, Vol. 63, April 1974, pp. 561-580.

[35]   R.J. McEliece and J.B. Shearer , "A Property of Euclid's Algorithm and an Application to Padé Approximation", *SIAM J. Appl. Math*, Vol. 34, 1978, pp. 611-617 .

[36]   M. Morf , A. Vieira and D. T. Lee , Ladder Forms for Identification and Speech Processing , *Proc. Conf. on Decision and Control* , Dec. 7-9, 1977 .

[37]   G. Nemeth and M. Zimanyi, "Polynomial Type Padé-Approximants", *Math. of Comp.*, Vol. 38, 1982, pp. 553-565.

[38]   S. Paszkowski, "Recurrence Relations in Padé-Hermite Approximation", *J. of Comp. and Appl. Math*, Vol. 19, 1987, pp. 99-107.

[39]   J. Rissanen , "Solution of Linear Equations with Hankel and Toeplitz Matrices ", *Numer. Math* , Vol. 22, 1974 , pp. 361-366.

[40]   J. Rissanen, Recursive Evaluation of Padé Approximants for Matrix Sequences, *IBM J. Res. Develop.*, 1972, pp. 401-406.

[41]   J. Rissanen, "Algorithms for Triangular Decomposition of Block Hankel and Toeplitz Matrices with Application to Factoring Positive Matrix Polynomials", *Math. Comp.*, Vol. 27, 1973, pp. 147-154.

[42]   H. Rutishauser, "Der Quotient-Differenzen-Algorithm", Z. *Angew. Math. Phys.*, Vol. 5, 1954, pp. 233-251.

[43]   Y. Starkand, "Explicit Formulas for Matrix-valued Padé Approximants", *J. of Comp. and Appl. Math*, Vol. 5, No. 1, 1979, pp. 63-65.

[44]   Y. Sugiyama , "An Algorithm for Solving Discrete-time Wiener-Hopf Equations based on Euclid's Algorithm ", *IEEE Trans. Inform. Theory* , Vol. 32 ; 1986, pp. 394-409.

[45]   W.F. Trench , "An Algorithm for the Inversion of Finite Hankel Matrices", *SIAM J. Appl. Math* , Vol. 13 , 1965, pp. 1102-1107 .

[46]   H. Wakita, "Direct Estimation of the Vocal Tract Shape by Inverse Filtering of Acoustic Speech Waveforms", *IEEE Trans. Audio and Electroacoustics*, Vol. AU-21, No. 5, Oct 1973, pp. 417-427.

[47]   R.A. Wiggens and E.A. Robinson , "Recursive Solution to the Multichannel Filtering Problem ", *J. Geophys. Res.* , Vol. 70, 1965 , pp. 1885-1891 .

[48]   P. Wynn, "The Rational Approximation of Functions which are formally defined by a power series expansion", *Math. Comp.*, Vol. 14, 1960, pp. 147-186.

[49]   S. Zohar , "Toeplitz Matrix Inversion: The Algorithm of W.F. Trench ", *J. ACM* , Vol. 16 , 1969, pp. 592-601 .

NOTICE

AVIS

The quality of this microform is heavily dependent upon the quality of the original thesis submitted for microfilming. Every effort has been made to ensure the highest quality of reproduction possible.

If pages are missing, contact the university which granted the degree.

Some pages may have indistinct print especially if the original pages were typed with a poor typewriter ribbon or if the university sent us an inferior photocopy.

Previously copyrighted materials (journal articles, published tests, etc.) are not filmed.

Reproduction in full or in part of this microform is governed by the Canadian Copyright Act, R.S.C. 1970, c. C-30.

La qualité de cette microforme dépend grandement de la qualité de la thèse soumise au microfilmage. Nous avons tout fait pour assurer une qualité supérieure de reproduction.

S'il manque des pages, veuillez communiquer avec l'université qui a conféré le grade.

La qualité d'impression de certaines pages peut laisser à désirer, surtout si les pages originales ont été dactylographiées à l'aide d'un ruban usé ou si l'université nous a fait parvenir une photocopie de qualité inférieure.

Les documents qui font déjà l'objet d'un droit d'auteur (articles de revue, tests publiés, etc.) ne sont pas microfilmés.

La reproduction, même partielle, de cette microforme est soumise à la Loi canadienne sur le droit d'auteur, SRC 1970, c. C-30.

Canada

THE UNIVERSITY OF ALBERTA

Computer Modelling of the Adsorption of Non-Volatile

Organic Compounds on XAD-2 Resin

BY

Donald Kenneth Noot

A THESIS

SUBMITTED TO THE FACULTY OF GRADUATE STUDIES AND RESEARCH

IN PARTIAL FULFILMENT OF THE REQUIREMENTS FOR THE DEGREE OF:

MASTER OF SCIENCE

IN

ENVIRONMENTAL SCIENCE

DEPARTMENT OF CIVIL ENGINEERING

EDMONTON, ALBERTA

FALL, 1988

THE UNIVERSITY OF ALBERTA

RELEASE FORM

NAME OF AUTHOR: Don Noot

TITLE OF THESIS: Computer Modelling of the Adsorption of Non-Volatile

Organic Compounds on XAD-2 Resin.

DEGREE: Master of Science

YEAR THIS DEGREE GRANTED: 1988

Permission is hereby granted to THE UNIVERSITY OF ALBERTA LIBRARY to reproduce single copies of this thesis and to lend or sell such copies for private, scholarly or scientific research purposes only.

The author reserves other publication rights, and neither the thesis nor extensive abstracts from it may be printed or otherwise reproduced without the author's written permission.

#46 355 Sandringham Cres.

London, Ontario, Canada

N6C 5K9

Date:

THE UNIVERSITY OF ALBERTA

FACULTY OF GRADUATE STUDIES AND RESEARCH

The undersigned certify that they have read, and recommend to the
Faculty of Graduate Studies and Research for acceptance, a thesis entitled:

Computer Modelling of the Adsorption of Non-Volatile

Organic Compounds on XAD-2 Resin

submitted by Donald Kenneth Noot

in partial fulfilment of the requirements for the degree of

Master of Science

in Environmental Science

_____
Supervisor

_____

_____

Date: July 8, 1988

To Doreen, Alexander and Ashley

Abstract

This study was performed in an attempt to gain understanding of the competitive adsorption effects of non-volatile organic compounds on XAD-2 resin in order to improve their recovery from water samples. Single solute isotherms were performed for the pesticide Lindane and the herbicide Triallate. The resulting Freundlich parameters were used to predict the competitive adsorption effects in a bi-solute system with a computer model based on Ideal Adsorbed Solution Theory. Bi-solute isotherms were experimentally determined and compared to computer predictions. The model was shown to predict the trends in adsorption, but imprecise isotherm data lead to errors in the predictions. The Equilibrium Column Model was used to predict column breakthrough in a bi-solute system. Column experimentation showed breakthrough to occur before predictions, since the model's assumption of no resistance to mass transfer was not valid for short bed contact times.

v

Acknowledgements

Table of Contents

List of Appendices

List of Tables

List of Figures

List of Abbreviations

ACS	American Chemical Society
APE	Average Percent Error
DCM	Dichloromethane
DCPA	Dimethyl-2,3,5,6-tetrachloroteraphthalate
DOM	Dissolved Organic Matter
ECD	Electron Capture Detector
ECM	Equilibrium Column Model
GC	Gas Chromatography
GC/MS	Gas Chromatography/Mass Spectrometry
HCE	Hexachloroethane
HCB	Hexachlorobenzene
HPLC	High Performance Liquid Chromatography
IAST	Ideal Adsorbed Solution Theory
Kd	Distribution Coefficient
LLS	Linear Least Squares
MADAM-HSD	Michigan Adsorption Design and Application Model - Homogenous Surface Diffusion
nM	nanoMolar
NLLS	Non-Linear Least Squares
RSS	Residual Sum of Squares
TCEP	tris(2-Chloroethyl) phosphate
TLC	Thin Layer Chromatography
TOC	Total Organic Carbon

1.0 Summary

XAD-2 resin is commonly used in the sampling of trace organic contaminants in drinking water and source waters for chemical and biological testing. This study was performed in an attempt to gain understanding of the competitive adsorption effects of compounds associated with health risk with respect to sampling methodology. The pesticide Lindane and herbicide Triallate were chosen as model compounds.

Single solute adsorption experiments showed that resin which had been previously used in a routine sampling procedure exhibited no loss in adsorption capacity or rate of adsorption for Lindane.

Two computer models were utilized in the study. A model based on Ideal Adsorbed Solution Theory was used to predict competitive behaviour in a bi-solute system from single solute isotherm data. Bi-solute isotherms were conducted as experimental verification of the model's predictions. The model predicted the trends in adsorption, but imprecise isotherm data and non-Freundlich adsorption behaviour resulted in erroneous predictions. The predictions were less accurate for Lindane, the more weakly adsorbing compound.

The Equilibrium Column Model (ECM) was used to predict breakthrough of Lindane and Triallate in column adsorption experiments. Column experiments performed at various resin contact times demonstrated that resistance to mass transfer is significant, resulting in immediate breakthrough at short contact times. ECM predictions were in error since the model assumes no mass transfer resistances. This assumption was not valid under the experimental conditions tested.

2.0 Introduction

Much study in recent years has been directed to the analysis of trace organic contaminants in water supplies and finished drinking water. The detection and identification of more and more compounds has been facilitated by advances in analytical techniques, and the knowledge of their presence has sparked public and scientific concern. Many studies have been performed to identify some of the compounds and to gain more understanding of the possible health effects associated with them. One means of screening for potential health risk is bacterial mutagenicity testing.

Mutagenicity testing is a biological procedure which determines if compounds present in the sample will cause genetic damage. Since the levels of organics in the water matrix are generally very low, a concentration step must be employed prior to biological testing. One common means of achieving this concentration step is by resin adsorption/desorption. The Amberlite® XAD resins, especially XAD-2, have been utilized often in these applications. These resins also provide one means of concentrating samples prior to chemical testing.

In resin adsorption/desorption, as with other methods of extraction, certain groups of chemicals are extracted more efficiently than others. Many factors affect a compound's extraction efficiency, including the compound's affinity for the resin and solubility in the water matrix. Also, since a limited capacity for adsorption exists (adsorption sites), competitive adsorption can play an important role in the extraction efficiency of a compound.

Computer models have recently been developed for activated carbon adsorption, in which the competitive adsorption effects of organic compounds can be predicted. Since few studies involving XAD-2 resin have dealt with the development of a rational sampling protocol, this study involves the application

2

of the computer adsorption models to gain a better understanding of competitive adsorption effects on XAD-2 resin.

The objectives of this study were twofold: 1) to evaluate the application of the computer models, which were developed for use with activated carbon, to the adsorption of non-volatile organic chemicals on XAD-2 resin, and 2) to aid in the development of a rational sampling protocol in order to improve the extraction and hence detection of compounds associated with health risk in water.

3.0 Scope of Investigation

At the beginning of the study, a scope of the investigation was established. As a result the study was divided into five phases.

The first phase consisted of a review of the literature and model compound selection. Several criteria were established and experimentation performed in order to select compounds to be used in the adsorption experiments. Phase 1 began in April, 1987 and ended in October, 1987. Some overlap with Phase 2 occurred since adsorption experiments began prior to completion of compound selection experimentation.

Single solute isotherm experiments were performed in Phase 2 of the study, since the IAST computer model requires single solute isotherm data as input. All isotherms were executed using pure water solutions. To determine the effects of resin re-use in routine sampling, adsorption experiments were also performed with resin which had been preloaded with background organics through repeated use in a prior study.

Single solute experiments began in September, 1987 and the last was performed in April, 1988. Most of the study was spent attempting to improve the quality of the single solute isotherm results. Various difficulties were encountered and many different modifications made to the experiments. The results did improve, but even the last isotherms obtained were not of as high quality as originally hoped for.

Phase 3 involved obtaining bi-solute isotherm results for use as experimental verification of computer model predictions. Several bi-solute isotherms were performed during March and April, 1988.

Phase 4 of the study consisted of using a computer model based on Ideal Adsorbed Solution Theory (IAST) to predict the competitive adsorption effects from single solute isotherm data, and comparing these predictions to

4

experimental bi-solute data. This phase began when bi-solute isotherm data became available, in April, 1988 and was completed in June, 1988.

The last phase of the study, phase 5, involved use of a simple column model, the Equilibrium Column Model (ECM), to predict column behaviour such as order of breakthrough and bed volumes-to-breakthrough. Using the output from this model, column experiments were designed and performed in an attempt to experimentally verify the model predictions. All column work was performed in May and June of 1988.

Figure 3. gives a graphic representation of the time schedule for the five phases of the study.

4.0 Technical Background

4.1. Introduction

Despite recent advances in the detection and identification of trace organic contaminants in water, it is evident that only a small fraction of the substances in waters have been characterized (Giabbai et al., 1983). Many sources exist for the diverse range of natural and synthetic organic compounds in water. Many studies have been performed to assess the potential health risks that may be associated with exposure to these compounds. Initially, the approach of these studies was the identification of the compounds present in the water and review of the relevant toxicity data (Fawell and Fielding, 1985). The toxicity data were relatively limited for this application, however, which led to a difficulty in establishing a practical significance of the chemical findings. Therefore a different approach evolved which combined both chemical analysis and genotoxicity tests (for example, bacterial mutagenicity tests) in an attempt to correlate potential health risk and chemical content.

With the increased awareness of the health risk associated with organics in drinking water, future trends for regulatory agencies include monitoring and reporting requirements for many organic chemicals, with special attention to pesticides (Cortruvo, 1985). More synthetic organic chemicals are being included as revisions to drinking water standards occur in both Canada and the United States (Toft, 1985). With these regulatory trends comes the need for standardized methods of recovery and analysis to be used in the monitoring of drinking water supplies and finished waters.

Many different methods have been utilized in the analysis of organic micropollutants in water. Some of these methods include liquid/liquid extraction, freeze drying, reverse osmosis and adsorption/desorption on activated carbon or synthetic resins. Each method has advantages and

6

disadvantages, and as such some are more particularly suited to accomplish specific objectives (Wilcox et al., 1986). In studies which incorporate mutagenicity testing, the method of choice has often been resin adsorption/desorption (Daignault et al., 1988), with the Amberlite® XAD resins being used most frequently. This method has low initial and operating expenses, is simple to use, and large amounts of water can be sampled resulting in high concentration factors. A high concentration factor is highly desirable since the trace organics in water are usually present at extremely low levels and thus must be concentrated for biological testing, as well as chemical analysis. Some disadvantages of the method include extensive resin cleaning procedures and artifact interferences. Also, due to the non-polar polymeric structure of the XAD-2 and XAD-4 resins, generally non-polar compounds are extracted while polar compounds are not (XAD-7 and XAD-8 are slightly more polar than XAD-2 and XAD-4 in polymeric structure). This is perhaps the most severe disadvantage, since the compounds extracted and the efficiency of extraction depend on many parameters, ranging from the experimental sampling conditions to the water matrix being sampled (Daignault et al. 1988).

In using resins, many researchers employ different experimental adsorption and desorption conditions. Adsorption conditions include flow rate (contact time), water-to-resin ratio (resin capacity), temperature and pH. Desorption conditions include the specific organic solvent or mixture used as eluant, the flowrate and the volume of eluant (bed volumes) used. As such, inter-study comparisons are often difficult due to the differences in the water matrix and experimental conditions (Wilcox et al., 1986; Noot et al., 1988).

While many researchers utilize their own experimental methods, there is little evidence in the literature involving mutagenicity testing which suggests an experimentally determined sampling protocol for resin adsorption/desorption

processes. For example, Van Rossum (1985) mentions that some compounds may be displaced from the XAD resin during sampling by more strongly adsorbing substances, but does not test at different sample volumes to determine the effect. Therefore this study was devised to attempt to gain an understanding of the competitive adsorption effects between model compounds and thereby aid in sampling method design.

4.2 Technical Information on XAD-2 Resin

XAD-2 resin, manufactured by Rohm and Haas (Philadelphia, PA.) is a styrene/divinylbenzene crosslinked copolymeric adsorbent. This synthetic resin is supplied in the form of white beads in the 20-50 mesh size fraction. Each bead consists of a large number of smaller microspheres. As a result of this macroreticular structure, the pore size distribution is quite uniform. Other characteristics include chemically homogenous non-ionic structure, good physical durability and large surface area. Although water readily penetrates the pores, it has been suggested that the materials being adsorbed do not penetrate to a substantial amount (Rohm and Haas, technical bulletin, 1978). This fact, along with the relatively weak physical adsorption (Van der Waal's forces) facilitates the desorption of the adsorbed compounds by solubility changes (solvent changes). The physical characteristics of XAD-2 resin are given in Table 4.2.1.

4.3 Uses of XAD-2 Resin

Amberlite XAD-2 resin has been used in many different applications. The following list is by no means exhaustive, but demonstates the diversity of applications of the resin.

- separation of proteins (Cheetham, 1979; Dunlop, 1978)

- separation/extraction of drugs (O'Connor, 1975; Ibrahim et al., 1975; Cantwell, 1976; Stolman and Pranitis, 1977; Mohammed and Cantwell, 1978)
- drug analysis in forensics (Bogusz, 1982; Bogusz et al., 1978)
- stationary phase in TLC (Pietrzyk et al., 1979; Rao and McLennon, 1977)
- stationary phase in HPLC (Kroeff and Pietrzyk, 1978; Baum et al., 1980; Pietrzyk and Chu, 1977; Hux et al., 1982)
- ion exchange (Khan and Cantwell, 1985)
- organics in air (Gluck and Melcher, 1980; Farwell at al., 1977)
- organics in wastewater (Glaze et al., 1973; Lawrence and Tosine, 1976; Rogers and Mahood, 1977)
- organics in rain (Strachan and Huneault, 1984)
- mutagenicity testing (De Raat and Van Ardenne, 1984; Huck et al., 1987)
- organic acids in water (Rosenfeld et al., 1984)
- pesticides and other toxins in water (Coburn et al., 1977; Levesque and Mallet, 1983; LeBel et al., 1986).

One of the first studies in which XAD-2 resin was utilized to extract neutral organics from drinking water was that by Burnham et al. (1972). Since then, many researchers have used XAD-2 resin for the analysis of organic contaminants in water. The reader is referred to a recent review compiled by Daignault et al. (1988) which describes the use of XAD resins in organic analysis in water. One of the common uses of XAD-2 resin is the concentration of organics for mutagenicity testing. A recent review on this topic was compiled by Noot et al. (1988).

4.4 Computer Models

This section first describes the theoretical basis of the two computer models used, and then revie briefly the use of the models by others. The models were originally obtained from Dr. John C. Crittenden of Michigan Technological University. Details concerning their running on the University of Alberta's computer system are provided by Huck and Andrews (1988).

4.4.1 Ideal Adsorbed Solution Theory

Ideal Adsorbed Solution Theory (IAST) was originally developed from thermodynamic considerations including ideal gas behaviour and Gibb's equation relating the amount of a substance adsorbed to the change in surface tension with the activity of the solution phase (Kong and DiGiano, 1986). Initially it described adsorption from a gas phase to a solid phase, and was later extended to describe adsorption from dilute liquids. The theory is useful in that competitive adsorption in multi-component systems can be predicted from single solute data. The following five equations are used in the prediction of multi-component equilibria (Crittenden et-al., 1985c):

$$q_T = \sum_{i=1}^{N} q_i \tag{1}$$

$$z_i = \frac{q_i}{q_T} \qquad i = 1 \text{ to } N \tag{2}$$

$$C_i = z_i C_i^{\circ} \qquad i = 1 \text{ to } N \tag{3}$$

$$1/q_T = \sum_{i=1}^{N} z_i/q_i^o \tag{4}$$

$$\pi_m = \frac{RT}{A} \int_0^{q_i^o} \frac{d \ln C_i^o}{d \ln q_i^o} \, d q_i^o = \pi_i^o \tag{5}$$

$$= \frac{RT}{A} \int_0^{q_j^o} \frac{d \ln C_j^o}{d \ln q_j^o} \, d q_j^o = \pi_j^o = \ldots \text{ for } j = 2 \text{ to } N$$

Equation 1 and 2 account for mass balance where

q_T is the total surface loading,

q_i is the surface loading for component i, and

z_i is the mole fraction of component i on the surface.

Equation 3 is analogous to Raoult's law, where

C_i is the equilibrium liquid phase concentration, and

C_i^o is the single solute equilibrium liquid phase concentration.

Equation 4 states that at the spreading pressure of the mixture, no area change per mole occurs from the single solute isotherms upon mixing. The spreading pressure (π) is 'a measure of the decrease in surface tension caused by the presence of sorbed phase' (Kong and DiGiano, 1986).

Equation 5 equates the spreading pressures of the single solute isotherms to that of the mixture, where

π_m = spreading pressure of the mixture,

π_i^o & π_j^o = single solute spreading pressures of individual

components,

R = ideal gas constant,

T = absolute temperature, and

A = specific surface area of the adsorbent.

If an isotherm equation is used to describe the data, equation 5 simplifies and can be manipulated to eliminate C_i. Typically, the Freundlich equation is used. The model is then able to calculate both liquid and solid phase concentrations if the Freundlich parameters K and 1/n, the initial liquid phase concentration and the adsorbent doses are known (Crittenden et al., 1985c).

In predicting multi-component adsorption, errors may occur from an extrapolation of the single solute isotherms to zero and high concentrations (Crittenden et al., 1985c). If the single solute isotherm is not linear in the range tested, or is not entirely accurate, then problems with the prediction will arise since the errors in the single solute data are amplified as extrapolation occurs. A plot of ($d \ln C_i^{\circ}$ / $d \ln q_i^{\circ}$) versus q_i° shows the range of extrapolated data used in the predictions, and therefore may be used to evaluate the extent of the extrapolation of single solute isotherms.

Since IAST was developed from ideal gas behaviour, it assumes that the activity coefficients are unity in both solid and liquid phases. A non-ideal lower activity may occur in the solid phase. No satisfactory method is available, however, to account for this effect (Kong and DiGiano, 1986).

For the purpose of comparing the predicted solid phase concentrations to experimentally determined multi-component isotherm data, a calculation of the Average Percent Errors (APEs) is used. This calculation includes division by the observed (experimental) value, which results in a normalized estimate of fit. As such, APEs represent a superior means of comparison over the Residual Sum of Squares method, for data of differing magnitudes (eg. solutes with different adsorption behaviour). The following equation is used to calculate the APEs:

$$APE = \frac{100}{N} \sum \frac{\left|observed\ value - predicted\ value\right|}{observed\ value} \qquad (6)$$

where N = number of sample points

4.4.2 Equilibrium Column Model

The Equilibrium Column Model (ECM) is a relatively simple column model in that it assumes no resistance to mass transfer. The model, which uses IAST to predict competitive adsorption effects in multi-component solutions, may be used to predict the elution order, breakthrough and highest effluent concentrations (overshoot concentrations) of each component (Crittenden et al., 1987). The model requires Freundlich single solute isotherm parameters, influent concentrations and physical adsorbent property data as input. Since no resistance to mass transfer is assumed, a square breakthrough wave is predicted rather than the observed 'S shaped' curve.

In order to predict breakthrough, ECM divides the column into zones that contain unique combinations of the components, the combination depending on their relative intensity of adsorption. The first zone at the influent end contains all components, but mostly the most strongly adsorbing. This compound is present only in this zone. The second most strongly adsorbed compound is present only in the first two zones, but mostly in the second, since the most strongly adsorbing compound competes more effectively in the first zone and therefore displaces the weaker compounds. Similar arguments are made for all other components. As such, the most weakly adsorbing compound will be present mainly in the last (near the effluent end) zone.

When breakthrough of all but the most strongly adsorbing compound occurs, the effluent concentration will be higher than the influent concentration

due to its displacement by stronger adsorbers. This high concentration is termed the overshoot concentration.

Output of the model includes the bed volumes fed to breakthrough, the velocity of the centre of mass of each wavefront and the treatment capacity for each component, as well as the concentration in individual zones, the average surface loading and single solute treatment capacities.

4.4.3 Use of the Computer Models by Others

In a survey of the literature, only one research paper was found to have applied competitive modelling to synthetic resin adsorption (Kong and DiGiano, 1986). In this study, resin (XE-340) and carbon adsorption of volatile chlorinated hydrocarbons were compared. Based on kinetics experiments, the resin was allowed to equilibrate for 14 days and the carbon for 7 days. IAST was used to model the adsorption, which was fitted to the Singer-Yen isotherm equation (see Appendix 4). This three parameter equation is a modification of the Freundlich equation and better describes the equilibrium data at very low concentrations. IAST was shown to predict some of the competition on the resin, but not for all compounds. For compounds with little difference in competitiveness, the model predicted larger shifts from the single solute isotherm than was experimentally observed in multi-component isotherms.

van Vliet et al. (1980) compared phenol adsorption on two activated carbons and eight synthetic adsorbents, among them XAD-2 resin. Adsorption data were fitted to an isotherm equation developed by the authors. Kinetics and batch experiments were performed to determine data required for column modelling. Experimental column breakthrough was shown to be predicted by a fixed-bed adsorption model, which incorporated mass transfer considerations.

The IAST computer model (used in the current study) was developed for use with activated carbon. Crittenden et al. (1985c) observed that IAST predictions were satisfactory for one- and two-carbon chlorinated hydrocarbons on three different activated carbons. Andrews et al. (1987) showed IAST to successfully predict the competitive adsorption of trihalomethanes. IAST was also shown to predict multicomponent adsorption in background mixtures of unknown composition (Crittenden et al., 1985b).

Crittenden et al. (1987) used the ECM to predict pilot scale fixed-bed adsorber breakthrough of volatile organics. The results indicated that for small empty bed contact times, the effects of mass transfer were appreciable, and the actual breakthrough occurred before the model prediction. Breakthrough of trihalomethanes in full-scale carbon contactors was successfully modelled using ECM (Huck and Andrews, 1988).

The adsorption of the pesticide Lindane on activated carbon was studied with respect to background dissolved organic matter (DOM, Smith et al., 1987). The kinetics and capacity of adsorption were studied and mass transfer parameters obtained. The adsorption of Lindane in a fixed-bed adsorber was predicted using the Michigan Adsorption Design and Applications Model employing Homogenous Surface Diffusion (MADAM-HSD). Results showed that the presence of DOM reduced the rates of transport of Lindane, resulting in a decrease in the rate and capacity of Lindane adsorption. Lindane breakthrough was successfully predicted by MADAM-HSD.

Other uses of the results from adsorption models include the design of fixed-bed adsorbers (Crittenden et al., 1985a) and evaluating the cost and performance of adsorption systems (Clark, 1987).

5.0 Materials, Methods and Development

5.1 Solvents

All solvents used in the study (acetone, hexane, dichloromethane (DCM), and methanol) were either pesticide grade or purchased as ACS grade and then doubly distilled. The only exception was the methanol used for the resin washing procedure (discussed later), which was used as ACS grade. Solvents were purchased from Fisher Scientific and BDH Chemicals Canada Ltd.

5.2 Model Compounds and Reagents

Lindane, Triallate, *trans*-Chlordane, Methoxychlor and p,p' DDE were obtained indirectly from Standards and Information (Pesticide Laboratory), Laboratory Services Division, Agriculture Canada. These compounds were of high purity since they were intended for use as analytical standards. Tris(2-chloroethyl) phosphate (TCEP) was purchased from Aldrich Chemical Company Inc. in 97% pure form. Hexachloroethane (purity not stated) was obtained from Terochem Laboratories Inc. Dimethyl-2,3,5,6-tetrachloroteraphthalate (DCPA) was purchased from Alpha Products. All compounds were used as received except DCPA.

The stated purity for DCPA was 97+%, but GC/MS analysis revealed that it was highly contaminated with Hexachlorobenzene (HCB), and thus required purification prior to use. This compound was purified by column chromatography using florisil. The florisil was activated at 550°C for 2 hours and then deactivated with water (3%, w/w). The contaminated DCPA was dissolved in DCM and diluted with hexane before application to a 50 g Florisil column. The HCB was eluted with hexane and two other minor contaminants with 25% DCM in hexane. The DCPA was then eluted with DCM. The eluant

composition was monitored by GC/ECD and those fractions containing the most DCPA were pooled and rotary evaporated to dryness. The residue was dried overnight at 50°C. A solution of this DCPA showed a very clean GC trace.

Anhydrous granular sodium sulphate (Na_2SO_4) was received from different suppliers during the study (Fisher Scientific, BDH Chemicals Canada Ltd.) and was heated to 550°C overnight before use as a water extractant from organic solvents.

Glass wool used as plugs in sodium sulphate filters was washed successively with acetone, hexane and acetone.

5.3 XAD-2 Resin

5.3.1 Resin Purification

XAD-2 resin was obtained from BDH Chemicals Canada Ltd., and was cleaned according to the Health and Welfare Canada method (LeBel et al., 1979) and suggestions from the manufacturer (Rohm and Haas, technical bulletin). This method consisted of first rinsing the resin with distilled water to remove resin fines and salts used to preserve freshness. Batches of resin were stirred with water, the resin allowed to settle, and the supernatant decanted. This step was repeated until the fines had been removed. Next the resin was rinsed four times with ACS grade methanol, letting the resin soak for 15 minutes before decanting. The resin was then transferred to a sintered glass funnel using acetone, and was swirled in acetone and allowed to soak for 15 minutes. The acetone was then removed (vacuum filtered) and a second acetone rinse applied. The same procedure was followed after this rinse with hexane, DCM, and acetone again (each 2 rinses). From previous experience with the resin, it was found that wetting the resin with clean water, and then rinsing with acetone,

hexane and acetone further reduced the amounts of resin artifacts present (Huck, 1986), so this step was also incorporated. Finally, the resin was transferred to double distilled methanol and stored at 4°C.

Resin which had been used to extract organics in water treated at a pilot scale drinking water treatment plant was collected. This resin became discolored (brownish-yellow) after use. The resin was used to sample water from the post-filter position for different oxidants, and had undergone many sampling cycles consisting of adsorption, desorption, and regeneration. Even though elution and regeneration was performed for each sampling cycle, the discoloration was not totally removed, suggesting that background organic matter had irreversibly (under the elution and regeneration conditions) adsorbed. (Resin was also prepared at the pilot plant which had undergone 1 and 2 sampling cycles at the post-filter position of non-disinfected water, but this resin was not utilized in this study). This previously used resin was stored in double distilled methanol at 4°C and cleaned prior to use as described above, except the salt/fines removal step and the final artifact reduction step were eliminated. The cleaning process was included to remove any artifacts or organics which may have desorbed during storage. The term "preloaded" resin is used from this point on to describe this previously used resin, although some of the organics not removed during elution and regeneration may have been removed in the cleaning process.

Prior to use, the resin (fresh and preloaded) was rinsed with approximately 20 bed volumes of distilled water to remove the methanol.

For some experiments, XAD-2 resin which had been submitted to the cleaning procedure was crushed in a ball mill and wet sieved. The 100-200 mesh fraction was collected and rinsed thoroughly with methanol to remove

very fine particles adhering to the larger particles. The crushed resin was then submitted to the normal Health and Welfare cleaning procedure and was stored in water until use in isotherm experiments.

5.3.2 Resin Drying Procedure

A procedure to partially dry the resin to a consistent water content was found in van Vliet et al. (1980) and modified for use with our lab equipment. Resin was placed in a small sintered glass frit column and placed in an International Clinical Centrifuge, model CL. A cap was placed on top of the fritted column and the resin was spun at 3000 rpm for 2 minutes (switch on to switch off). This procedure resulted in an average dry resin percentage of 56.6% with a standard deviation of 0.504 and a percent relative standard deviation of 0.89% for all the data in the study (the maximum percent relative standard deviation for an individual test group was 0.63%). This dry resin percentage was extremely close to the value reported by van Vliet et al. (1980) of 56.3%.

The procedure was modified slightly for use with crushed resin of the 100-200 mesh size. Crushed resin was spun at 1000 rpm for 1 minute. The average percent dry resin varied in two runs from 53.5 to 46.1%.

The data for the percent dry resin test performed throughout the study are given in Table 5.3.1.

5.4 Water Preparation

Water used for experimental work was prepared on two different Milli-Q® systems. The first system consisted of University distilled water passed through a Filtrasorb 400 granular activated carbon column, then on to the four bowl Milli-Q unit. This unit utilized the following Milli-Q cartridges: Super-C Carbon, Ion-

Ex, Ion-Ex, and Organex-Q, followed by a Milli-Pak filter (0.22 μm). Since this system was suspected of having high total organic carbon (TOC) content, the later experiments were performed with water from the second Milli-Q system. This system again used University distilled water passed through a Filtrasorb 400 column and into a six bowl Milli-Q unit consisting of Super-C Carbon, Ion-Ex, Ion-Ex, Organex-Q, Super-C Carbon and Super-C Carbon cartridges. This water was then passed through a column of XAD-2 resin in an attempt to reduce any XAD adsorbable TOC content (some experiments were performed with water from Milli-Q system 1 which was also passed through the XAD column). Appendix 2, which contains each isotherm's preparation and analysis information, gives water preparation details.

Table 5.4.1 and 5.4.2 provide TOC data of water prepared by both systems.

All water used for equilibration experiments was buffered with 1 mL/L of a pH 7.0 phosphate buffer and pH adjusted to pH 7.5. The phosphate buffer was prepared by adding 25.76 g of $NaH_2PO_4 \cdot H_2O$ and 41.84 g of K_2HPO_4 (modified from Standard Methods, 408C) to one liter of water.

5.5 Distribution Coefficient Experiments

Equilibration experiments to determine the distribution coefficients (Kd = solid phase concentration (μg/g) ÷ liquid phase concentration (μg/L)) were performed by spiking 100 μL of an acetone solution of the compound into 1 L of Milli-Q water buffered to pH 7.5. The concentrations of the spiking solutions were adjusted so that final concentrations would be 172 nanomolar (based on 50 μg/L of Lindane), and were as follows:

compound	spiking solution concentration (mg/L in acetone)
Lindane	500
Triallate	520
HCE	407
p,p' DDE	548
Methoxychlor	592

Assuming no evaporation, the amount of acetone in aqueous solution as a result of spiking would be 78 mg/L, or higher than the concentration of analyte. This was unavoidable, however, since spiking the compounds into water with a water-miscible solvent is necessary to ensure dissolution in the water. Also, it would not be expected that this amount of acetone would compete for adsorption on the resin, although changes in the compound's solubility in the aqueous phase would result. This would be a minor effect, however, and as already stated, the addition of acetone was unavoidable, and some evaporation would occur.

5.5.1 Liquid Phase Analysis

Liquid phases for Lindane, HCE and DDE were extracted with 100, 75, 50 mL of DCM, while Triallate and Methoxychlor liquid phases were extracted with 100, 75, 50 mL of hexane (see Results and Discussion, section 6.1.2).

All solvent extracts (for Kd determination and all experiments with liquid phase extraction) were passed through a sodium sulphate filter plugged with a small wad of glass wool, to remove traces of water, into a round bottom flask. Concentration via rotory evaporation was then performed. If DCM was the solvent, it was taken to near dryness (~ 0.5 mL) and then 10 mL of hexane added and evaporated to ~ 1 mL. This step was employed in an attempt to reduce the DCM in the final sample to be injected on the EC detector, since it is

very sensitive to chlorinated compounds and even a small amount of DCM could upset the detector. Final samples were then made up by rinsing the round bottom flasks with hexane or an acetone/hexane mixture and made up to specific volumes.

5.5.2 Solid Phase Analysis

After equilibration, the resin was collected by draining the water/resin from the 1 L bottles through a 1 L separatory funnel plugged with a small wad of glass wool. The bottles were rinsed several times with the liquid phase to remove all resin beads. Excess water on the beads and wool was blown out by nitrogen or air flow. The resin was then eluted using the standard Health and Welfare procedure, scaled down for these small amounts of resin. Three (3) mL of the eluant mixture (15% acetone in hexane) was added to the separatory funnel and allowed to drain into a 125 mL separatory funnel until the organic phase began to elute. The resin and eluant were then equilibrated for 15 minutes, after which another 2-3 mL eluant was allowed to pass over the resin. The aqueous phase was discarded, and the organic phase drained through sodium sulphate into volumetric glassware. The 1 L separatory funnel, resin, small separatory funnel and sodium sulphate filter were then rinsed with about 10 mL eluant and the sample made up to volume (if required) with hexane.

5.6   Isotherm Experiments

5.6.1 Isotherm Preparation

Isotherm water was prepared by adding the phosphate buffer (1 mL/L) to the Milli-Q water. The pH of this water was usua v about 6.8, so the pH was then raised to 7.5 by addition of 1% NaOH while being magnetically stirred. If the pH was overshot, a 10% HCl solution was added to decrease the pH. The .

water was then spiked with a solution of the compound made up in acetone, and stirred overnight. This solution was then dispensed into 500 mL bottles.

Resin which had been subjected to the drying procedure was rapidly weighed onto a teflon® or plastic weighing boat and added to the bottles by rinsing the boat with the spiked water. The bottles were then filled and capped with teflon lined caps and placed in a rotory equilibration apparatus which turned at 28 rpm. All isotherms were equilibrated at 20°C. Equilibration times varied from 7 to 17 days before analysis of both liquid and solid phase was performed. Sample bottles were also included (2 or 3 for each isotherm) which did not contain any resin; these bottles were denoted as isotherm blanks. The liquid phase concentrations in these bottles were determined in order to obtain the initial liquid phase concentrations.

5.6.2 Liquid Phase Extractions

Liquid phase extractions were performed using DCM and hexane. The extraction procedure used in most isotherm experiments was three sequential DCM extractions. In later experiments, an extra DCM extraction was added or a final extraction with hexane was performed (see Appendix 2 for actual method used for individual experiments).

5.6.3 Solid Phase Elution

The resin used in early isotherm experiments (Isotherms 1 - 4) was eluted according to the Health and Welfare method, as discussed in section 5.6.2. In later isotherms (Isotherm 5 - 16), a modified elution procedure was used, which consisted of a small change in the Health and Welfare procedure. This change was implemented because for the higher resin dose samples, the resin clumped together in the acetone/hexane mixture, and poor resin/eluant contact resulted from clumping

and trapped air bubbles. Rather than using 15% acetone in hexane as the eluant, the resin was first rinsed with acetone to remove the water (and some of the analyte), and then eluted with hexane. Both rinsings were collected in a small separatory funnel so that the final ratio of acetone to hexane was 15%. The mixture was then swirled vigorously, and the aqueous layer discarded (checks on the aqueous layer during development showed no analyte (Lindane) to be present). The eluant was then drained through sodium sulphate as before, and the resin, separatory funnel and filter rinsed with hexane.

For the crushed resin isotherms, a different procedure for separating the resin from the liquid was developed. The bottle contents were poured through a glass fritted column (about 2 cm diameter, 7 cm height) and the liquid pulled through into a filter flask by vacuum. The bottle was rinsed several times with filtrate to ensure all the resin was collected. The resin was eluted in the fritted columns, and the eluant collected as before in a small separatory funnel. This method worked very well and therefore was used for subsequent bead resin isotherms as well (see Appendix 2 for specific method used in individual experiments).

5.6.4 Isotherm Data Reduction

Once solid and liquid phase concentrations were known, the data were fitted to the Freundlich equation: $Q_e = K * C_e^{1/n}$

where: Q_e = equilibrium solid phase concentration ($\mu g/g$)

. C_e = equilibrium liquid phase concentration ($\mu g/L$)

and K and n are empirical constants (see Appendix 4 for more details about the Freundlich equation)

The Freundlich parameters K and $1/n$ were determined by linear least squares and by non-linear least squares techniques.

5.7 Column Experiments

XAD-2 resin columns were prepared in glass tubes of 0.56 and 0.7 cm diameter. Resin was contained with glass wool plugs. The water solution was magnetically stirred while being gravity fed to the column by teflon® tubing. Samples of volumes ranging from 50 to 250 mL were collected and extracted with DCM three times (50 mL each for 250 mL samples and 15 mL each for 50 mL samples). Samples were reduced in volume and internal standard was added for GC analysis.

5.8 GC Analysis

The gas chromatograph (GC) used in this study was a Hewlett-Packard 5790A (serial # 2244A01560) equipped with an electron capture detector (ECD). A Hewlett-Packard 3390A integrator (serial # 2149A13990) was used for peak detection and integration.

All isotherm samples were spiked with the internal standard, *t*-Chlordane, the amount depending on the final make-up volume of the sample. Solid phase samples and low-resin-dose liquid phase samples were made up to 25 or 35 mL, while other liquid phase samples were made up to volumes ranging from 2 to 15 mL (as liquid phase concentration decreased, the make-up volume also decreased). This was done since the range of concentrations in the liquid phase varied by several orders of magnitude, and the use of different make-up volumes reduced the range of area counts or area ratios (ratio of sample counts / internal standard counts) encountered. Samples and standards were injected using the solvent wash technique, and the slope and y-intercept of the average area ratio versus mass ratio for standard plots were calculated. The mass ratio of sample compound to internal standard was then calculated by:

mass ratio = (average area ratio - y-intercept) / slope

The mass of sample compound in the sample was then calculated by:

mass of compound = mass ratio * mass of internal standard added

For liquid phase samples, this mass was then divided by the volume of the liquid phase extracted (usually 0.5 L) to yield the liquid phase concentration in μg/L. For solid phase samples, this mass was divided by the dry weight of resin, to yield the solid phase concentration in μg/g.

Where the standard plot was linear, one slope and intercept were used for all samples within that region. Where the plot was non-linear, sample mass ratios were calculated using the slope and intercept between the standard points where the sample fell. Standards were injected each day that samples were analysed. Two or more replicate injections were used for each sample and standard. Typical standard calibration plots are given in Figures 5.1a and 5.1b for Lindane, and Figures 5.2a and 5.2b for Triallate.

Distribution coefficient and liquid-liquid extraction experiment samples did not contain internal standards. In these cases, the liquid phase concentrations were calculated according to:

Liquid Conc. (μg/L) = (ave. area counts - y-intercept) / slope *

(injection vol. Std. / injection vol. Sample) / dilution factor

where dilution factor = volume extracted / final make-up volume

Similarly, the solid phase concentrations (for Kd's) were calculated as:

Solid Conc. (μg/g) = ((ave. area counts - y-intercept) / slope *

(injection vol. Std. / injection vol. Sample) *

final make-up volume) / dry resin weight

Two GC columns were used in the course of this experiment. Initially a Supelco SPB-1 column (0.25 mm ID, 0.25 μm film thickness, approximately 30 m long) was installed and later a J+W Scientific DB-1 (0.25 mm ID, 0.25 μm film

ickness, approximately 20 m long) was installed. Both were methyl silicone phases and performed similarly. However because of the different lengths, the column head pressure was reduced for the DB-1 to establish a similar flow rate to the SPB-1. Both columns had been used previously.

The GC conditions were as follows:

injector temperature	235 - 250°C
detector temperature	300°C
carrier and make-up gas	5% Methane in Argon
septum purge flow	5 mL/min
split vent flow	5 mL/min
column head pressure	20 psi for SPB-1
	12 psi for DB-1

Oven temperature

isothermal   range from 120°C for HCE to 280°C for

DDE (other compounds around 240°C)

program for liquid extraction experiments (SPB-1)

120° (0.5 min) - 10°/min - 265° (5.5 min)

program for bi-solute isotherms (DB-1)

170° (2 min) - 2°/min - 290°

6.0 Results and Discussion

As discussed previously, the study was divided into five sections or phases. The first phase consisted of the selection of the compounds to be used for the laboratory experiments. The second phase involved the generation of single solute data. The third phase consisted of the generation of bi-solute data. The fourth phase involved computer modelling of competitive adsorption using IAST and the data collected in phases two and three. In the fifth and last phase, the Equilibrium Column Model was used with the single solute data and column experimental data. Each phase is dealt with separately in this section.

6.1 Phase 1: Selection of Experimental Model Compounds

To aid in the selection of model compounds to be used for experimental work, relevant literature was reviewed for organic chemicals identified in drinking water and those studied on XAD-2 resin. The lists compiled are given in Appendix 1. The following set of criteria was established to be used in the selection of the model compounds:

1) chemical identified in drinking water

2) similar chemical structure and behaviour to mutagen(s), but preferably non-mutagenic (due to health threat with handling)

3) less volatile chemicals should be used to reduce volatility losses

4) adsorptive behaviour should be different for different compounds, i.e. choose compounds with different adsorptive strengths (relatively, from strongly to weakly adsorbed)

5) methods of analysis should be relatively easy and similar for all compounds

6) chemicals should be easy to obtain

Since the compounds of interest in actual drinking water samples are present at very low concentrations, the same low range of concentrations should be used to model the adsorption effects. The compounds which are strongly adsorbing onto XAD-2 resin are non-polar in nature, and thus their solubilities in water would be very low. For these reasons, it was decided to select halogenated compounds to facilitate the use of Electron Capture Detection (ECD), which is very sensitive to these compounds, enabling low concentrations to be used. Also, many chlorinated compounds are those commonly associated with health risk, and therefore would satisfy the objective of the study, namely to study resin adsorption in order to ultimately improve recovery (for testing and analysis) of chemicals associated with health risk.

With these considerations in mind, a short list of chemicals was compiled. The following compounds were obtained and preliminary testing was performed to determine compound behaviour with respect to analytical methods and resin adsorption:

- p,p'-DDE (1,1-Dichloro-bis(4-chlorophenyl)ethylene)

  $C_{14}H_8Cl_4$ [72-55-9]

  organochlorine pesticide, metabolite of DDT, o,p-DDE non-mutagenic

- Lindane (γ - BHC, 1,2,3,4,5,6-hexachlorocyclohexane)

  $C_6H_6Cl_6$ [58-89-9]

  organochlorine pesticide, non-mutagenic but carcinogenic

- Hexachloroethane (HCE)

  C_2Cl_6 [67-72-1]

  used in industry (solvent, explosives, rubber vulcanizing)

- Tris(2-chloroethyl) phosphate (TCEP)

  $C_6H_{12}Cl_3PO_4$ [115-96-8]

non-mutagenic

- Dimethyl-2,3,5,6-tetrachloroteraphthalate (DCPA)

  $C_{10}H_6O_4Cl_4$ [1861-32-1]
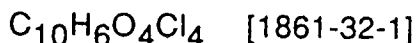
  pre-emergence herbicide, one of many phthlate esters found in water

- Methoxychlor (1,1,1-Trichloro-2,2-bis[4-methoxyphenyl)ethane)

  $C_{16}H_{15}Cl_3O_2$ [1861-32-1]
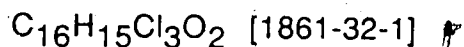
  organochlorine insecticide (used in Edmonton for mosquito control)

- Triallate (S-2,2,3-Trichloroallyl diisopropylthiocarbamate)

  $C_{10}H_{16}Cl_3NOS$ [1861-32-1]
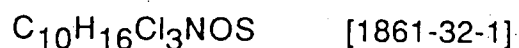
  herbicide (Avadex BW)

All of these compounds are listed in the list of organic compounds identified in drinking water (see Appendix 1) except for Triallate and Methoxychlor. Small amounts of most compounds were obtained for preliminary testing from another laboratory, while Tris(2-chloroethyl) phosphate (TCEP) and Dimethyl-2,3,5,6-tetrachloroteraphthalate (DCPA) were purchased (Aldrich and Alpha respectively).

6.1.1 Liquid Extraction Experiments

Since both the liquid phase and solid phase would be analysed to determine the mass balance for isotherm work, liquid extraction experiments were performed to determine compound behaviour in this analysis. Stock solutions of four compounds (HCE, Lindane, Triallate and DDE) were made up in acetone to facilitate dissolution when spiked into the water. The first extraction experiment consisted of four compounds being spiked into 1 L of distilled/deionized water at the 10 µg/L level. Three 100 mL dichloromethane (DCM) extracts were collected separately, rotory evaporated (rotovapped) to ~1

mL and made up to 100 mL hexane. A check on rotovap losses was performed by spiking the stock solution into 100 mL DCM and following the same procedure as the extracts. The separatory funnel was also rinsed with DCM to check for glass adsorption. A standard was made by spiking the stock solution into 100 mL hexane, and all extracts were compared to this standard. The results for this first extraction experiment are presented in Table 6.1.1. Triallate was not detected in the extracts as it is less sensitive to ECD than the other compounds, and was below detection limits. The greater than 100% recoveries in the rotovap check could be caused by a spiking error, but a more reasonable explanation is the GC quantitation method used. Firstly, no internal standard was used so that injection errors could have occurred, and also only one standard was used, i.e. the slope and intercept passed through the standard values and zero. From subsequent GC work, it became evident that the GC calibration does not pass through the zero point, thus these errors are most likely explained by the poor GC quantitation. The results indicated, however, that Lindane and DDE were well recovered and HCE was not. The results also did not exhibit the expected ratios between extracts, i.e. each extract should contain relatively the same percentage of the liquid phase concentration prior to extraction, but this was not the case.

Due to the problems with this experiment, subsequent extraction experiments were performed at higher spiked concentrations. The second experiment was performed at the 100 μg/L level for five compounds (Methoxychlor was added). The results are given in Table 6.1.2. In this case, Lindane and Triallate were extracted well, but not HCE, DDE and Methoxychlor. These compounds were also detected in the separatory funnel rinse, indicating a problem with glass adsorption. Indeed, glass adsorption is a common problem in studies involving organics in water.

The improper extract ratios also occurred, which could possibly be explained by glass adsorption. If the DCM rinse was not sufficient to remove all the glass-adsorbed compounds, then the initial liquid phase concentration would have been lower than 100 µg/L prior to the first extract, and thus the lower percent recoveries in the second and third extracts would make more sense.

In an attempt to reduce glass adsorption, and increase extraction efficiencies, a third experiment was performed using hexane rather than DCM as solvent. The spiking level was supposed to be at 50 µg/L, but due to a calculation error, it was only at 5 µg/L. A sixth compound, DCPA, was also added. Table 6.1.3 shows the results which indicated good extraction for all compounds except HCE. Since this compound was the most volatile of the group, it is possible that some was lost in the rotovap step. Since one of the criteria for compound selection was ease of analysis, HCE was no longer considered. Only one compound was detected in the second extract, and none in the third since the initial liquid phase concentration was only 5 µg/L. The apparent loss of Methoxychlor in the rotovap check cannot be explained.

Due to the problems with the previous experiments, another extraction experiment was performed at 50 µg/L using DCM as the solvent. The results, presented in Table 6.1.4, were similar to those of previous experiments with respect to high rotovap checks, low recoveries for some compounds and relative percent removals between extracts. Also, it was noticed that the DCPA was grossly contaminated with Hexachlorobenzene (HCB) (determined by Gas Chromatography - Mass Spectromemetry). As such, the recovery for this compound was also reported, but the exact levels of HCB and DCPA were not known (although they totalled 50 µg/L).

Due to the calculation error in the third experiment, this extraction with the seven compounds at the 50 µg/L level and extraction with hexane was repeated. The results in Table 6.1.5 showed greater accuracy than previous extraction experiments. This is evident in the rotovap check values, which for most compounds were very close to 100% recovered. This change over previous experiments was probably due to the fact that three GC standards instead of just one were used to quantitate the samples. Since some of the compounds exhibited rather high negative y-intercepts, the use of a calibration plot changed the recovery values by a substantial amount. Also, the solutions with lower concentrations were made up to 2 mL and the high concentration solutions to 25 mL to reduce the range of area counts, thus improving quantitation by reducing non-linear effects of the detector.

Most compounds were nearly totally recovered in the hexane extracts, with HCE, DDE and Methoxychlor being the exceptions. The volatility of HCE makes this compound difficult to work with, but reasons for less than quantitative extraction of DDE and methoxychlor are not so clear. DDE showed a rather high value in the separatory funnel rinse of 14%, and as a result 92.5% of the compound can be accounted for (this is much higher than previous extraction experiments). If glass adsorption was the main cause for low recoveries of DDE, it is possible that the solubility in water had been exceeded, although it was also recovered to a lesser extent than the other compounds in the third experiment (hexane extraction at 5 µg/L). The low recovery of Methoxychlor is difficult to explain, especially in the low rotovap check. The raw GC data for Methoxychlor showed less reproducibility than for other compounds, with a percent relative standard deviation of 27% while the other compounds showed normal precision (the worst being 4% for Hexachlorobenzene, others about 2%).

The behaviour of DDE and Methoxychlor in liquid-liquid extractions and GC analysis did not satisfy the criteria set forward for model compound selection. Also, the solubilities for these compounds were found to be approximately 40 μg/L (Vershuren, 1983). Since tests were performed at this level and above, these compounds were not considered to be good candidates for model compounds. In all extraction experiments, Lindane and Triallate were quantitatively extracted. Therefore these compounds were considered good candidates for model compounds.

6.1.2 Distribution Coefficient Determinations

The purpose of these experiments was to enable selection of the compounds to be used as model compounds, based on the relative adsorption characteristics on XAD-2 resin. Equi-molar solutions (172 nanomolar) of HCE, Lindane, Triallate, p,p' DDE and Methoxychlor were prepared based on previous work done with Lindane at 50 μg/L (.72 nM). Solutions of the compounds were equilibrated with XAD-2 resin at two different resin doses for each compound, with the doses being the same for all compounds to allow comparison. Unfortunately, different equilibration times were used for different compounds, ranging from 5 days to 13 days since procedures were being developed. Values were available, however, for each compound at a long equilibration time. Triallate and p,p' DDE were extracted from the aqueous solution using hexane, while Lindane, Methoxychlor and HCE were extracted using DCM. This was done to improve the compound extraction according to the results obtained in the liquid extraction experiments (although for multicomponent analysis, the use of one solvent was desirable). The DCM extracts of Methoxychlor and HCE were concentrated using Kuderna-Danish evaporation to reduce the losses encountered during rotary evaporation. Three

standards were used to quantitate the Kd samples. The resin was eluted as described in the Material and Methods section 5.5.

The results of the distribution coefficient determination tests are given in Table 6.1.6. The Kd values shown for Lindane were determined in previous experiments. The first lindane bottle listed (#11) contained an initial liquid phase concentration of 5 µg/L (17 nM). The results for Methoxychlor are not listed as problems were encountered in detection of the compound in the liquid phase extracts due to the reduced sensitivity of Methoxychlor (compared to DDE, Methoxychlor has one less chlorine atom and two oxygen atoms).

The variation in the values for Kd obtained at different resin loadings could have been caused by a non-linear isotherm and variations in the total amount of compound recovered. The total amount recovered for Lindane was rather variable and this was most likely due to the variation in the GC quantitation, since these samples were analysed at an earlier date (when fewer standards were used and the GC was still being configured for optimum performance).

Because of the variability in the Lindane values, it was decided that the differences in Kd for Lindane and HCE were not significant. However, the much larger values obtained for Triallate and to a lesser extent for DDE would appear to be caused by a real difference in adsorption characteristics. Accordingly, Triallate was the most strongly sorbed compound, and Lindane and HCE were the most weakly sorbed compounds, with DDE being intermediately sorbed.

Despite the variations observed, the experiment was still useful for selecting compounds which were adsorbed to different extents. Volatility problems with HCE made this compound a poor choice, so that Lindane was chosen as the weak adsorber. Triallate was chosen as the strong adsorber.

These compounds were also well behaved in the liquid extraction experiments. Isotherm work then began with these two compounds.

Kd values had yet to be determined for DCPA and TCEP. The compound DCPA required purification prior to use (see section 5.3). Original attempts at the determination of the Kd for TCEP had failed due to the very low ECD sensitivity of this compound compared to the others. Rather than performing a Kd experiment with 2 bottles, a preliminary isotherm was performed for TCEP with 5 bottles, at an elevated initial liquid phase concentration to allow detection in the liquid phase after equilibration. The liquid phase samples for both of these compounds were extracted with DCM.

The distribution coefficient data for TCEP and DCPA are presented in Table 6.1.7. The results showed that DCPA was adsorbed c, roximately to the same extent as Lindane. The Kd for TCEP was much lower than that for other compounds, indicating that it was adsorbed less strongly. This was to be expected since the solubility in water of TCEP was likely to be much higher than the other very hydrophobic compounds tested.

6.1.3 Summary

Several criteria were put forward with respect to choosing chemicals to be used as model compounds for the study. Experiments to determine the relative adsorption affinities of the compounds for XAD-2 resin showed the compounds from weakly adsorbing to strongly adsorbing were: TCEP < HCE ~ Lindane ~ DCPA < p,p' DDE < Triallate. Compounds which were ruled out were HCE for volatility problems, and DDE for difficulties with quanititative extraction from the liquid phase and low solubilities. Triallate was chosen as the strong adsorber since its Kd was large and it was extracted quantitatively.

Lindane and DCPA both exhibited moderate Kd's, but Lindane was chosen since isotherm work had already begun on Lindane before the Kd experiment for DCPA was complete. TCEP could have been used for the weakly adsorbing compound, if time had allowed isotherm work on three compounds. Some problems may have arisen from its insensitivity compared to the other compounds, and from significant procedural change for solid phase analysis (see section 6.2.2). Therefore isotherm work was performed on Lindane and Triallate.

6.2 Phase 2: Generation of Single Solute Data

6.2.1 Adsorption Kinetics on XAD-2 Resin

Before any equilibration experiments could be performed, the time allowed for equilibration had to be decided. Andrews et al. (1987) used an equilibration time of 7 days to study competitive adsorption of trihalomethanes on activated carbon. One study in the literature was found in which isotherm work on a resin was performed (Kong and DiGiano, 1986). In this study an equilibration time of 14 days was used for isotherms of volatile organic chemicals on XE-340 resin. Since no data were found on the adsorption of non-volatile compounds on XAD-2 resin, kinetics studies were carried out.

The first kinetics experiment was to be performed at an initial liquid phase concentration of 50 µg/L but was actually done at 5 µg/L due to a calculation error. The results are given in Table 6.2.1. The amount of resin added was not enough to significantly reduce the liquid phase concentration at the 5 µg/L level, but it appeared that the solid phase concentration remained approximately the same after 2 days.

The experiment was repeated at the 50 μg/L level. The results are presented in Table 6.2.2. No samples were analysed between 3 and 7 days since the equilibration was thought to occur within 2 or 3 days. The scattered and low recoveries are probably due to GC quantitation error since an internal standard was not used at this point. A plot of the liquid phase concentration decrease with time is given in Figure 6.2.1. From this plot it can be seen that liquid phase concentration decreased only slightly between 3 and 7 days, so that the equilibration time was taken to be 7 days.

6.2.2 Single Solute Isotherms

Bench scale adsorption data were gathered by using the bottle point isotherm method. A solution of one organic compound in pure water was dispensed into bottles to which various amounts of XAD-2 resin were weighed. The pure water was buffered to a pH of 7.5, which was the average pH of the settled water at the Rossdale pilot plant in Edmonton in January, 1987. Bottles of 500 mL volume were used for all isotherms. Once loaded, these bottles were rotated at 28 rpm for various times, at 20°C. The resin was then separated from the liquid phase and the two phases analysed for residual concentration. These solid and liquid phase concentrations were then fitted to the Freundlich equation and plotted on a log-log scale.

Over the course of the study, 13 single solute isotherms were performed. In this section, the isotherms are discussed in chronological order, with discussion of the problems encountered and methods development which occurred with time. All experimental details about each isotherm experiment (such as equilibration times, methods of extraction, etc.) have been compiled in Appendix 2. All Freundlich parameters for the isotherms are given in Table 6.2.3 for easy comparison. This table includes Linear Least Squares (LLS) and

Non-Linear Least Squares (NLLS) estimates, as well as the 95% confidence interval for NLLS analysis.

Initially, only the solid phase from each isotherm bottle was to be analysed, and the liquid phase concentration was to be calculated from average isotherm blank values (i.e. bottles containing no resin) less the solid phase values. In the case where both solid and liquid phases are analysed, the isotherm blank value is only used for a mass balance check, i.e. for calculation of percent recoveries.

The solid phases from the first adsorption isotherm of Lindane on XAD-2 were analysed, but the results were disappointing. Table 6._.4 shows the solid phase results, where the liquid phase was calculated from the blank less the solid phase values. It can be seen that the solid phase concentration did not monotonically decrease with increasing resin weights. This translated to a high degree of scatter, as the plot in Figure 6.2.8 demonstrates. The numbers in this figure correspond to the resin weights in the bottles, with the lowest resin weight being bottle 1 and the highest resin weight being bottle 20 (see Table 6.2.4). It can be seen that for small changes in the resin weights between bottles, large variations in solid and liquid phase concentrations were observed. The low resin weight samples were in the proper region of the plot (upper right), but the calculated liquid phases for the high resin weight bottles were not in the proper region (lower left). Rather, they were shifted to the right, or towards higher liquid phase concentrations. This indicated that the solid phase concentrations were low, causing erroneously high calculated liquid phase concentrations.

Because of these poor results, the liquid phases from this experiment were extracted. The results of both analysed solid and liquid phases values are given in Table 6.2.5, and the plot is shown in Figure 6.2.3. These results were

much better, although some scatter from linearity occurred in the low resin weight region (upper right). In this and other isotherm experiments, mass balances were generally not worse for points which appeared from the plots to be outliers.

The Freundlich parameters for this isotherm are included in Table 6.2.3 The change in the parameters from linear to non-linear least squares shows the influence of the scatter upon the data. The parameters for the region consisiting of the ten points in the middle of the isotherm (between the scattered points) are also given.

The scatter was initially thought to be a resin size distribution problem. A dry resin sieve analysis showed that the resin size distribution (after washing) fell between 20 and 60 mesh (see Appendix 3). Since about 85% of the beads were in the 20-28 mesh size, it was thought that if beads of predominantly large or small size were weighed into the low resin weight bottles, the difference in surface areas could cause variations in adsorption capacity. Therefore a separate experiment was performed in which replicate bottles containing 20-28 mesh beads and 28-35 mesh beads were equilibrated with a Lindane solution and analysed. The results showed no significant difference between adsorption capacities for the two resin size fractions (see Appendix 3).

The next Lindane isotherm was run at the 100 µg/L level (up from 50 µg/L). It was hoped that this change would reduce the problem of scatter in the low resin weight bottles. Also, this change increased the range of liquid phase concentrations encountered for the isotherm. The results for this experiment are given in Table 6.2.6. Since the value for 0c (resin-free sample c) was much lower than that for 0a (and also lower than the amount recovered in solid phase samples 9-15), only the value for 0a was used for percent recovery compounds.

The non-monotonical decrease in solid concentration and increase in liquid concentration was present in this isotherm as well. The Freundlich plot is given in Figure 6.2.4. The Freundlich parameters were similar to those in Isotherm 1 (see Table 6.2.3). The plot shows that the scatter in the upper right region may have been reduced compared to Isotherm 1. But the scatter was evident throughout the entire plot for Isotherm 2. The scatter was not caused by errors in the analysis of the liquid or solid phases, since good total recoveries were obtained (i.e. when a solid phase concentration was high, the liquid phase concentration was correspondingly low and vice versa). The variation in the mass balances was not large enough to account for the scatter in the isotherm. This was tested by plotting the isotherm as determined only by liquid phase analysis (and calculating the solid phase values), therefore assuming 100% recovery. In this case the isotherm was very similar to the plot where both solid and liquid phases were used. Also, a deviation of 5 or 10% in a value does not cause a large shift in the position on a log-log plot. Therefore it was thought that the scatter may have been due to non-homogeneity within the resin.

This postulated resin non-homogeneity was also used to explain the scatter in the next two isotherms performed with Triallate. Isotherm 3 was a preliminary isotherm performed to provide estimates of the Freundlich parameters for Triallate adsorption, to be used in the design of a full Triallate isotherm. The results of Isotherm 3 are given in Table 6.2.7 and Figure 6.2.5.

The full Triallate isotherm was Isotherm 5. The results are presented in Table 6.2.8 and Figure 6.2.6. This experiment included two points (resin weights) which were replicated three times each. As can be seen in Table 6.2.7, two of the low resin weight replicates, bottles 3 and 4, agree very well, but bottle 5 is quite different. The deviation points to a difference in resin adsorption

and not an analytical problem with one of the phases, since the percent recoveries for all three bottles were good. The other replicates were bottles 10, 11 and 12. While the solid phase concentrations for these bottles were similar, the liquid phase values were all different. Figure 6.2.7 shows the plot in a different format with all the points numbered and the replicated bottle points numbered in bold.

The difference in Freundlich parameters for Triallate compared to Lindane (larger K, smaller 1/n) confirmed that this compound was more strongly adsorbed.

The next step taken to reduce the scatter was to attempt to homogenize the resin by crushing it into smaller particles. A recent paper on dynamic (column) modelling with activated carbon (Weber and Wang, 1987) suggested using the 80-100 mesh fraction. This size was large enough to not yield effects such as pressure drop and flow channeling encountered with finely powdered carbon, yet small enough to yield comparable equilibration results with the fine carbon. Also reported was the fact that particle size (ranging from 16 to 325 mesh) had no effect on final adsorptive capacity for the compounds studied. It was thought that if these principles could be applied to XAD-2 resin, then perhaps crushing and sieving the resin would provide more satisfactory results.

Isotherm 6 was performed at the 100 µg/L level using 100-200 mesh resin. This size fraction was chosen as the smallest fraction which would not cause practical difficulties in separation from the liquid phase. The results are given in Table 6.2.9. Replicate bottles were 3, 4, 5 and 10, 11, 12. The high resin weight replicates' solid phase concentrations agreed very well, but the liquid phase value for # 11 was slightly different than the others. Two of the low

resin weight samples replicated extremely well, but bottle # 3 was different in both solid and liquid phase. The high percent recoveries in the high resin weight bottles pointed to incomplete extraction of the high liquid phase concentration samples (more Lindane was recovered from the resin in the high resin weight samples than from the resin-free samples). As a result, future isotherm liquid phase samples were extracted with larger volumes of DCM, more extracts, or DCM followed by hexane extracts (see Appendix 2 for isotherm procedure details).

Figure 6.2.8 shows that the scatter in this isotherm was reduced, but was still evident in the low resin weight region. In the high resin weight zone, the plot looked very good as it was quite linear and the points were equally spaced (the isotherms were designed to produce equal spacing between points; see Appendix 5). A large gap then separated the points 7 and 8 (see Figure 6.2.9 for plot with bottle points numbered, replicates in bold). This effect can also be seen by the jump in liquid phase concentrations from sample # 7 (17.4 µg/L) to # 8 (0.96 µg/L) in Table 6.2.9.

A possible explanation for this jump was that some component(s) of the total organic carbon (TOC) remaining in the 'pure' water were preferentially adsorbing onto the resin, thereby competing for adsorption at the low resin weights. Measurements of TOC in the Milli-Q water had been on the order of 100 µg/L, which was the same initial liquid phase concentration used for Lindane and Triallate in the isotherms. If this competition existed, the Lindane adsorption plot would be shifted to the right and down (lower solid phase concentration and higher liquid phase concentration), as is the case in this experiment. If the resin weight between bottles 7 and 8 was enough to fully remove the adsorbing TOC, then a sharp decrease in liquid phase concentration could occur since the 'extra' resin in the bottle would now adsorb

Lindane. Also, the variation in scatter from isotherm to isotherm could have been caused by the changing condition of the Milli-Q cartridges. This postulation did not explain the scatter, however, since a competitive adsorbent should simply displace the plot, and not scatter it.

The increase in the value for the Freundlich K in this experiment compared to bead isotherms for Lindane pointed to either a greater capacity of the crushed resin or faster adsorption kinetics. Since there was no evidence for the former, the latter explanation is more likely.

The results of the preliminary Tris (2-chloroethyl) phosphate (TCEP) isotherm (Isotherm 4) were also in agreement with the TOC competition postulation. The initial liquid phase concentration of this isotherm was increased since the ECD sensitivity for this compound was lower than for other compounds, and as such, the Kd experiment for this compound had not been successful. The isotherm results are given in Table 6.2.10. Bottles 4 & 5 were replicate bottles, and they agreed extremely well. The percent recoveries were low, but very similar in value. The Freundlich plot is given in Figure 6.2.10. The plot is very linear, with very little scatter.

The fact that this isotherm was very linear was encouraging. It was thought that this experiment may have been successful since the concentration was high enough to reduce TOC competition.

The Freundlich K for this compound was much lower than for Lindane and Triallate and the 1/n value was higher, indicating that this compound was adsorbed less strongly than the others (see Table 6.2.3).

Problems with compound detectability, however, were encountered in the low liquid phase concentration samples. Also, since TCEP is more soluble in water, 'extra' samples consisting of the aqueous layers in the elution

procedure (which was normally discarded) were collected and analysed. TCEP was detected in significant amounts in all of these 'extra' samples. Solid phase concentrations were then calculated as the sum of TCEP recovered from the resin elution and the aqueous layers. Due to these analysis problems, it was decided not to perform more experiments with TCEP.

In an attempt to reduce the TOC of the isotherm make-up water, the Milli-Q prepared water was contacted with XAD-2 resin. Water was contacted in a batch mode and also in a column mode. The results in Table 6.2.11 show that both modes increased the TOC of the water. This increase could have been caused by small amounts of organic solvent from the resin washing procedure still present on the resin, which was rinsed off into the water. In any case, it was hoped that the TOC adsorbable on the resin would be removed, and the water prepared by column mode was used in Isotherm 7. The results of this Triallate isotherm are presented in Table 6.2.12 and the plot is given in Figure 6.2.11. Even though the water was filtered through resin and the initial liquid phase concentration was increased from 100 to 500 µg/L, the non-montonic progression and scatter still persisted. The Freundlich parameters for this isotherm (Table 6.2.3) showed increased adsorption capacity (larger K). This occurred because of the initial liquid phase concentration increase, which caused the driving force for adsorption to increase. Since the increased capacity was noticed, it meant that the isotherm bottles had not reached equilibrium. Therefore the equilibration time was increased in the next isotherm experiment.

Isotherm 8 consisted of Lindane on crushed resin at the 500 µg/L level. The equilibration time of this isotherm was 9 days. The results in Table 6.2.13 indicate that the replicated bottles (8, 9 and 10) demonstrated excellent

agreement. The plot in Figure 6.2.12 exhibited monotonic progression and relatively good linearity.

From these results, it was decided to perform another kinetics experiment at the increased initial concentration and for a longer duration. Bottles were loaded with 500 µg/L Lindane and equilibrated for various times. Fresh and also preloaded resin (resin put through many sampling cycles, see section 5.3) was utilised in order to compare the kinetics between them. The results are presented in Table 6.2.14. The plot of liquid phase decrease with time is shown in Figure 6.2.13. The plot clearly shows that equilibration was not achieved at 7 days, but that 14 days would be a better time period. Also, no substantial difference was observed between fresh and preloaded resin.

As a result of the kinetics experiment, the next single solute isotherms were equilibrated for 12 days (14 day times were planned but they could not be analysed at that time). All isotherms after Isotherm 8 were performed with resin beads, since crushed resin did not yield better results and also crushing preloaded resin may have altered its adsorption characteristics.

Isotherm 12 consisted of a Lindane isotherm on fresh resin. The results are given in Table 6.2.15 and Figure 6.2.14. This isotherm exhibited less scatter than previous single solute isotherms. There appears to be, however, a curving character to the isotherm. In the high resin weight region (lower left on plot), the data plot in a linear fashion, but then the plot seems to curve down in the upper right region corresponding to low resin weights.

This effect was also noticed in Isotherm 13, which was loaded at the same time as Isotherm 12 (i.e. same make-up water). Isotherm 13 was the same experiment as Isotherm 12 except that preloaded resin was used instead of fresh. The data are given in Table 6.2.16 and the plot in Figure 6.2.15. These last two isotherms are compared in Figure 6.2.16. It can be seen that

these two isotherm plots very nearly replicate themselves, at least within the variation seen from earlier experiments.

The last Lindane isotherm performed was Isotherm 16. This experiment was meant to be a check on the reproducibility of the two-week isotherms. The results are given in Table 6.2.17 and Figure 6.2.17. This plot also has some curvature, but the curving starts at a lower liquid phase concentration than the plots for Isotherms 12 and 13. This type of curvature could be explained by the TOC interference postulation, that is if a small amount of preferentially adsorbing background compound(s) was present, the adsorption curve in the low resin weight region would be shifted down due to competition. Another possible explanation is that the Freundlich equation simply does not describe the adsorption of Lindane on XAD-2 resin over the concentration range encountered, such that plotting the data in the linearized form of the equation does not result in a linear plot. To determine if the data was better described by another isotherm equation, the data for Isotherms 12 and 16 were plotted using the linearized from of the Langmuir equation (see Appendix 4 for a brief discussion of this equation). Due to the very large concentration range (isotherms were designed for plotting with the Freundlich equation), two plots must be used for each isotherm. Figures 6.2.18 and 6.2.19 show the Langmuir plots for Isotherm 12, and Figures 6.2.20 and 6.2.21 the Langmuir plots for Isotherm 16. These plots were relatively linear. Small curvatures in the lower left of Figures 6.2.19 and 6.2.21 occurred because the lowest resin weight sample points for both isotherms (upper right on Freundlich plot) showed some departure from the curving trend on the Q versus C plot. If the curvature in t' Freundlich plots was actually caused by a limit being approached for th~ ₃lid phase concentration, then the departure from the curving trend for the owest resin weight bottle (largest liquid phase concentration) would be c .culi tc

explain. Indeed, the solid phase concentration should then flatten out in this region. But rather, it did not flatten out, but appeared to increase again at the approximate slope of the high resin weight region, especially for Isotherm 16. This would suggest that the shifting of the curve was caused by competitive adsorption. A similar shifting was also seen in the crushed resin Isotherm 8 (Figure 6.2.12).

A long equilibration time isotherm for Triallate was also performed. The results for Isotherm 14 are presented in Table 6.2.18 and Figure 6.2.22. This plot exhibited a systematic departure from linearity, which apparently did not fit the Freundlich equation. This type of plot is typical of adsorption isotherms which exhibit multi-layer coverage on the adsorbent. One adsorption equation which takes multi-layer adsorption into account is the Brunauer-Emmett-Teller (BET) equation (see Appendix 4). This isotherm was plotted in the linearized form of the equation with the high C/Cs points given in Figure 6.2.23 and the low C/Cs points plotted in Figure 6.2.24. These plots also were not linear, suggesting the adsorption does not fit the BET equation.

6.2.3 Summary

Much of the study was spent attempting to obtain single solute isotherm parameters of good quality for use with the computer models. Isotherms showed a large degree of scatter. Sample analysis was precluded as the source of errors since good total recoveries were obtained. Many different experimental modifications were attempted, such as modifying the extraction and elution procedures, increasing the initial liquid phase concentration, utilizing crushed resin, attempting to further purify the make-up water and increasing the equilibration time. In the end, the single solute data were not of

the quality hoped for at the beginning of the study. The low resin weight region of the isotherms showed the largest degree of scatter and non-linearity. One possible explanation is the fact that the concentrations used in this study were relatively low, even though they exceeded the actual concentrations of these types of compounds in real water samples. Many problems can occur in the analysis of low level organics, as was also seen in this study. Another possible explanation is that small amounts of resin may have dried during weighing into the isotherm bottles. A brief test showed that dry resin exhibited an increased adsorption capacity (see Appendix 3). More experimentation is required, however, to further investigate this effect.

Many different values for the Freundlich parameters were gathered for each of the two compounds. The values for the early resin beads experiments are not reliable since the bottles were analysed prior to reaching equilibrium. The Lindane isotherms using 100-200 mesh resin showed the highest capacity for the adsorption of Lindane. Figure 6.2.25 shows the Lindane Isotherm plots for Isotherm 8 and 12. Isotherm 8 was equilibrated for 9 days with crushed resin, and Isotherm 12 was equilibrated for 17 days with beaded resin. The plot shows that the crushed resin exhibited a higher capacity than the bead resin (higher solid phase concentration). The difference between the plots for Isotherms 8 and 12 is much larger than the difference between the plots for Isotherms 12 and 16 (see Figure 6.2.26), which is an estimate of the reproducibility or variability of the experiments. This suggests that at the equilibrium times used the increase in capacity for crushed resin is a real effect. This large difference is also evident from the table of Freundlich parameters for all single solute isotherms (Table 6.2.3).

One explanation of the increased capacity is that by crushing the resin, much more surface area is exposed for adsorption. This is in contrast to the

results for activated carbon of Weber and Wang (1987) who stated that the capacity for adsorption was the same for different size fractions. The average pore size for XAD-2 resin is very uniform and small at 90 Angstroms or 0.009 µm (Rohm and Haas technical bulletin). In granular activated carbon, the pores cover a large size range, typically from 10 to 100000 Angstroms (Montgomery, 1985). In the case of the granular carbon, much of the pore structure is available for adsorption, whereas for the resin, the small pore size can exclude the organic molecules for pore adsorption (Rohm and Haas, technical bulletin). Indeed, styrene/divinylbenzene cross-linked polymers are used in size exclusion chromatography. Much more study would be necessary, however, to determine if the compounds used in this study were actually adsorbed only on the surface and not in the pores.

Another possible explanation for the increased capacity is that the beaded resin had possibly not reached equilibrium. Since pore diffusion is often a very slow step, this explanation is more probable. When the resin is crushed, the kinetics may increase due to the increase in surface area of adsorbent readily available in solution. In this case, the analyte need only diffuse through the stationary liquid film about the resin particle, and any pore distances which must be traversed are considerably shorter. Therefore the resin used in the bead form did not appear to reach equilibrium, even in the two-week equilibration times.

Another factor which may have reduced the adsorption kinetics for beaded resin was the fact the tumbling divice used to turn the bottles may have been spinning at a high rotational speed. At 28 rpm, the resin beads may have been "centrifuged" out towards the bottle cap, and not actually mixed in solution. The crushed resin, however, may have remained in solution as a fine suspension, thus contacting the liquid phase more efficiently.

Figure 6.2.27 allows comparison of the plots from both final single solute isotherms for Lindane (Isotherm 12) and Triallate (Isotherm 14). It can be seen that the plots converged in the low resin weight region of the plot, but diverged in the high resin weight zone. For this reason, the values of the Freundlich K (which are obtained at a liquid phase concentration of 1 µg/L) were larger for Triallate, since at the initial liquid phase concentrations used, large resin weights were required to bring the liquid phase concentration down to 1 µg/L (see Table 6.2.3 for Freundlich data). Also, the Triallate plot had a low slope. This means that the isotherm for Triallate was very favorable for adsorption, that is, the solid phase concentration was maintained quite high over a large range of resin doses. As such for a given resin dose, Triallate was removed from the water to a greater extent.

Another set of isotherm plots which is interesting to note is presented in Figure 6.2.28, which contains the plots of Isotherm 2 (Lindane) and Isotherm 7 (Triallate). It is intriguing to see that the scatter in the plots was almost identical, following the same pattern and also scattering in the same region of the plots. This could be pure coincidence. No explanation for this phenomenon can be given.

6.3   Phase 3:   Generation of Bi-solute data

6.3.1   Bi-solute Isotherms

Once single solute Freundlich parameters were obtained, the IAST model was used to predict competitive adsorption. In order to verify these predictions, bi-solute adsorption isotherms were performed.

Three bi-solute isotherms were conducted. Isotherms 10 and 11 were replicate experiments except for equilibration times which were 7 and 14 days respectively. The isotherms were loaded at initial liquid phase concentrations of 500 µg/L Lindane and 523 µg/L Triallate (equi-molar concentrations of ~1.72 µmole/L). The results for Isotherm 10 are given in Table 6.3.1a for Lindane and 6.3.1b for Triallate, and the Freundlich plot is shown in Figure 6.3.1.

The results for Isotherm 11 are given in Tables 6.3.2a for Lindane and 6.3.2b for Triallate, and the Freundlich plot is shown in Figure 6.3.2. These isotherms were very similar except for a shift in the 14 day plot to higher solid phase and lower liquid phase concentrations. Figure 6.3.3 shows the Lindane plots from these two isotherms and Figure 6.3.4 shows the Triallate plots. It can be seen that significant adsorption occurred in the second week of equilibration. These data, along with the kinetics data generated at the same time as these experiments, showed that equilibration times of 14 days were required.

When these bi-solute plots were compared to the 2 week equilibration single solute isotherm plots, it was apparent that the amount of shift due to competition was small. Figure 6.3.5 shows the Lindane single solute data from Isotherm 12 and the bi-solute data from Isotherm 11. Figure 6.3.6 shows the Triallate single solute data from Isotherm 14 and the bi-solute data from Isotherm 11.

Due to the small competitive effect, another bi-solute isotherm was performed with the initial liquid phase concentration of Triallate being approximately five times that of Lindane (on a molar basis). The results of this isotherm (Isotherm 15) are presented in Tables 6.3.3a for Lindane and 6.3.3b for Triallate. The Freundlich plot is given in Figure 6.3.7. Some problems with scatter occurred again with this experiment, with the pattern of scatter being the same for both compounds (as such, analytical errors cannot be ruled out as the

cause, i.e. if some of a sample was lost, then both compounds would be affected in the same way).

The plots from the bi-solute Isotherm 15 are compared to the single solute isotherm plots in Figure 6.3.8 for Lindane and Figure 6.2.9 for Triallate. For both compounds, the bi-solute plots were displaced from their respective single solute plots in the low resin weight zone of the plot. Lindane, however, was displaced to a greater extent than Triallate. These were the expected results, since when little resin was present, the more strongly adsorbed compound (Triallate) competed more effectively for the resin's active sites. Also, for high resin weights, the adsorption behaviour approached single solute adsorption, since the large amounts of resin available reduced competition effects.

6.3.2 Summary

Three bi-solute isotherms were performed in the latter part of the study. The results from Isotherm 10 were not used for modelling purposes since the equilibration time was too short. Isotherm 11 was performed at equi-molar initial liquid phase concentrations while Isotherm 15 was performed at an approximate 5 to 1 molar ratio (Triallate to Lindane). The competitive shift in adsorption was more evident in Isotherm 15. This points to the fact that even though the single solute Freundlich parameters for the two compounds were significantly different (indicating different adsorption strengths), the difference was not great enough to show large competitive adsorption effects. The competitive shifts from single solute data occurred only in the low resin weight bottles. If two compounds of very different adsorption strengths had been chosen, then a shift over a larger range of the isotherm could have been expected.

A large degree of scatter was present in the low resin weight region of Isotherm 15 for both compounds.

6.4   Phase 4:   Modelling Using Ideal Adsorbed Solution Theory

6.4.1   The Use of Linear Least Squares Estimates of K and 1/n

Once the bi-solute Freundlich isotherms were completed, the experimentally determined data were compared to computer model predictions of the competitive adsorption. IAST was used to predict the competitive adsorption effects from the single-solute Freundlich parameters used as input. Initially, both linear least squares (LLS) and non-linear least squares (NLLS) estimates of the parameters K and 1/n were used. As seen earlier, for most isotherms there was a relatively large difference between LLS and NLLS estimates, indicating that some curvature was present (see Table 6.2.3). Also, curvature is evident in the Freundlich plots for isotherms 12 (Lindane) and 14 (Triallate). Since these two isotherms were deemed to most accurately represent the single-solute adsorption of these two compounds onto beaded resin, the parameters from these isotherms were used for IAST input. To determine which estimates more accurately represented the data, the single solute data along with the LLS and NLLS best-fit lines were plotted on one graph. Figure 6.4.1 shows the plots for Isotherm 12 (Lindane) and Figure 6.4.2 for Isotherm 14 (Triallate). It can be seen that the two high concentration (liquid and solid) samples in Isotherm 12 influenced the NLLS to a large extent, which caused the NLLS line to deviate considerably in the lower concentration region (lower left of the plot). The LLS best fit line did not deviate more in one region than another, and therefore better represented the actual data. The difference between the LLS and NLLS lines is less severe for the Triallate plot.

Since there was a large discrepancy between the LLS and NLLS estimates for the Lindane isotherm, both estimates were used in the model to determine which values produced a better prediction. Figure 6.4.3 shows the IAST prediction for Lindane competition with Triallate as determined in the bi-solute Isotherm 11, using LLS single solute parameters, while Figure 6.4.4 shows predictions using NLLS parameters. It can be seen that for LLS estimates the prediction was approximately parallel to the single solute line, whereas for NLLS the prediction crossed the single solute line. Where the prediction crossed the single solute line, the model predicted that the capacity of the resin for Lindane was higher with Triallate present than without it . . This incorrect result occurs in the same high resin weight region where the NLLS line deviated from the actual isotherm data. These results indicated that the NLLS estimates were unsatisfactory for the Lindane prediction (similar results occurred for Triallate, except that the prediction with NLLS values crossed the single solute line in the low resin weight region - data not shown). Therefore the LLS estimates of the Freundlich parameters were used for all modelling in the study.

6.4.2 IAST Predictions

IAST predictions were generated for bi-solute isotherms 11 and 15 for both Lindane and Triallate. In Isotherm 11, the compounds were spiked at an approximately equi-molar initial liquid phase concentration. Since the competitive displacement was not very large, Isotherm 15 was performed at an approximately 5 to 1 molar initial ratio (Triallate to Lindane). The single solute parameters used in the modelling were those from Isotherm 12 for Lindane and Isotherm 14 for Triallate. The Average Percent Errors (APEs) of the solid phase predictions compared to the bi-solute data were calculated to aid in evaluation

of the predictions. These values are presented in Table 6.4.1 for both compounds and both isotherms.

The plot of the Lindane prediction for Isotherm 11 was previously given in Figure 6.4.3. The figure shows that the predicted curve was shifted down and to the right of the actual bi-solute data. The model predicted a larger displacement for Lindane than was experimentally determined. The APE for this prediction was 18.4%. The solid phase values for high resin weights (lower left region) were predicted relatively well, but in the low resin weight region, the predicted values were lower than the experimental data. As such, this region was responsible for the relatively high APE. It can be seen, however, that the predicted and actual curves were very similar in shape, with a leveling off in the upper right region. An explanation for this curving is that at low resin doses, the Triallate competed more effectively than Lindane, and therefore the Lindane was displaced more. When the resin dose increased, the competition was less severe due to the increased surface area for adsorption, and the Lindane adsorption became more like single solute behaviour. This can be seen in the bi-solute data in this figure.

Although the curves were similar shape, the prediction covered a smaller liquid phase range than the bi-solute data. This was consistent with the model predicting a larger displacement, in that the liquid phase concentration of the highest resin weight sample is predicted to be larger than what was experimentally determined.

The fact that the bi-solute isotherm shows a slightly higher capacity than the single solute isotherm in the high resin weight region is a result of using the linear least squares best fit line for Isotherm 12 (single solute). It can be seen in Figure 6.2.15 that the low resin weight samples deviated from the linearity in the

high resin weight samples, which caused a decrease in the slope of the best fit line.

The IAST prediction for Isotherm 15 is given in Figure 6.4.5. 'The bi-solute data for this isotherm exhibited a large degree of scatter, but the prediction followed the same trend as with Isotherm 11. The prediction was again shifted down and to the right, and covered a smaller liquid phase range than the bi-solute data, indicating that the model predicted a larger displacement. The solid phase concentrations were predicted relatively well with the exception of the two lowest resin weight samples. These points were primarily responsible for the APE of 17.1%.

The IAST prediction for Triallate in Isotherm 11 is shown in Figure 6.4.6. Visually, the prediction appeared to be much better than for Lindane, but in fact the APE of 19.6% was very similar. This was primarily due to the lower solid phase concentrations than predicted in the low resin weight zone of the plot. Since Triallate was the stronger adsorber, the predicted and actual displacement from single solute behaviour was less than that of Lindane.

Figure 6.4.7 shows that the predicted displacement from single solute adsorption of Triallate in Isotherm 15 was less than in Isotherm 11. This is reasonable since the initial liquid phase concentration of Lindane was decreased in Isotherm 15, resulting in less competition for Triallate. The large degree of scatter in the bi-solute data for Isotherm 15 makes a comparison of the prediction to experimental data very difficult. No bi-solute data points were present in the middle region of the plot, but rather were concentrated at the ends of the plot. This behaviour was also seen in some single solute isotherms, and the cause is unknown. The high APE of 45.2% was primarily caused by the scatter in the low resin weight bi-solute data points.

The observation that IAST predicted larger displacement compared to observed data was also found by Kong and DiGiano (1986) for compounds which did not exhibit very different adsorption strengths.

It becomes evident that 'good quality' single solute and bi-solute isotherms are required to adequately predict and verify competitive adsorption effects. To demonstrate this, Lindane adsorption was predicted for bi-solute Isotherm 15 using the single solute data from Isotherm 16 instead of Isotherm 12 (Isotherm 16 was a check on the reproducibility of the two-week isotherms, and gave lower scatter as seen by a value of R^2 of 0.977 for Isotherm 16 compared to 0.900 for Isotherm 12). Figure 6.2.26 illustrates that the two isotherms appeared to be reproduced relatively well. But the small change between these two isotherms caused a significant difference in the model's prediction. Figure 6.4.8 shows the prediction and isotherm data. It can be seen when comparing to Figure 6.4.5 (prediction using single solute Isotherm 12), that the shape and relative position of the prediction curve has changed. Less leveling in the low resin weight region occurred, and the line was shifted in slope in keeping with the shift in slope from Isotherm 16 to 12. The result is a lower APE of only 10.9% compared to the previous APE of 17.1%. This improvement in prediction with a relatively small change in the single solute isotherm indicates the high dependence of the model on input data fluctuations. As such, single solute isotherms must be very accurate for the model to produce accurate predictions.

One possible source of error when using IAST is the assumption that the experimental single solute Freundlich parameters can be extrapolated to zero and high concentrations. IAST often requires larger single solute solid phase concentrations than observed in multi-component isotherms, especially for weaker adsorbing compounds (Crittenden et al., 1985). If the isotherm shows

deviation from linearity in the range tested, and IAST extrapolates to a larger range, these outlying values may be very far from the actual adsorption behaviour in that region. This will obviously cause errors in the predictions. The fact that the isotherms used for modelling show either scatter or curvature, points to this as a probable cause of the errors in the predictions.

To determine if the single solute isotherms were a possible source of error due to IAST extrapolation, a plot of $(d \ln C_i^o / d \ln q_i^o$ i.e. the slope of the isotherm) versus q_i^o was generated to show the range of extrapolated data used in the predictions. Values of q_i used in IAST were obtained from the model's output, and q_i^o (the solid phase concentration of the single solute at the same spreading pressure as the bi-solute) was calculated as follows:

$$q_i^o = \Sigma \ q_j \ n_j \ / \ n_i \quad \text{for } j = 1 \text{ to } 2 \text{ (for two components)}$$

The results of this calculation yield the solid phase concentration at each resin dose used by IAST. The range of these results for the predictions of bi-solute isotherms 11 and 15 are given in Table 6.4.2. Also given are the ranges for the single solute isotherms 12 and 14 (the parameters of which were used for modelling). A plot of all data points used in IAST as well as the two range points for the single solute isotherms is given in Figure 6.4.9 for predictions on Isotherm 11. Figure 6.4.10 show these results for Isotherm 15 predictions. It can be seen that the model has extended the single solute isotherm for Lindane by a large amount. The range of solid phase concentrations used for Triallate, however, was within the experimental single solute isotherm data.

Thus the errors in the predictions can be attributed to three factors: 1) the single solute isotherms exhibited scatter and showed some lack of fit

(systematic departure) from the Freundlich equation in the region tested, 2) for Lindane the IAST model extrapolated the single solute values, and 3) the bi-solute isotherm data also showed scatter and therefore may not be entirely accurate.

The lack of fit and scatter in the single solute isotherms in the range tested causes errors since a degree of uncertainty in actual adsorption behaviour is present. The correlation coefficient, R^2, for the least squares linear regression in Isotherm 12 was 0.900 and for Isotherm 14 was 0.848, indicating the relatively poor fit of the data. The cause of this scatter is, however, not known (see section 6.2.3 for possible explanations).

For Lindane, the single solute isotherm was extrapolated to higher solid and liquid phase concentrations by the model. It is probable that the extrapolated data do not reflect actual adsorption behaviour in the extrapolated range since the model draws upon the poor quality single solute estimates.

For Triallate, the IAST model used a range that was experimentally determined, and therefore, extrapolation was not the cause of prediction errors. Rather, one source of the errors was the poor single solute isotherm data. The single solute plot for Isotherm 14 in Figure 6.2.22 showed a high degree of curvature. This is also seen in the low R^2 of 0.848. Since the data do not fit the Freundlich equation, errors are generated when using the model which assumes Freundlich behaviour.

Another source of the errors in the predictions was the scatter in the bi-solute isotherm data. These data were subject to the same sort of scatter seen in single solute isotherms, which when compared to the evenly spaced model predictions lead to high APEs.

6.4.3 Summary

The IAST computer model was used to predict the competitive adsorption of Lindane and Triallate. The trends in the competition were predicted, but differences between actual bi-solute data and predictions were observed. The model predicted a higher displacement from single solute adsorption than was actually observed. The APEs for all predictions were less than 20% except for Triallate in Isotherm 15. Model predictions are in error because of inadequate single solute and bi-solute isotherm data. Single solute isotherms showed scatter and curvature, which caused poor precision and accuracy of the Freundlich parameters. It is not known, however, whether the cause of the curvature was actual adsorption behaviour or experimental error (presence of TOC or resin drying for example). When IAST extrapolated the isotherms, it is most probable that the adsorption behaviour in the extrapolated zones was not accurate. This points to the fact that accurate isotherm data and good Freundlich behaviour is essential to the model's ability to predict multi-component adsorption.

Since the predictions are compared to experimental bi-solute data, any scatter or inaccuracy in the bi-solute data caused differences from the predicted behaviour. The bi-solute Isotherm 11 showed less scatter than bi-solute Isotherm 15. The largest APE was generated for the prediction of Triallate in Isotherm 15. The cause was scatter in the low resin weight samples of the isotherm.

6.5 Phase 5: Column Modelling Using Equilibrium Column Model

6.5.1 Column Experiments

The computer model ECM was run with the appropriate input data to obtain predictions of column breakthrough for a Lindane and Triallate mixture (1:5 molar ratio). The surface loading was determined from the flow conditions of XAD-2 column sampling at the Rossdale Pilot Plant in Edmonton. A column experiment was designed from the model output data, and the experiment performed with certain fractions of the effluent being collected and extracted for analysis on GC. The results, given in Table 6.5.1, show that immediate breakthrough of both Lindane and Triallate occurred, at approximately 75% of the influent concentration. A plot of the efflu t concentration divided by the influent concentration (C/C°) versus the volur of solution passed is given in Figure 6.5.1. Also plotted is the flow rate, normalized to fit on the same scale. The solution was gravity fed and the flow rate changed with time due to flow restrictions in the column, most probably caused by air bubbles which formed within the resin bed. The Triallate curve showed two large drops in effluent concentration, which was probably an analysis problem. Since another experiment was performed, the samples around these points were not analysed.

A second column experiment was performed since immediate breakthrough occurred in the first experiment. The column used in the first experiment was 0.56 cm diameter X 1.4 cm height, (height-to-diameter ratio of 2.5). The height-to diameter ratio was increased to 6.7 (0.7 X 4.7 cm) in the second experiment in order to increase the empty bed contact time (EBCT) of the solution within the resin bed. The surface loading was kept the same as in the first experiment. The results for the second experiment are presented in Table 6.5.2, and the breakthrough plot is given in Figure 6.5.2. Immediate breakthrough was again noticed, although at much lower normalized concentrations than the first experiment. It was seen that the Lindane

breakthrough curve was always at higher concentrations than that of Triallate. This was to be expected, since Lindane was the more weakly adsorbing compound and as such, was displaced by Triallate. The increase in EBCT was shown to dramatically affect the adsorption of the two compounds. This suggested that the kinetics of adsorption were relatively slow, and that the EBCTs used were inadequate for quantitative removal of these compounds from water. The importance of EBCT was also seen in the decrease in normalized concer ation of the last two samples. The Lindane and Triallate curves decreased as the flow rate decreased due to reduction in head pressure. The decrease for Triallate was more pronounced since it was the more strongly adsorbing compound and as such, was more affected by flow (EBCT) changes.

In order to further investigate the effect of EBCT on column adsorption, a third experiment was performed using the same column dimensions and influent concentrations as the second experiment, but at a flow rate reduced by a factor of eight. The results are given in Table 6.5.3 and Figure 6.5.3. Both Lindane and Triallate were detected in the first effluent sample collected, but at very low levels compared to previous experiments. After approximately 11.5 L of solution passed, the effluent concentration of Lindane was 21.9% of the influent, and Triallate was present at only 7.9% of the influent level. It should be noted that the normalized concentration scale in Figure 6.5.3 does not extend to unity, but only to 0.35 in order to expand the breakthrough curves. The decrease in effluent concentrations with a reduced flow rate was evident at 3.5 L of solution passed. The overall effect of the increased EBCT from that of experiment 2 was a dramatic decrease in effluent concentrations.

The plot in Figure 6.5.1 showed the Lindane and Triallate normalized effluent concentrations to be similar, but the plot in Figure 6.5.2 displays a large difference between the two compounds. These results suggest that the EBCT in

experiment 1 of 0.82 second was so short that competitive adsorption effects were negligible. At the intermediate EBCT of 2.7 seconds in experiment 2, the effects of competition can be seen in the lower Triallate normalized effluent concentration compared to that of Lindane. The same competitive trend also appeared toward the end of experiment 3. Therefore, the EBCT within the resin bed is an extremely important parameter in multicomponent systems.

6.5.2 ECM Predictions

The computer model ECM was used to predict the breakthrough for the conditions of these experiments. The experimental conditions as well as the volume of solution to breakthrough predictions are given in Table 6.5.4. The breakthrough predictions for the first experiment of over 10 L were obviously in error compared to experimental results, since 90% breakthrough was reached at 5 L of solution passed. This demonstrated the importance of resistance to mass transfer considerations at such short EBCTs, which the model does not take into account. It is difficult to determine the accuracy of the model's predictions for the second and third experiments since full breakthrough concentrations were not obtained for the volumes of solution passed. It is clear, however, that as the EBCT increased, the adsorption efficiency also increased. For longer EBCTs in which equilibrium is more closely approached within the column, the model becomes more accurate since the mass transfer considerations become less important. This result for ECM was also demonstrated by Crittenden et al. (1987) for different EBCTs in activated carbon contactors.

The increase in the predictions of volume of solution passed to breakthrough from experiment 1 to experiment 2 was due to the increased bed volume of resin since the surface loading was held constant. An increase in the

resin capacity predictions between experiments 2 and 3 also existed, and was due to the decrease in flow rate (increase in EBCT).

The assumption of no resistance to mass transfer was not valid under the experimental conditions tested. ECM has advantages, however, over other column models which take mass transfer resistance considerations into account, due to the reduction in experimentation required to determine the necessary input parameters.

6.5.3 Comparison to Other Results

The results of these experiments demonstrate the importance of the EBCT for sampling efficiency. For comparison purposes, the EBCTs used by different researchers in the use of XAD-2 and XAD-4 resin is presented below:

research paper	EBCT (seconds)	application
...l., 1977	8.1 - 11.9	pesticide sampling from water
Junk et al., 1974	2.0 - 3.4	trace organics analysis in water
LeBel et al., 1987	19.5	trace organics analysis in water
van Vliet et al., 1980	128	phenol column adsorption on XAD-4

The diversity in methods used by different researchers is evident from these data. The shortest EBCT of 2.0 - 3.4 seconds used by Junk et al. (1974) resulted in quantitative recoveries for some compounds. and recoveries as low

as 47% for others. The short EBCT may have been a factor in the low recoveries, especially for multisolute systems.

The longer EBCTs used by Coburn et al. (1977) and LeBel et al. (1987) would be expected to yield better recoveries. The long EBCT of 128 seconds used by van Vliet et al (1980) was used in research column modelling experiment. The use of such long EBCTs in routine sampling procedures would be impractical, however.

6.5.4 Summary

The computer model ECM was evaluated in the prediction of breakthrough of a bi-solute system on XAD-2 resin. At a short EBCT, resistance to mass transfer effects were important and the model did not predict the experimentally determined breakthrough. At longer EBCTs, the full breakthrough concentrations were not experimentally observed, and thus, model predictions could not be verified. As the EBCT increased, resistance to mass transfer considerations became less important as time was allowed for equilibration to occur. The model would be expected to be more accurate under these conditions.

If the ideal breakthrough curve is to be obtained for the conditions used in the experiments, a smaller resin size may be required. This would reduce the film diffusion rate, since the stationary liquid film about the particles decreases in thickness as the particle size decreases. Practical difficulties with head loss may be encountered with smaller particles, however.

The higher normalized effluent concentration for Lindane over Triallate indicated the important role of EBCT upon competitive adsorption effects. The results showed that the more strongly adsorbing compound (Triallate) was

retained to a higher degree on the column, while the more weakly adsorbing compound (Lindane) was displaced.

In comparing the results to sampling conditions used by other researchers, a large range in EBCTs was observed. In establishing sampling procedures, the EBCT is restricted by practical limitations, but should be long enough to allow equilibration.

6.6 Recommendations

Several recommendations can be made as a result of the findings in this study.

- Similar modelling studies should use model compounds which exhibit larger differences in their adsorptive behaviour. For the more weakly adsorbing compound, the single solute isotherm should be experimentally determined to high concentration regions in order to reduce extrapolation by IAST. Since many isotherms displayed curvature when plotted in the linearized form of the Freundlich equation, different isotherm equations such as the Langmuir or the Singer-Yen should be incorporated for use within the computer models.

- Long EBCTs should be used for resin column experiments. For routine sampling of a specific water matrix, the EBCT should be varied to determine the longest practical EBCT, in order to ensure equilibration within the resin bed. This will improve extraction efficiency.

- The effects of drying the resin should be investigated further since preliminary tests show that the effect may be a useful one in improving sampling recoveries.

- The kinetics of adsorption of non-volatile organics on bead resin as well as crushed resin should be further investigated. It may be possible to increase adsorption efficiencies by utilizing a smaller size of resin particle. A trade-off between increased adsorption kinetics and increased head loss would likely have to be made for column adsorption tests.

7.0 Conclusions

The following conclusions may be drawn from this investigation of the adsorption of non-volatile organic compounds on XAD-2 resin:

1) Resin which had been previously used in routine sampling procedures exhibited neither loss in adsorptive capacity nor reduction in the rate of adsorption for Lindane, the only compound tested in this regard.

2) The computer model based on IAST predicted the trends in competitive adsorption between Lindane and Triallate. A larger displacement from single solute adsorption was predicted for bi-solute systems than was experimentally observed. Errors in predictions were caused by imprecise single solute and bi-solute data. IAST extrapolated the imprecise Lindane single solute isotherm data which then magnified the error. As such, the model's application to resin adsorption cannot be disputed nor verified.

3) The computer model ECM did not predict adsorption breakthrough in bi-solute column experiments as mass transfer parameters cannot be ignored in the range of resin empty bed contact times experimentally encountered.

4) The scatter associated with the isotherm data cannot be explained. Many different experimental modifications were employed to reduce scatter but were unsuccessful.

5) The difference in the adsorptive capacities for Lindane and Triallate was not large enough to cause significant displacement of the isotherms in bisolute experiments. The demonstration of a clear effect of competition was also complicated by the scatter in the isotherms which resulted in a degree of uncertainty in adsorption behaviour. If compounds exhibiting a larger difference in adsorption behaviour were used, the scatter for each

isotherm would become relatively less important, and the competitive adsorption effects would be more pronounced.

6) Crushed resin in the 100-200 mesh size fraction showed a higher capacity for Lindane than resin beads, at the equilibrium times used. This was attributed to faster adsorption kinetics for smaller particles.

7) The kinetics of adsorption on resin beads was relatively slow. Isotherm bottle should be turned at a rotational speed of less than 28 rpm, to reduce a "centrifuge" effect. Extensive kinetics studies should be performed to accurately determine the rate of adsorption. Studies using XAD-2 resin beads should allow for longer than 14-day equilibration times.

8) The adsorption of Triallate was more favorable than that of Lindane. This was indicated by a larger Freundlich K, and a lower Freundlich $1/n$ (slope). A lower slope indicates that at lower liquid phase concentrations, a higher solid phase concentration is maintained.

9) The relative adsorption affinities on XAD-2 resin for the compounds tested were as follows: TCEP < HCE ~ Lindane ~ DCPA < p,p' DDE < Triallate.

Table 4.2.1   Physical Properties of XAD-2 Resin
(modified from Rohm and Haas, technical bulletin)

Property	Amberlite XAD-2
Appearance	hard, spherical opaque beads
Solids	51 to 55
Porosity (mL pore/mL bead - dry basis)	0.40 to 0.45
Surface Area (m^2/g - dry basis)	330
Effective Size (mm)	0.30 to 0.45
Harmonic Mean Particle Size (mm)	0.45 to 0.60
Average Pore Diameter ($Å$ - dry basis)	90
True Wet Density in Distilled Water (g/mL)	1.02
Skeletal Density (g/mL)	1.07
Bulk Density (lbs/ft^3)	40 to 44
(g/cm^3)	0.64 to 0.70

Table 5.3.1 Percent Dry Resin Data for Entire Study

Date	# of samples	Mean Percent Dry Resin	Standard Deviation	Percent Relative Standard Deviation
Fresh beads				
July, 1987	11	56.7	0.31	0.54
Oct., 1987	6	56.9	0.079	0.14
Feb., 1988	6	55.9	0.35	0.63
March, 1988	4	56.4	0.32	0.57
March, 1988	5	56.5	0.45	0.80
April, 1988	6	56.5	0.39	0.70
Preloaded beads				
Aug., 1987	2	55.2	-	-
March, 1988	7	56.6	0.31	0.54
April, 1988	6	56.48	0.39	0.70
Seived Beads (Oct., 1987)				
20-28 mesh	2	57.5	-	-
28-35 mesh	2	55.6	-	-
Crushed Fresh Resin (100-200 mesh)				
Jan., 1988	5	53.5	0.96	1.80
March, 1988	8	46.1	2.01	4.37

Table 5.4.1 TOC Data for Milli-Q System 1

| Sample | Date, 1988 | TOC (µg/L) | | |
		Jan. 27	Feb. 1	Feb. 2
Milli-Q		64	107	162
Buffered Milli-Q		112		
Batch contacted*		187^	218^^	
Column contacted*			658^^^	186

* buffered Milli-Q water contacted with XAD-2 resin
^ one day equilibration, magnetically stirred
^^ three day equilibration, rotor stirred
^^^ initial column rinse
Note: values reported are average of 2 or 3 replicates

Table 5.4.2 TOC Data for Milli-Q System 2

| Sample | Date (1988) | TOC (µg/L) | |
		Mar. 29	Apr. 5
Milli-Q		122	
Resin Filtered		122	
Buffered		61	139

Note: values reported are average of 3 replicates

Table 6.1.1   Solvent Extraction Results - Dichloromethane (10 µg/L)
Average area counts and percent of total for 4 compounds

	HCE	Lindane	Triallate	p,p' DDE
Standard	129524	25041	1388	31219
Rotovap check	124770	29519	1678	35796
	96.3	117.9	120.9	114.7
Separatory Funnel rinse	ND*	ND	ND	ND
Extract 1	71523	22003	ND	23522
	55.2	87.9		75.3
Extract 2	9828	5008	ND	3956
	7.6	20.0		12.7
Extract 3	ND	691	ND	1002
		2.8		3.2
Total % recovered in Extracts	62.8	110.6		91.2

Table 6.1.2 Solvent Extraction Results - Dichloromethane (100 μg/L)
Average area counts and percent of total for 5 compounds

	HCE	Lindane	Triallate	p,p' DDE	Methoxychlor
Standard	2059975	1288250	37606	1301775	150558
Rotovap check	58000 95.0	1319900 102.5	38139 101.4	1355400 104.1	145610 96.7
Separatory Funnel rinse	38121 1.9	ND	ND	100484 7.7	5416 3.6
Extract 1	1237550 60.1	1278500 99.2	33616 89.4	500130 38.4	87487 58.1
Extract 2	5998 0.3	7979 0.6	ND	28734 2.2	ND
Extract 3	ND	ND	ND	19717 1.5	ND
Total % recovered in Extracts	60.4	99.8	89.4	42.1	58.1

* ND denotes Not Detected

Table 6.1.3 Solvent Extraction Results - Hexane (5 µg/L)
Area counts and percent of standard for six compounds

	HCE	Lindane	Triallate	p.p'DDE	Methoxychlor	DCPA
Standard	64003	26134	1069	21280	1327	18659
Rotovap check	47262 / 73.8	26124 / 100.0	1129 / 105.6	21448 / 100.8	976 / 73.5	19325 / 103.6
Sep. funnel rinse	2513 / 3.9	ND*	ND	387 / 1.8	ND	ND
Extract 1	24935 / 39.0	27625 / 105.7	1162 / 108.6	19076 / 89.6	1461 / 110.1	18874 / 101.2
Extract 2	ND	ND	ND	494 / 2.3	ND	ND
Extract 3	ND	ND	ND	ND	ND	ND
Total % recovered in Extracts	39.0	105.7	108.6	92.0	110.1	101.2

ND denotes Not Detected

Table 6.1.4 Solvent Extraction Results - Dichloromethane (50 µg/L)

Area counts and percent of standard for 7 compounds
(50 µg/L each except HCB and DCPA*)

	HCE	HCB	Lindane	Triallate	DCPA	p,p'DDE	Methoxychlor
Standard	1371267	220403	395853	12585	84367	216330	47784
Rotovap check	1405967	233863	471150	13526	85298	257590	48654
	102.5	106.1	119.0	107.5	101.1	119.1	101.8
Sep. funnel rinse	21466	5572	ND**	ND	1918	7654	ND
	1.6	2.5			2.3	3.5	
Extract 1	1074800	164370	452315	11904	71788	77352	35124
	78.4	74.6	114.3	94.6	85.1	35.8	73.5
Extract 2	41679	24438	23960	983	7136	11632	588
	3.0	11.1	6.1	7.8	8.5	5.4	1.2
Extract 3	1521	7528	1430	ND	2717	9768	ND
	0.1	3.4	0.4		3.2	4.5	
Total % recovered in Extracts	81.5	89.1	120.7	102.4	96.8	45.6	74.7

* Hexachlorobenzene and Dimethyl-2,3,5,6-tetrachloroteraphthalate at unknown levels (50 ppb combined)
** ND denotes Not Detected

Table 6.1.5 Solvent Extraction Results - Hexane (50 µg/L)
Area counts and percent of standard for 7 compounds
(50 µg/L each except HCB and DCPA*)

	HCE	HCB	Lindane	Triallate	DCPA	p,p' DDE	Methoxychlor
Standard	4224800	690693	2787025	89998	959725	2672025	356998
Rotovap check	2830635 / 67.7	688680 / 99.7	2797150 / 100.4	89530 / 99.5	952935 / 99.3	2547900 / 95.4	254910 / 73.5
Sep. funnel rinse^	1693850 / 3.3	440530 / 5.1	70217 / 0.3	66859 / 6.0	54745 / 0.6	4703250 / 14.0	419885 / 9.3
Extract 1	1939200 / 47.1	587247 / 85.0	2716733 / 97.5	79659 / 88.7	896103 / 93.5	2003500 / 75.3	187503 / 56.1
Extract 2^	77701 / 0.3	93681 / 1.1	243025 / 0.8	11980 / 1.2	81276 / 0.8	812015 / 2.5	12493 / 0.9
Extract 3^	0.18 14739 / 0.2	36051 / 0.4	47012 / 0.2	5260 / 0.6	32982 / 0.4	216980 / 0.7	6084 / 0.7
Total % recovered in Extracts (plus sep. fun. rinse)	47.6	86.5	98.6	90.4	94.7	78.5	57.6
	50.9	91.6	98.9	96.4	95.2	92.5	66.9

* Hexachlorobenzene and Dimethyl-2,3,5,6-tetrachloroteraphthalate at unknown levels (50 ppb combined)
^ These solutions made up to 2 mL, others in 25 mL

Table 6.1.6   Distribution Coefficient Determination for Lindane, HCE, Triallate and DDE

Compound (equil'n time)	Dry Resin Dose (g/L)	Equilibrium Concentration		Kd (L/g)	Percent Recovered
		Liquid (ug/L)	Solid (ug/g)		
Lindane					
12	0.1142	0.16	38.81	247	91.9
5	0.6244	0.51	63.87	126	80.8
5	1.0733	0.67	62.32	93	135.1
Hexachloroethane (HCE)					
13	0.6232	0.18	64.27	356	98.8
13	0.7384	0.17	50.02	293	91.1
Triallate.					
12	0.6230	0.0056	87.17	15672	103.6
12	0.7391	0.0039	68.36	17421	96.4
p,p' DDE					
12	0.6243	0.069	72.45	1053	82.8
12	0.7380	0.071	66.62	932	90.0

Table 6.1.7   Distribution Coefficient Determination for DCPA and TCEP

Compound (equil'n time)	Dry Resin Dose (g/L)	Equilibrium Concentration		Kd (L/g)	Percent Recovered
		Liquid (ug/L)	Solid (ug/g)		
Dimethyltetrachloroteraphthalate (DCPA)					
7	0.5727	0.38	99.0	260	100.1
7	0.7385	0.24	72.3	304	94.1
Tris(2-Chloroethyl) phosphate (TCEP)					
7	0.1194	149	3428	23.0	76.4
7	0.4475	47.5	1288	27.2	85.4
7	1.5987	9.94	395	39.7	87.7
7	4.5432	3.21	138	42.8	85.9
7	4.5456	3.14	139	44.1	86.7

Table 6.2.1 Adsorption Kinetics of Lindane at 5 µg/L

| Bottle # | Resin Dry Weight (g) | Equilibration Time | CONCENTRATION (µg/L) | | |
			Liquid Phase	Solid Phase*	Total Recovered
1	0.0111	24 hrs	4.3	0.4	4.7
2	0.0119	47 hrs	3.9	0.9	4.7
3	0.0116	5 days	4.4	1.0	5.3
5	0.0120	6 days	4.2	1.0	5.2
6	0.0116	7 days	4.4	1.1	5.5
Blank	0	5 days	5.1	-	5.1
Preloaded	0.0119	6 days	4.7	0.5	5.2
Preloaded	0.0119	6 days	4.6	0.5	5.1

* Concentration if the solute on the resin was made up in 1 L.

Table 6.2.2 Adsorption Kinetics of Lindane at 50 µg/L

| Bottle # | Resin Dry Weight (g) | Equilibration Time | Concentration | | Percent Recovered |
			Liquid (µg/L)	Solid (µg/g)	
1	0.4562	5 hrs	37.1	43.2	86.0
2	0.4574	24 hrs	16.9	99.7	94.7
3	0.4575	2 days	6.7	110.2	86.5
4	0.4573	3 days	4.0	126.2	93.6
5	0.4579	7 days	0.32	108.6	91.6
Blank a	0	3 days	66.0		
Blank b	0	7 days	54.7		

* Blank a used for bottles 1-4 and Blank b for bottle 5

Table 6.2.3 Freundlich Parameters for All Isotherms

Isotherm Number [*]	Description	Linear Least Squares K	1/n	Non-Linear Least Squares[**] K	1/n
1 (7)	Lindane 50 ppb, beads	233.25	0.4478	121.7 (292.8 - -49.45)	0.6747 (1.083- 0.2667)
2 (8)	Lindane 100 ppb, beads	279.03	0.449	343.6 564.6 - 122.6)	0.3932 (0.5528 - 0.2336)
3 (7)	Prelim. Triallate 104 ppb, beads	566.18	0.3011	882.9 (2222 - -456.0)	0.208 (0.6317 - -0.2157)
4 (7)	Prelim. TCEP 500 ppb, beads	54.47	0.8279	51.9 (59.6 - 44.19)	0.8372 0.8672 - 0.8072)
5 (7)	Triallate 104 ppb, beads	590.38	0.162	582.2 (1126 - 38.45)	0.1887 (0.4465 - -0.6897)
6 (7)	Lindane 100 ppb, crushed	811.96	0.4905	932.8 (1471 - 394.0)	0.4465 (0.6210 - 0.2719)
7 (7)	Triallate 523 ppb, beads	980.11	0.4389	1744 (3464 - 23.47)	0.3172 0.5190 - 0.1154)
8 (9)	Lindane 500 ppb, crushed	1299.06	0.5781	291 (742.8 - -160.7)	0.8524 (1.127 - 0.5779)
9 (7)	Lindane, 500 ppb Preloaded beads	368.51	0.4317	909.7 (2563 - -743.2)	0.2569 (0.5773 - -0.0636)
10 (7)	Lindane (bi-solute) 500 ppb, beads	763.49	0.3732	847.2 (1338 - 356.6)	0.3535 (0.4562 - 0.2509)
10 (7)	Triallate (bi-solute) 523 ppb, beads	1638.41	0.272	1419 (2610 - 227.3)	0.3046 (0.4577 - 0.1515)

Isotherm, Number [*]	Description	Linear Least Squares		Non-Linear Least Squares [**]	
		K	1/n	K	1/n
11 (14)	Lindane (bi-solute) 500 ppb, beads	922.65	0.4163	1116 (1550 - 681.7)	0.377 (0.4471 - 0.307)
11 (14)	Triallate (bi-solute) 523 ppb, beads	2833.1	0.2446	2705 (3986 - 1424)	0.2551 (0.3439 - 0.1663)
12 (17)	Lindane 500 ppb, beads	538.39	0.5811	1474 (2396 - 550.8)	0.3487 (0.4610 - 0.2364)
13 (17)	Lindane, 500 ppb Preloaded beads	618.37	0.5469	1659 (2688 - 630.3)	0.3165 (0.4287 - 0.2043)
14 (17)	Triallate 523 ppb, beads	3761.25	0.3032	3289 (12320 - 5744)	0.3499 (0.8634 - -0.1637)
15 (16)	Lindane (bi-solute) 100 ppb, beads	473.83	0.3291	439 (810.7 - 67.36)	0.3595 (0.5819 - 0.1372)
15 (16)	Triallate (bi-solute) 523 ppb, beads	2858.37	0.1621	2737 (4867 - 607.8)	0.1826 (0.3384 - 0.0268)
16 (16)	Lindane 500 ppb, beads	393.52	0.6908	180.3 (526.1 - -165.6)	0.8173 (1.148 - 0.4865)

[*] equilibration time in days given in brackets
[**] 95 % confidence interval given in brackets

Table 6.2.4   Isotherm 1 Solid Phase Results - Lindane
Solid phase analysed after 7 days equilibration

Bottle #	Dry Resin Weight (g)	Equilibrium Concentration	
		Solid (ug/g)	Liquid (ug/L)
0a	-	-	51.5
0b	-	-	51.1
0c	-	-	51.0
1	0.0044	1261	40.1
2	0.0053	1746	32.5
3	0.0068	780	40.5
4	0.0085	1054	33.2
5	0.0109	622	37.6
6	0.0133	1021	24.0
7	0.0173	647	28.8
8	0.0220	518	28.3
9	0.0277	602	17.8
10	0.0337	418	23.0
11	0.0426	445	13.2
12	0.0544	371	10.8
13	0.0681	321	7.49
14	0.0849	215	14.7
15	0.1089	148	19.0
16	0.1350	158	8.58
17	0.1694	97.8	18.0
18	0.2167	96.0	9.57
19	0.2700	85.0	5.28
20	0.3414	60.9	9.57

Table 6.2.5 Isotherm 1 Results - Lindane
Both phases analysed after 7 days equilibration

Bottle #	Dry Resin Weight (g)	Equilibrium Concentration Liquid (µg/L)	Solid (µg/g)
0a	0	51.5	-
0b	0	51.1	-
0c	0	51.0	-
1	0.0044	40.3	1261
2	0.0053	32.8	1746
3	0.0068	40.5	780
4	0.0085	30.8	1054
5	0.0109	35.8	622
6	0.0133	24.8	1021
7	0.0173	29.0	647
8	0.0220	26.1	518
9	0.0277	17.3	602
10	0.0337	22.9	418
11	0.0426	10.7	445
12	0.0544	5.30	371
13	0.0681	2.74	321
14	0.0849	2.17	215
15	0.1089	1.21	148
16	0.1350	0.523	158
17	0.1694	0.326	97.8
18	0.2167	0.199	96.0
19	0.2700	0.180	85.0
20	0.3414	0.177	60.9

Table 6.2.6 Isotherm 2 Results - Lindane
Both phases analysed after 8 days equilibration

Bottle #	Dry Resin Weight (g)	Equilibrium Concentration Liquid (µg/L)	Solid (µg/g)	Percent Recovered
0a	-	96.6		
0c	-	85.1		
2	0.0041	73.9	2360	96.7
3	0.0062	73.5	1941	100.9
4	0.0111	68.9	1068	95.9
5	0.0128	50.4	1778	99.2
8	0.0446	9.16	907	93.3
9	0.0625	2.42	738	97.9
10	0.0866	1.89	530	96.9
11	0.1200	2.60	385	98.4
12	0.1745	0.596	271	98.4
13	0.2412	0.520	195	97.7
14	0.3455	0.934	133	96.3
15	0.4933	0.116	95.8	97.9

Experimental Note: bottles 0b, 1, 6 & 7 lost due to breakage.

Table 6.2.7 Isotherm 3 Results - Preliminary Triallate
Both phases analysed after 7 days equilibration

Bottle #	Resin Dry Weight (g)	Equilibrium Concentration Liquid (µg/L)	Solid (µg/g)	Percent Recovered
B1	-	100.6	-	
B2	-	100.9	-	
B3	-	100.8	-	
13	0.0082	41.2	3451	97.3
14	0.0133	69.8	956	94.6
15	0.0250	10.1	1843	101.4
16	0.0487	14.0	902	101.1
18	0.1594	0.018	316	100.1
20	0.5088	0.035	93.9	94.8

Table 6.2.8 Isotherm 5 Results - Triallate
Both phases analysed after 7 days equilibration

Bottle #	Dry Resin Weight (g)	Equilibrium Concentration		Percent Recovered
		Liquid (µg/L)	Solid (µg/g)	
B1	-	97.1	-	
B2	-	94.2	-	
B3	-	98.1	-	
1	0.0082	47.5	2855	98.0
2	0.0127	66.1	1067	96.5
3	0.0161	64.6	973	99.4
4	0.0161	65.3	875	96.8
5	0.0164	49.0	1516	102.3
6	0.0225	46.5	1118	100.5
7	0.0287	55.3	683	98.1
8	0.0337	27.6	1026	100.2
9	0.0472	12.0	923	102.8
10	0.0595	7.10	773	102.8
11	0.0603	4.54	743	97.6
12	0.0591	12.3	720	101.0
13	0.0800	1.92	602	101.9
14	0.0985	0.232	500	102.3

Table 6.2.9 Isotherm 6 Results - Lindane on 100-200 mesh resin
Both phases analysed after 7 days equilibration

Bottle #	Resin Dry Weight (g)	Equilibrium Concentration Liquid (µg/L)	Solid (µg/g)	Percent Recovered
0a	-	91.8	-	
0b	-	91.5	-	
0c	-	93.4	-	
1*	0.0043	43.0	5042	94.0
2	0.0058	37.7	4592	98.4
3	0.0079	16.6	4877	101.8
4	0.0082	24.6	4162	100.6
5	0.0082	24.5	4153	100.8
6	0.0137	17.2	2772	101.0
7	0.0215	17.4	1756	100.8
8	0.0361	0.96	1318	104.1
9	0.0542	0.65	878	104.0
10	0.0817	0.39	585	104.1
11	0.0815	0.51	587	104.2
12	0.0823	0.39	580	103.9
13	0.1313	0.27	368	105.0
14	0.2719	0.14	173	102.4

* Some of this sample's solid phase may have been lost

Table 6.2.10 Isotherm 4 Results - Preliminary TCEP
Both phases analysed after 7 days equilibration

Bottle #	Dry Resin Weight (g)	Equilibrium Concentration Liquid (µg/L)	Solid (µg/g)	Percent Recovered
0a	-	747	-	
0b	-	714	-	
1	0.0597	149	3428	76.4
2	0.2237	47.5	1288	85.4
3	0.7993	9.94	395	87.7
4	2.2716	3.21	138	85.9
5	2.2728	3.14	139	86.7

Table 6.2.11 TOC Results for Isotherm 7 Water Preparation
TOC in µg/L (average of 2 or 3 replicate injections)

Sample Date	Jan. 27	Feb. 1	Feb. 2
Milli-Q	64	107	162
Buffered Milli-Q	112		
Batch Contacted*	187^	218^^	
Column Contacted*		658^^^	186

* buffered Milli-Q water equilibrated with XAD-2 resin
^ one day equilibration, magnetically stirred
^^ three day equilibration, rotor stirred
^^^ initial column rinse

Table 6.2.12 Isotherm 7 Results - Triallate
Both phases analysed after 7 days equilibration

Bottle #	Resin Dry Weight (g)	Equilibrium Concentration Liquid (µg/L)	Equilibrium Concentration Solid (µg/g)	Percent Recovered
0a	-	440.2		
0b	-	455.7		
0c	-	458.7		
1	0.0087	165.2	14843	93.6
2	0.0127	266.8	6776	97.2
3	0.0203	80.8	9126	100.1
4	0.0206	97.1	8710	100.9
5	0.0206	197.1	5896	97.4
6	0.0328	61.8	6117	102.5
7	0.0549	14.8	4013	100.9
8	0.0863	2.56	2754	105.8
10	0.2220	1.69	1095	108.1
11	0.2232	2.36	1070	106.3
12	0.2238	0.61	1108	110.0
13	0.3712	0.49	669	110.2
14	0.5629	0.69	437	109.2

Experimental Note: bottle #9 broke in the equilibrator

**Table 6.2.13   Isotherm 8 Results - Lindane on
100-200 mesh resin**
Both phases analysed after 9 days equilibration

Bottle #	Resin Dry Weight (g)	Equilibrium Concentration Liquid (µg/L)	Solid (µg/g)	Percent Recovered
0a	-	448.1		
0b	-	450.1		
0c	-	458.8		
1	0.0010	341.7	47189	95.7
2	0.0039	234.6	27310	98.6
3	0.0060	186.9	20871	97.1
4	0.0091	143.9	16161	97.0
5	0.0159	46.9	12781	100.3
6	0.0228	20.0	9365	98.7
7	0.0516	6.2	4299	99.5
8	0.0961	1.97	2352	100.4
9	0.0969	1.77	2333	100.4
10	0.0945	1.76	2427	101.8
11	0.1835	0.98	1286	104.6
12	0.3003	0.66	804	106.9
13	0.5871	0.30	402	104.5

Table 6.2.14 Kinetics Experiment - Lindane on Fresh and Preloaded Resin Beads

Bottle #	Resin Dry Weight (g)	Equilibrium Concentration Liquid (µg/L)	Solid (µg/g)	Percent Recovered
0a	-	610		
0b	-	560		
1F	0.0433	251	4078	103.3
2F	0.0427	125	5553	102.3
3F	0.0427	50.6	6372	101.6
4F	0.0423	32.4	6558	100.3
1P	0.0424	238	4043	99.3
2P	0.0428	134	5313	100.7
3P	0.0425	74.1	6108	101.5
4P	0.0422	25.8	6543	98.8

Note: some of sample 4P (liquid phase) was lost (≤10%)

Table 6.2.15 Isotherm 12 Results - Lindane on Fresh Resin
Both phases analysed after 17 days equilibration

Bottle #	Resin Dry Weight (g)	Equilibrium Concentration Liquid (µg/L)	Solid (µg/g)	Percent Recovered
0a	-	514		
0b	-	507		
0c	-	499		
1*	0.0043	411	11882	101.0
2	0.0107	290	10194	100.6
3*	0.0342	25.1	7043	100.0
4*	0.0685	9.16	3629	100.0
5*	0.1766	3.10	1425	100.0
6	0.3366	1.88	743	99.1
7	0.5675	1.091	449	100.8
8	1.4130	0.435	182	101.4

* Solid phase calculated from liquid value since some solid phase was lost

Table 6.2.16 Isotherm 13 Results - Lindane on Preloaded Resin
Both phases analysed after 17 days equilibration

Bottle #	Resin Dry Weight (g)	Equilibrium Concentration		Percent Recovered
		Liquid (μg/L)	Solid (μg/g)	
0a	-	514		
0b	-	507		
0c	-	499		
1	0.0048	413	10599	101.8
2	0.0104	301	10034	100.7
3*	0.0330	26.6	7265	100.0
4*	0.0668	7.93	3731	100.0
5*	0.1690	2.66	1491	100.0
6	0.3484	1.34	729	100.5
7	0.5705	0.900	449	101.3
8	1.4169	0.334	180	100.8

* Solid Phase calculated from liquid value since some solid phase was lost

Table 6.2.17 Isotherm 16 Results - Repeat of Lindane Isotherm
Both phases analysed after 16 days equilibration

Bottle #	Resin Dry Weight (g)	Equilibrium Concentration		Percent Recovered
		Liquid (μg/L)	Solid (μg/g)	
1	0.0031	345	22368	94.2
2	0.0151	186	10828	100.0
3	0.0515	25.18	4702	99.7
4*	0.1774	3.522	1335	93.2
5	0.4871	1.294	495	94.5
6	1.3388	0.493	168	88.0

* some of sample 4 - liquid phase (≤10 %) was lost

Table 6.2.18 Isotherm 14 Results - Triallate
Both phases analysed after 17 days equilibration

Bottle #	Resin Dry Weight (g)	Equilibrium Concentration		Percent Recovered
		Liquid (μg/L)	Solid (μg/g)	
0a	-	461		
0b	-	506		
1	0.0032	248	38572	97.3
2	0.0088	228	13712	92.7
3	0.0145	172	10014	91.5
4	0.0307	6.40	8105	99.6
5	0.0566	0.398	4632	103.8
6	0.0978	0.123	2645	102.2
7	0.1705	0.0720	154	104.0
8	0.2815	0.0594	873	97.1

Table 6.3.1a Bisolute Isotherm 10 - Lindane Results
Equi-molar solution of Lindane and Triallate
Both phases analysed after 7 days equilibration

Bottle #	Resin Dry Weight (g)	Equilibrium Concentration		Percent Recovered
		Liquid (μg/L)	Solid (μg/g)	
0a	-	526		
0b	-	519		
1	0.0031	471	8107	98.9
2	0.0093	390	7283	99.8
3	0.0175	320	5252	95.6
4	0.0311	165	4877	89.0
5	0.0496	77.1	4554	100.4
6	0.0757	32.7	3218	98.8
7	0.1166	13.63	2162	98.3
8	0.1874	7.78	1363	98.5

Table 6.3.1b   Bisolute Isotherm 10 - Triallate Results
Equi-molar solution of Lindane and Triallate
Both phases analysed after 7 days equilibration

Bottle #	Resin Dry Weight (g)	Equilibrium Concentration Liquid (µg/L)	Equilibrium Concentration Solid (µg/g)	Percent Recovered
0a	-	451		
0b	-	392		
1	0.0031	407	9521	103.3
2	0.0093	305	10065	109.3
3	0.0175	279	5795	106.9
4	0.0311	137.8	5112	101.0
5	0.0496	46.13	4677	113.1
6	0.0757	9.429	3215	110.1
7	0.1166	1.718	2133	110.7
8	0.1874	0.655	1321	110.0

Table 6.3.2a   Bisolute Isotherm 11 - Lindane Results
Equi-molar solution of Lindane and Triallate
Both phases analysed after 14 days equilibration

Bottle #	Resin Dry Weight (g)	Equilibrium Concentration Liquid (µg/L)	Equilibrium Concentration Solid (µg/g)	Percent Recovered*
0c	-	494		
0d	-	428		
1	0.0045	399	11429	101.6
2	0.0077	368	9834	105.1
3	0.0174	229	8123	103.7
4	0.0298	108	6445	99.4
5	0.0493	25.8	4833	101.7
6	0.0763	15.2	3234	103.0
7	0.1184	8.07	2068	100.7
8	0.1826	4.09	1356	101.1

* since some of sample 0d was lost, percent recovered calculated with 0c

Table 6.3.2b . Bisolute Isotherm 11 - Triallate Results
Equi-molar solution of Lindane and Triallate
Both phases analysed after 14 days equilibration

Bottle #	Resin Dry Weight (g)	Equilibrium Concentration Liquid (µg/L)	Solid (µg/g)	Percent Recovered*
0c	-	451		
0d	-	392		
1	0.0045	356	12743	104.4
2	0.0077	279	12920	105.9
3	0.0174	182	8260	104.4
4	0.0298	69.3	6624	102.8
5	0.0493	2.88	4722	103.9
6	0.0763	1.061	3113	105.6
7	0.1184	0.188	1975	103.8
8	0.1826	0.0866	1280	103.8

* since some of sample 0d was lost, percent recovered calculated with 0c

Table 6.3.3a Bisolute Isotherm 15 - Lindane Results
1 to 5 molar ratio solution of Lindane and Triallate
Both phases analysed after 17 days equilibration

Bottle #	Resin Dry Weight (g)	Equilibrium Concentration Liquid (µg/L)	Solid (µg/g)	Percent Recovered
0a	-	86.1		
0b	-	87.2		
1	0.0043	71.5	2267	104.9
2	0.0088	47.7	2317	102.1
3	0.0137	56.0	1359	107.5
4	0.0256	27.3	1239	104.7
5	0.0323	21.1	1041	101.9
6	0.0559	1.76	825	108.5
7	0.0892	1.161	527	109.8
8	0.1379	0.823	334	107.3

Note: from sample #7, the maximum Lindane recovered was 95.1 µg/L

Table 6.3.3b Bisolute Isotherm 15 - Triallate Results
1 to 5 molar ratio solution of Lindane and Triallate
Both phases analysed after 17 days equilibration

Bottle #	Resin Dry Weight (g)	Equilibrium Concentration Liquid (µg/L)	Solid (µg/g)	Percent Recovered
0a	-	333	-	
0b	-	335		
1	0.0043	264	8902	101.8
2	0.0088	166	9812	101.4
3	0.0137	198	5135	101.2
4	0.0256	90.8	4976	103.4
5	0.0323	67.3	4294	103.3
6	0.0559	0.143	3252	108.9
7	0.0892	0.0879	2032	108.6
8	0.1379	0.0838	1268	104.7

Note: from sample #6, the maximum Triallate recovered was 363.7 µg/L

Table 6.4.1 Solid Phase Average Percent Errors for IAST Predictions

Compound Modelled	Single Solute Isotherm Data	Bi-solute Isotherm	Solid Phase APEs
Lindane	12	11	18.4
	12	15	17.1
	16	15	10.9
Triallate	14	11	19.6
	14	15	45.2

Table 6.4.2 Solid Phase Concentration Range for Single Solute Isotherms 12 and 14 and for IAST Predictions

Prediction of Bi-solute Isotherm	Single Solute Isotherm	Solid Phase Concentration Range (μg/g)		
		Compound	Single Solute	IAST
11	12	Lindane	182 -11882	4072 - 45367
	14	Triallate	873 - 38572	2125 -23671
15	12	Lindane	182 -11882	2862 - 36633
	14	Triallate	873 - 38572	1493 - 19218

Table 6.5.1 Column Experiment #1 Results
EBCT = 0.82 seconds

Sample Number	Mid-point Volume (L)	Effluent Concentration (C/C°)		Normalized Flow Rate
		Lindane	Triallate	
1	0.125	0.768	0.726	1.10
2	0.375	0.823	0.701	1.24
6	1.375	0.832	0.807	1.27
11	2.625	0.873	0.857	1.24
16	3.875	0.904	0.890	1.24
21	5.125	0.928	0.922	1.28
26	6.375	0.916	0.945	1.24
31	7.625	0.960	0.973	1.31
36	8.875	0.969	0.873	1.25
41	10.125	0.887	0.385	1.20
46	11.375	0.988	0.920	1.27
51	12.625	0.936	0.748	1.20
56	13.875	0.963	0.794	1.32
61	15.125	0.937	0.748	1.25
66	16.375	0.931	0.481	1.24
71	17.625	1.026	0.829	1.29
75Blank (C°)	18.625	1.000	1.000	

Table 6.5.2 Column Experiment 2 Results
EBCT = 2.72 seconds

Sample Number	Mid-point Volume (L)	Effluent Concentration (C/C°) Lindane	Triallate	Normalized Flow Rate
Blank 1a	0	1.006	0.996	
Blank 1b	0	1.014	1.000	
Blank 2a	6.5	1.000	1.027	
Blank 3a	17.1	0.979	0.977	
1	0.025	0.304	0.232	0.76
2	0.075	0.380	0.331	0.89
4	0.175	0.412	0.370	0.88
6	0.35	0.509	0.449	1.16
9	0.875	0.493	0.416	0.99
12	2.475	0.560	0.438	0.98
15	4.725	0.592	0.432	0.91
17	6.225	0.649	0.462	1.01
20	9.475	0.704	0.439	1.16
22	11.975	0.741	0.498	1.09
24	14.475	0.718	0.439	0.96
26	16.975	0.672	0.305	0.87

Table 6.5.3   Column Experiment 3 Results
EBCT = 21.7 seconds

Sample Number	Mid-point Volume (L)	Effluent Concentration (C/C°) Lindane	Triallate	Normalized Flow Rate
1	0.025	0.033	0.022	0.27
2	0.075	0.020	0.019	0.28
3	0.125	0.021	0.021	0.28
4	0.175	0.018	0.020	0.25
5	0.225	0.016	0.018	0.23
6	0.275	0.022	0.022	0.28
7	0.35	0.035	0.030	0.33
9	0.85	0.040	0.028	0.28
11	1.05	0.049	0.032	0.32
17	3.407	0.044	0.025	0.24
25	4.85	0.096	0.043	0.32
32	6.35	0.119	0.048	0.33
38	11.42	0.219	0.079	0.33
Blank	0	1.000	1.000	

Table 6.5.4   Summary of Column Experiment Data

Column Experiment	1	2	3
Column Diameter (cm)	0.56	0.7	0.7
Bed Length (cm)	1.4	4.7	4.7
Average Flow Rate (mL/min)	25	40	5
EBCT (min)	0.82	2.72	21.7
Influent Concentrations (μg/L)			
Lindane	92.7	54.1	54.5
Triallate	430	467	441
Computer Predictions			
Volume of Solution to Breakthrough (L)			
Lindane	10.1	54.4	56.8
Triallate	12.4	61.2	64.9

Figure 3.1 Time Schedule for the Five Phases of the Study

100
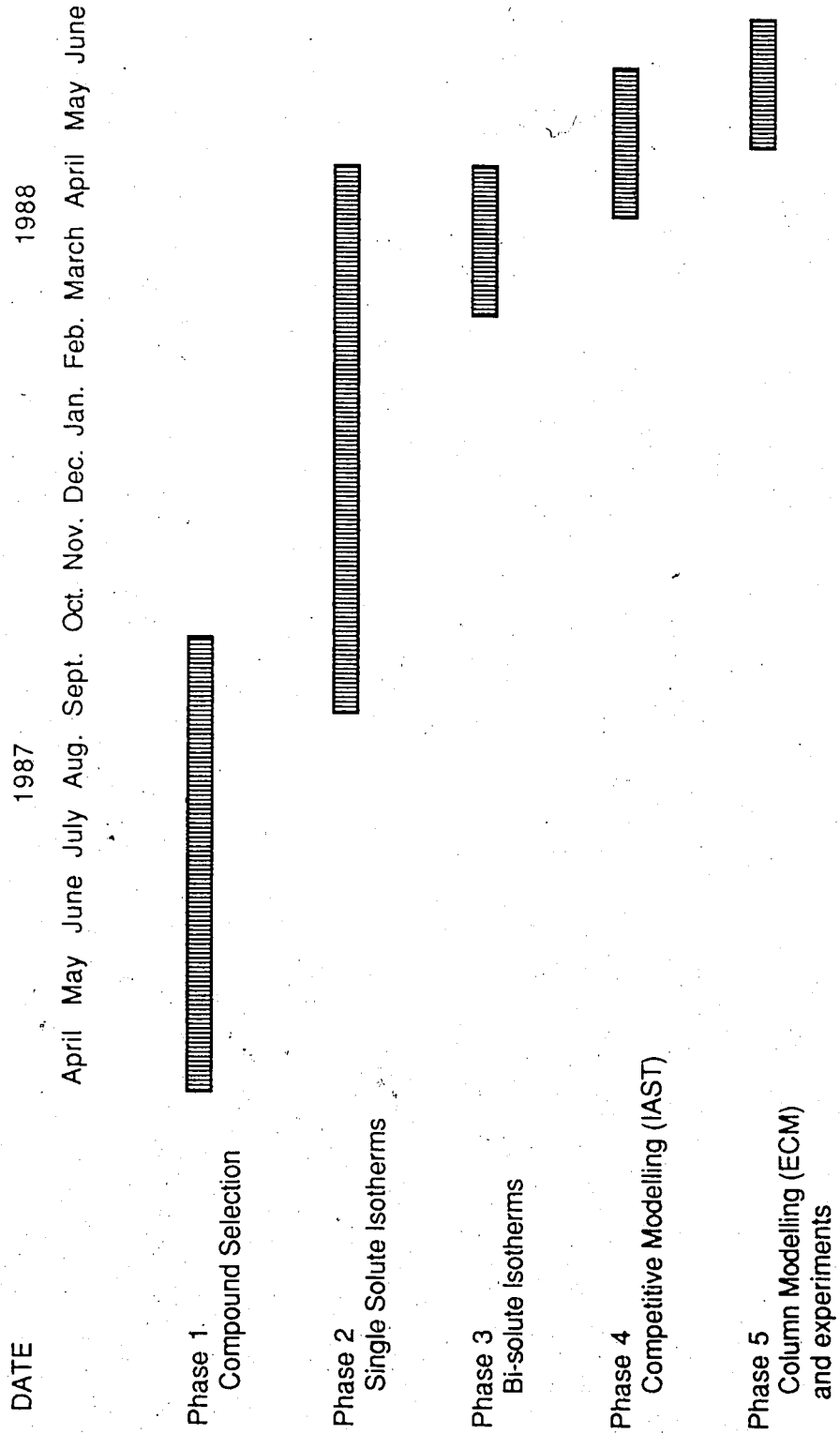
Figure 5.1a Total Lindane Calibration Plot for Isotherms 10 & 11
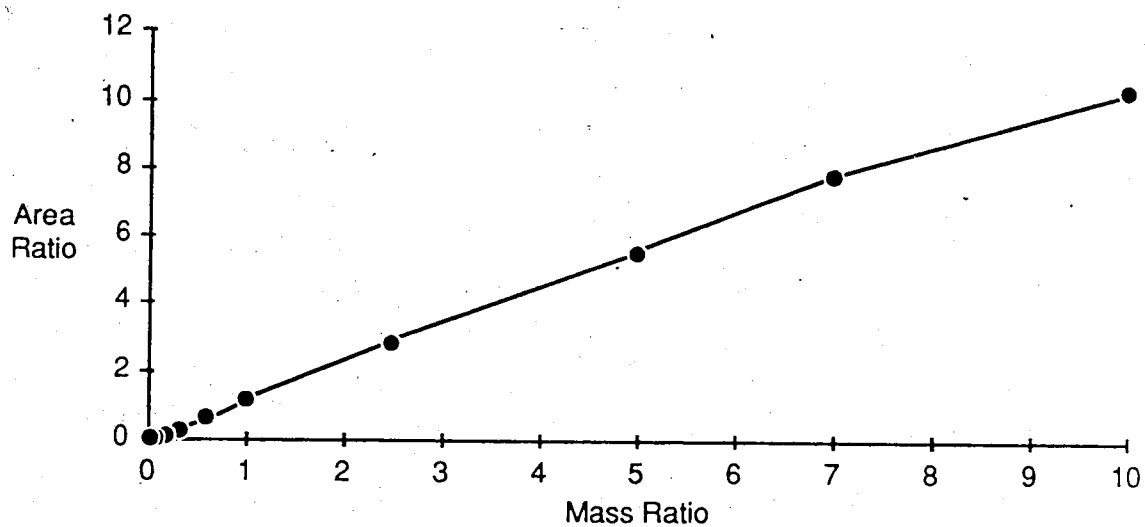
Figure 5.1b Partial Lindane Calibration Plot for Isotherms 10 & 11
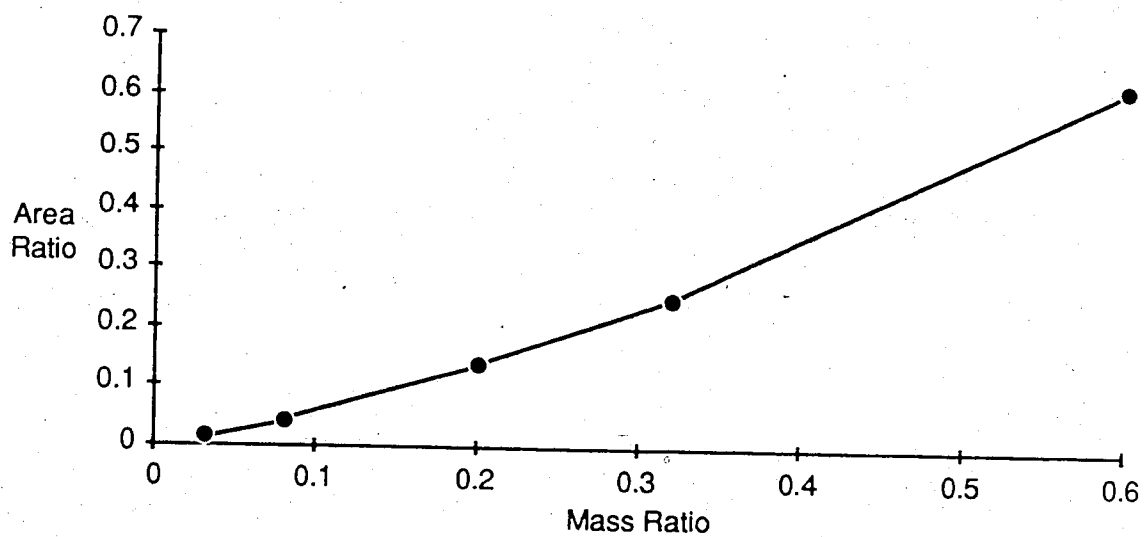
Figure 5.2a Total Triallate Calibration Plot for Isotherms 10 & 11
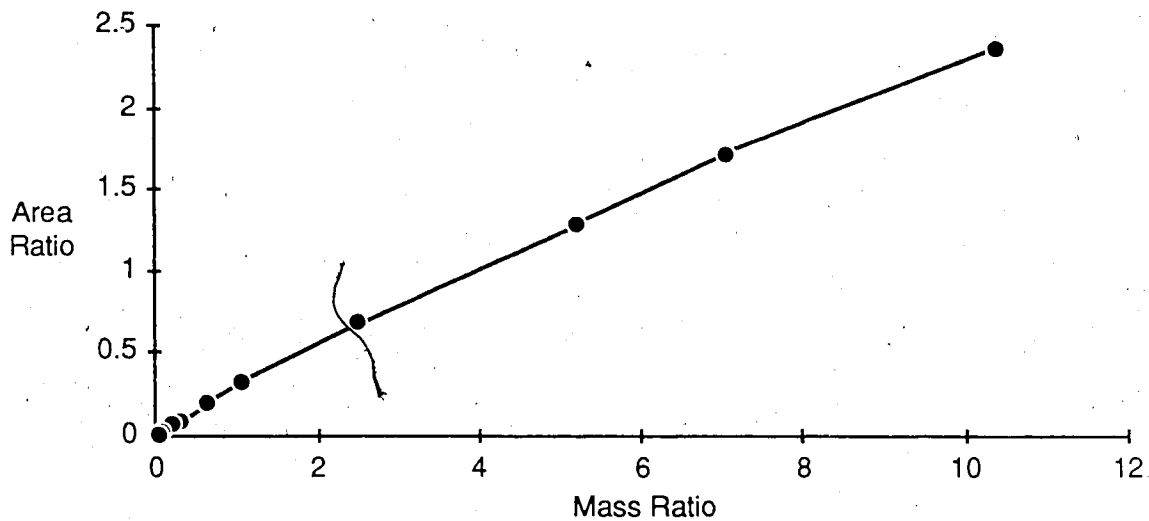
Figure 5.2b Partial Triallate Calibration Plot for Isotherms 10 & 11
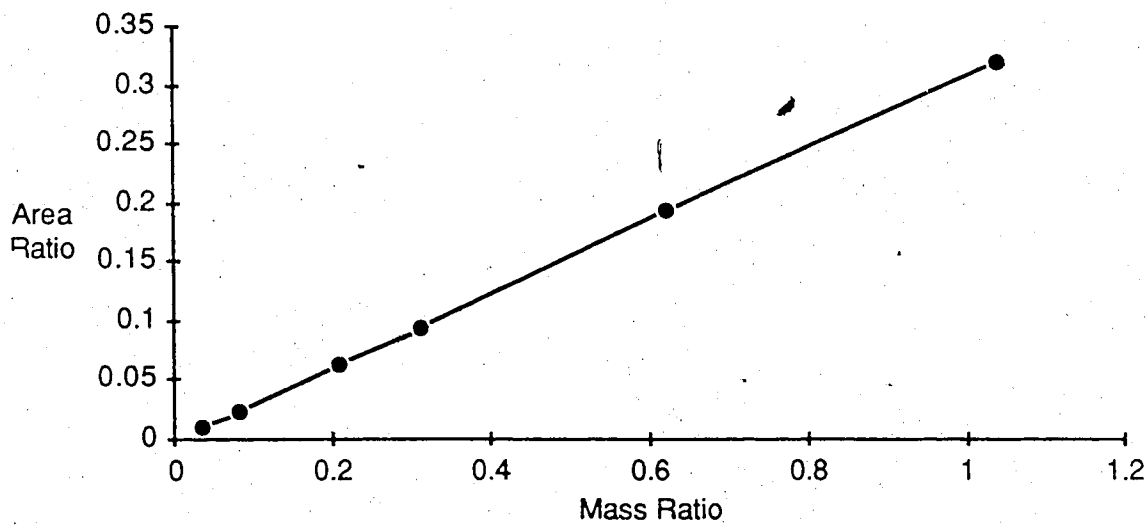
Figure 6.2.1 Adsorption Kinetics of Lindane on XAD-2 Resin
50 µg/L Initial Liquid Phase Concentration
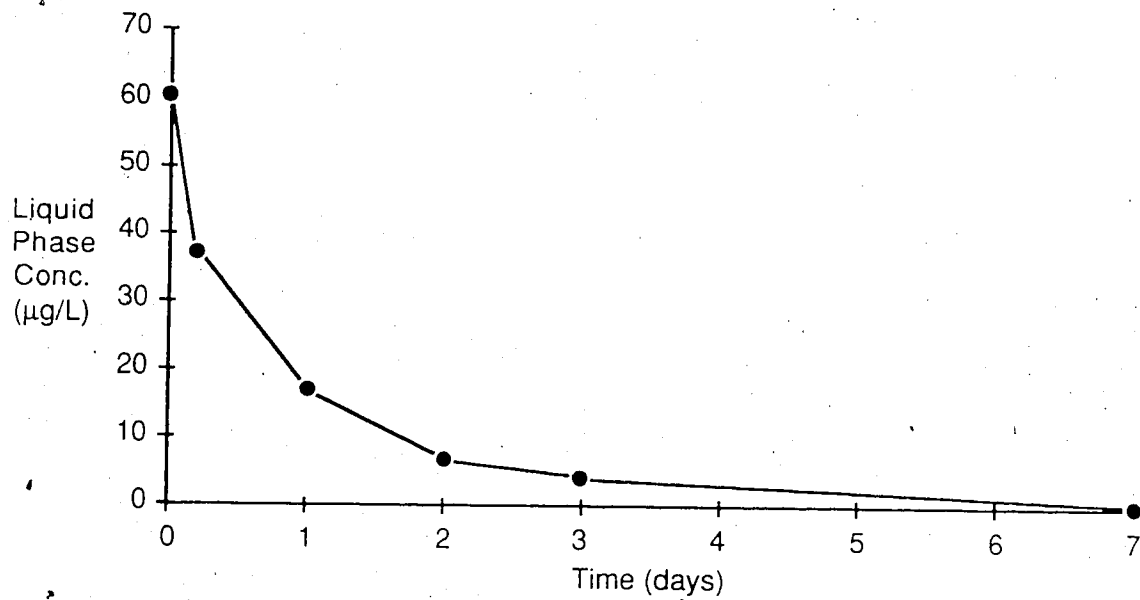
Figure 6.2.2 Isotherm 1 - As Determined by Solid Phase Analysis
Every 5th Bottle Numbered
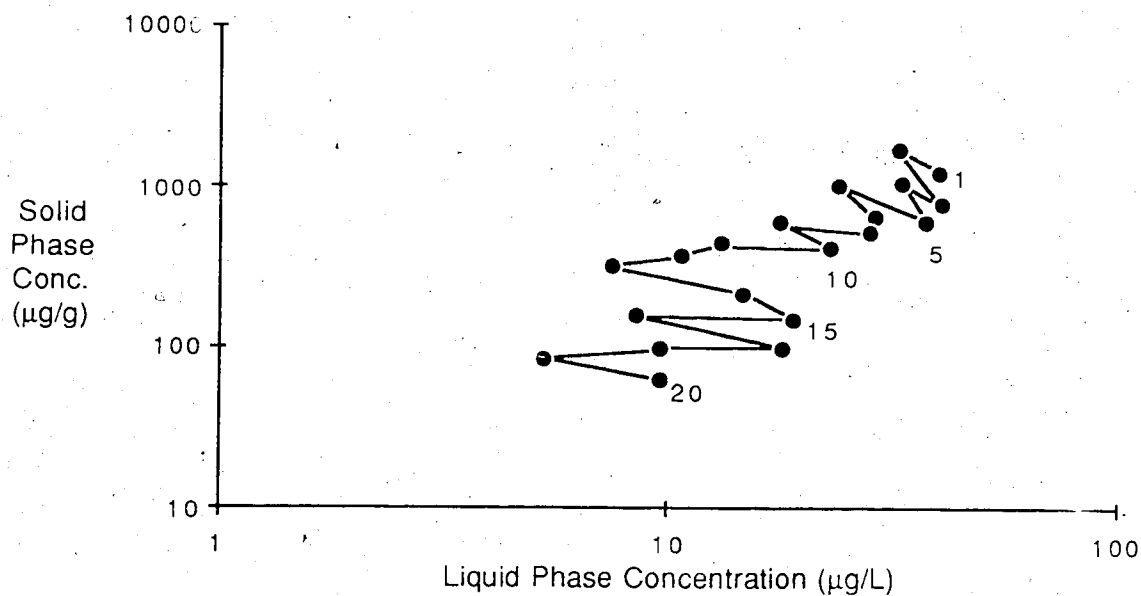
Figure 6.2.3 Isotherm 1 - Both Phases Analysed

Isotherm 1
Lindane

LABORATORY PARAMETERS
MIIII-Q Water: pH=7.5, Temp=20°C
Fresh XAD-2 Resin
Equilibration Time: 7 Days

SOLID PHASE CONCENTRATION, μg/g

LIQUID PHASE CONCENTRATION, μg/L
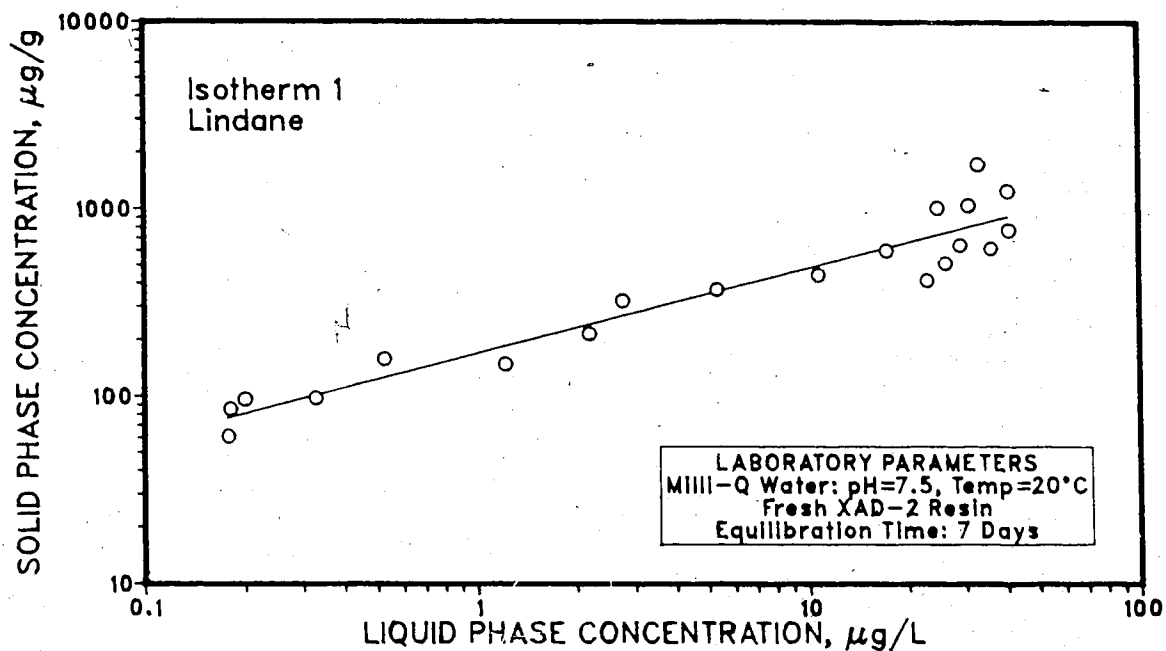
Figure 6.2.4 Isotherm 2 - Lindane on Fresh Resin

Isotherm 2
Lindane

LABORATORY PARAMETERS
MIJII-Q Water: pH=7.5, Temp=20°C
Fresh XAD-2 Resin
Equilibration Time: 8 Days

SOLID PHASE CONCENTRATION, μg/g

LIQUID PHASE CONCENTRATION, μg/L
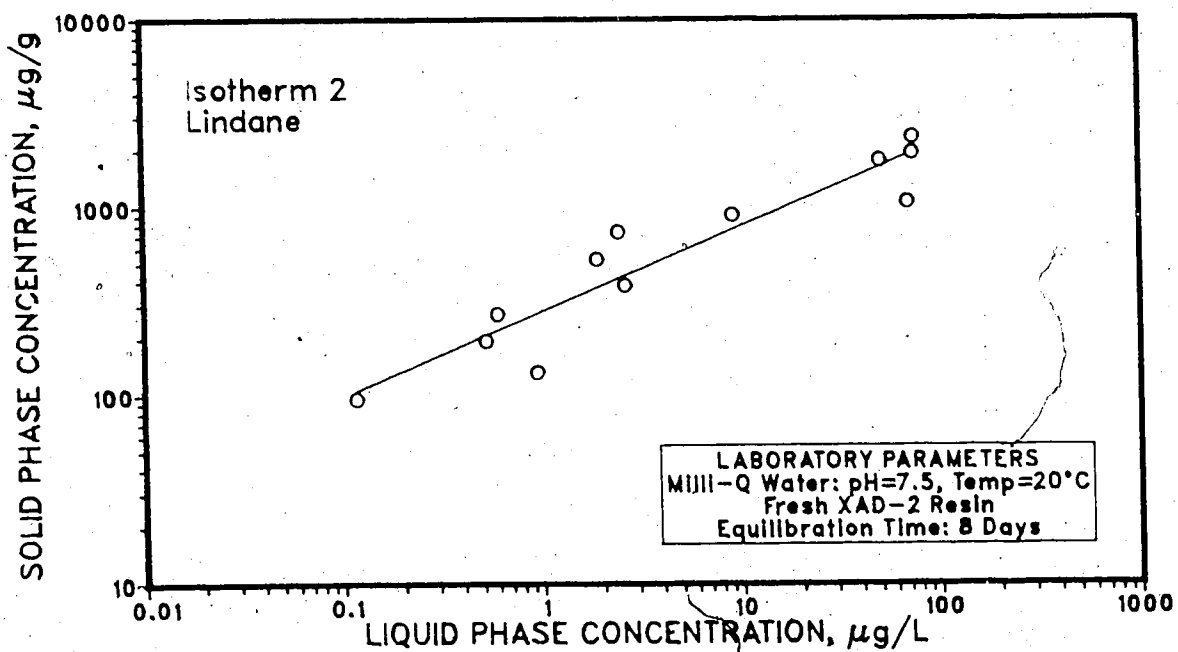
Figure 6.2.5 Isotherm 3 - Preliminary Triallate on Fresh Resin
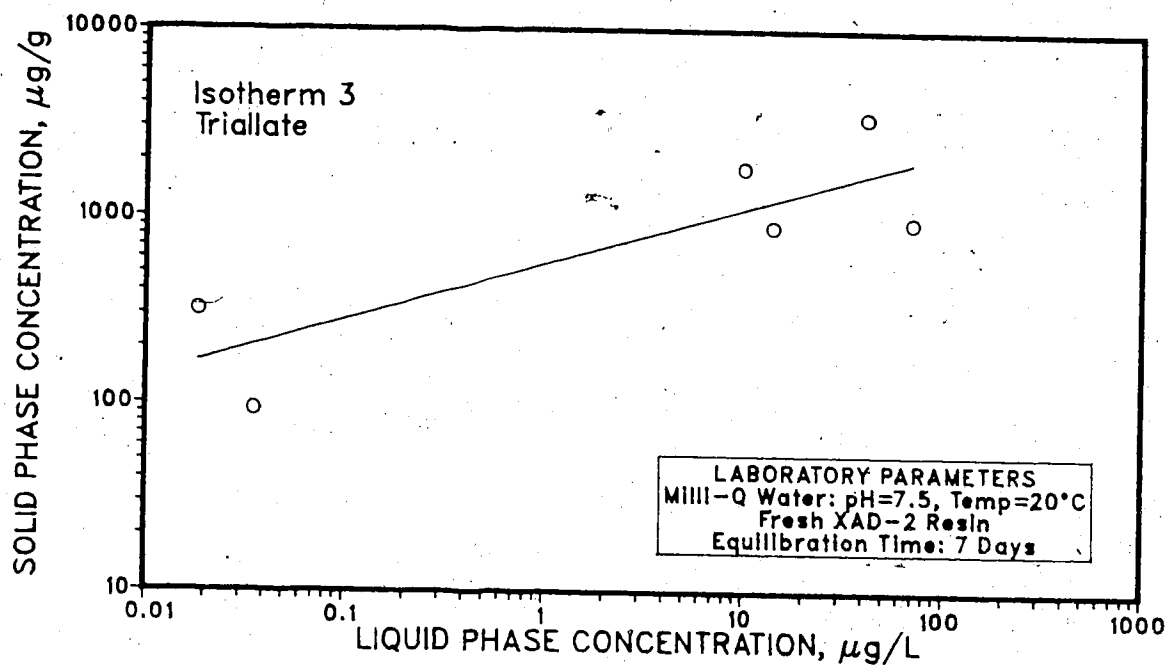
Figure 6.2.6 Isotherm 5 - Triallate on Fresh Resin
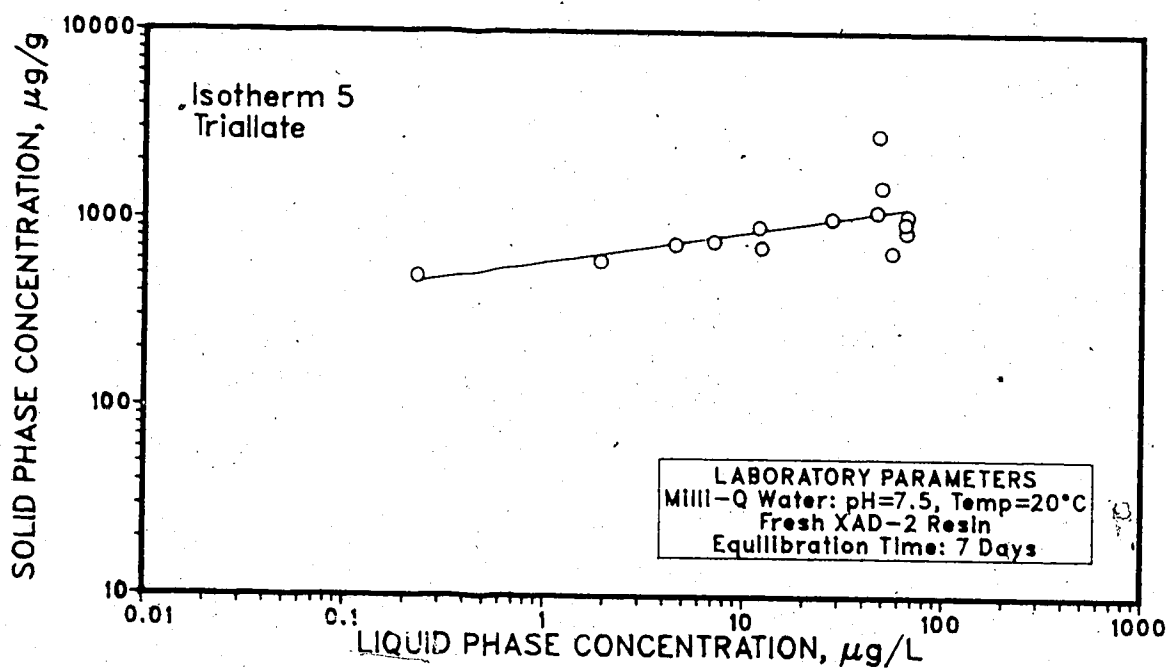
Figure 6.2.7 Isotherm 5 - Replicates Samples Numbered in Bold
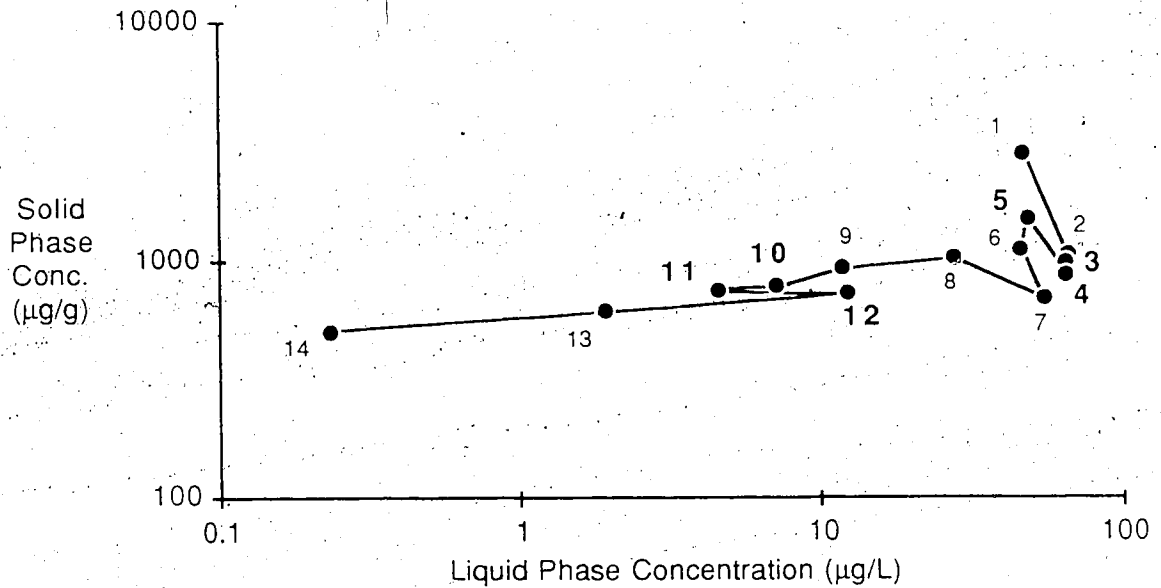
Figure 6.2.8 Isotherm 6 - Lindane on Crushed Resin
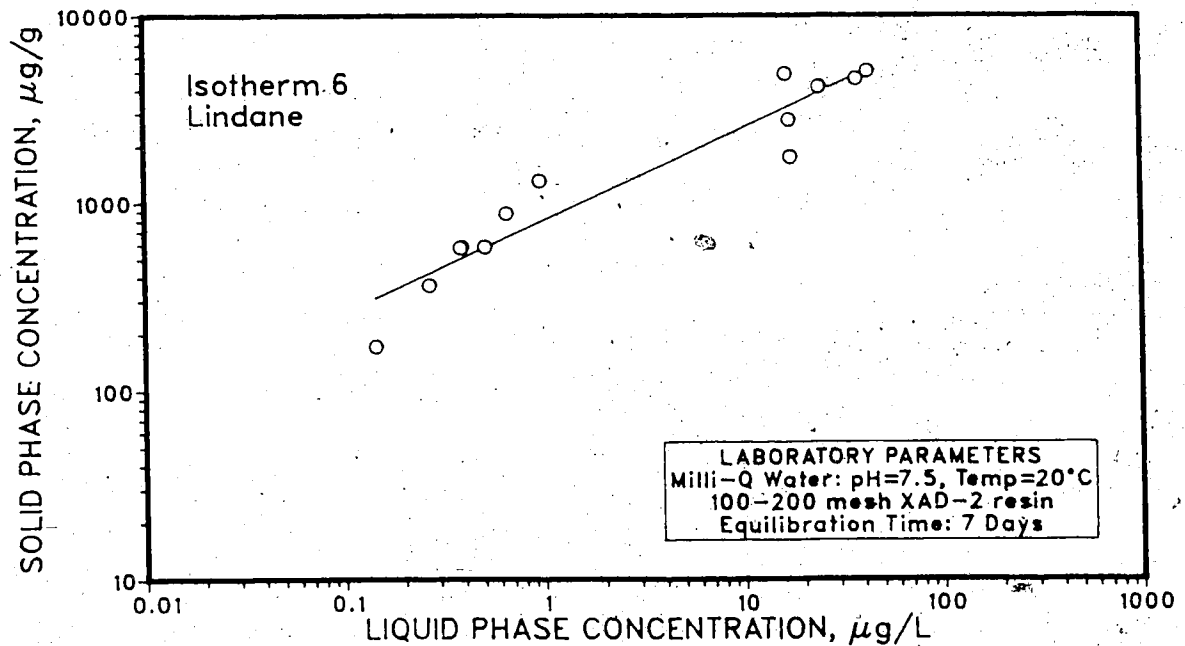
Figure 6.2.9 Isotherm 6 - Replicate Samples Numbered in Bold
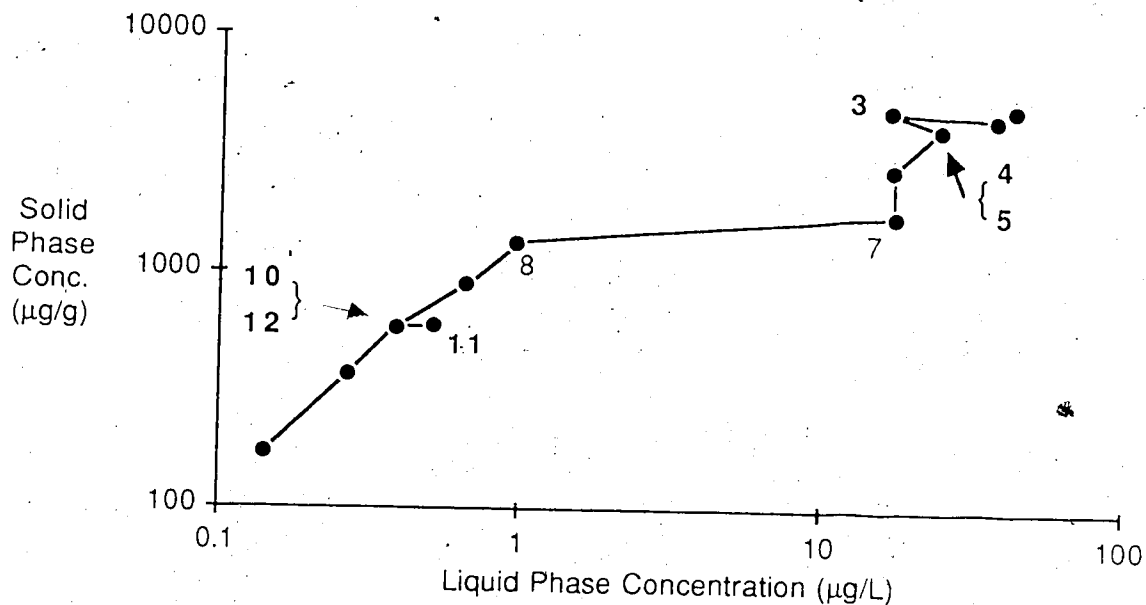
Figure 6.2.10 Isotherm 4 - TCEP on Fresh Resin
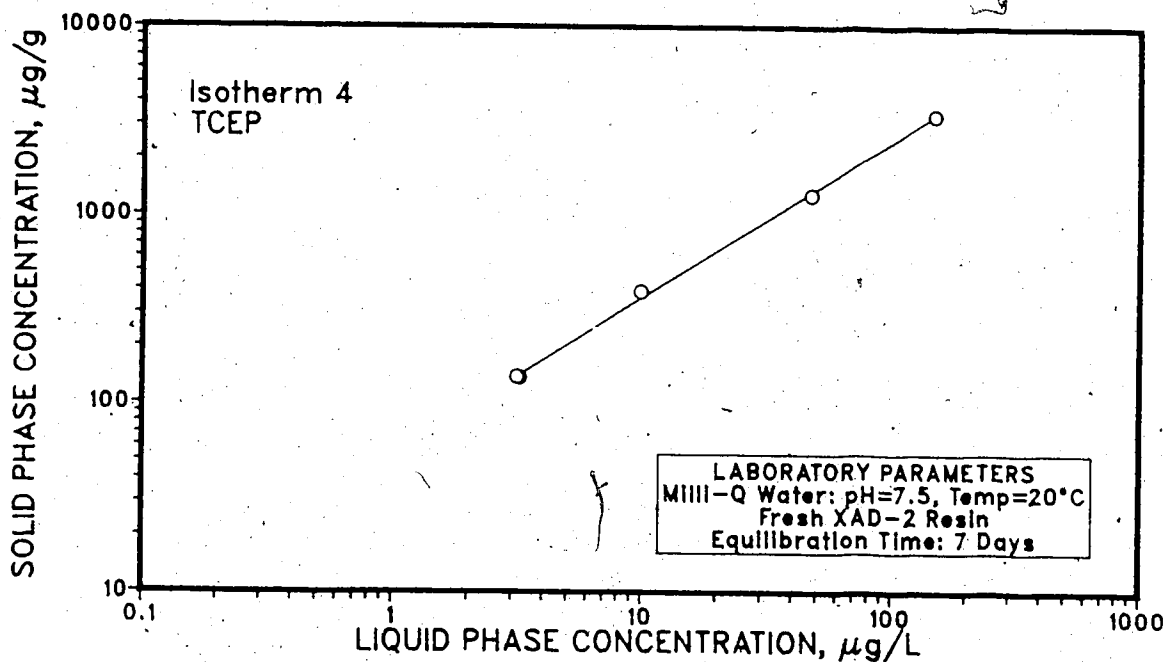
Figure 6.2.11 Isotherm 7 - Triallate on Fresh Resin
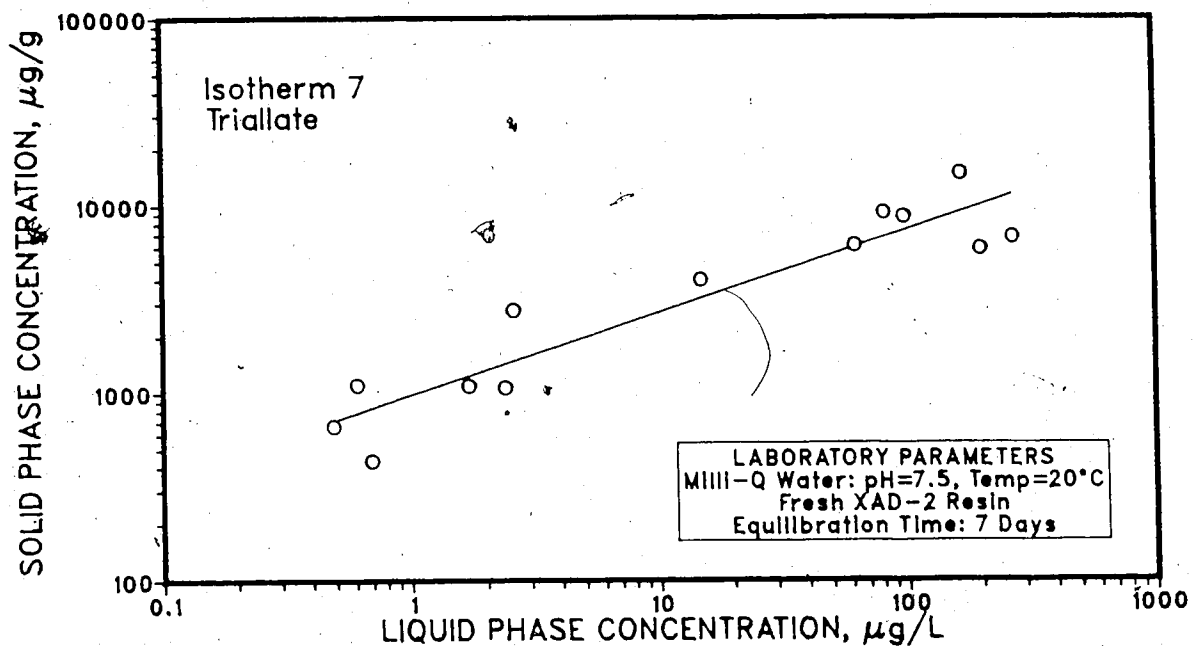
Figure 6.2.12 Isotherm 8 - Lindane on Crushed Resin
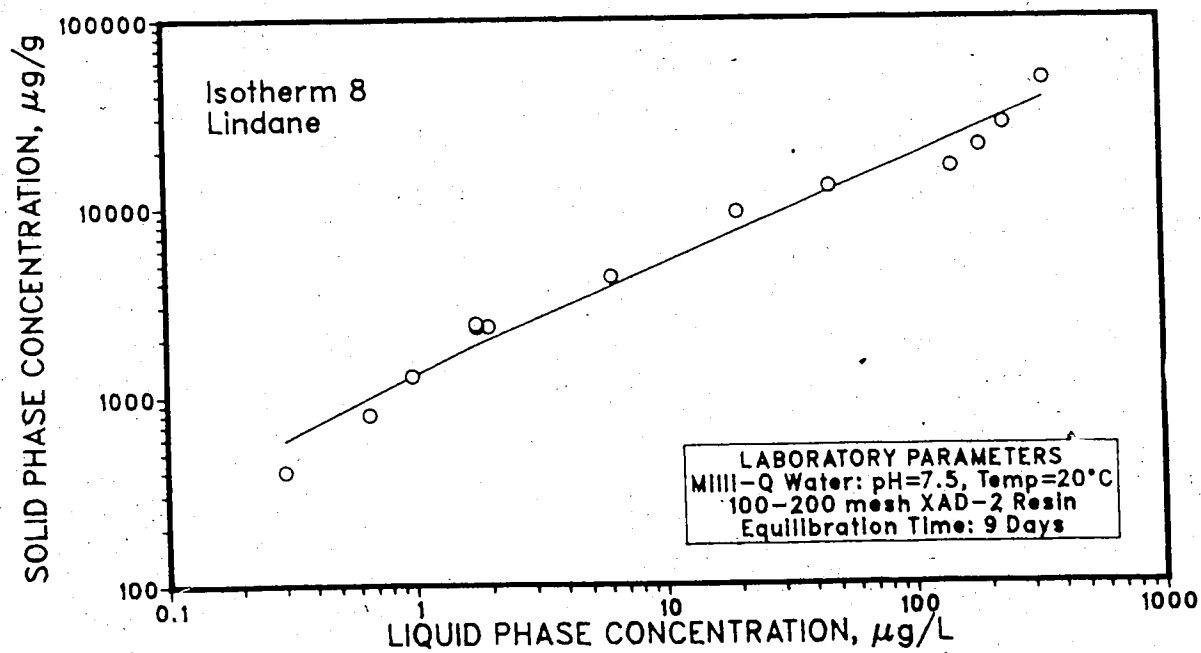
Figure 6.2.13 Kinetics of Lindane Adsorption on Fresh and Preloaded Resin
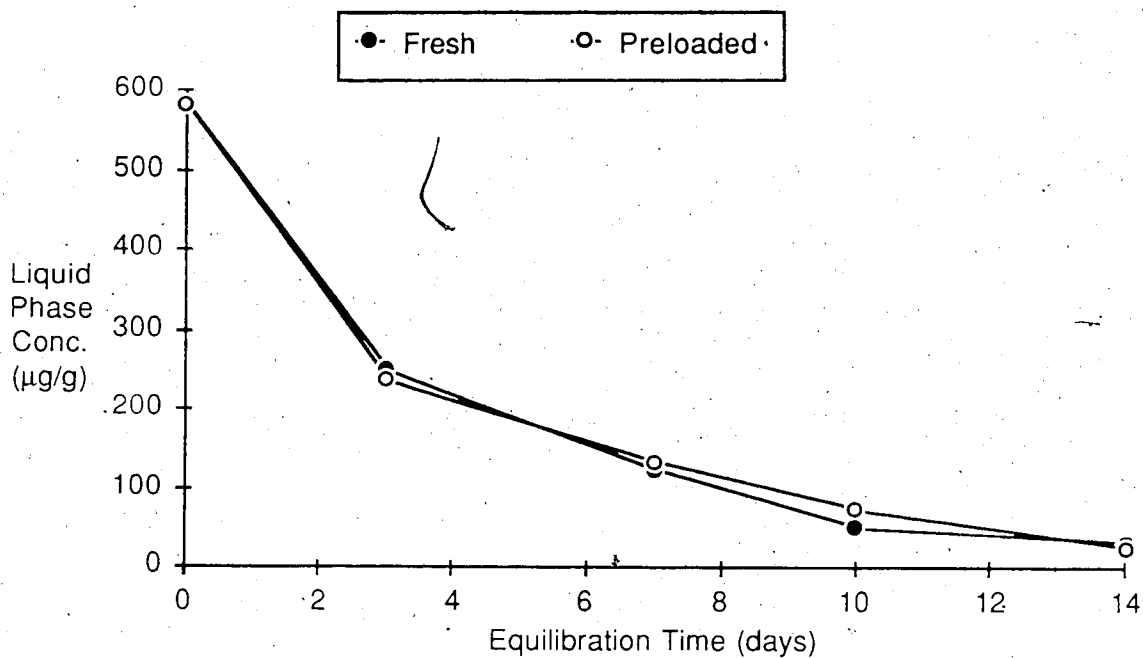
Figure 6.2.14 Isotherm 12 - Lindane on Fresh Resin
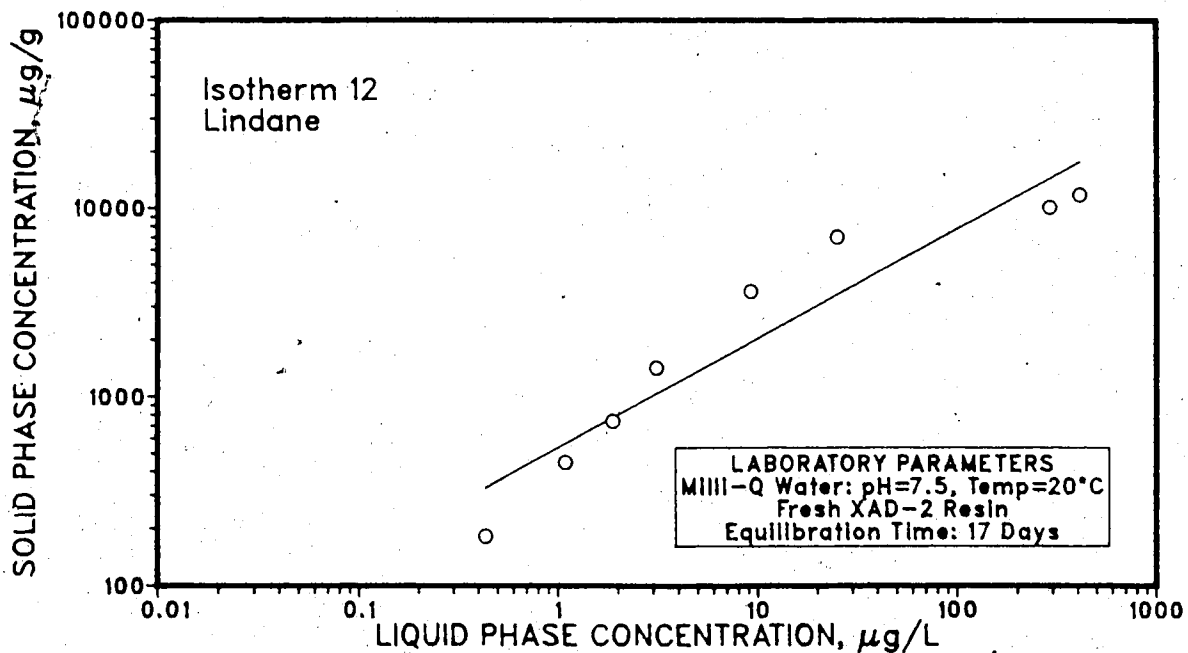
Figure 6.2.15   Isotherm 13 - Lindane on Preloaded Resin
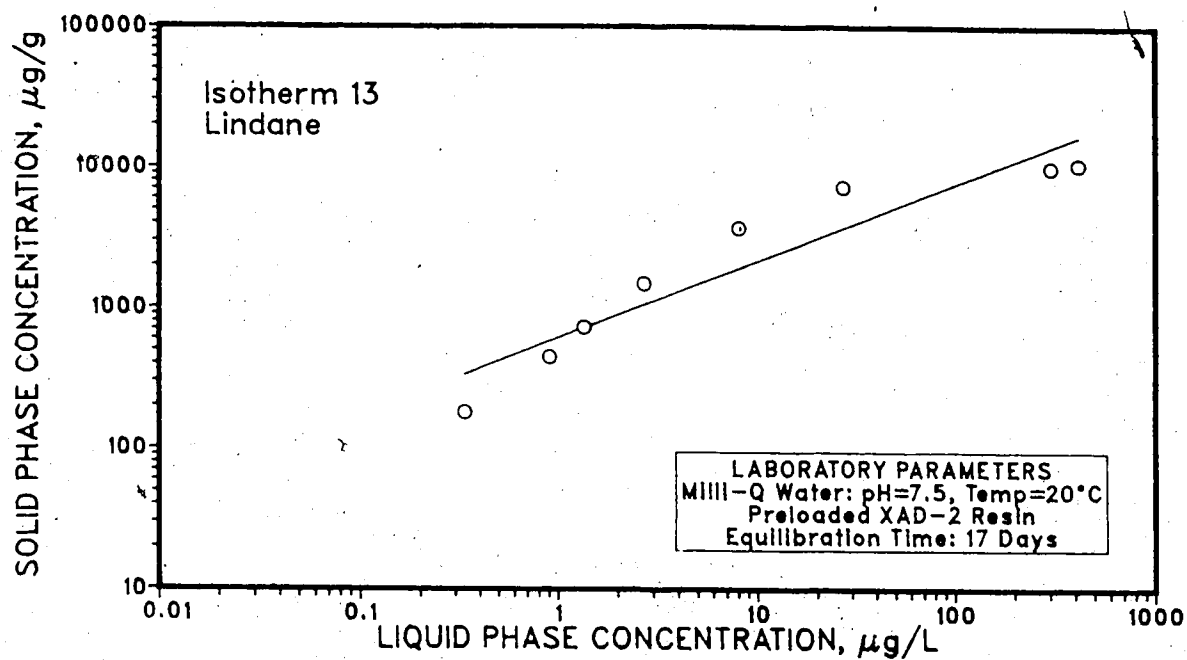
Figure 6.2.16   Comparison of Fresh and Preloaded Resin in
Lindane Isotherms 12 and 13
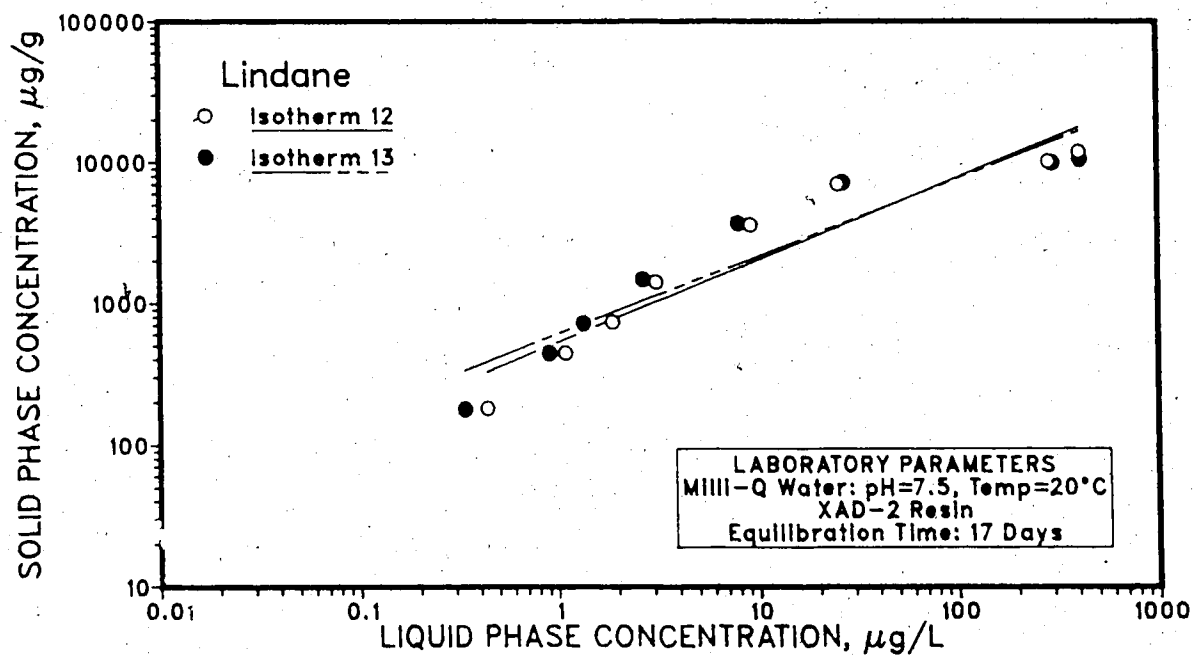
Figure 6.2.17 Isotherm 16 - Lindane on Fresh Resin
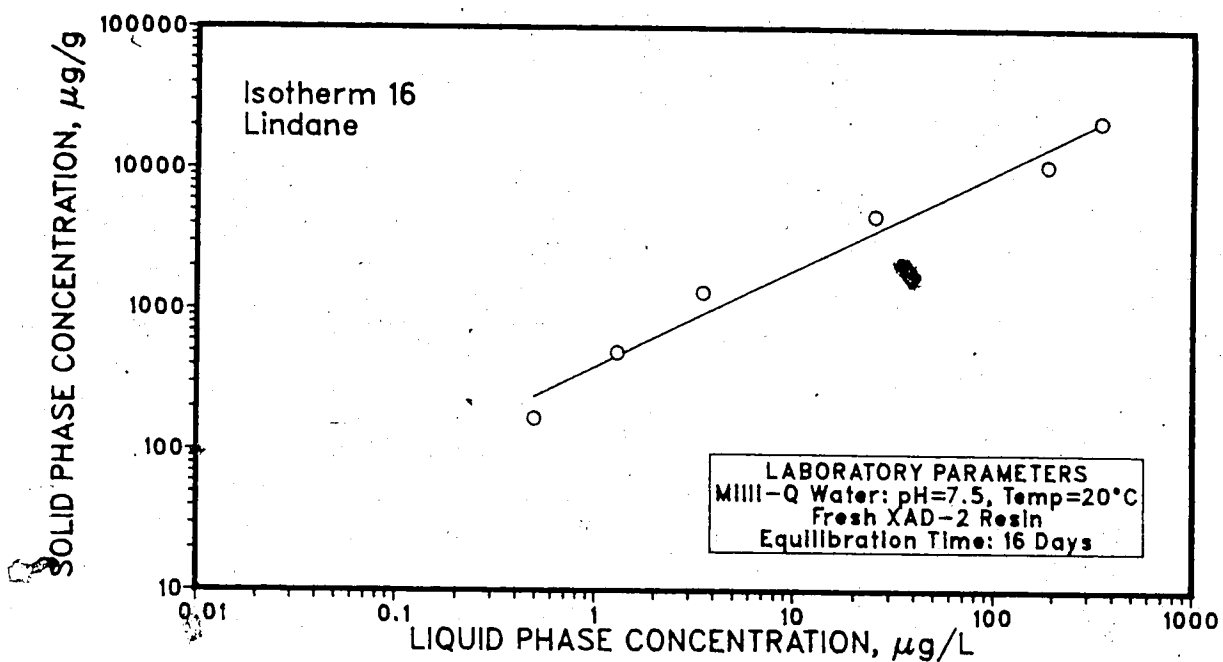
Figure 6.2.18 Langmuir Plot of Isotherm 12
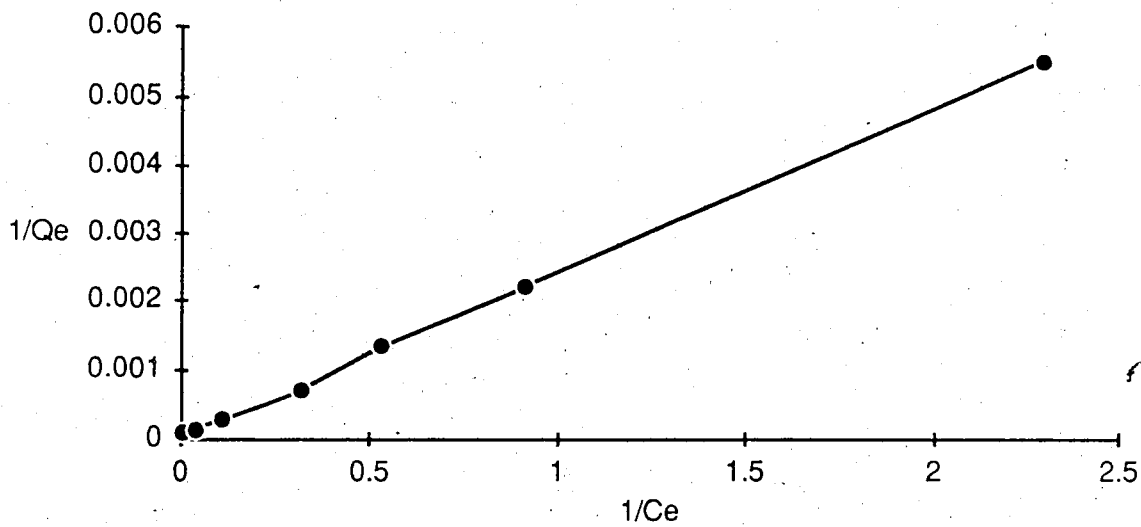
Figure 6.2.19 Partial Langmuir Plot of Isotherm 12
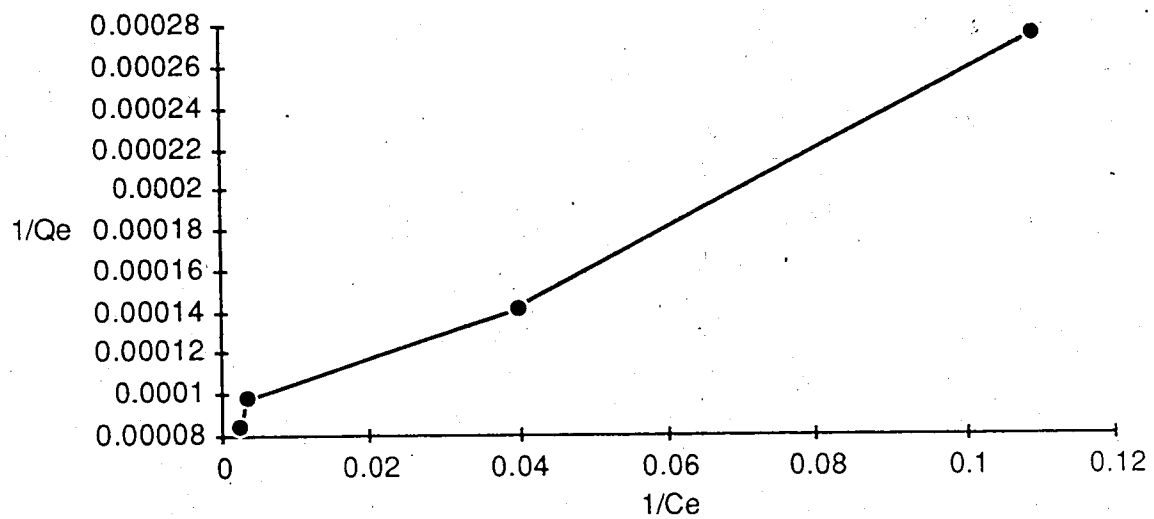
Figure 6.2.20 Langmuir Plot of Isotherm 16
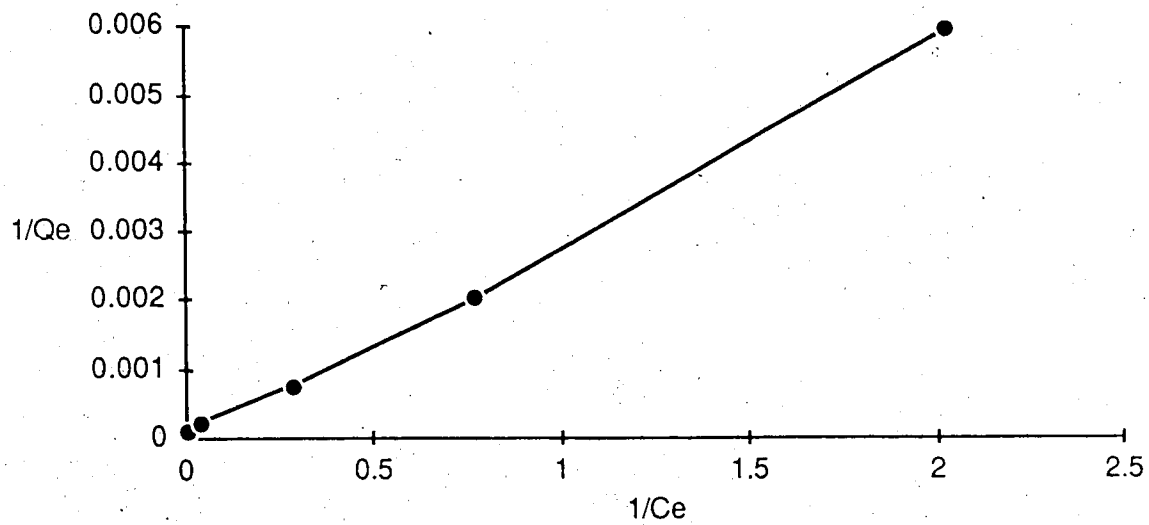
Figure 6.2.21 Partial Langmuir Plot of Isotherm 16
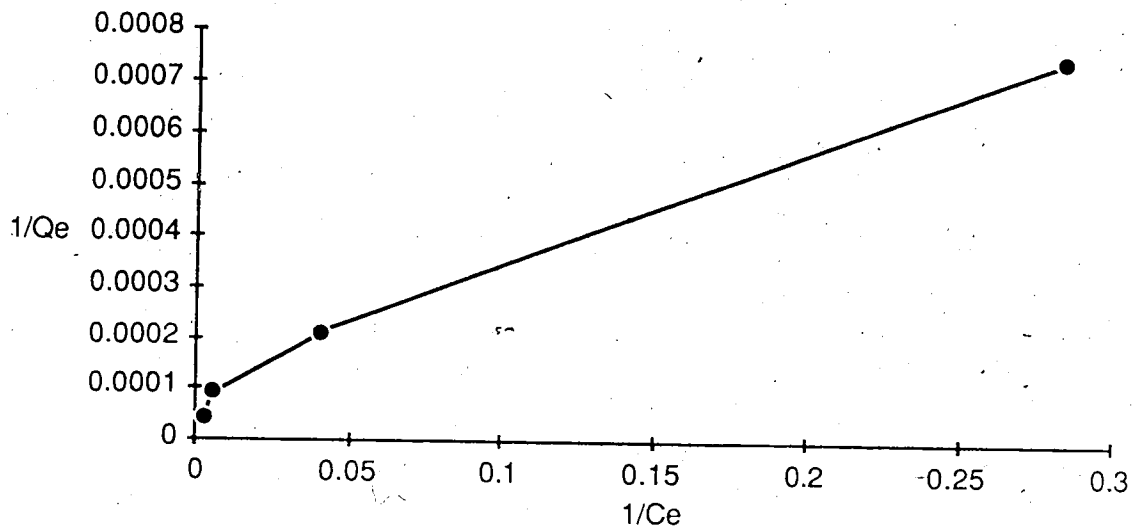
Figure 6.2.22 Isotherm 14 - Triallate on Fresh Resin
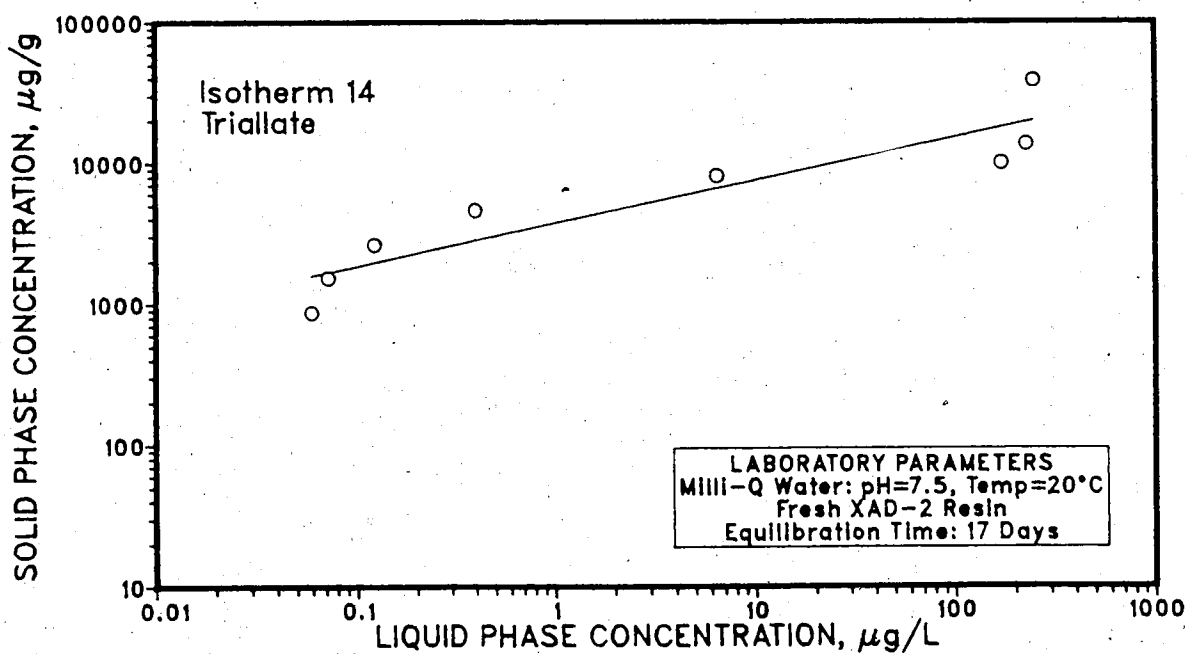
Figure 6.2.23 Partial BET Plot of Isotherm 14 (high C/Cs)
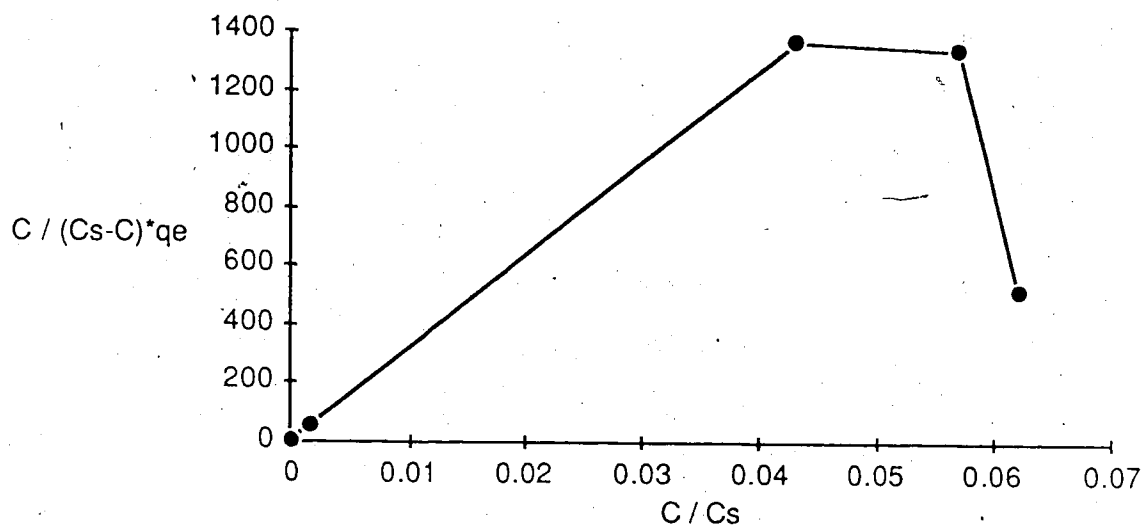
Figure 6.2.24 Partial BET Plot of Isotherm 14 (low C/Cs)
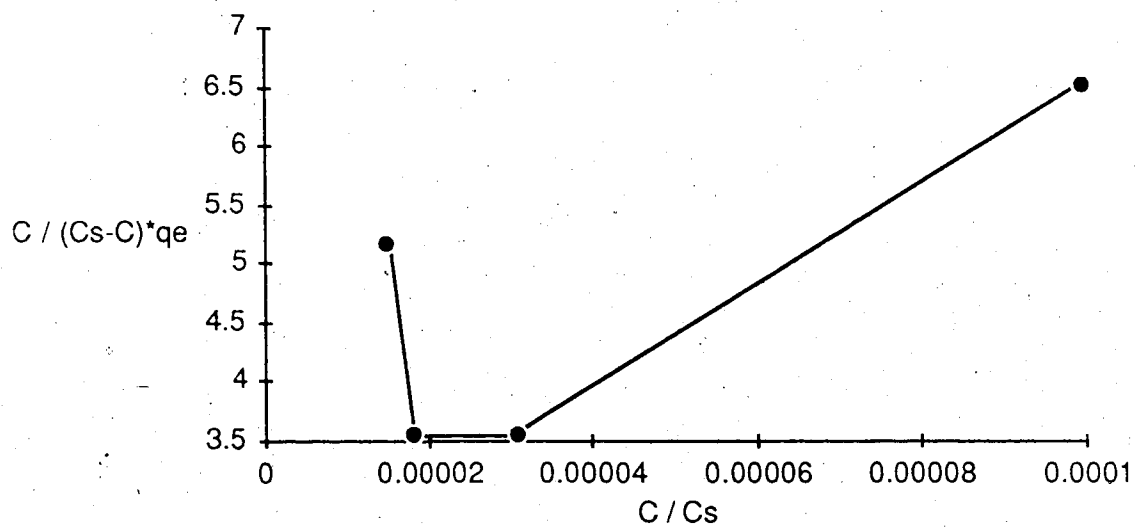
Figure 6.2.25 Comparison of Crushed and Fresh Resin in Lindane Isotherms 8 & 12
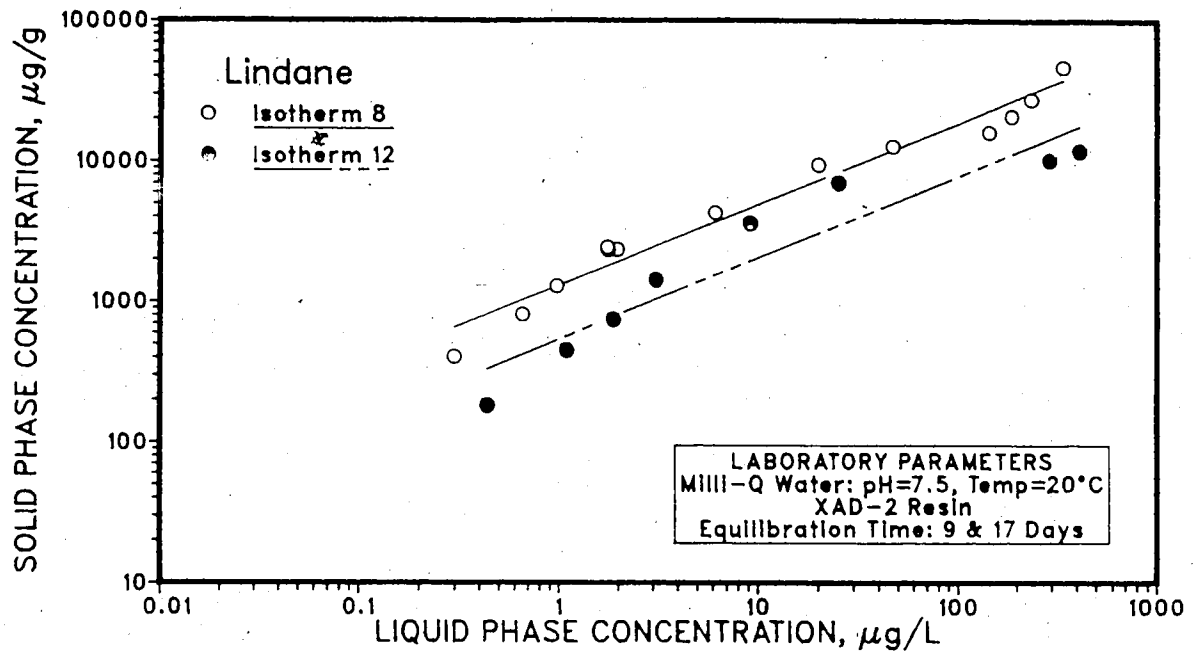
Figure 6.2.26 Comparison of Lindane Isotherms 12 & 16
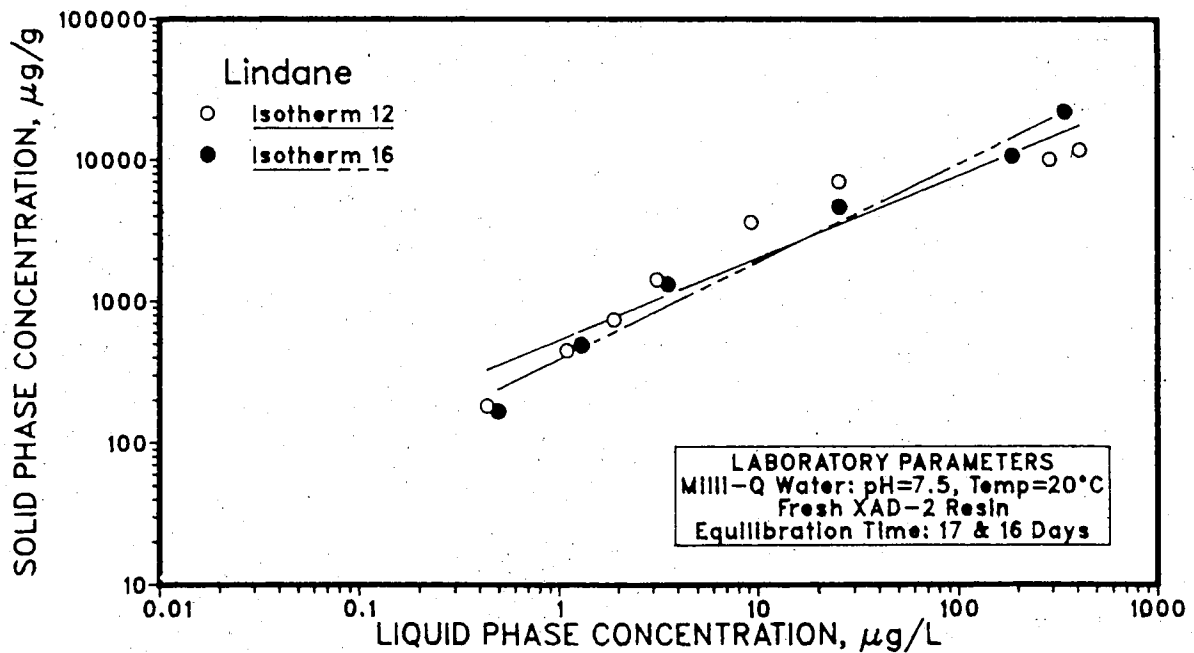
Figure 6.2.27 Comparison of Lindane and Triallate Single Solute Isotherms 12 &14
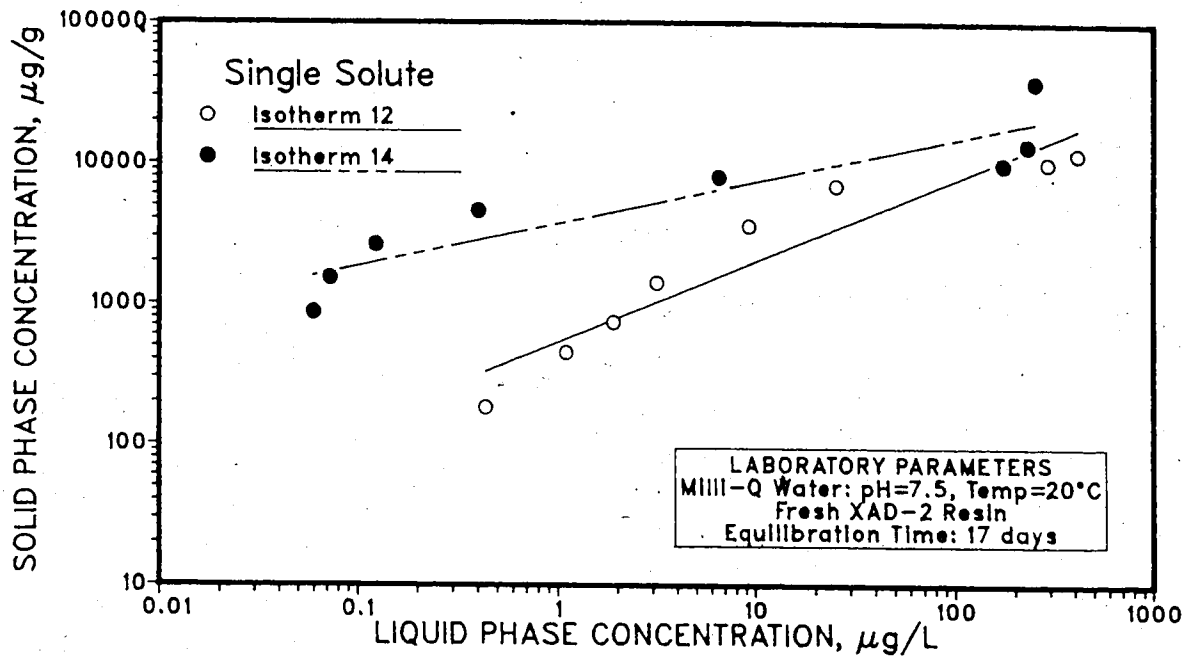
Figure 6.2.28 Comparison of Lindane and Triallàte Single Solute Isotherms 2 & 7
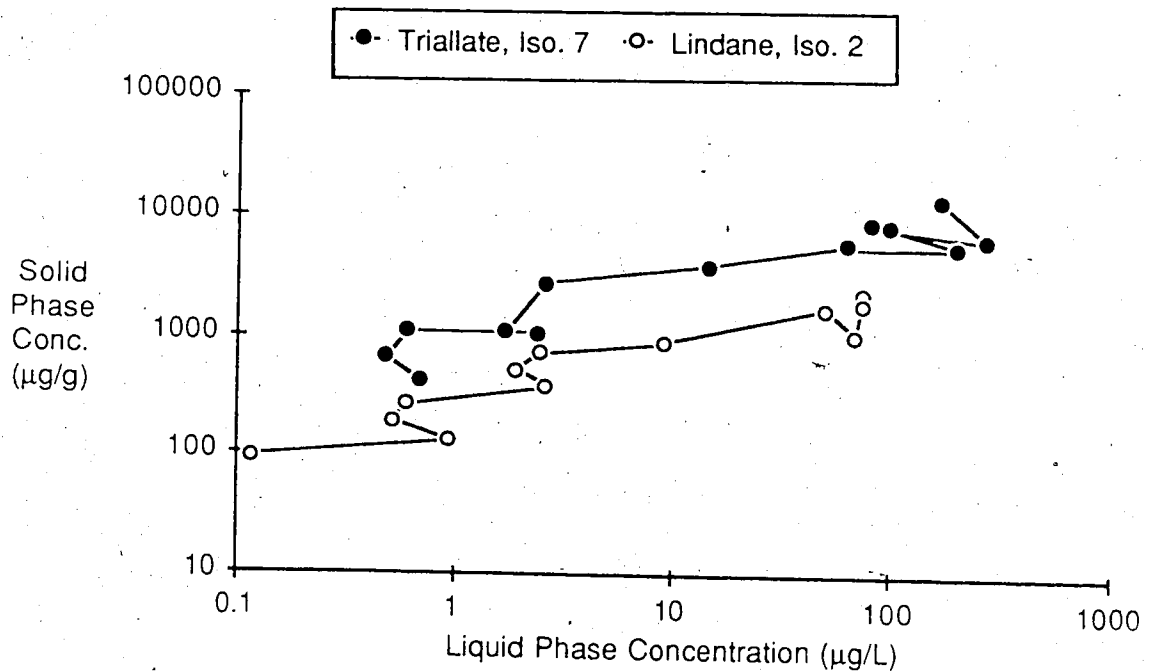
Figure 6.3.1 Bi-solute Isotherm 10 - Triallate and Lindane at 1:1 Molar Ratio
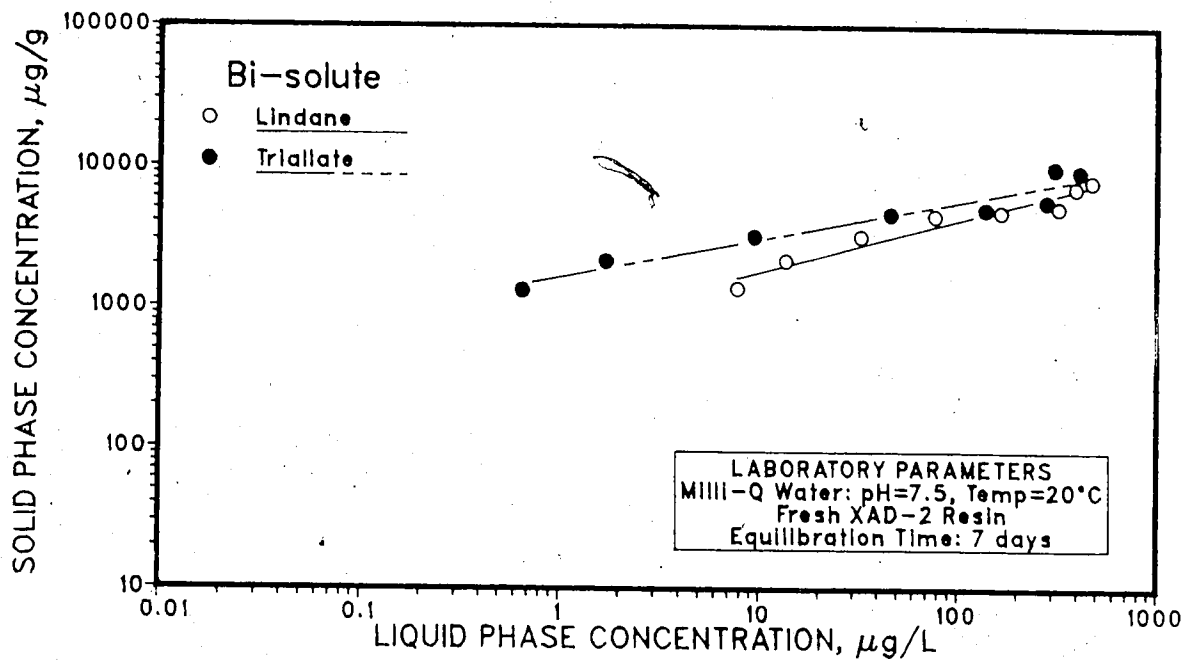
Figure 6.3.2 Bi-solute Isotherm 11 - Triallate and Lindane at 1:1 Molar Ratio
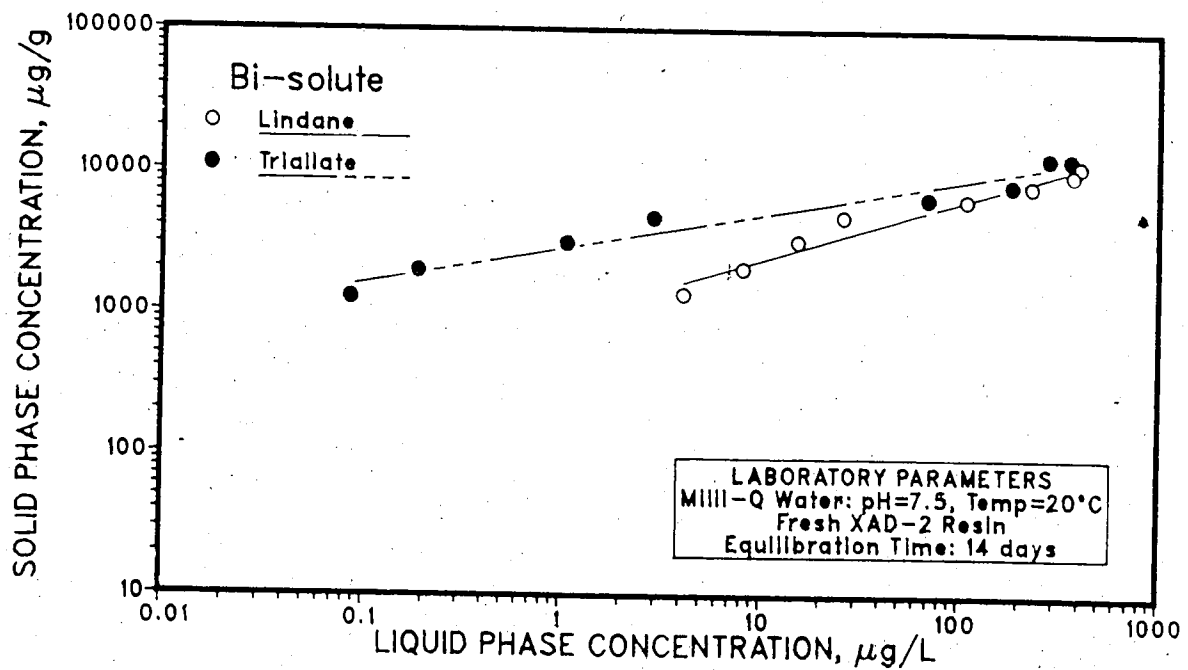
Figure 6.3.3 Comparison of Lindane Plots in Bi-solute
Isotherms 10 & 11
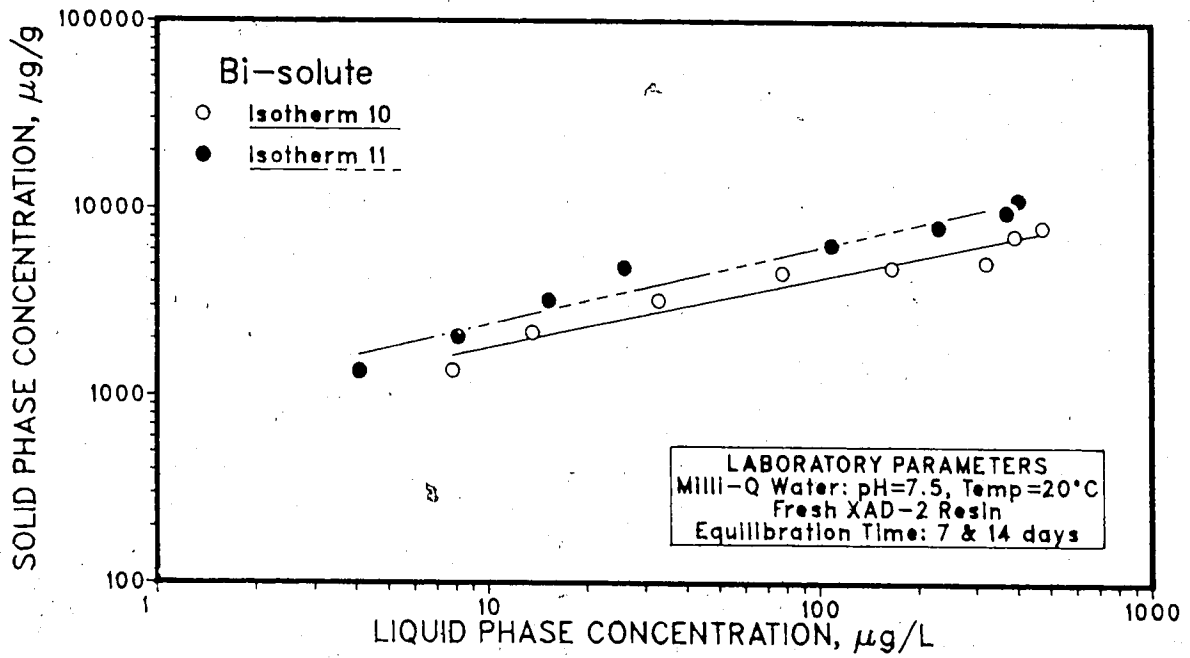
Figure 6.3.4 Comparison of Triallate Plots in Bi-solute
Isotherms 10 & 11
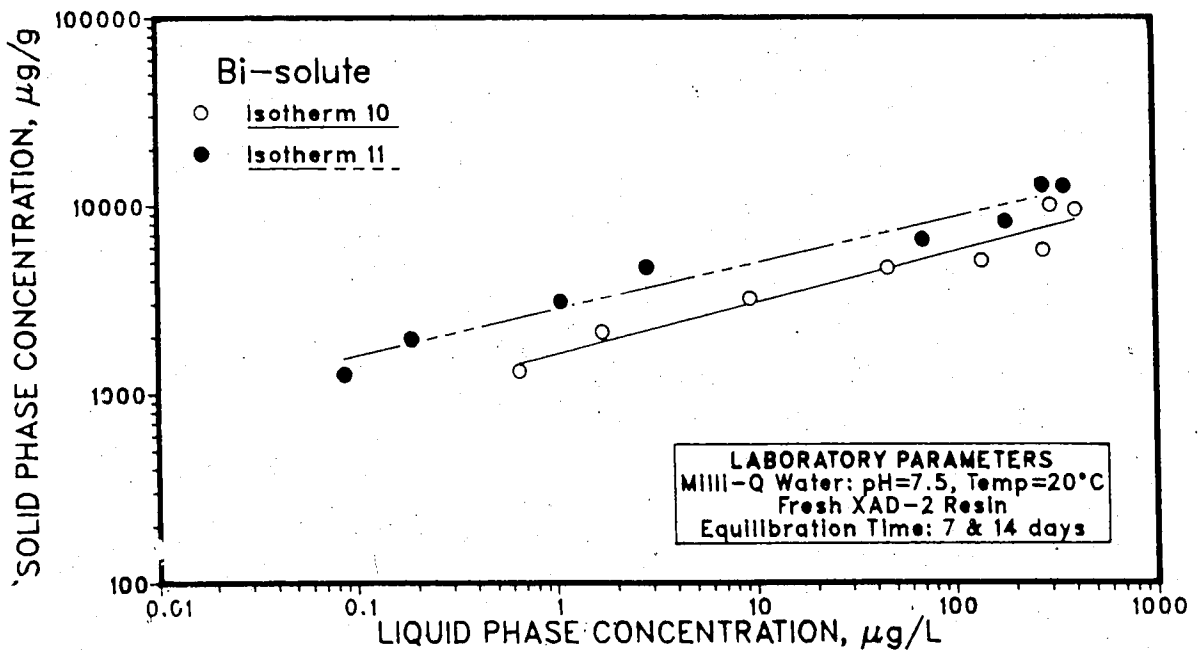
Figure 6.3.5 Comparison of Lindane Adsorption in Single Solute
Isotherm 12 and Bi-solute Isotherm 11
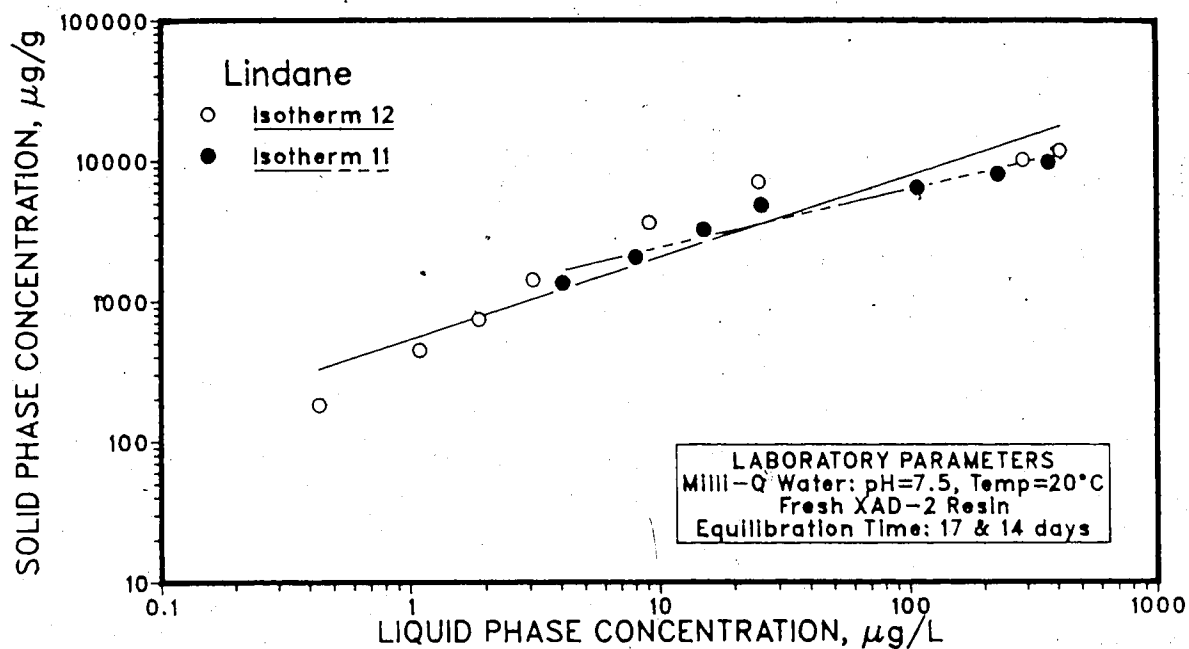
Figure 6.3.6 Comparison of Triallate Adsorption in Single Solute
Isotherm 14 and Bi-solute Isotherm 11
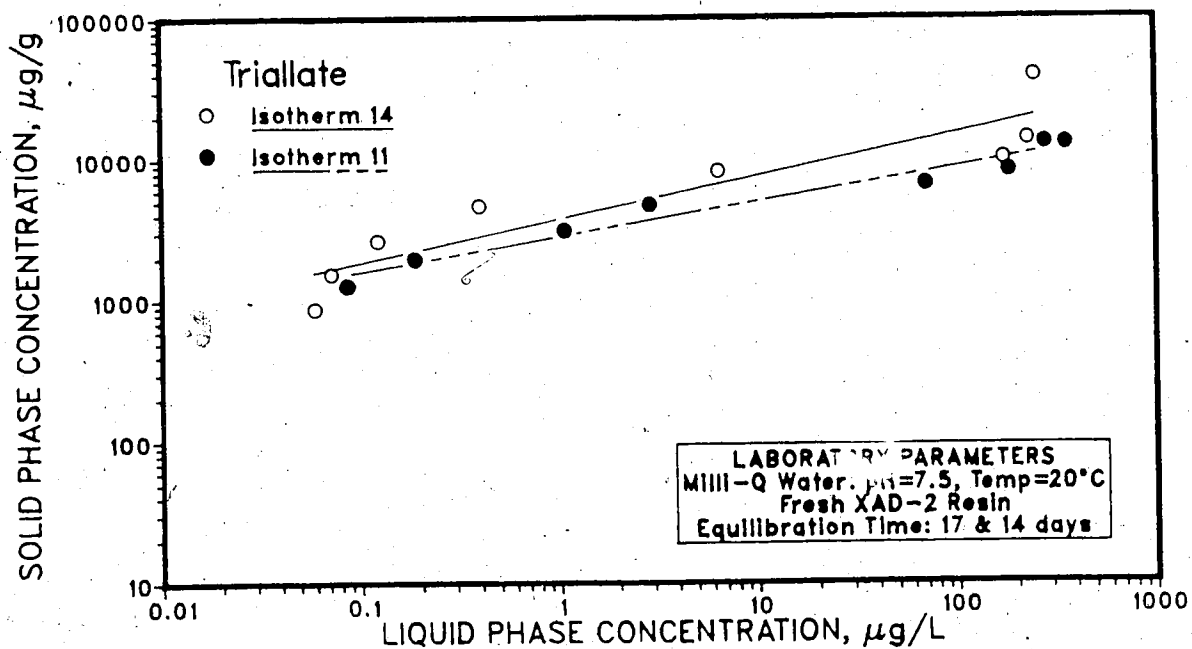
Figure 6.3.7 Bi-solute Isotherm 15 - Triallate and Lindane at 5:1 Molar Ratio
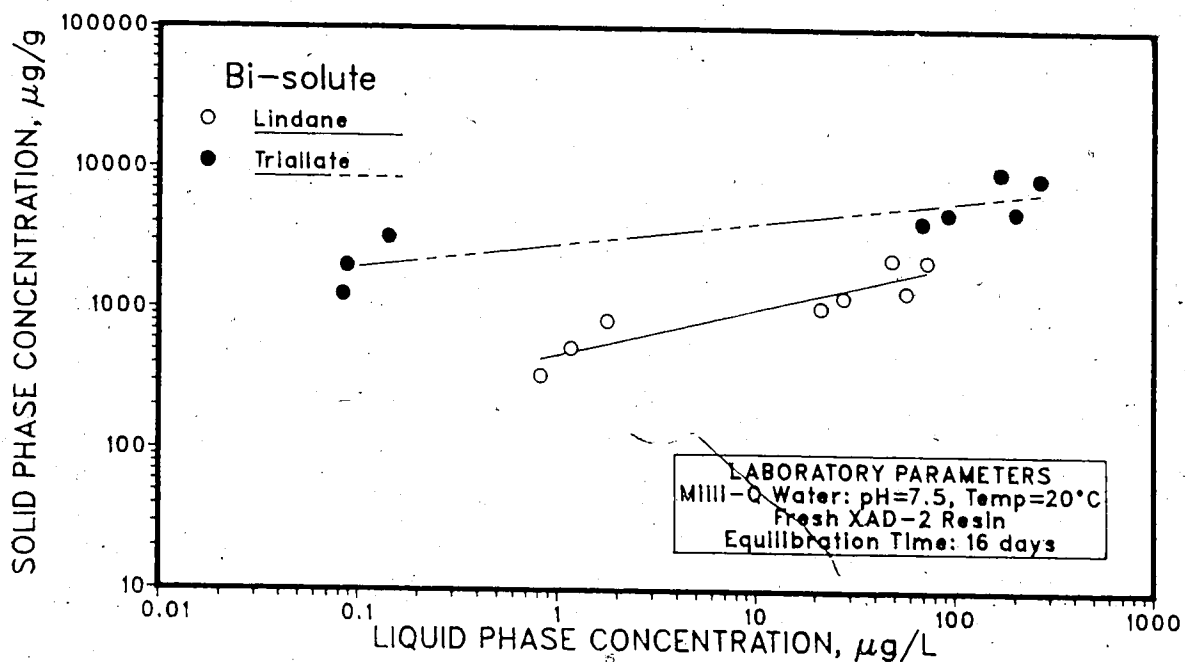
Figure 6.3.8 Comparison of Lindane Adsorption in Single Solute Isotherm 12 and Bi-solute Isotherm 15
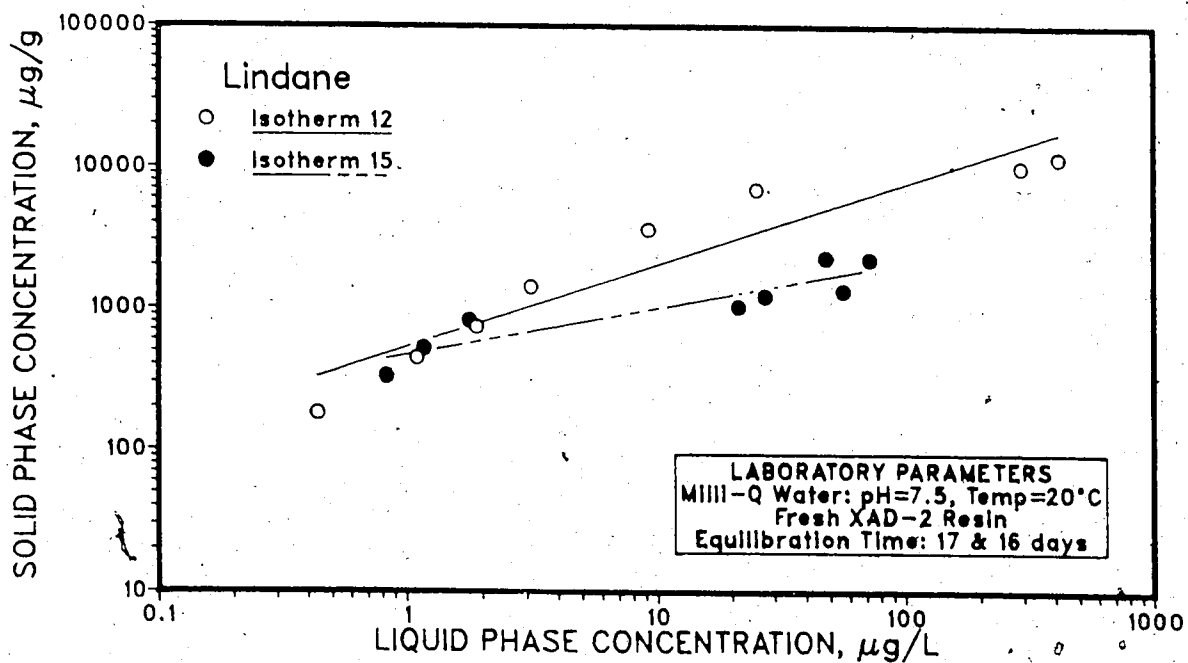
Figure 6.3.9 Comparison of Triallate Adsorption in Single Solute Isotherm 14 and Bi-solute Isotherm 15
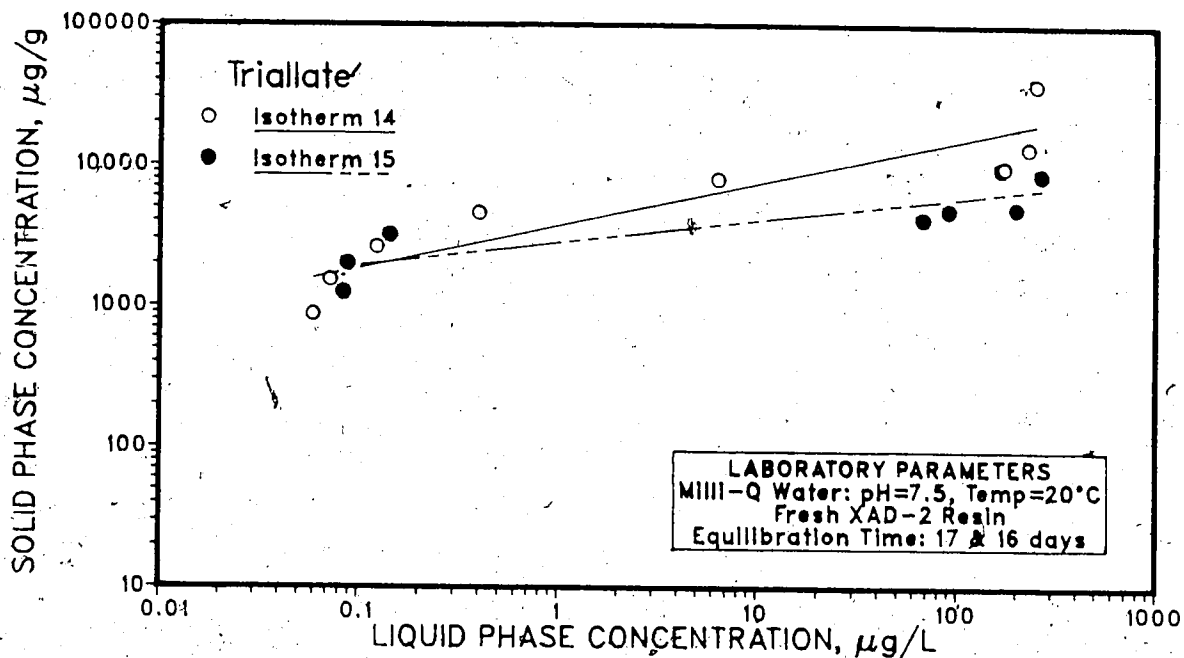
Figure 6.4.1 Comparison of Linear Least Squares to Non-Linear Least Squares Fit for Lindane Isotherm 12
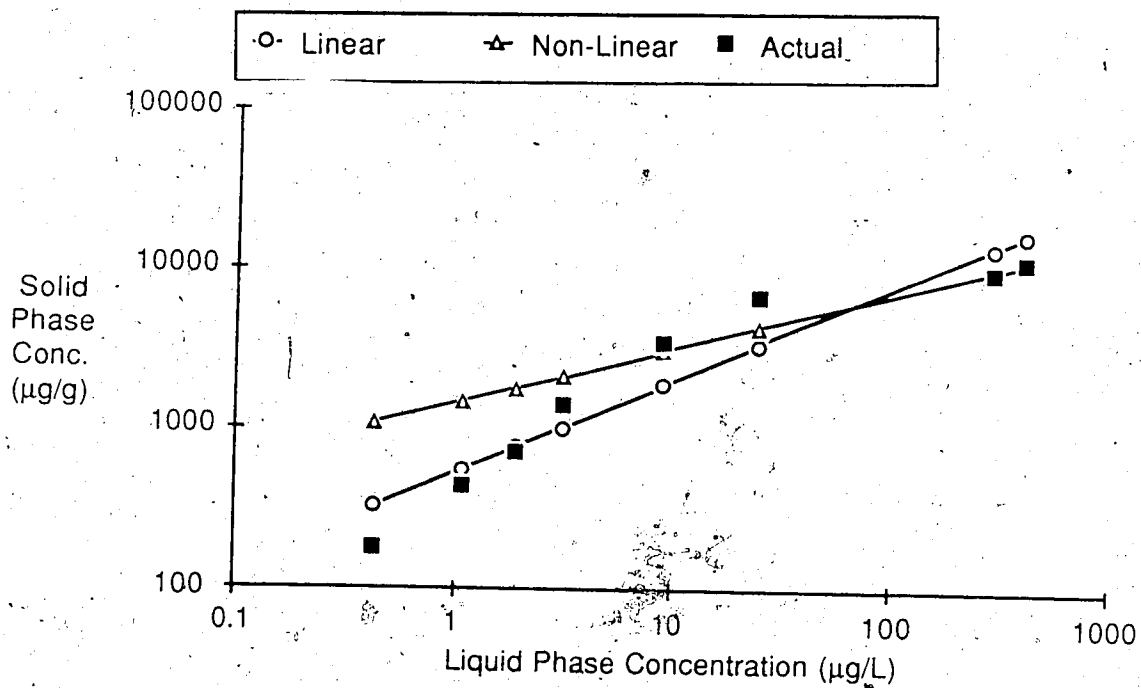
Figure 6.4.2 Comparison of Linear Least Squares to Non-Linear Least Squares Fit for Triallate Isotherm 14
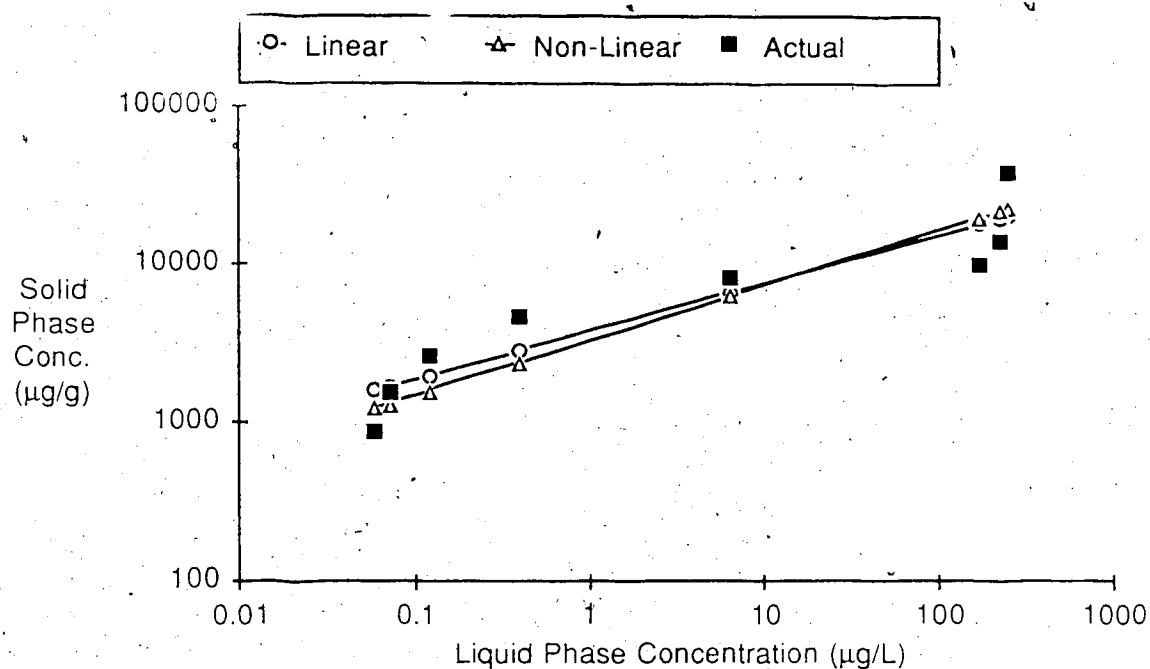
Figure 6.4.3 IAST Prediction of Lindane in Isotherm 11 - Linear Least Squares
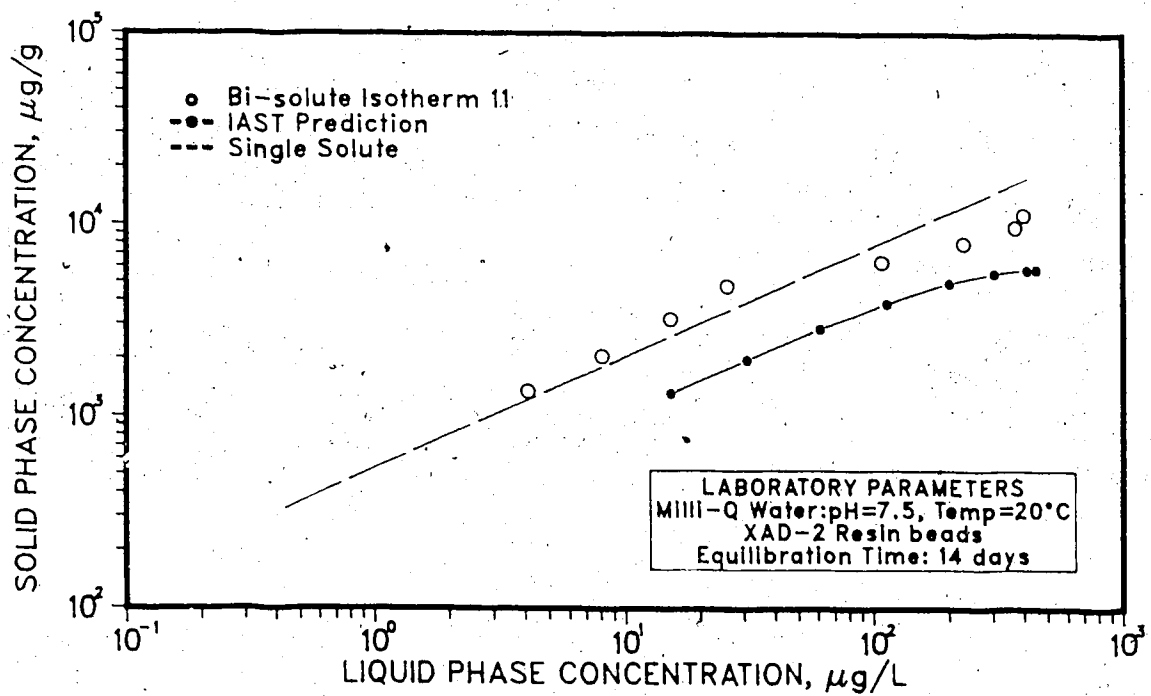
Figure 6.4.4 IAST Prediction of Lindane in Isotherm 11 - Non-Linear Least Squares
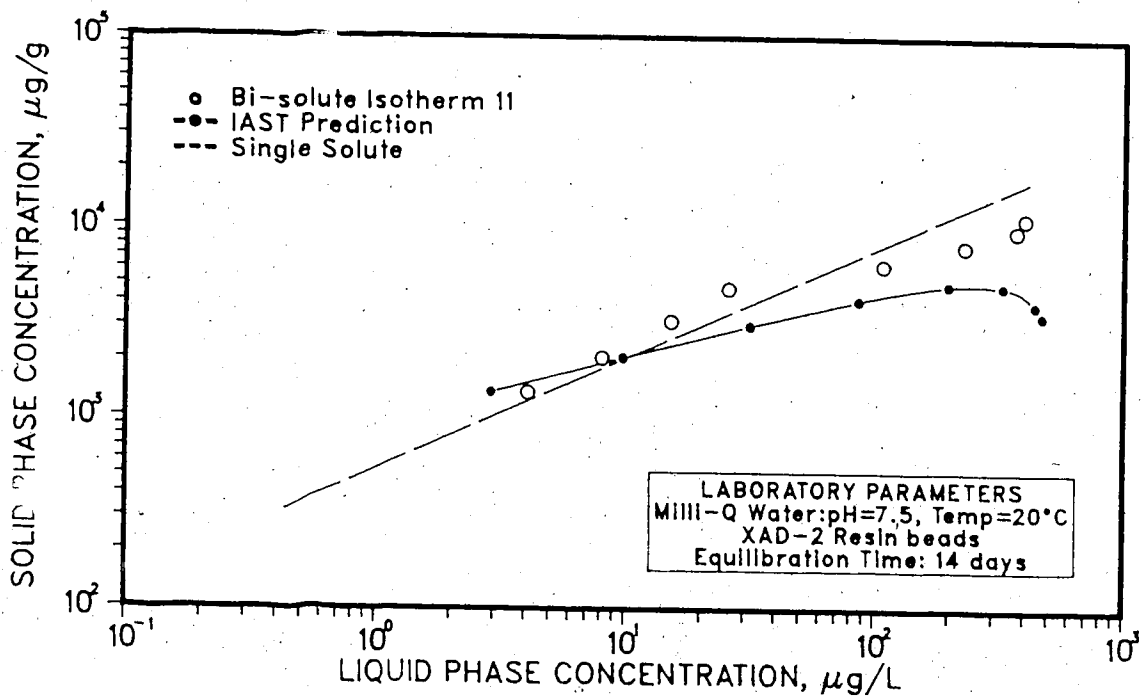
Figure 6.4.5 IAST Prediction of Lindane in Bi-solute Isotherm 15
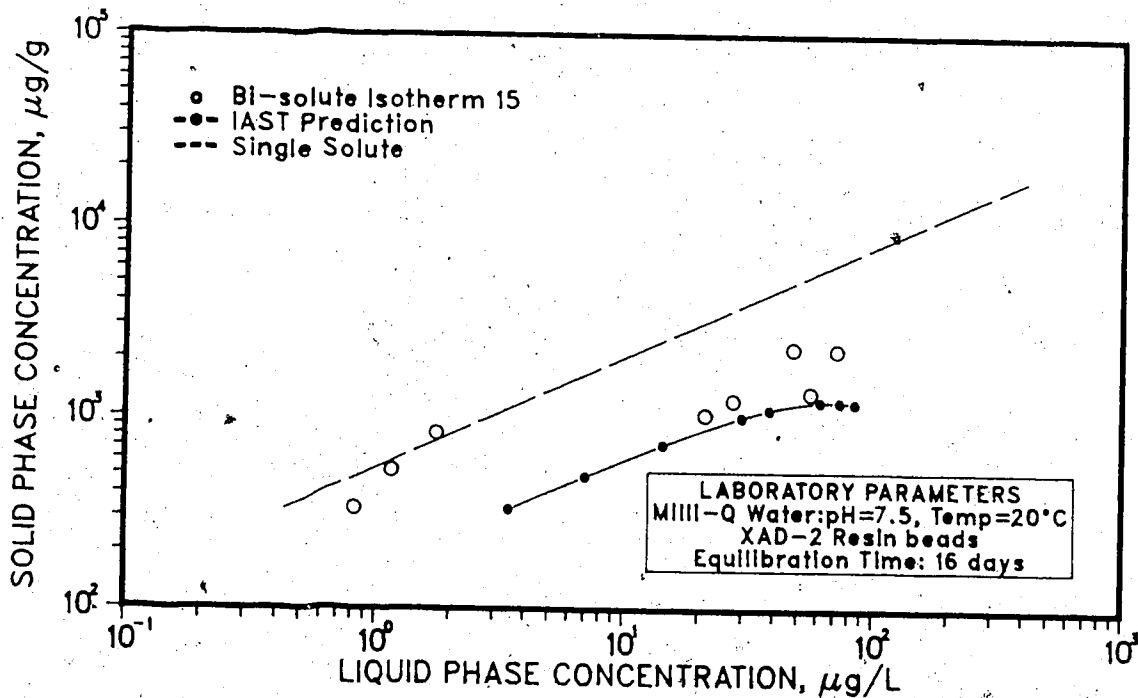
Figure 6.4.6 IAST Prediction of Triallate in Bi-solute Isotherm 11
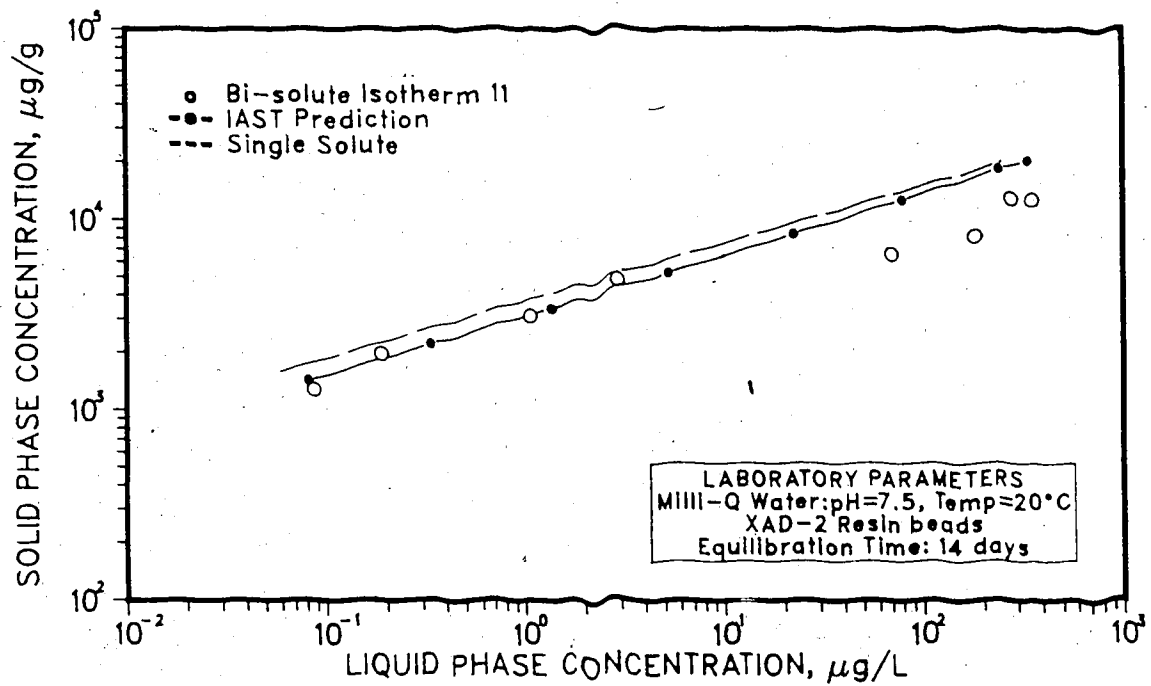
Figure 6.4.7 IAST Prediction of Triallate in Bi-solute Isotherm 15
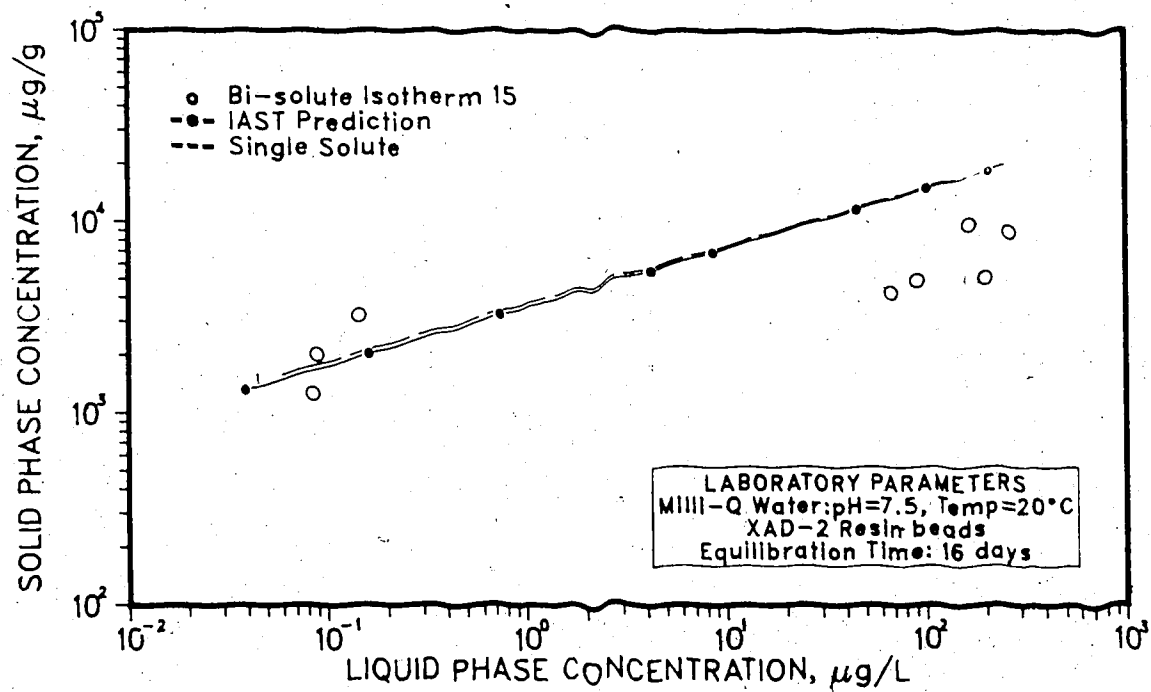
Figure 6.4.8 IAST Prediction of Lindane in Bi-solute Isotherm 15
using Single Solute Isotherm 16
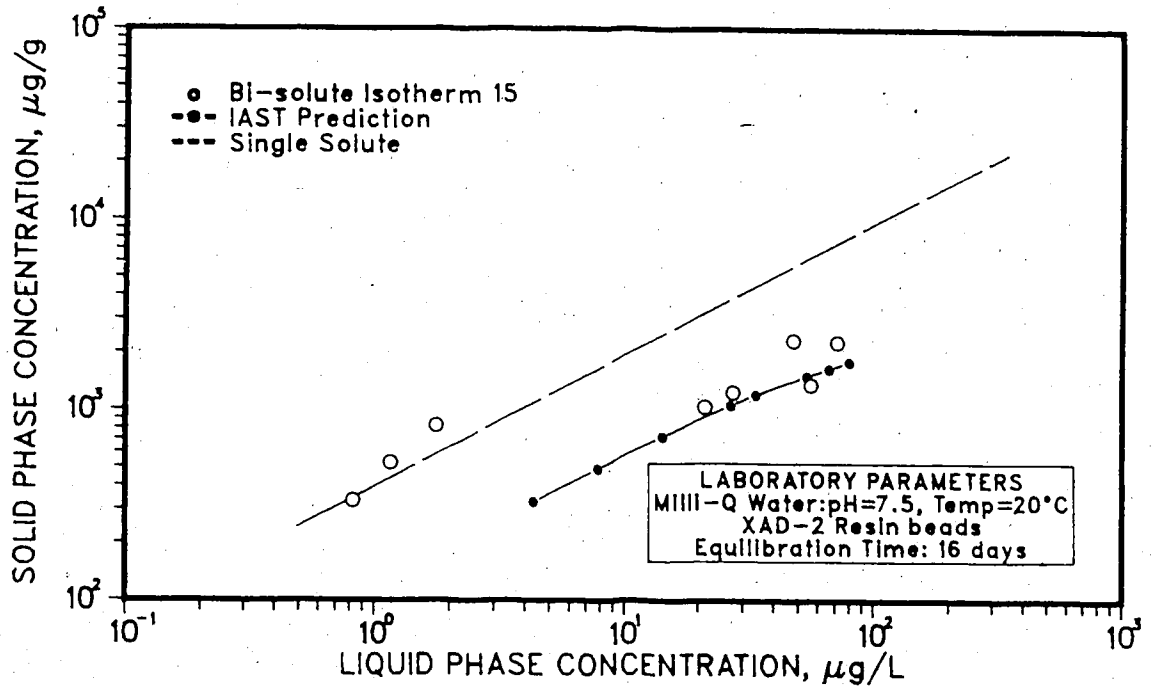
Figure 6.4.9 Solid Phase Concentration Range Used in IAST
Predictions for Bi-solute Isotherm 11
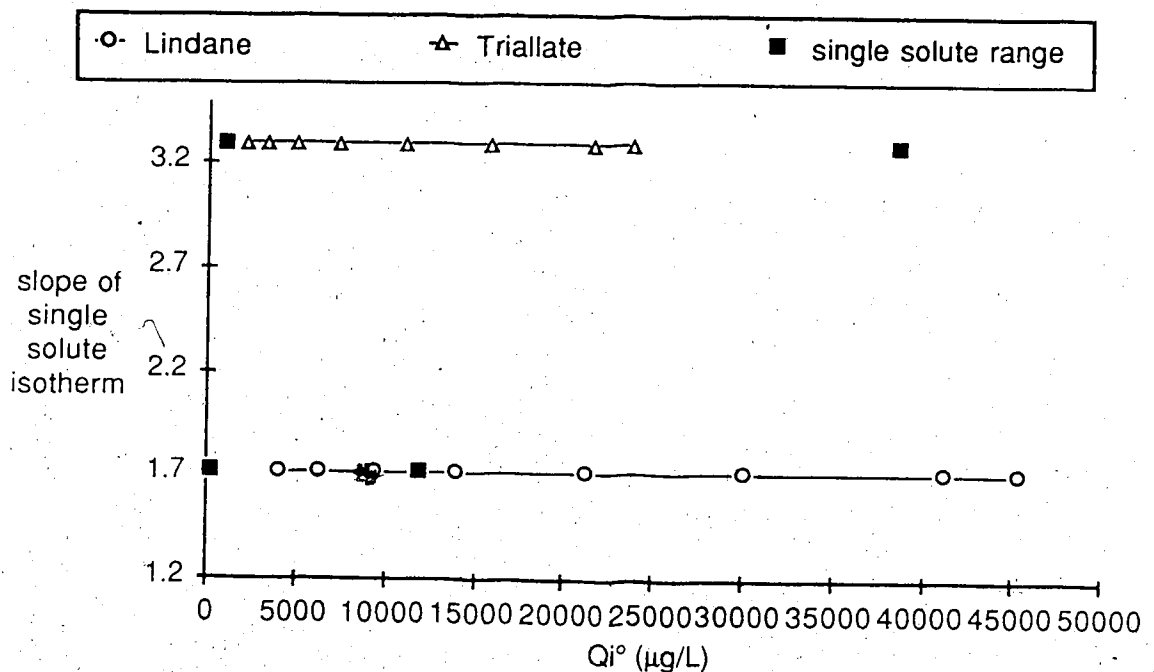
Figure 6.4.10 Solid Phase Concentration Range Used in IAST Predictions for Bi-solute Isotherm 15
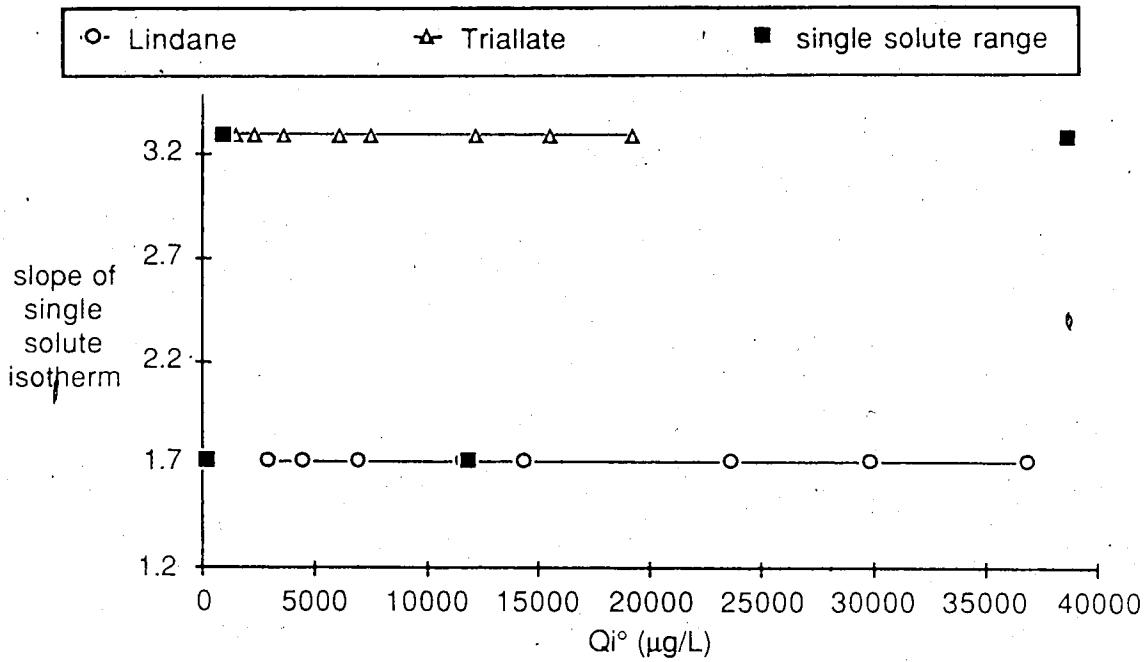
Figure 6.5.1 Column Experiment #1 Effluent Concentration Curves
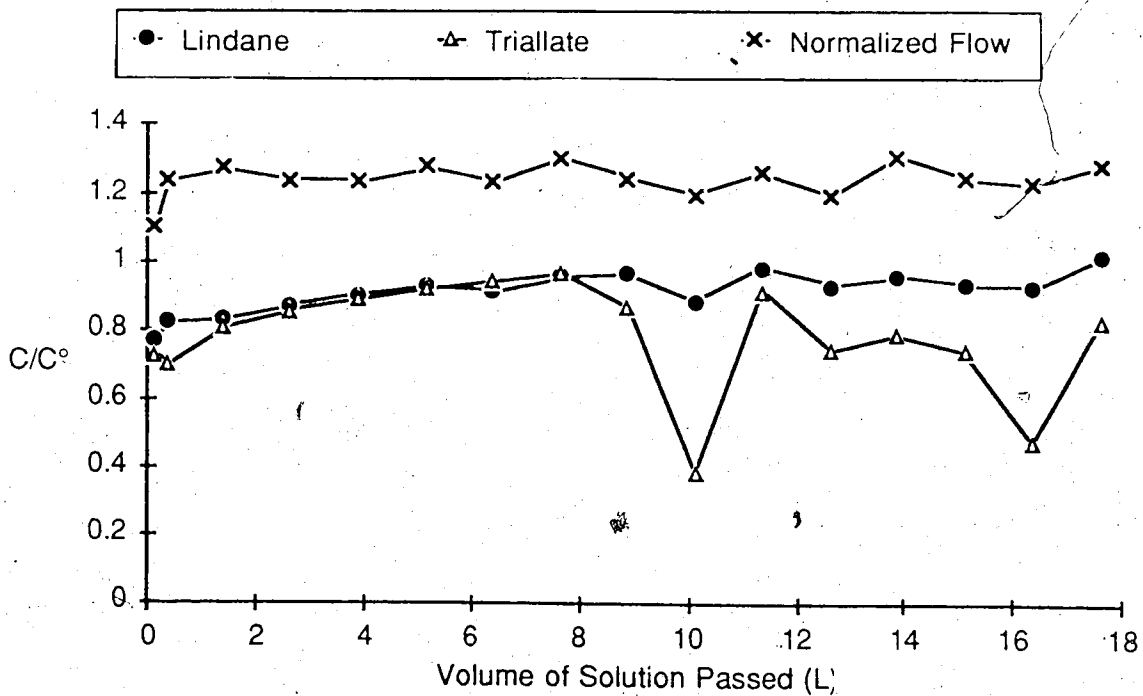
Figure 6.5.2   Column Experiment #2 Effluent Concentration Curves
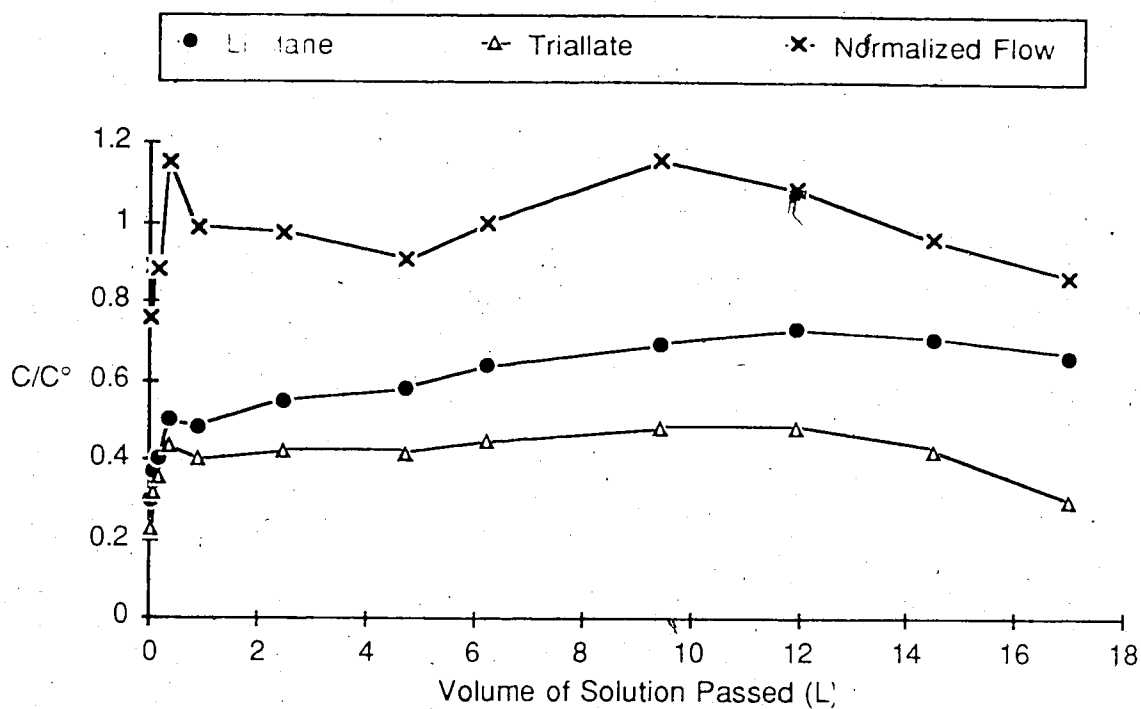
Figure 6.5.3   Column Experiment #3 Effluent Concentration Curves
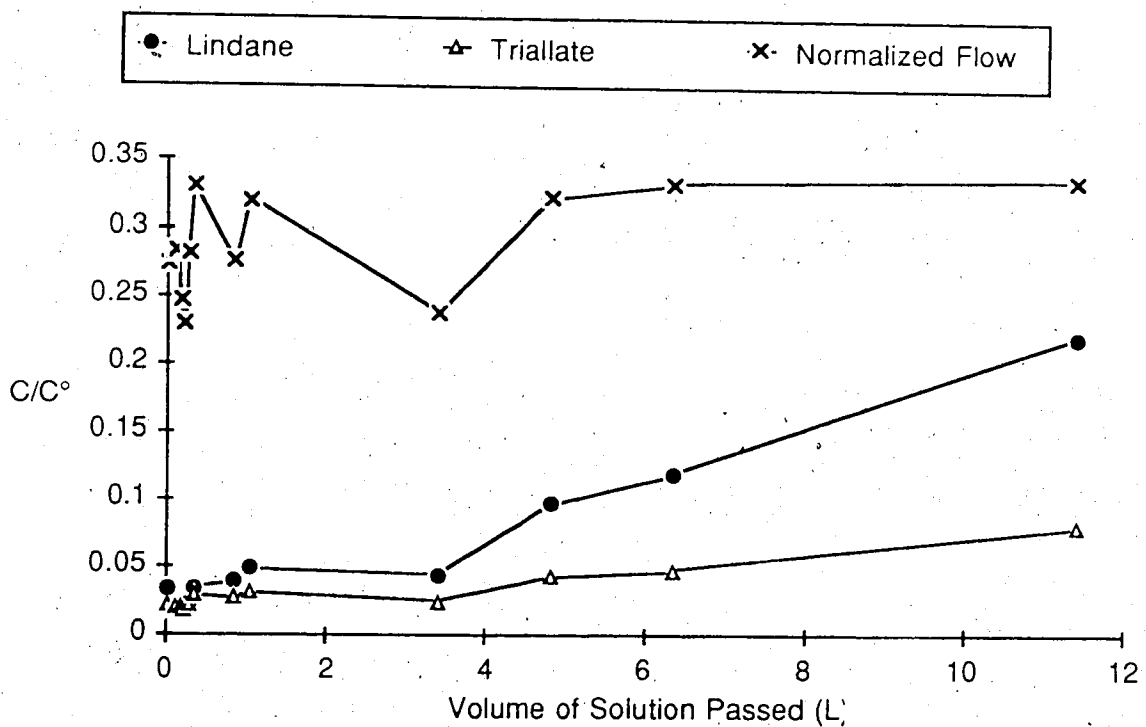
8.0 References

1. Andrews, R.C., P.M. Huck, J.C. Crittenden, E. Knettig, L.C. Gammie and D.T. Williams (1987). The Use of Ideal Adsorbed Solution Theory to Predict Multicomponent Adsorption of Trihalomethanes. Proceedings of the American Water Works Association Annual Conference, Kansas City, Missouri, June 13-18, 839-860.

2. APHA-AWWA-WPCF (1985). 408 (Chlorine Residual). In Standard Methods for the Examination of Water and Wastewater, 16th Edition, 305.

3. Baum, R.G., R. Saetre and F.F. Cantwell (1980). Liquid Chromatography Columns of Microparticle Amberlite XAD-2. Anal. Chem., 52, 15-19.

4. Benoit F.M. and D.T. Williams (1981). Determination of Hexachlorocyclopentadiene at the Nanogram Per Liter Level in Drinking Water. Bull. Environ. Contam. Toxicol., 27, 303-308.

5. Bogusz, M. (1982). Enzymatic Hydrolysis of Tissues before Amberlite XAD-2 Extraction in Poisoning Cases. Forensic Sci. Int., 20 (1), 27-33.

6. Bogusz, M., J. Gierz and J. Bialka (1978). Isolation of Drugs from Autopsy Material by XAD-2 Adsorption-Elution Technique. A Routine Procedure. Arch. Toxicol., 41 (2), 153-162.

7. Burnham, A.K., G.V. Calder, J.S. Fritz, G.A. Junk, H.J. Svec and R. Willis (1972). Identification and Estimation of Neutral Organic Contaminants in Potable Water. Anal. Chem., 44 (1), 139-142.

8. Cantwell, F.F. (1976). Pre-column Reactions to Eliminate Interferents in the Liquid Chromatographic Analysis of p-Hydroxybenzoates in Complex Pharmaceuticals. Anal. Chem., 48, 1854-1859.

9.   Cheetham, P. (1979).   Removal of Triton X-100 from Aqueous Solution using Amberlite XAD-2. Anal. Biochem., 92 (2), 447-452.

10. Cheh A.M., J. Shochdopole, C. Heilig, P.M. Koski and L. Cole (1980). Destruction of Direct-Acting Mutagens in Drinking Water by Nucleophiles: Implications for Mutagen Identification and Mutagen Elimination from Drinking Water. In R.L. Jolley, R.L. Brungs and R.B. Cumming (Eds.), Water Chlorination: Environmental Impact and Health Effects, Vol. 3, Ann Arbor Science, Ann Arbor, Michigan, 803-815.

11. Clark, R.M. (1987). Evaluating the Cost and Performance of Field-Scale Granular Activated Carbon Systems. Environ. Sci. Technol., 21, 573-580.

12. Coburn, J.A., I.A. Valdmanis and A.S.Y. Chau (1977). Evaluation of XAD-2 for Multiresidue Extraction of Organochlorine Pesticides and Polychlorinated Biphenyls from Natural Waters. J. Assoc. Off. Anal. Chem., 60 (1), 224-228.

13. Coleman W.E., J.W. Munch, W.H. Kaylor, R.P. Streicher, H.P. Ringhand and J.R. Meier (1984). Gas Chromatography/Mass Spectroscopy Analysis of Mutagenic Extracts of Aqueous Chlorinated Humic Acid. A Comparison of the By-Products to Drinking Water Contaminants. Environ. Sci. Technol., 18, 674-681.

14. Cortruvo, J.A. (1985). Organic Micropollutants in Drinking Water: An Overview. Sci. Tot. Environ., 47, 7-26.

15. Crittenden, J.C., G. Friedman, D.W. Hand, J. Berrigan and T. Speth (1985a). Design of Fixed-Beds to Remove Multicomponent Mixtures of Volatile Organic Chemicals. Proceedings of the American Water Works Association Annual Conference, Washington, D.C., June 23-27, 1327-1346.

16. Crittenden, J.C., P. Luft and D.W. Hand (1985b). Prediction of Multicomponent Adsorption Equilibria in Background Mixtures of Unknown Composition. Water Res., 12, 1537-1548.

17. Crittenden, J.C., P. Luft, D.W. Hand, J.L. Oravitz, S.W.Loper and M. Ari (1985c). Prediction of Multicomponent Adsorption Equilibria Using Ideal Adsorbed Solution Theory. Environ. Sci. Technol., 19 (11), 1037-1043.

18. Crittenden J.C., T.F. Speth, D.W. Hand, P. Luft, and B. Lykins (1987). Evaluating Multicomponent Competitive Adsorption in Fixed Beds. J. Environ. Eng., 113 (6), 1363-1375.

19. Daignault, S.A., D.K. Noot, D.T. Williams and P.M. Huck (1988). A Review of the Use of XAD Resins to Concentrate Organic Compounds in Water. Accepted by Water Research, June, 1988.

20. De Raat, W.K. and R.A.M. Van Ardenne (1984). Sorption of Organic Compounds from Urine in Mutagenicity Testing: Choice of Sorbent. J. Chromatogr., 310, 41-49.

21. de Greef E., J.C. Morris, C.F. van Kreijl and C.F.H. Morra (1980). Health Effects in the Chemical Oxidation of Polluted Waters. In R.L. Jolley, R.L. Brungs and R.B. Cumming (Eds.), Water Chlorination: Environmental Impact and Health Effects, Vol. 3, Ann Arbor Science, Ann Arbor, Michigan, 913-924.

22. Dunlop, E.H. (1978). Physicochemical Aspects of the Removal of Protein-bound Substances by Charcoal and other adsorbents of Potential Value in Systems of Artificial Liver Support. Parts 1 & 2. Med. Biol. Eng. Comput., 16 (4), 343-349, 350-362.

23. Fawell, J.K. and M. Fielding (1985). Identification and Assessment of Hazardous Compounds in Drinking Water. Sci. Tot. Environ., 47, 317-341.

24. Farwell, S.O, F.W. Bowes and D.F. Adams (1977). Evaluation of XAD-2 Resin as a Collection Sorbent for 2,4-D Herbicides in Air. J. Environ. Sci. Health, B12 (1), 71-83.

25. Giabbai, M., L. Roland, M. Ghosal, J.H. Reuter and E.S.K. Chian (1983). Investigation of a Comprehensive Approach for Trace Analysis of Dissolved Organic Substances in Water. J. Chromatogr., 279, 373-382.

26. Glaze,W.H., I.V. Henderson, J.E. Bell and V.A. Wheeler (1973). Analysis of Organic Materials in Wastewater Effluents after Chlorination. J. Chromatogr. Sci., 11 (11), 580-584.

27. Gluck, S.J. and R.G. Melcher (1980). Concentration and Determination of the Propylene glycol butyl ether esters of 2,4-D in Air. Am. Ind. Hyg. Assoc. J., 41 (12), 932-934.

28. Haworth S., T. Lawlor, K. Mortelmans, W. Speck and E. Zeiger (1983). Salmonella Mutagenicity Test Results for 250 Chemicals. Environmental Mutagenesis, 5, Supplement 1, 3-142.

29. Huck, P.M. (1986). Combined Chemical and Biological Evaluation of Drinking Water Treatment Alternatives on a Pilot Scale (UP-A-391). Final report submitted to Health and Welfare Canada, Ottawa, Ontario. Department of Supply and Services Contract No. 1ST84-00176.

30. Huck, P.M., S.A. Daignault, D.K. Noot, R.C. vonBorstel, D. Savage, W.B. Anderson, D. Kellendonk, C.E. Rodger and D.T. Williams. (1987). Assessment of the Products of Reactions of Drinking Water Disinfectants with Humic Substances and Trace Organic Contaminants. Sci. Tot. Environ., 62, 315 328.

31. Huck, P.M. and R.C. Andrews (1988). A Study Using Computer Software to Model the Performance of Carbon Adsorbers in a Large Canadian Drinking Water Treatment Plant (UP-A-452). Final Report submitted to

Health and Welfare Canada, Ottawa, Ontario. Department of Supply and Services Contract Number 1ST85-00220.

32. Hux, R.A., H.Y. Mohammed and F.F. Cantwell (1982). Precolumns of Amberlite XAD-2 for Direct Injection Liquid Chromatographic Determination of Methaqualone in Blood Plasma. Anal. Chem., 54, 113-117.

33. Ibrahim, G., S. Andryauskas and M.L. Bastos (1975). Application of Amberlite XAD-2 Resin for General Toxicological Analysis. J. Chromatogr., 108 (1), 107-116.

34. Junk G.A., J.J. Richard, M.D. Grieser, D. Witiak, J.L. Witiak, M.D. Arguello, R. Vick, H.J. Svec, J.S. Fritz and G.V. Calder (1974). Use of Macroreticular Resins in the Analysis of Water for Trace Organic Contaminants. J. Chromatogr., 99, 745-762.

35. Khan, A.S. and F.F. Cantwell (1985). Properties of Low-Capacity Macroporous Anion-Exchangers and Their Use with High-pH Eluents for the Determination of Weak Acids in Urine. Talanta, 32 (9), 901-906.

36. Kong, E.J. and F.A. DiGiano (1986). Competitive Adsorption among VOCs on Activated Carbon and Carbonaceous Resin. J.A.W.W.A., 78 (4), 181-188.

37. Kopfler F.C., H.P. Ringhand, W.E. Coleman and J.R. Meier (1985). Reaction of Chlorine in Drinking Water, with Humic Acids and In Vivo. In R.L. Jolley, R.J. Bull, W.P. Davis, S Katz, M.H. Roberts Jr. and V.A. Jacobs (Eds.), Water Chlorination: Chemistry, Environmental Impact and Health Effects, Vol.5, Lewis Publishers Inc., Michigan, 161-173.

38. Kringstad K.P., P.O. Ljundquist, F. de Sousa and L.M. Stromberg (1983). On the Formation of Mutagens in the Chlorination of Humic Acid. Environ. Sci. Technol., 17 (9), 553-555.

39. Kroeff, E.P. and D.J. Pietrzyk (1978). Investigation of the Retention and Separation of Amino Acids, Peptides, and derivatives on Porous Copolymers by High Performance Liquid Chromatography. Anal. Chem., 50 (3), 502-511.

40. Lawrence, J. and H.M. Tosine (1976). Adsorption of Polychlorinated Biphenyls from Aqueous Solutions and Sewage. Environ. Sci. Technol., 10 (4), 381-383.

41. LeBel G.L., D.T. Williams and F. Benoit (1987). Use of Large-Volume Resin Cartridges for the Determination of Organic Contaminants in Drinking Water Derived from the Great Lakes. In I.H. Suffet and M. Malaiyandi (Eds.), Organic Pollutants in Water: Sampling, Analysis and Toxicity Testing, American Chemical Society, Washington, D.C., 309-325.

42. LeBel G.L., D.T. Williams, G. Griffith and F.M. Benoit (1979). Isolation and Concentration of Organophosphorous Pesticides from Drinking Water at the ng/L Level, Using Macroreticular Resin. J. Assoc. Off. Anal. Chem., 62 (2), 241-249.

43. LeBel G.L., D.T. Williams, J.J. Ryan and B.P.Y. Lau (1986). Evaluation of XAD-2 Resin Cartridge for Concentration/Isolation of Chlorinated Dibenzo-p-Dioxins and Furans From Drinking Water at the Parts-per-Quadrillion Level. In C. Rappe, G. Choudhary and L. Keith (Eds.), Chlorinated Dioxins and Dibenzofurans in Perspective, Lewis Publishers, Michigan, 329-341.

44. Levesque, D. and V.N. Mallet (1983). Development of an Analytical Method for Aminocarb and Some Derivatives in Water Using XAD Resins and Gas Chromatography. Intern. J. Environ. Anal. Chem., 16, 139-147.

45. Lykins B.W. Jr. and W. Koffskey (1986). Products Identified at an Alternative Disinfection Pilot Plant. Environ. Health Perspect., 69, 119-128.

46. Meier J.R., H.P. Ringhand, W.E. Coleman, J.W. Munch, R.P. Streicher, W.H. Kaylor and K.M. Schenck (1985). Identification of Mutagenic Compounds Formed During Chlorination of Humic Acid. Mut. Res., 157, 111-122.

47. Meier J.R., H.P. Ringhand, W.E. Coleman, K.M. Schenck, J.W. Munch, R.P. Streicher, W.H. Kaylor and F.C.Kopfler (1986). Mutagenic By-Products from Chlorination of Humic Acid. Environ. Health Perspect., 69, 101-107.

48. Mohammed, H.Y. and F.F. Cantwell (1978). Liquid Chromatographic Analysis of Pharmaceutical Syrups Using Pre-Columns and Salt-Adsorption on Amberlite XAD-2. Anal. Chem., 50, 491-496.

49. Montgomery, J.M., Consulting Enginneers, Inc. (1985). Water Treatment Principles and Design, Wiley-Interscience, New York, 177-183.

50. Mortelmans K., S. Haworth, T. Lawlor, W. Speck, B. Tainor and E. Zeiger (1983). Salmonella Mutagenicity Tests:II. Results for 270 Chemicals. Environmental Mutagenesis, 8, Supplement 7, 1-119.

51. Nestmann E.R., R. Otson, G.L. LeBel and D.T. Williams (1983). Correlation of Water Quality Parameters with Mutagenicity of Drinking Water Extracts. In R.L. Jolley, W.A. Brungs, J.A. Cortruvo, R.B. Cumming, J.S. Mattice and V.A. Jacobs (Eds.), Water Chlorination: Environmental Impact and Health Effects, Vol. 4, Ann Arbor Science, Ann Arbor, Michigan, 1151-1164.

52. Noot, D.K., S.A. Daignault, R.C. von Borstel, D.T. Williams and P.M. Huck (1988). A Review of the Use of Mutagenicity Testing to Assess Drinking Water Treatment Processes. Submitted to J.A.W.W.A., July, 1988.

53. Noordsij A., L.M. Puyker and M.A. Van der Gaag (1985). The Quality of Drinking Water Prepared from Bank-Filtered River Water in the Netherlands. Sci. Tot. Environ., 47, 273-292.

54. O'Connor, S.C. (1975). Macroreticular Resin Chromatography of Antibiotics. Methods Enzymol., 43, 296-299.

55. Pietrzyk, D.J.; T.D. Rotsch, S.W. Chan Leuthauser (1979). Applications of the Porous Amberlite XAD Copolymers as Stationary Phases in TLC. J. Chromatogr. Sci., 17 (10), 555-561.

56. Pietrzyk, D.J. and C.H. Chu (1977). Separation of Organic Acids on Amberlite XAD Copolymers by Reversed Phase High Pressure Liquid Chromatography. Anal. Chem., 49 (6), 860-867.

57. Rao, G.S. and D.A. McLennon (1977). Thin-layer Chromatographic Analysis of Phenytoin and its Hydroxy Metabolites. J. Chromatogr., 137 (1), 231-233.

58. Rogers, I.H and H.W. Mahood (1977). The Use of a Macroreticular Resin in the Analysis of Kraft Pulping Effluents for Resin Acids. Tech. Rep. - Fish. Mar. Serv. (Can.), 730, 13 pp.

59. Rohm and Haas Co., Amberlite XAD-2, Technical Bulletin, Philadelphia, PA, November, 1978.

60. Rosenfeld, J.M., M. Mureika-Russel and A. Phatak (1984). Macroreticlar Resin XAD-2 as a Catalyst for the Simultaneous Extraction and Derivatization of Organic Acids from Water. J. Chromatogr., 283, 127-135.

61. Samoiloff M.R., J. Bell, D.A. Birkholz, G.R. Webster, E.G. Arnott, R. Pulak and A. Madrid (1983). Combined Bioassay-Chemical Fractionation

Scheme for the Determination and Ranking of Toxic Chemicals in Sediments. Environ. Sci. Technol., 17 (6), 329-334.

62. Sato Г., M. Mukaida, Y. Ose, H. Nagase and T. Ishikawa (1985). Mutagenicity of Chlorinated Products from Soil Humic Substances. Sci. Tot. Environ., 47, 229-241.

63. Smith, E.H., S.K. Tseng and W.J. Weber, Jr. (1987). Modeling the Adsorption of Target Compounds in the Presence of Background Dissolved Organic Matter. Environm. Progress, 6 (2), 18-25.

64. Stolman, A. and P.A.F. Pranitis (1977). XAD-2 Resin Drug Extraction Methods for Biologic Samples. Clin. Toxicol., 10 (1), 49-60.

65. Strachan, W.M.J. and H. Huneault (1984). Automated Rain Sampler for Trace Organic Substances. Environ. Sci. Technol., 18, 127-130.

66. Suffet I.H., L. Brenner, J.T. Coyle and P.R. Cairo (1978). Evalution of the Capacity of GAC and XAD-2 Resin to Remove Trace Organics from Treated Water. Environ. Sci. Technol., 12 (12), 1315-1322.

67. Suffet I.H., L. Brenner and B. Silverman (1976). Identification of 1,1,1-Trichloroacetone in Two Drinking Waters: A Known Precursor in Haloform Reaction. Environ. Sci. Technol., 10 (13), 1273-1275.

68. Tabor M.W. and J.C. Loper (1985). Analytical Isolation, Separation and Identification of Mutagens from Nonvolatile Organics of Drinking Water. Intern. J. Environ. Anal. Chem., 19, 281-318.

69. Toft, P. (1985). The Control of Organics in Drinking Water in Canada and the United States (Standards, Legislation and Practice). Sci. Tot. Environ., 47, 45-58.

70. Tokiwa H. and Y. Ohnishi (1986). Mutagenicity and Carcinogenicity of Nitroarenes and Their Sources in the Environment. <u>CRC Crit. Rev. Tox.</u>, <u>17</u> (<u>1</u>), 23-60.

71. Van' Rossum, P.G. (1985). Progress in the Isolation and Characterization on Non-Volatile Mutagens in a Drinking Water. <u>Sci. Tot. Environ.</u>, <u>47</u>, 361-370.

72. van Vliet, B.M., W.J. Weber, Jr. and H. Hozumi (1980). Modeling and Prediction of Specific Compound Adsorption by Activated Carbon and Synthetic Adsorbents. <u>Water Res.</u>, <u>14</u>, 1719-1728.

72b Verschueren, Karel (1983). Handbook of Environmental Data on Organic Chemicals, Second Edition. Van Nostrand Reinhold Company, New York, New York, 434,821.

73. Weber, W.J. Jr. (1972). Physicochemical Processes for Water Quality Control, Wiley-Interscience, New York, 206-211.

74. Weber, W.J. Jr., and C.K. Wang (1987). A Microscale System for Estimation of Model Parameters for Fixed-Bed Adsorbers. <u>Environ. Sci. Technol.</u>, <u>21</u>, 1096-1102.

75) Wilcox, P., F. van Hoof and M. van der Gaag (1986). Isolation and Characterisation of Mutagens from Drinking Water. In A. Léonard and M. Kirsch-Volders (Eds.), Proceedings of the 16th Annual Meeting of the European Environmental Mutagen Society, 25-30 August 1986, 92-103.

76. Williams, D.T., E.R. Nestmann, G.L. LeBel, F.M. Benoit and R. Otson (1982). Determination of Mutagenic Potential and Organic Contaminants of Great Lakes Drinking Water. <u>Chemosphere</u>, <u>11</u> (<u>3</u>), 263-276.

77. Zoeteman B.C.J., J. Hrubec, E. de Greef and H.J. Kool (1982). Mutagenic Activity Associated with By-Products of Drinking Water Disinfection by Chlorine, Chlorine Dioxide, Ozone and UV-Irradiation. Environ. Health Perspect., 46, 197-205.

	A	B	C	D	E
1	Compound	mutagenic*	XAD-2**	comments	reference
2					
3	* negative, positive, weak, intermediate or strong (relative) or carcinogenic				
4	** adsorbable on XAD-2 yes, no, possibly or on XAD-4				
5					
6	Acenaphthene		y(7,68)		7, 68
7	Methylchloroacetate	-		Humic Acid (HA)	62
8	Methyldichloroacetate	-		HA	62
9	Ethylchloroacetate	-		HA	62
10	Ethyldichloroacetate	-		HA	62
11	Ethyltrichloroacetate			HA	62
12	Dichloroacetic acid	-(62)		HA	13, 37, 46, 62
13	Trichloroacetic acid	-(62)		HA	13, 37, 46, 62
14	alpha-Hydroxy-alpha-methyl bezeneacetic acid		y		17
15	Phenylacetic acid		y		13
16	1,1-Dichloroacetone	possible		HA	62
17	1,3-Dichloroacetone	i(10)	p	HA(38)	10, 38
18	1,1,1-Trichloroacetone		y(pH4;67)		66, 67,
19	1,1,3,3-Tetrachloroacetone				38
20	Pentachloroacetone	+(62)		HA(62)	38, 62
21	Hexachloroacetone				38
22	Benzeneacetonitrile				17
23	Chloroacetonitrile	-(50)	y		37, 50
24	Bromochloroacetonitrile	+(23)		HA,Fulvic Acid (FA	13, 77, 23
25	Dibromochloroacetonitrile				16
26	Dichloroacetonitrile	+(50,23)		HA,FA	13, 37, 47, 50, 23
27	Trichloroacetonitrile	-(37) +(50)		HA,FA	13, 37, 46, 20
28	Acetophenone		y		66, 77
29	Dihydroactinidiolide		y		13
30	Benzaldehyde			sediment(61)	61, 13
31	2-Methylbenzaldehyde			sediment	12
32	3- or 4-Methylbenzalbehyde			sediment	12
33	Dichloroacetaldehyde				5
34	Trichloroacetaldehyde				5

Organic Compounds in Drinking Water

	A	B	C	D	E
1	Compound	mutagenic*	XAD-2**	comments	reference
2					
35	Alkanes C10,11,12,15-17,19,20				45
36	Anilines				53
37	Chloroanilines		4		53
38	Trichloroaniline	c	4		40
39	Nitroanilines		4		53
40	9,10-Di(chloromethyl)anthracene	s	p		2
41	3,5-Di-t-butyl-4-hydroxybenzaldehyde				4
42	Ethylbenzaldehyde		y		17
43					
44	benzene	c(23)	y		51, 77, 23
45	Alkyl benzenes		y(4)		7, 53
46	Dibromodihydroxybenzene, diacetate ester			FA	3
47	Dichlorodihydroxybenzene, diacetate ester			FA	3
48	Trichlorodihydroxybenzene, diacetate ester			FA	3
49	Chlorobenzenes	c	4		53
50	Chlorobenzene		y		40
51	Dichlorobenzene				13
52	1,2-Dichlorobenzene	-(28)	y(68)		28, 45, 68,
53	1,3-Dichlorobenzene	-(28)	y(68)		45, 68, 28
54	1,4-Dichlorobenzene	-(28)			45, 28
55	Trichlorobenzene		y		4, 13, 4
56	1,2,4-Trichlorobenzene	-(70)			45
57	1-Chloro-2-nitrobenzene				45, 70
58	1-Chloro-4-nitrobenzene	+(28) -(70)			28, 45, 70
59	(1-Chloroethyl)dimethylbenzene		y		17
60	p-Chloro-1-methylenepropylbenzene		y		17
61	Ethylbenzene		y(4)		45, 51, 7,
62	1,3-Diethylbenzene				45
63	1,4-Diethylbenzene				45
64	1,2-Dimethylbenzene	-(28)		sediment	61, 28
65	1,2,3-Trimethylbenzene				45
66	1,2,4-Trimethylbenzene				45

Organic Compounds in Drinking Water

	A	B	C	D	E
1	Compound	mutagenic*	XAD-2**	comments	reference
2					
67	1,2,5-Trimethylbenzene				45
68	1,2,3,4-Tetramethylbenzene				45
69	1,2,3,5-Tetramethylbenzene				45
70	1,2,4,5-Tetramethylbenzene				45
71	1-(1,3-Dimethyl-3-butenyl)-3-methoxybenzene		y		17
72	Isopropylbenzene		y		7
73	2,4-Dimethyl-1-(1-methoxypropyl)benzene		y		17
74	Benzyl bromide	i	p		2
75	Benzyl chloride	w	p		2
76	Nitrobenzene	-(28,70)	4(24)		28, 45, 53, 70
77	p,p'-bis(Dimethylamino)benzophenone		4		53
78	2-(Methylthio)benzothiazole				16
79	Hexachlorobutadiene		y		14
80	Trichlorobutanal				5
81	1,2-Epoxybutane	w	p		2
82	1-Bromobutane	+			40
83	Butan-2,3-dione	+			40
84	3-Chloro-?-butanone				5
85	1,1-Dichloro-2-butanone			FA	13, 5
86	1,3-Dichloro-2-butanone				5
87	3,3-Dichloro-2-butanone			HA,FA	13, 5
88	1,1,1-Trichloro-2-butanone			FA	13, 5
89	1,1,3-Trichloro-2-butanone				13, 5
90	Dichlorobutenal				5
91	2,3,3-Trimethyl-1-butene				5
92	Chloromethylbutene			sediment	12
93	1-Chloro-3-buten-2-one		y		13
94	3-Chloro-3-buten-2-one				5
95	Tetrachloro-3-buten-2-one				5
96	Pentachloro-3-buten-2-one				5
97	Trimethylcyclohexenylbutenone		y	FA	13, 5
98					17

	A	B	C	D	E
	Compound	mutagenic*	XAD-2**	comments	reference
1					
2					
99	Bromoform	+(28,23)		FA	28, 13, 77, 23
100	Chloroform	-	y	HA,FA	13, 46, 37, 51, 66, 76, 77
101					
102	Campestrol			sediment	12
103	Carbazole	c			40
104	Citonellyl propionate			sediment	12
105	Cholesterol			sediment	12
106	Chloral	+(23,62)	y	HA(62)	23 62
107	Chrysene		y		14
108	Chrysene-5,6-oxide	i	p		2
109	Clofibrate	c			40
110	cyclododecane			sediment	12
111	cis-1,2-Diethylcyclobutane			sediment	12
112	1,5-Di-t-butyl-3,5-dimethylbicyclo(3,1,0)hexanone				4
113	3,3-Dimethyl-1,5-bis(isobutyl)bicyclo(3,1,0)hexanone-2				16
114	7-Butylbicyclo[4.1.0]heptane				12
115	2,6-Bis(t-butyl)2,5-cyclohexadiene-1,4-dione			sediment	16
116	Cyclohexene oxide	w	p		2
117	3,5-Dimethylcyclohexen-1-one			sediment	12
118	3-Methyl-2-cyclohexen-1-one			sediment	12
119	Dicyclopentadiene				16
120	Hexachlorocyclopentadiene	-(37,28)	y	light sensitive	4, 13, 29, 37, 46,19
121	Trichlorocyclopentenedione				
122	trans-2-Methylcyclopentanol			sediment	12
123	1-Hexyl-3-methylcyclopentane			sediment	12
124	1,1,3-Trimethyl-cyclopentane			sediment	12
125	3-Methyl-2-(2,4-pentadienyl)-2-cyclopenten-1-one		y		17
126	Tetrachlorocyclopropene			FA	13, 37
127	Cumene				45
128	p-cymene				45
129	Dichloro-p-cymene	w	p		2
130	Bromo-p-cymene	w	p		2

Organic Compounds in Drinking Water

	Compound	mutagenic*	XAD-2**	comments	reference
131					
132	2,2-Dimethyl-3,5-decadiyne and isomers		y		17
133	Dimethyl decalin and isomers		y		17
134	4-Decanone			sediment	12
135	1,4-Dioxane	-(28) c(23)			28, 23
136	2-Methyl-1-dodecanol			sediment	12
137	Dodecanone		y		17
138	1-Dotriacontanol			sediment	12
139					
140	2-Methyl-2-phenyl epoxide		y		17
141	Bromoethane	+(23)			23
142	Iodoethane	+(23)			23
143	1,2-Dichloroethane	+,c(23)	y		51, 23
144	1,1,1-Trichloroethane	c			40
145	1,1,2-Trichloroethane	c			40
146	Tetrachloroethane	+,c			40
147	1,1,2,2-Tetrachloroethane	-(28)			66
148	Hexachloroethane	-(28) c(23)	y	FA,FA	13, 28, 46, 23
149	Dimethylphenyl ethanone		y		17
150	1,2-Dichloroethylene	-(50)	y		51, 50
151	Trichloroethylene	-(50) +,c(23)	y		50, 51, 66, 23
152	1-Phenylethanone			sediment	12
153	Tetrachloroethylene	-(28)	y		51, 28
154	Bis(2-chloroethyl) ether	+			40
155	Bis(2-chloroisopropyl) ether		4(53)		77, 53
156					
157	Fatty acids		4		53
158	d-Fenchone				45
159	3-Chloro-4-(dichloromethyl)-5-hydroxy-2(5H)-furanone	s			10
160	Dihydro-5,5-dimethyl-2(3H)-furanone			sediment	12
161					
162	Diacetoneglucose		4		53

Organic Compounds in Drinking Water

	Compound	mutagenic*	XAD-2**	comments	reference
1					
2					
163	Glycidaldehyde	i	p		2
164					
165	Heptanal			Ozone	16
166	1-Ethoxy-2-heptanone			sediment	12
167	6-Methyl-2-heptanone			sediment	12
168	Methylhepten-2-one		y		17
169	Hexadecanol			sediment	12
170	4-Methylhexanal			sediment	12
171	3,3-Dimethylhexane			sediment	12
172	2-Hexanethiol			sediment	12
173	2-Ethyl-1-hexanol			sediment	12
174	1-Hexen-3-ol			sediment	12
175	4-Hydroxy-5-methyl-2-hexanone			sediment	12
176					
177	Indane		4		53
178	Indene		y		7
179	2,3-Dihydroindene		y		7
180	Alkyl-2,3-Dihydroindene		y		7
181	Methylindene		y		7
182	2,2,4-Trimethylpenta-1,3-dioldiisobutyrate			2 isomers	4
183	o-Neoisomenthol			sediment	12
184	Isooctyl alcohol			sediment	12
185	Isophorone		y		13
186					
187	Dichloromethane		y		11
188	Bromochloromethane	+(23)			23
189	Bromodichloromethane	-(50) +(23)	y	FA	13, 50, 51, 66, 76, 77, 23
190	Dibromochloromethane	+(23)	y	FA	13, 51, 66, 76, 23
191	Tetrachloromethane	c		carbon tetrchloride	40
192	bis-(2-Chloroethoxy)-methane		y		14
193	Trichloronitromethane	+			40
194	Triphenylmethane				45

Organic Compounds in Drinking Water

	Compound	mutagenic*	XAD-2**	comments	reference
1					
2					
195	alpha,alpha-Dimethyl benzenemethanol		y		17
196	Mucochloric acid	w		MX-CHCl	10
197	Nitrogen Mustard	i	p	alogen'd alkylamin	2
198					
199	Naphthalene		y	see PAHs #377	13
200	1-Chloromethylnaphthalene	i	p		2
201	Nonadecanal			sediment	12
202	1,9-Nonanediol			sediment	12
203	2-Nonenal			sediment	12
204					
205	Organo-chlorine pesticides, see separate list			see #313	41, 45
206	Organo-phosphorous pesticides, see separate list		y	see #356	41
207				sediment	12
208	13-Octadecenal			sediment	12
209	17-Octadecenal			sediment	12
210	1,2,7,8-Diepoxy Octane	w	p		2
211	3,7-Dimethyl-6-octen-1-ol			sediment	12
212	1,3,3-Trimethyloxindole		4(53)		77, 53
213					
214	6,10,14-Trimethyl-2-pentadecanone			sediment	12
215	Ethyl-2-acetyl-4-pentenoate		y		17
216	1,5-Dibromopentane	+(23)			23
217	2,2,3,4-Tetramethylpentane			sediment	12
218	2-Methyl-3-pentanol			sediment	12
219	2,2-Dichloro-3-pentanone			FA	3
220	4-Hydroxy-4-methyl-2-pentanone			sediment	12
221	2-Methyl-3-pentanone			sediment	12
222	3-Methyl-4-penten-2-one		y		17
223	Alylphenols		4		53
224	Bromodichlorophenol, acetate ester			FA	3
225	Tribromophenol, acetate ester			FA	3
226	2,4,6-Trichlorophenol	-	c(23)	HA(46)	37, 46, 23

Organic.Compounds in Drinking Water

	A	B	C	D	E
1	Compound	mutagenic*	XAD-2**	comments	reference
2					
227	Tetramethylphenol				17
228	4-Nonylphenol		y		45
229	2,6-Di-t-butyl-4-amino-methylphenol			may be bromo	4
230	Monochloro phenoxyalkanoic acid		4	MCPA (herbicide)	53
231	Dichloro phenoxyalkanoic acid		4	2,4-D (herbicide)	53
232					
233	PAHs, see separate list		y	see #377	41
234	Phosphate triesters, see separate list			see #420	41
235					
236	1-(1-cyclohexenyl)piperidine		y		17
237	Butylphenylmethyl phthalate		y		17
238	Dibutyl phthalate isomers		y		17
239	Dibutyl phthalate	+(23)	y(66)		45, 66, 23
240	Diethyl phthalate	+(23)	y(68)		45, 61, 68, 23
241	Diisobutyl phthalate				45
242	Dimethylphthalate	+			40
243	Dipropyl phthalate				45
244	Dioctyl phthalate				45
245	1,2-Butylbenzyl phthalate				45
246	Di-2-ethylhexyl phthalate	+,c (23)			45, 23
247	3-Nitrophthalic acid		y		17
248	Polychlorinated biphenyls		y	PCBs	23
249	Dichloropropanal	+			37
250	Trichloropropanal	+			37
251	1-Bromopropane	+			40
252	Bromodichloropropane				16
253	Tetramethylbenzenepropanoic acid		y		17
254	1,3-Dibromo-2-propanol		y		17
255	1-Chloropropanone	-		HA(46)	37, 46
256	1,3-Dichloropropanone	+		HA(10)	37, 46, 10
257	1,1-Dichloro-2-propanone	+		HA,FA	13, 46, 10
258	1,1,1-Trichloro-2-propanone	+		HA (same as #50)	13, 46, 10

Organic Compounds in Drinking Water

	Compound	mutagenic*	XAD-2**	comments	reference
259	1,1,3-Trichloropropanone	+		HA	46, 10
260	1,1,1,3-Tetrachloro-2-propanone	+		HA	13, 9
261	1,1,3,3-Tetrachloro-2-propanone	+		HA	13, 46, 10
262	Pentachloro-2-propanone	+	y	HA	13, 46, 10
263	2-Chloro-1-(4-ethylphenyl)-2-methyl-1-propanone				17
264	2-Chloropropenal	+(46)		HA(38,46)	37,38, 9
265	2,3-Dichloropropenal	+			37
266	3,3-Dichloropropenal	+		HA,FA	13, 37, 46, 10
267	2,3,3-Trichloropropenal	+(46,47)		HA(46,47)	37, 46, 10
268	Dichloropropene	+		FA	40
269	Pentachloropropene	+(37)		FA	13, 37
270	3-Propoxy-1-propene			sediment	12
271	3,3,3-Trichloropropene oxide	i	p		2
272	Dichloropropenenitrile			FA	13, 37
273	Trichloropropenenitrile			FA	13, 37
274	Benzo[a]pyrene-4,5-oxide	s	p		2
275					
276	Dimethylquinoline				16
277	Dihydrotrimethylquinoline				16
278	Trimethylquinoline				16
279	2,6-Di-t-butyl-1,4-benzoquinone		y		17
280					
281	Diacetone-L-sorbose		y		13
282	Styrene	+,c(23)	y	sediment(61)	61, 23
283	Styrene oxide	i	p		2
284	n-Butylbenzene sulphonamide		4		53
285	Sulphones		4		53
286	molecular Sulphur		y		17
287					
288	Terpenoids		4	various molec. wts	53
289	Polychlorinated terphenyls	c			40
290	Tetradecanal			sediment	12

Organic Compounds in Drinking Water

	A Compound	B mutagenic*	C XAD-2**	D comments	E reference
1	Compound	mutagenic*	XAD-2**	comments	reference
2					
291	5-Methyltetralin		y		17
292	Dimethyltetralin		y		17
293	Alkyl benzothiophenes		y		7
294	2,2-Benzothiophene		y		7
295	Bromotrichlorothiophene			FA	3
296	Tetrabromothiophene			FA	3
297	Trichlorothiophene				37
298	Tetrachlorothiophene			FA	3
299	Toluene		y		51, 66, 76
300	2-Ethyltoluene				45
301	3-Ethyltoluene				45
302	4-Ethyltoluene				45
303	m/p-tolunitrile		y		13
304	2-Nitrotoluene	-(28,70)			28, 45, 70
305	2,4-Dinitrotoluene-		y(68)		45, 68
306	1,12-Tridecadiene			sediment	12
307					
308	Xylene		y	all three isomers	45, 51, 76(o+m)
309	Diacetone-D-xylose		y		13
310					
311					
312					
313	Organo-chlorine pesticides				
314	Aldrin		y		41
315	alpha-BHC		y		41, 45, 76
316	beta-BHC		y		41, 45, 76
317	gamma-BHC	-(28)	y	lindane	41, 45, 28
318	1,2-Dichlorobenzene	-(28)	y		41, 28
319	1,4-Dichlorobenzene	-(28)	y		41, 28
320	1,2,3-Trichlorobenzene	-(28)	y		41, 28
321	1,3,5-Trichlorobenzene	-(28)	y		41, 28
322	2,4,5-Trichlorotoluene		y		41

Organic Compounds in Drinking Water

	A	B	C	D	E
1	Compound	mutagenic*	XAD-2**	comments	reference
2					
323	1,2,3,4-Tetrachlorobenzene	-(28)	y		41, 28
324	1,2,3,5-Tetrachlorobenzene	-(28)	y		41, 28
325	Hexachlorobenzene	-(28)	y(68)		45, 68, 28
326	Pentachloronitrobenzene	-(28)			45, 28
327	Hexabromobiphenyl		y		41
328	alpha-Chlordane	(50 isomer?			41, 45, 20
329	gamma-Chlordane		y		41, 45
330	Oxychlordane		y		41, 45
331	alpha-Chlordene		y		45
332	beta-Chlordene				45
333	gamma-Chlordene				45
334	Dimethyl-2,3,5,6-tetrachloroterephthalate			DCPA	45
335	o,p'-DDD	-(50)			45
336	m,p'-DDD				45, 20
337	p,p'-DDD				45
338	o,p'-DDE	-(50)			45, 20
339	p,p'-DDE				41, 45
340	o,p'-DDT				45
341	p,p'-DDT				41, 45
342	Dieldrin	-(28)	y		41, 45, 28
343	alpha-Endosulfan		y		41
344	beta-Endosulfan		y		41
345	Endosulfan-2				45
346	Endrin				45
347	Heptachlor		y		45
348	Heptachlor epoxide		y		41, 45
349	Mirex	-(50)	y		41, 20
350	Photomirex		y		41
351	Perthane				45
352	Octachlorostyrene		y		41
353					
354					

Organic Compounds in Drinking Water

	A	B	C	D	E
1	Compound	mutagenic*	XAD-2**	comments	reference
2					
355					
356	Organo-phosphorous pesticides				
357	Azinphos-methyl				41
358	Diazinon				41
359	Dimethoate				41
360	Dursban	+(28)			41, 28
361	EPN				41
362	Ethion				41
363	Fenitrothion				41
364	Imidan				41
365	Malathion	-(28)			41, 28
366	Methylparathion	+(28)			41, 28
367	Parathion	+(28)			41, 28
368	Phosalone				41
369	Phosphamidon				41
370	Ronnel				41
371	Ruelene				41
372	Supracide				41
373	Trithion				41
374					
375					
376					
377	Polynuclear aromatic hydrocarbons			PAHs	
378	Acenaphthalene	+		acenaphthylene ?	40
379	Acenaphthylene		y		7
380	Anthracene	+(50)	y(68)		41, 68, 76, 50
381	Benzo[a]anthracene		y		14
382	Dibenzo[a,h]anthracene		y		14
383	2-Methylanthracene				41, 76
384	9-Methylanthracene				41
385	9,10-Di(chloromethyl)anthracene	s	p		2
386	Anthraquinone				41, 76

Organic Compounds in Drinking Water

	A	B	C	D	E
1	Compound	mutagenic*	XAD-2**	comments	reference
2					
387	Bibenzyl				
388	Biphenyl	-(28)			41, 76
389	3,3'-Dimethylbiphenyl				41, 76, 28
390	4,4'-Dimethylbiphenyl				41, 76
391	(Diethyl or methyl)biphenyl		y		41
392	Fluoranthene	+(23)			17
393	Fluorene		y(68)		41, 76, 23
394	9H-fluorene		y		41, 68, 76
395	9-Methylfluorene	+(23)			17
396	9-Fluorenone				23
397	Naphthalenene	-(50)	y(7,68)		41, 76
398	Alkyl naphthalenes				41, 50, 68, 76, 7
399	1-Ethylnaphthalene				7
400	2-Ethylnaphthalene				41
401	1-Methylnaphthalene	+(23)	y(7)		41
402	2-Methylnaphthalene				41, 76, 7, 23
403	1,2-Dimethylnaphthalene				41
404	1,3-Dimethylnaphthalene				41
405	1,4-Dimethylnaphthalene				41
406	1,5-Dimethylnaphthalene				41
407	2,3-Dimethylnaphthalene				41
408	2,3,5-Trimethylnaphthalene				41
409	2,3,6-Trimethylnaphthalene				41, 76
410	Phenanthrene				41
411	1-Methylphenanthrene	+(23)			41, 76, 17
412	2-Methylphenanthrene	+(23)			23
413	9-Methylphenanthrene	+(23)			23
414	Pyrene		y(68)		41, 68, 76
415	cis-Stilbene	-(28)			41, 76, 28
416	trans-Stilbene	-(28)			41, 28
417					
418					

Organic Compounds in Drinking Water

	A	B	C	D	E
1	Compound	mutagenic*	XAD-2**	comments	reference
2					
419					
420	Phosphate esters			TAAPs	
421	Trialkyl phosphates		4		53
422	Tributyl phosphate		y(66)		41, 45, 66, 76
423	Tributoxyethyl phosphate				41, 76
424	p-tert-Butylphenyldiphenyl phosphate				41
425	Tris(2-chloroethyl) phosphate	-(28)			41, 76, 28,
426	Tris(1,3-dichloropropyl) phosphate	+(50)			41, 76, 77, 50,
427	Tricresyl phosphate	-(28)		cresyl=tolyl	76, 28,
428	Triethyl phosphate				41, 76
429	2-Ethylhexyldiphenyl phosphate				41
430	o-Isopropylphenyldiphenyl phosphate				41
431	Triphenyl phosphate				41, 76
432	Propyl phosphate				76
433	Tri-o-tolyl phosphate	-(28)		tolyl=cresyl	41, 28,
434	Tri-m-tolyl phosphate				41
435	Tri-2,4-xylyl phosphate				41

	A	B	C	D	E
1	Compound	Recovery (%)*	Concentration (ppm)	Comments**	Reference
2					
3	* sorbed, desorbed or total (total if not specified)				
4	** Single Solute, Multi-Solute, elution solvent, etc.				
5					
6	Benzyl acetate	100	0.01-0.1	ave. SS, MS, pure & tap w., ether	34
7	Chloroacetic acid	4 s	8	urine, SS	20
8	Acetophenone	92	0.01-0.1	ave. SS, MS, pure & tap w., ether	34
9	Hexadecylamine	94	0.01-0.1	ave. SS, MS, pure & tap w., ether	34
10	Didecylmethylammonium bromide	85 s	20	urine, SS	20
11	N-Methylaniline	84	0.01-0.1	ave. SS, MS, pure & tap w., ether	34
12	3,4-Dichloroaniline	74 s	20	urine, SS	20
13	Atrizine	83	0.01-0.1	ave. SS, MS, pure & tap w., ether	34
14					
15	Benzaldehyde	101	0.01-0.1	ave. SS, MS, pure & tap w., ether	34
16	Benzene	100	100	SS, ether or methanol	7
17		95 s	0.6	urine, SS	20
18		99 s	60	pure w., SS	20
19		95 s 87d 83t	60	urine, pH 2, SS, acetone	20
20	Chlorobenzene	95	0.01-0.1	ave. SS, MS, pure & tap w., ether	34
21	o-Dichlorobenzene	88	0.01-0.1	ave. SS, MS, pure & tap w., ether	34
22	m-Dichlorobenzene	93	0.01-0.1	ave. SS, MS, pure & tap w., ether	34
23	1,2,4,5-Tetrachlorobenzene	74	0.01-0.1	ave. SS, MS, pure & tap w., ether	34
24	Ethylbenzene	81	0.01-0.1	ave. SS, MS, pure & tap w., ether	34
25	Iodobenzene	81	0.01-0.1	ave. SS, MS, pure & tap w., ether	34
26	Nitrobenzene	91	0.01-0.1	ave. SS, MS, pure & tap w., ether	34
27	Benzene sufonic acid	31	3	SS, ether or methanol	7
28	Methyl benzoate	101	0.01-0.1	ave. SS, MS, pure & tap w., ether	34
29	Benzoic acid	23	1	SS, ether or methanol	7
30		100	1	pH 3.2, SS, ether or methanol	7
31	Benzonitrile	88	0.01-0.1	ave. SS, MS, pure & tap w., ether	34
32	Benzophenone	93	0.01-0.1	ave. SS, MS, pure & tap w., ether	34
33	Benzothiazole	100	0.01-0.1	ave. SS, MS, pure & tap w., ether	34
34	Benzil (ketone?)	97	0.01-0.1	ave. SS, MS, pure & tap w., ether	34
35	Benzyl alcohol*	91	0.01-0.1	ave. SS, MS, pure & tap w., ether	34
36					
37	Hexabromobiphenyl	74.0 - 61.9	10 ng/L	(low - high vol.), MS, tap w.,15% acetone/hexane	41
38	Polychlorinated biphenyls	91 (ave)	0.125-2.0	river w., MS, ether	12

Compounds Studied on XAD-2 Resin

	A Compound	B Recovery (%)*	C Concentration (ppm)	D Comments**	E Reference
1	Compound	Recovery (%)*	Concentration (ppm)	Comments**	Reference
2					
39	Arochlor 1245	56 s	2	urine, pH 2, SS	20
40		76 s	50	pure w., pH 2, SS	20
41	Hexachlorobutadiene	66		MS, pure w., 15% acetone/hexane	68
42	Ethylbutyrate	100	100	SS, ether or methanol	7
43					
44	o-Cresol	100	0.3	SS, ether or methanol	7
45	Cinnamyl alcohol	85	0.01-0.1	ave. SS, MS, pure & tap w., ether	34
46	Benzyl chloride	88	0.01-0.1	ave. SS, MS, pure & tap w., ether	34
47	Cumene	93	0.01-0.1	ave. SS, MS, pure & tap w., ether	34
48	p-Cymene	92	0.01-0.1	ave. SS, MS, pure & tap w., ether	34
49					
50	Methyl decanoate	95	0.01-0.1	ave. SS, MS, pure & tap w., ether	34
51	Decanol	91	0.01-0.1	ave. SS, MS, pure & tap w., ether	34
52	Dodecanol	93	0.01-0.1	ave. SS, MS, pure & tap w., ether	34
53					
54	Ethylene diamine	18 s	18	urine, SS	20
55	2-Phenoxyethanol	102	0.01-0.1	ave. SS, MS, pure & tap w., ether	34
56	Anisole ether	87	0.01-0.1	ave. SS, MS, pure & tap w., ether	34
57	Benzyl ether	99	0.01-0.1	ave. SS, MS, pure & tap w., ether	34
58	Hexyl ether	75	0.01-0.1	ave. SS, MS, pure & tap w., ether	34
59	2-Methoxynaphthalene ether	97	0.01-0.1	ave. SS, MS, pure & tap w., ether	34
60	Phenyl ether	91	0.01-0.1	ave. SS, MS, pure & tap w., ether	34
61					
62	Dibutyl fumarate	92	0.01-0.1	ave. SS, MS, pure & tap w., ether	34
63	Diethyl fumarate	86	0.01-0.1	ave. SS, MS, pure & tap w., ether	34
64	Di-2-ethylhexyl fumarate	84	0.01-0.1	ave. SS, MS, pure & tap w., ether	34
65					
66	2,6-Dimethyl-4-heptanone	93	0.01-0.1	ave. SS, MS, pure & tap w., ether	34
67	n-Hexanol	85	200	SS, ether or methanol	7
68		93	0.01-0.1	ave. SS, MS, pure & tap w., ether	34
69	2-Ethylhexanol	99	0.01-0.1	ave. SS, MS, pure & tap w., ether	34
70					
71	Indole	89	0.01-0.1	ave. SS, MS, pure & tap w., ether	34
72					
73	Methylisobutyl ketone	100	100	SS, ether or methanol	7
74					

Compounds Studied on XAD-2 Resin

	A	B	C	D	E
1	Compound	Recovery (%)	Concentration (ppm)	Comments	Reference
2					
75	Diethyl malonate	103	0.01-0.1	ave. SS, MS, pure & tap w., ether	34
76	Methyl methacrylate	35	0.01-0.1	ave. SS, MS, pure & tap w., ether	34
77	Bis-(2-chloroethoxy)methane	2		MS, pure w., 15% acetone/hexane	68
78					
79	Naphthalene	100	0.05	SS, ether or methanol	7
80	2-Hydroxy-3-naphthoic acid	39	0.6	SS, ether or methanol	7
81					
82	Methyl octanoate	98	0.01-0.1	ave. SS, MS, pure & tap w., ether	34
83	Benzoxazole	92	0.01-0.1	ave. SS, MS, pure & tap w., ether	34
84					
85	Methyl palmitate	70	0.01-0.1	ave. SS, MS, pure & tap w., ether	34
86	Phenol	45	0.4	SS, ether or methanol	7
87		69 s	2	urine, SS	20
88		81 s	200	pure w., SS	20
89	p-Chlorophenol	85 s	39	urine, SS	20
90	2,4-Dimethylphenol	100	0.4	SS, ether or methanol	7
91	2-Methylphenol	100	0.3	SS, ether or methanol	7
92	p-Nitrophenol	100	0.2	SS, ether or methanol	7
93		89 s	12	urine, SS	20
94	2,4-Dinitro-2-aminophenol	43	0.4	SS, ether or methanol	7
95					
96	Phenylenediamine	98	0.9	SS, ether or methanol	7
97	Dibutyl phthalate	99	0.01-0.1	ave. SS, MS, pure & tap w., ether	34
98	Diethyl phthalate	92	0.01-0.1	ave. SS, MS, pure & tap w., ether	34
99		47		MS, pure w., 15% acetone/hexane	68
100	Dimethyl phthalate	91	0.01-0.1	ave. SS, MS, pure & tap w., ether	34
101	Dioctyl phthalate	11 s	250	urine, SS	20
102	Dimethoxyethyl phthalate	94	0.01-0.1	ave. SS, MS, pure & tap w., ether	34
103	Di-2-ethylhexyl phthalate	88	0.01-0.1	ave. SS, MS, pure & tap w., ether	34
104					
105	Benzo-a-pyrene	61 s	9	urine, pH 2, SS	20
106					
107	Quinoline	84	0.01-0.1	ave. SS, MS, pure & tap w., ether	34
108	Isoquinoline	83	0.01-0.1	ave. SS, MS, pure & tap w., ether	34
109					
110	Salicaldehyde	100	0.01-0.1	ave. SS, MS, pure & tap w., ether	34

Compounds Studied on XAD-2 Resin

	A	B	C	D	E
1	Compound	Recovery (%)	Concentration (ppm)	Comments	Reference
2					
111	Methyl salicylate	96	0.01-0.1	ave. SS, MS, pure & tap w., ether	34
112	p-Toluene sulfonic acid	23	9	SS, ether or methanol	7
113					
114	m-Chlorotoluene	80	0.01-0.1	ave. SS, MS, pure & tap w., ether	34
115	alpha, o-Dichlorotoluene	96	0.01-0.1	ave. SS, MS, pure & tap w., ether	34
116	2,4-Dichlorotoluene	71	0.01-0.1	ave. SS, MS, pure & tap w., ether	34
117		109		MS, pure w., 15% acetone/hexane	68
118	1,2,4-Trichlorotoluene	99	0.01-0.1	ave. SS, MS, pure & tap w., ether	34
119	o-Nitrotoluene	80	0.01-0.1	ave. SS, MS, pure & tap w., ether	34
120					
121	2-Undecanone	88	0.01-0.1	ave. SS, MS, pure w., ether	34
122					
123					
124					
125	Organochlorine pesticides and compounds				
126					
127	Aldrin	94	0.01	pure w., MS, ether	12
128		75	0.016	river w., MS, ether	12
129		47	0.01-0.1	ave. SS, MS, pure & tap w., ether	34
130	1,2-Dichlorbenzene	80.7 - 68.3	10 ng/L	(low - high vol.), MS, tap w.,15% acetone/hexane	41
131		28		MS, pure w., 15% acetone/hexane	68
132	1,3-Dichlorbenzene	28		MS, pure w., 15% acetone/hexane	68
133	1,4-Dichlorbenzene	70.0 - 67.0	10 ng/L	(low - high vol.), MS, tap w.,15% acetone/hexane	41
134	1,2,3-Trichlorbenzene	86.0 - 79.7	10 ng/L	(low - high vol.), MS, tap w.,15% acetone/hexane	41
135	1,3,5-Trichlorbenzene	70.0 - 69.6	10 ng/L	(low - high vol.), MS, tap w.,15% acetone/hexane	41
136	1,2,3,4-Tetrachlorbenzene	86.9 - 88.7	10 ng/L	(low - high vol.), MS, tap w.,15% acetone/hexane	41
137	1,2,3,5-Tetrachlorbenzene	87.5 - 103.3	10 ng/L	(low - high vol.), MS, tap w.,15% acetone/hexane	41
138	Pentachlorbenzene	76.7 - 90.8	10 ng/L	(low - high vol.), MS, tap w.,15% acetone/hexane	41
139	Hexachlorbenzene	76.0 - 89.7	10 ng/L	(low - high vol.), MS, tap w.,15% acetone/hexane	41
140		90		MS, pure w., 15% acetone/hexane	68
141	cis-Chlordane	92	0.04	pure w., MS, ether	12
142		73	0.022	river w., MS, ether	12
143	trans-Chlordane	89	0.04	pure w., MS, ether	12
144		79	0.024	river w., MS, ether	12
145	DDE	81	0.01-0.1	ave. SS, MS, pure & tap w., ether	34
146	p,p' DDT	103	0.04	pure w., MS, ether	12

Compounds Studied on XAD-2 Resin

	A	B	C	D	E
1	Compound	Recovery (%)*	Concentration (ppm)	Comments**	Reference
2					
147		95	0.041	river w., MS, ether	12
148	DDT	96	0.01-0.1	ave. SS, MS, pure & tap w., ether	34
149	Dieldrin	96	0.01	pure w., MS, ether	12
150		76	0.025	river w., MS, ether	12
151	Endrin	96	0.1	pure w., MS, ether	12
152		80	0.03	river w., MS, ether	12
153	Heptachlor	95	0.01	pure w., MS, ether	12
154		78	0.009	river w., MS, ether	12
155	Lindane	93	0.01	pure w., MS, ether	12
156		100	0.008	river w., MS, ether	12
157		95	0.01-0.1	ave. SS, MS, pure & tap w., ether	34
158	Methoxychlor	108	0.1	pure w., MS, ether	12
159		105	0.095	river w., MS, ether	12
160	Mirex	97	0.03	pure w., MS, ether	12
161		52	0.023	river w., MS, ether	12
162	Photomirex	72.0 - 68.4	10 ng/L	(low - high vol.), MS, tap w.,15% acetone/hexane	41
163	Octachlorostyrene	79.3 - 79.8	10 ng/L	(low - high vol.), MS, tap w.,15% acetone/hexane	41
164		74.7 - 89.0	10 ng/L	(low - high vol.), MS, tap w.,15% acetone/hexane	41
165	2,4,5-Trichlorotoluene	81.3 - 79.4	10 ng/L	(low - high vol.), MS, tap w.,15% acetone/hexane	41
166					
167					
168					
169	Organophosphorous compounds				
170					
171	Aminocarb and derivatives				
172	4-Dimethylamino-3-methylphenol carbama	93	0.01	pH 7, pure w., ethyl acetate	44
173	4-Dimethylamino-3-methylphenol	61	0.04	pH 7, pure w., ethyl acetate	44
174	4-(N-Methyl-N-formylamino)-3-	42	200	pH 7, pure w., ethyl acetate	44
175	methylphenol methylcarbamate				
176	4-(Formylamino)-3-methylphenol	11	5	pH 7, pure w., ethyl acetate	44
177	methylcarbamate				
178	4-Dimethylamino-3-methylphenol carbama	6	0.002	pH 7, pure w., ethyl acetate	44
179	4-(Formylamino)-3-methylphenol	98	0.2	pH 7, pure w., ethyl acetate	44
180					
181	Atrizine	83	0.01-0.1	ave. SS, MS, pure & tap w., ether	34
182	Chlorpyrifos	92	100 ng/L	MS on column. 15% acetone/hexane	Bel et al. 19

Compounds Studied on XAD-2 Resin

158

	Compound	Recovery (%)*	Concentration (ppm)*	Comments**	Reference
1					
2					
183		86	10 ng/L	MS on column. 15% acetone/hexane	Bel et al. 19
184	Diazinon	99	100 ng/L	MS on column. 15% acetone/hexane	Bel et al. 19
185		103	10 ng/L	MS on column. 15% acetone/hexane	Bel et al. 19
186	Diazinon-oxon	92	100 ng/L	MS on column. 15% acetone/hexane	Bel et al. 19
187		99	10 ng/L	MS on column. 15% acetone/hexane	Bel et al. 19
188	Dimethoate	34	100 ng/L	MS on column. 15% acetone/hexane	Bel et al. 19
189		34	10 ng/L	MS on column. 15% acetone/hexane	Bel et al. 19
190	EPN	93	100 ng/L	MS on column. 15% acetone/hexane	Bel et al. 19
191		92	10 ng/L	MS on column. 15% acetone/hexane	Bel et al. 19
192	Ethion	102	100 ng/L	MS on column. 15% acetone/hexane	Bel et al. 19
193		94	10 ng/L	MS on column. 15% acetone/hexane	Bel et al. 19
194	Fenitrothion	104	100 ng/L	MS on column. 15% acetone/hexane	Bel et al. 19
195		96	10 ng/L	MS on column. 15% acetone/hexane	Bel et al. 19
196	Malathion	96	100 ng/L	MS on column. 15% acetone/hexane	Bel et al. 19
197		103	10 ng/L	MS on column. 15% acetone/hexane	Bel et al. 19
198	Methadathion	92	100 ng/L	MS on column. 15% acetone/hexane	Bel et al. 19
199		100	10 ng/L	MS on column. 15% acetone/hexane	Bel et al. 19
200	Ethyl parathion	95	100 ng/L	MS on column. 15% acetone/hexane	Bel et al. 19
201		102	10 ng/L	MS on column. 15% acetone/hexane	Bel et al. 19
202	Methyl parathion	93	100 ng/L	MS on column. 15% acetone/hexane	Bel et al. 19
203		97	10 ng/L	MS on column. 15% acetone/hexane	Bel et al. 19
204	Phosalone	100	100 ng/L	MS on column. 15% acetone/hexane	Bel et al. 19
205		97	10 ng/L	MS on column. 15% acetone/hexane	Bel et al. 19
206	Phosmet	92	100 ng/L	MS on column. 15% acetone/hexane	Bel et al. 19
207		101	10 ng/L	MS on column. 15% acetone/hexane	Bel et al. 19
208	beta-Phosphamidon	39	100 ng/L	MS on column. 15% acetone/hexane	Bel et al. 19
209		39	10 ng/L	MS on column. 15% acetone/hexane	Bel et al. 19
210	Ronnel	92	100 ng/L	MS on column. 15% acetone/hexane	Bel et al. 19
211		96	10 ng/L	MS on column. 15% acetone/hexane	Bel et al. 19
212	Ruelene	95	100 ng/L	MS on column. 15% acetone/hexane	Bel et al. 19
213					
214					
215					
216	Polynuclear aromatic hydrocarbons				
217					
218	Acenaphthene	92	0.01-0.1	ave. SS, MS, pure & tap w., ether	34

Compounds Studied on XAD-2 Resin

159

	A	B	C	D	E
1	Compound	Recovery (%)*	Concentration (ppm)*	Comments**	Reference
2					
219		77		MS, pure w., 15% acetone/hexane	68
220	Anthracene	83	0.01-0.1	ave. SS, MS, pure & tap w., ether	34
221		98		MS, pure w., 15% acetone/hexane	68
222	Benzo[a]anthracene	65		MS, pure w., 15% acetone/hexane	68
223	Dibenzo[a,h]anthracene	65		MS, pure w., 15% acetone/hexane	68
224	Biphenyl	101	0.01-0.1	ave. SS, MS, pure & tap w., ether	34
225	Chrysene	113		MS, pure w., 15% acetone/hexane	68
226	Fluorene	84	0.01-0.1	ave. SS, MS, pure & tap w., ether	34
227		112		MS, pure w., 15% acetone/hexane	68
228	Naphthalene	98	0.01-0.1	ave. SS, MS, pure & tap w., ether	34
229		100		MS, pure w., 15% acetone/hexane	68
230	1-Methylnaphthalene	87	0.01-0.1	ave. SS, MS, pure & tap w., ether	34
231	2-Methylnaphthalene	95	0.01-0.1	ave. SS, MS, pure & tap w., ether	34
232	Tetrahydronaphthalene	62	0.01-0.1	ave. SS, MS, pure & tap w., ether	34
233					
234					
235					
236	Polychlorinated dibenzo-p-dioxins (PCDD)				
237	and Polychlorinated dibenzofurans (PCDF)				
238					
239	1368-TCDD	34.2, 51.1	1 pg/L	MS, tap w., 15% acetone/hexane	43
240		25.8, 67.3	10 pg/L	MS, tap w., 15% acetone/hexane	43
241		28.2, 64.1	25 pg/L	MS, tap w., 15% acetone/hexane	43
242	2378-TCDF	88.3, 97.2	1 pg/L	MS, tap w., 15% acetone/hexane	43
243		89.5, 91.7	10 pg/L	MS, tap w., 15% acetone/hexane	43
244		101.0, 105.1	25 pg/L	MS, tap w., 15% acetone/hexane	43
245	2378-TCDD	73.2, 77.4	1 pg/L	MS, tap w., 15% acetone/hexane	43
246		67.3, 95.9	10 pg/L	MS, tap w., 15% acetone/hexane	43
247		105.7, 116.4	25 pg/L	MS, tap w., 15% acetone/hexane	43
248	12478-PnCDF	87.2, 91.1	1 pg/L	MS, tap w., 15% acetone/hexane	43
249		70.8, 82.4	10 pg/L	MS, tap w., 15% acetone/hexane	43
250		85.6, 100.3	25 pg/L	MS, tap w., 15% acetone/hexane	43
251	12347-PnCDD	106.3, 128.6	1 pg/L	MS, tap w., 15% acetone/hexane	43
252		76.9, 85.1	10 pg/L	MS, tap w., 15% acetone/hexane	43
253		103.9, 128.3	25 pg/L	MS, tap w., 15% acetone/hexane	43
254	123678-HxCDF	82.5, 89.0	1 pg/L	MS, tap w., 15% acetone/hexane	43

Compounds Studied on XAD-2 Resin

	A	B	C	D	E
1	Compound	Recovery (%)*	Concentration (ppm)	Comments**	Reference
2					
255		69.4, 78.7	10 pg/L	MS, tap w., 15% acetone/hexane	43
256		99.2, 101.4	25 pg/L	MS, tap w., 15% acetone/hexane	43
257	123678-HxCDD	86.7, 95.6	1 pg/L	MS, tap w., 15% acetone/hexane	43
258		72.6, 95.7	10 pg/L	MS, tap w., 15% acetone/hexane	43
259		110.9, 113.2	25 pg/L	MS, tap w., 15% acetone/hexane	43
260	123789-HxCDD	68.3, 69.5	1 pg/L	MS, tap w., 15% acetone/hexane	43
261		56.1, 74.0	10 pg/L	MS, tap w., 15% acetone/hexane	43
262		84.8, 94.4	25 pg/L	MS, tap w., 15% acetone/hexane	43
263	1234678-HpCDF	73.3, 91.6	1 pg/L	MS, tap w., 15% acetone/hexane	43
264		68.4, 77.0	10 pg/L	MS, tap w., 15% acetone/hexane	43
265		90.9, 95.6	25 pg/L	MS, tap w., 15% acetone/hexane	43
266	1234678-HpCDD	71.5, 75.0	1 pg/L	MS, tap w., 15% acetone/hexane	43
267		59.4, 83.7	10 pg/L	MS, tap w., 15% acetone/hexane	43
268		94.2, 110.5	25 pg/L	MS, tap w., 15% acetone/hexane	43
269	OCDF	46.7, 50.8	1 pg/L	MS, tap w., 15% acetone/hexane	43
270		42.2, 70.5	10 pg/L	MS, tap w., 15% acetone/hexane	43
271		77.6, 91.9	25 pg/L	MS, tap w., 15% acetone/hexane	43
272	OCDD	33.1, 35.9	1 pg/L	MS, tap w., 15% acetone/hexane	43
273		17.9, 44.5	10 pg/L	MS, tap w., 15% acetone/hexane	43
274		54.2, 64.0	25 pg/L	MS, tap w., 15% acetone/hexane	43
275					
276					
277					
278	Alkyl phosphates				
279					
280	Tributyl phosphate	112.9	10 ng/L	MS, tap w., 15% acetone/hexane	41
81	Tris(2-chloroethyl) phosphate	81.8	10 ng/L	MS, tap w., 15% acetone/hexane	41
282	Tris(1,3-dichloropropyl) phosphate	96.8	10 ng/L	MS, tap w., 15% acetone/hexane	41
283	Triphenyl phosphate	97.8	10 ng/L	MS, tap w., 15% acetone/hexane	41
284	Tributoxyethyl phosphate	101.6	10 ng/L	MS, tap w., 15% acetone/hexane	41
285	2-Ethylhexyldiphenyl phosphate	95.5	10 ng/L	MS, tap w., 15% acetone/hexane	41
286	o-Isopropylphenyldiphenyl phosphate	97.0	10 ng/L	MS, tap w., 15% acetone/hexane	41
287	Tri-o-tolyl phosphate	94.6	10 ng/L	MS, tap w., 15% acetone/hexane	41
288	Tri-m-tolyl phosphate	92.2	10 ng/L	MS, tap w., 15% acetone/hexane	41
289	p-tert-Butylphenyldiphenyl phosphate	95.9	10 ng/L	MS, tap w., 15% acetone/hexane	41
290	Tri-2,4-xylyl phosphate	90.7	10 ng/L	MS, tap w., 15% acetone/hexane	41

Compounds Studied on XAD-2 Resin

Appendix 2   Detailed Experimental Isotherm Information

Isotherm 1

Date run:	Sept. 17 - Sept. 24, 1987
Equilibration Time:	7 days
Compound:	Lindane
Resin:	Fresh beads
Initial Spiking:	1.5 mL of 500 mg/L into 15L = 50 µg/L
	overnight stir
Water Preparation:	System 1
Analysis: Liquid:	100, 50, 50 mL DCM
Solid:	5 mL 15 %,acetone/hexane + 5 mL hexane

Isotherm 2

Date run:	Nov. 24 - Dec. 2, 1987
Equilibration Time:	8 days
Compound:	Lindane
Resin:	Fresh beads
Initial Spiking:	2 mL of 500 mg/L into 10 L = 100 µg/L
	2 hour stir
Water Preparation:	System 1, then boiled the water
Analysis: Liquid:	100, 50, 30 mL DCM
Solid:	15 % acetone/hexane, stirred resin while eluting

Isotherm 3 (Preliminary Isotherm)

Date run:	Nov. 26 - Dec. 3, 1987
Equilibration Time:	7 days
Compound:	Triallate
Resin:	Fresh beads
Initial Spiking:	1.2 mL of 520 mg/L into 6 L = 104 µg/L
	overnight stir
Water Preparation:	System 1
Analysis: Liquid:	100, 50, 30 mL DCM
Solid:	15 % acetone/hexane, stirred resin while eluting,
	acetone rinse following elution

Isotherm 4 (Preliminary Isotherm)

Date run:	Dec. 1 - Dec. 9, 1987
Equilibration Time:	8 days
Compound:	TCEP
Resin:	Fresh beads
Initial Spiking:	50 µL of 500 mg/L into each 500 mL bottle
Water Preparation:	System 1
Analysis: Liquid:	100, 50, 30 mL DCM
Solid:	20 mL 15 % actone/hexane

Isotherm 5

Date run:	Dec. 10 - Dec. 17, 1987
Equilibration Time:	7 days
Compound:	Triallate
Resin:	Fresh beads
Initial Spiking:	1 mL of 1000 mg/L into 10 L = 100 µg/L
	overnight stir
Water Preparation:	System 1, boiled under vacuum @ room temperature
Analysis: Liquid:	100, 50, 30 mL DCM
Solid:	modified (acetone first, then hexane)

Isotherm 6

Date run:	Jan. 12 - Jan. 19, 1988
Equilibration Time:	7 days
Compound:	Lindane
Resin:	Fresh, crushed (100-200 mesh)
Initial Spiking:	2 mL of 500 mg/L inot 10 L = 100 µg/L
	overnight stir
Water Preparation:	System 1
Analysis: Liquid:	100, 50, 30 mL DCM
Solid:	modified, in glass fritted column

Isotherm 7

Date run:	Feb. 2 - Feb. 9, 1988
Equilibration Time:	7 days
Compound:	Triallate
Resin:	Fresh beads (vacuum suctioned to remove gas bubbles)
Initial Spiking:	5 mL (blown down to ~ 1) of 1000 mg/L into 10 L
	= 500 µg/L, 2 hour stir
Water Preparation:	System 1, through XAD-2 resin column
Analysis: Liquid:	3 x 100 mL DCM + 20 mL rinse
Solid:	modified, in glass fritted column

Isotherm 8

Date run:	Feb. 20 - Feb. 29, 1988
Equilibration Time:	9 days
Compound:	Lindane
Resin:	Fresh, crushed (100-200 mesh)
Initial Spiking:	10 mL (blown down to ~ 1.5) of 500 mg/L into 10 L =
	500 µg/L, overnight stir
Water Preparation:	System 1, through XAD-2 resin column
Analysis: Liquid:	100, 75, 50, 50, 50 mL DCM
Solid:	modified, in glass fritted column

Isotherm 9 (Preliminary Isotherm)

Date run:	March 8 - March 15, 1988
Equilibration Time:	7 days
Compound:	Lindane
Resin:	Preloaded beads
Initial Spiking:	0.35 mL of 10 mg/mL into 7 L = 500 µg/L
	overnight stir
Water Preparation:	System 2, through XAD-2 resin column
Analysis: Liquid:	100, 75, 50, 50 mL DCM + 100 mL hexane
Solid:	modified, in glass fritted column

Isotherm 10

Date run:	March 8 - March 15, 1988
Equilibration Time:	7 days
Compound:	Lindane & Triallate
Resin:	Fresh beads
Initial Spiking:	0.55 mL of 10 mg/mL Lindane into 11 L = 500 µg/L
	0.55 mL of 10.47 mg/mL Triallate into 11 L = 523 µg/L
	overnight stir
Water Preparation:	System 2, through XAD-2 resin column
Analysis: Liquid:	100, 75, 50, 50 mL DCM + 100 mL hexane
Solid:	modified, in glass fritted column

Isotherm 11

Date run:	March 8 - March 22, 1988
Equilibration Time:	14 days
Compound:	Lindane & Triallate
Resin:	Fresh beads
Initial Spiking:	0.55 mL of 10 mg/mL Lindane into 11 L = 500 µg/L
	0.55 mL of 10.47 mg/mL Triallate into 11 L = 523 µg/L
	overnight stir
Water Preparation:	System 2, through XAD-2 resin column
Analysis: Liquid:	100, 75, 50, 50 mL DCM + 100 mL hexane
Solid:	modified, in glass fritted column

Isotherm 12

Date run:	March 30 - April 16, 1988
Equilibration Time:	17 days
Compound:	Lindane
Resin:	Fresh beads
Initial Spiking:	750 µL of 10 mg/mL into 15 L = 500 µg/L
	overnight stir
Water Preparation:	System 2, through XAD-2 resin column
Analysis: Liquid:	100, 75, 50 mL DCM + 100 mL hexane
Solid:	modified, in glass fritted column

Isotherm 13

Date run: March 30 - April 16, 1988

Equilibration Time: 17 days

Compound: Lindane

Resin: Preloaded beads

Initial Spiking: 750 µL of 10 mg/mL into 15 L = 500 µg/L

                                   overnight stir

Water Preparation: System 2, through XAD-2 resin column

Analysis: Liquid: 100, 75, 50 mL DCM + 100 mL hexane

                  Solid: modified, in glass fritted column

Isotherm 14

Date run: March 30 - April 16, 1988

Equilibration Time: 17 days

Compound: Triallate

Resin: Fresh beads

Initial Spiking: 500 µL of 10.47 mg/mL into 10 L = 523 µg/L

                                   overnight stir

Water Preparation: System 2, through XAD-2 resin column

Analysis: Liquid: 100, 75, 50 mL DCM + 100 mL hexane

                  Solid: modified, in glass fritted column

Isotherm 15

Date run:	April 5 - April 21, 1988
Equilibration Time:	16 days
Compound:	Lindane & Triallate
Resin:	Fresh beads
Initial Spiking:	100 μL of 10 mg/mL Lindane into 10 L = 100 μg/L
	500 μL of 10.47 mg/mL Triallate into 10 L = 523 μg/L
	overnight stir
Water Preparation:	System 2, through XAD-2 resin column
Analysis: Liquid:	100, 75, 50 mL DCM + 100 mL hexane
Solid:	modified, in glass fritted column

Isotherm 16

Date run:	April 5 - April 21, 1988
Equilibration Time:	16 days
Compound:	Lindane
Resin:	Fresh beads
Initial Spiking:	500 μL of 10 mg/mL into 10 L = 500 μg/L
	overnight stir
Water Preparation:	System 2, through XAD-2 resin column
Analysis: Liquid:	100, 75, 50 mL DCM + 100 mL hexane
Solid:	modified, in glass fritted column

Appendix 3 Extra experiments on XAD-2 Resin

A3.1 Resin Size Distribution

A sieve analysis of XAD-2 resin was performed to determine the size distribution. The resin had been subjected to the cleaning procedure and the was dryed. The results in the following table (Table A3-1) show that about 85% of the resin fell between the 20-28 mesh size and about 12% between the 28-35 mesh size. This sieve analysis may have been in slight error since the dry resin clings to the seives by static charge. In order to minimize this effect, a large amount of resin was used. Also, once wetted, the beads may increase in size.

Table A3-1 Sieve Analysis of XAD-2 Resin

Sieve Size	Weight (g)			% Resin
(mesh)	Sieve	Sieve & Resin	Resin	Retained
20	420.88	422.50	1.62	0.8
28	411.55	576.39	164.84	85.4
35	373.03	395.50	22.47	11.6
60	360.20	364.26	4.06	2.1
100	388.33	388.44	0.11	0.1
		sum	193.1	

A3.2 Effects of Resin Bead Size on Adsorption Capacity

As a result of scatter in the single solute isotherms, particularly in the low resin weight region, a test was performed to determine the effect of resin bead size upon adsorption capacity. Wet resin was sieved into two size fractions, 20-28 and 28-35 mesh. Replicate bottles containing 50 µg/L Lindane and the same resin weights for the two size fractions were equilibrated for 7 days. Both phases were then analysed. The results in the following table (Table A3-2) show that out of the three replicates, two samples agreed and one was quite different. Because the liquid and solid phase values for the two size fractions were quite close, and also due to the deviation within replicates, no significant difference in the adsorption capacity between the size fractions was observed.

Table A3-2 Effect of Resin Bead Size on Adsorption Capacity
Both solid and liquid phases analysed

Bottle #	Sieve Fraction (mesh)	Dry Resin Weight (g)	Equilibrium Concentration		Total Percent Recovered
			Liquid Phase (ug/L)	Solid Phase (ug/g)	
2	28-35	0.3316	0.21	67.3	89.7
3	28-35	0.3315	0.20	61.7	82.2
4	28-35	0.3322	1.03	65.2	88.7
13	20-28	0.3318	0.18	65.5	87.2
16	20-28	0.3321	0.57	63.1	85.0
19	20-28	0.3319	0.17	68.0	90.7

A3.3 Comparison of Adsorption on Wet and Dry Resin

In order to determine the effect of dry resin on the adsorption capacity, a test to compare the adsorptive capacity of wet and dry resin was performed. In this test, four bottles were loaded with replicate resin weights. Two of the bottles were then dried at 110 °C for 2 hours. The bottles were then filled with a 523 µg/L Triallate solution and equilibrated for 10 days. The results in the following table (Table A3-3) show that the adsorption capacity for Triallate was much greater for dry resin than wet resin. The Triallate in the liquid phase samples for dry resin was high enough to detect, but since it was expected that the concentration would be much higher, a large amount of internal standard was added, making quantitation difficult.

This is an interesting result. A possible explanation may involve a resistance to transfer accross the liquid film surrounding the wetted beads. More study is required, however, in order to further clarify the results of this test.

Table A3-3 Comparison of Triallate Adsorption on Wet and Dry Resin
Both phases analysed after 10 days equilibration

Bottle #.	Resin Dry Weight (g)	Equilibrium Concentration Liquid (µg/L)	Solid (µg/g)	Percent Recovered
Wet 1	0.0142	224	7606	84.0
Wet 2	0.0136	326	8096	104.6
Dry 1	0.0143	nd*	18460	101.1
Dry 2	0.0144	nd*	18331	101.2

* nd denotes not detected

A3.4 Characterization of Modified Elution Method

In order to determine when Triallate was eluted in the modified elution procedure, the different eluant fractions of the solid phase analysis for a sample in the test above (A3.3) were collected and analysed separately. First about 1.5 mL acetone was passed to strip the water from the resin, then three fractions of 6, 4 and 10 mL hexane. The aqueous layer that forms upon mixing the acetone and hexane was also collected from another sample and analysed. The results in Table A3-4 show that most of the Triallate was eluted in the acetone rinse. A detectable but low amount was also recovered from the aqueous phase, probably due to the significant amount of acetone present in this phase.

These results appear to indicate that acetone alone would be a good eluant. Some means of removing the water, however, would then need to be devised.

Table A3-4 Characterization of Modified Elution Method

Elution Fraction	Mass Triallate in Fraction (µg)	Percent of Total
1.5 mL acetone	104	96.6
6 mL hexane	3.55	3.30
4 mL hexane	0.099	0.09
10 mL hexane	0.018	0.02
Aqueous layer	0.036	0.03

Appendix 4   Brief Description of Selected Isotherm Equations

A4.1 Freundlich Equation

The Freundlich equation is an empirically derived adsorption equation which is often useful in describing actual adsorption data. It attempts to account for differing energies of adsorption due to heterogeneity in surface active sites and the degree of coverage. The equation has the form:

$$q_e = K \, C^{1/n}$$

where q_e and C are the solid and liquid phase equilibrium concentrations, respectively, and K and $1/n$ are empirical constants describing adsorption capacity and adsorption intensity, respectively. Isotherm data are fitted to a logarithmic linear form:

$$\log q_e = \log K + 1/n \log C$$

where plotting $\log q_e$ versus $\log C$ results in a slope of $1/n$ and an intercept of $\log$. at C=1.

The Freundlich equation usually fits experimental data over moderate concentration ranges, but it does not reduce to a linear adsorption expression at low liquid phase concentrations.

(Montgomery, 1985 and Weber, 1972).

A4.2 Langmuir Equation

The Langmuir equation can be deduced from physical considerations (kinetic or thermodynamic) and generally fits a broad range of experimental data. The Langmuir equation has the following form:

$$q_e = (Q^\circ bC) / (1 + bC)$$

where q_e and C are as described above, Q° is the moles of solute adsorbed per unit weight of adsorbent in a complete monolayer surface coverage, and b

is an empirical constant related to energy of adsorption. Two linear forms are common:

$$C/q_e = 1/bQ° + C/Q°$$

where a plot of C/q_e versus C yields a slope of $1/Q°$ and an intercept of $1/bQ°$, or

$$1/q_e = 1/Q° + (1/bQ°)(1/C)$$

where a plot of $1/q_e$ versus $1/C$ yields a slope of $1/bQ°$ and an intercept of $1/Q$.

Underlying assumptions include constant energy of adsorption (homogenous surface) and that maximum adsorption corresponds to a monolayer of surface coverage. As such, the typical Langmuir plot shows a 'leveling off' of the isotherm at high solid and liquid phase concentrations. Also, at low liquid phase concentrations, the equation reduces to a linear adsorption relationship. (Montgomery, 1985 and Weber, 1972).

A4.3 Brunauer, Emmett and Teller (BET) Equation

The BET equation is similar to the Langmuir equation except that it accounts for multilayer coverage, with the Langmuir equation describing each layer. Assumptions include constant energy of adsorption, and that one layer need not be complete before the next layer forms. The equation has the form:

$$q_e = (BCQ°) / (C_s - C) [1 + (B - 1)(C/C_s)]$$

where all parameters are as described above and B is a constant related to the difference in energy of adsorbate in different layers.

Isotherms described by the BET equation show a characteristic backward 'S' shape.

(Montgomery, 1985 and Weber, 1972).

A4.4 Singer-Yen Equation

The Singer-Yen equation consisits of a modification of the Freundlich equation. An extra term is added which enables better description of adsorption data at very low concentrations according to Henry's Law (linear adsorption). The equation has the following form:

$$\log C = \log (q/q_x) - (n_f - 1) (1 - q/q_x) / \ln 10 + n_f \log(q_x/k_f)$$

where q and C are the solid and liquid phase equilibrium concentrations, respectively, and k_f, n_f and q_x are statistically determined from experimental data.

(Kong and DiGiano, 1986).

Appendix 5   Isotherm Design Procedure

1. Values must be known for the following parameters:
   Freundlich estimates of K and $1/n$
   Minimum liquid phase concentration, $C_{e,min}$ ($\mu g/L$)
   Volume of equilibration bottles, V (L)
   Number of bottles, b
   Minimum adsorbent weight, M_{min} (mg)

2. Use the following equation to calculate $C_{e,max}$ for a given initial liquid phase concentration, C_0, at the minimum adsorbent dose by iteration:

$$M = \frac{V * [C_0 - C_e] * 1000}{[K * C_e^{1/n}]}$$

ie. iterate until the calculated $M = M_{min}$.

This procedure will yield the liquid phase concentration range, $C_{e,min}$ to $C_{e,max}$.

3. Calculate the range of adsorbent doses required to give equal spacing on the Freundlich log - log plot. This is done by first calculating the maximum adsorbent dose, M_{max} using the above equation with $C_{e,min}$. Then, the logarithmic dose increment can be calculated by the following equation:

$$\text{log increment} = (\log(M_{max}) - \log(M_{min})) / (b - 1)$$

The doses can be equally spaced on a log plot by adding the logarithmic dose increment to $\log(M_{min})$ for $b - 1$ times, and then converting each value back. Note: these adsorbent doses are given in dry weights and therefore must be converted to wet weights (if applicable).
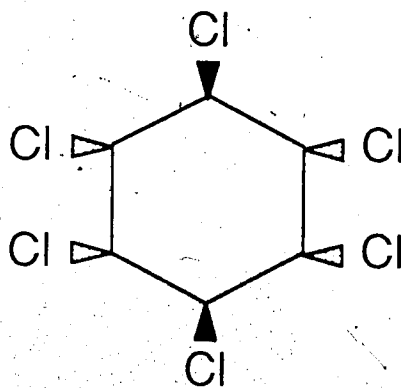
4. With all these data, C_e for each bottle can be calculated and the theoretical isotherm plotted.

Appendix 6   Compound Structures and Information for Lindane, Triallate and TCEP

Lindane   1,2,3,4,5,6-hexachlorocyclohexane   [58-89-9]

$C_6H_6Cl_6$

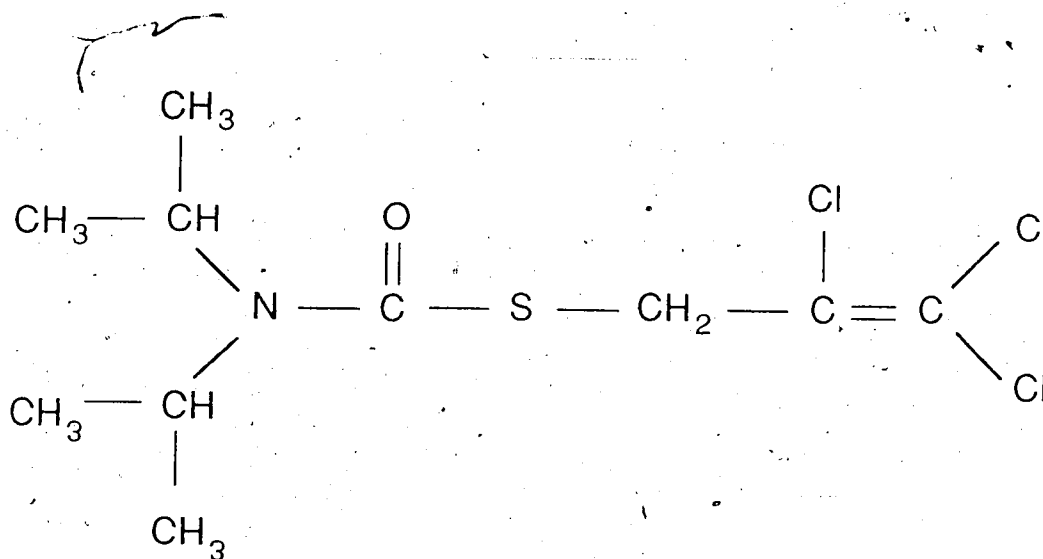Molecular Weight 290.85   Solubility in water 10 mg/L @ 20 °C

Melting Point 112.5 °C

Source: Agrochemicals Handbook, Royal Society of Chemistry, University of Nottingham, England, 1983.

Triallate S-2,3,3-Trichloroallyldiisopropyl thiocarbamate [2303-17-5]
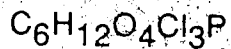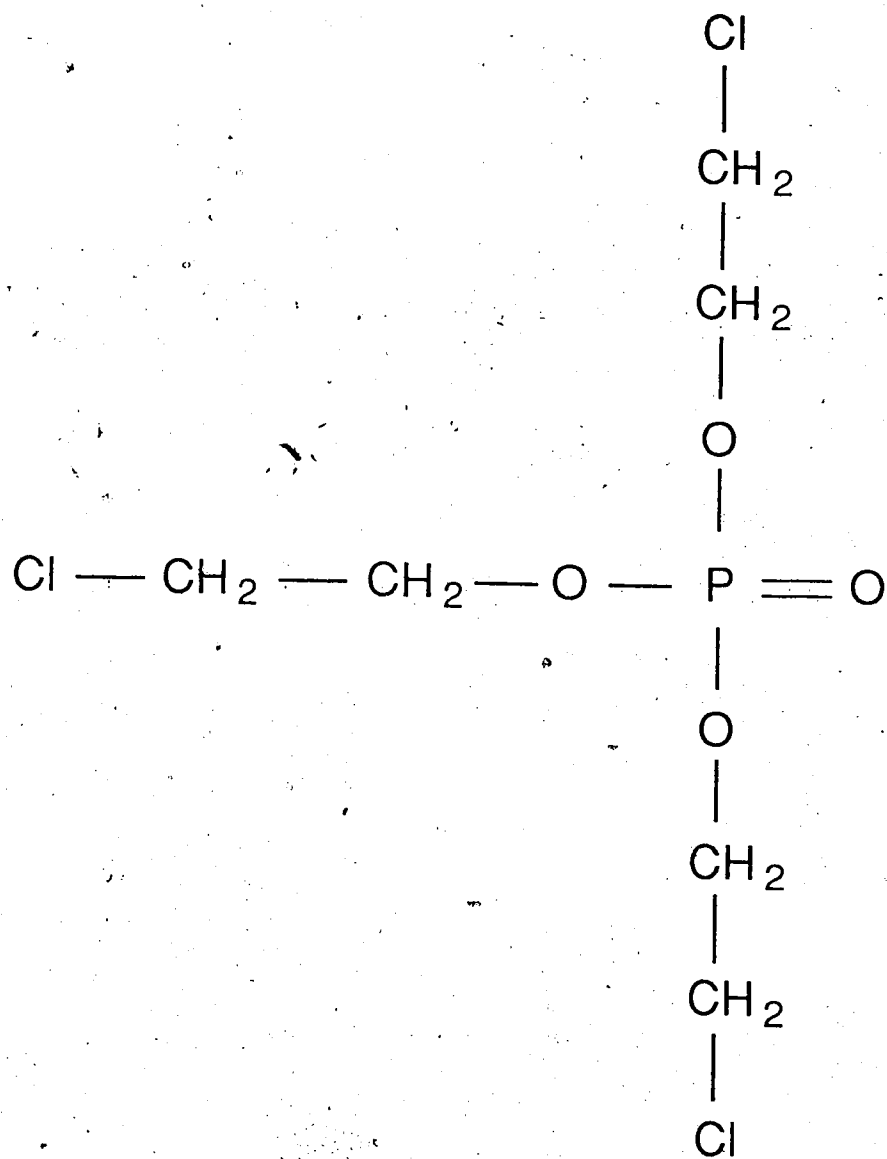

$C_{10}H_{16}Cl_3NOS$

Molecular Weight 304.66

Melting Point 29-30 °C

Solubility in water 4 mg/L @ 20 °C

Boiling point 117 °C @ 0.4 mbar

Source: Agrochemicals Handbook, Royal Society of Chemistry, University of Nottingham, England, 1983.

Tris(2-chloroethyl) phosphate (TCEP)

$$Cl-CH_2-CH_2-O-P(=O)(-O-CH_2-CH_2-Cl)(-O-CH_2-CH_2-Cl)$$

$C_6H_{12}O_4Cl_3P$

Molecular Weight 285.49

Melting Point 29-30 °C

Density 1.390

Boiling point 330 °C